



Intégrabilité dans la Correspondance AdS/CFT:l'analyse quasiclassique et l'approche de bootstrap

Nikolay Gromov

► To cite this version:

Nikolay Gromov. Intégrabilité dans la Correspondance AdS/CFT:l'analyse quasiclassique et l'approche de bootstrap. Mathematical Physics [math-ph]. Université Pierre et Marie Curie - Paris VI, 2007. English. <tel-00286218>

HAL Id: tel-00286218

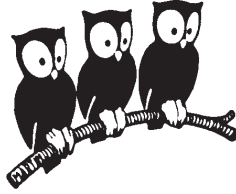
<https://tel.archives-ouvertes.fr/tel-00286218>

Submitted on 9 Jun 2008

HAL is a multi-disciplinary open access archive for the deposit and dissemination of scientific research documents, whether they are published or not. The documents may come from teaching and research institutions in France or abroad, or from public or private research centers.

L'archive ouverte pluridisciplinaire **HAL**, est destinée au dépôt et à la diffusion de documents scientifiques de niveau recherche, publiés ou non, émanant des établissements d'enseignement et de recherche français ou étrangers, des laboratoires publics ou privés.

Laboratoire de physique théorique
de l'École normale supérieure



Thèse de doctorat de l'Université Paris 6

Spécialité: Physique théorique

présenté par
Nikolay GROMOV

pour obtenir le grade de
Doctor de l'Université Paris 6

sujet

**Intégrabilité dans la Correspondance AdS/CFT:
l'analyse quasiclassique et l'approche de bootstrap**

Soutenue le 16 novembre 2007 devant le jury composé de

MM.	V. Kazakov	directeur de thèse
	I. Kostov	
	M. Staudacher	rapporteur
	A. Tseytlin	rapporteur
	A. Zabrodin	
	K. Zarembo	
	J.-B. Zuber	

Integrability in AdS/CFT correspondence: quasiclassical analysis and bootstrap approach

Abstract

In this thesis we consider a quasi-classical method applicable to integrable field theories which is based on classical integrable structure - the algebraic curve. We apply it to the Green-Schwarz superstring on $AdS_5 \times S^5$ space. We show that the proposed method reproduces perfectly the earlier results obtained by expanding the string action for some simple classical solutions. The construction is explicitly covariant and is not based on a particular parametrization of the fields and as a result is free from ambiguities.

On the other hand, the finite size corrections in some particularly important scaling limit are studied in this thesis for a system of Bethe equations. For the general superalgebra $\mathfrak{su}(N|K)$ the result for the $1/L$ corrections is obtained. We find an integral equation which describes these corrections in a closed form. As a by-product of this computation we found a new type of the duality among the systems of Bethe equations.

As an application we consider the conjectured Beisert-Staudacher (BS) equations with the Hernandez-Lopez dressing factor where the finite size corrections should reproduce quasi-classical results around general classical solution. Indeed, we show that our integral equation can be interpreted as a sum of all physical fluctuations and thus prove the complete 1-loop consistency of the BS equations. We demonstrate that any local conserved charge (including the AdS Energy) computed from the BS equations is indeed given at 1-loop by the sum of charges of fluctuations with an exponential precision for large S^5 angular momentum of the string.

As an independent result, the BS equations in $\mathfrak{su}(2)$ sub-sector were derived from the Zamolodchikovs' S-matrix.

Keywords

Gauge theory, String theory, Integrability, Duality

Résumé

Dans cette thèse, nous considérons une méthode quasi-classique applicable aux théories des champs intégrables, basée sur la structure classique intégrable codifiée dans la courbe algébrique. Nous appliquons cette méthode à la supercorde de Green - Schwarz sur l'espace $AdS_5 \times S^5$. Nous montrons que la méthode proposée reproduit parfaitement les résultats déjà obtenus précédemment par l'expansion de l'action autour de certaines solutions simples classiques.

D'autre part, les corrections de taille finie, dans une certaine limite importante, sont étudiées dans cette thèse pour un système des équations de Bethe. Le résultat pour les corrections $1/L$ a aussi été obtenu pour le supergroupe général $\mathfrak{su}(N|K)$. Nous trouvons une équation qui décrit ces corrections dans une forme complète. Comme un sous-produit de ce calcul, nous avons trouvé un nouveau type de la dualité entre les systèmes des équations de Bethe.

Comme application, nous avons examiné les équations conjoncturées par Beisert et Staudacher (BS) avec un facteur de "dressing" de Hernandez et Lopez où les corrections de taille finie devraient reproduire les calculs quasiclassiques autour du mouvement classique de la supercorde dans l'espace $AdS_5 \times S^5$. En effet, nous montrons que notre équation intégrale peut être interprétée comme une somme sur toutes les fluctuations physiques et ainsi nous prouvons que les équations de BS sont cohérentes avec la quantification quasiclassique. Autrement dit, nous démontrons que toutes les charges locales (y compris l'énergie AdS) calculées à partir des équations BS sont effectivement données à la première boucle par la somme des charges des fluctuations.

Un autre résultat présenté ici: nous avons obtenu les équations BS pour sous-secteur $\mathfrak{su}(2)$ à partir de la matrice S de Zamolodchikov et Zamolodchikov.

Mots clés

Théorie de jauge, Théorie des cordes, Intégrabilité, Dualité

Résumé substantiel

L'histoire de la mécanique quantique commence à partir de la suggestion de Louis de Broglie que les particules libres peuvent être décrites en termes des ondes, à l'instar des photons. Cette suggestion a été brillamment confirmée par l'observation des effets des interférences des électrons sur des cristaux. L'étape prochaine a été de décrire les particules dans un potentiel extérieure. Ce problème a été résolu par Schödinger, qui a découvert l'équation non relativiste correspondante. Cependant, sa généralisation relativiste avait un problème de densité négative et la description des systèmes des particules en interaction relativistes s'est trouvée inconsistente.

Grâce à la découverte de la théorie des champs la majorité de vieux problèmes a été résolue ou, au moins, clarifié mais les nouvelles difficultés des divergences ont apparues dans la théorie perturbative. Toutefois, pour décrire tous les phénomènes physiques qui peuvent être observés dans les conditions terrestres, les difficultés peuvent être surmontées. La description quasi complète des données expérimentales existantes a été donnée jusqu'ici par le Modèle Standard. Le seul ingrédient du Modèle Standard, qui manque encore de support expérimental est le boson de Higgs. On peut conclure, que à ce moment, il n'y a pas de nécessité directe expérimentale de sortir des compétences du Modèle Standard.

D'autre part, il existe de nombreuses raisons théoriques pour aller au delà des compétences du Modèle Standard. Le Modèle Standard est une théorie des champs quantiques relativistes, qui décrit trois interactions fondamentales de la nature. La théorie quantique cohérente, qui décrit toutes les quatre interactions connues, y compris la gravité quantique, en même temps, n'existe pas. Actuellement, un des problèmes principaux de la physique théorique est l'unification de la mécanique quantique et de la relativité générale, et ainsi l'unification des interactions gravitationnelles avec les autres. Jusqu'à présent, la théorie des cordes a été et le seul candidat, qui pouvait les unir. La plupart des problèmes de la gravité quantique semble être résolue dans la théorie des cordes. En particulier, les divergences sont régularisées sur l'échelle de Planck, d'une façon naturelle. Malheureusement, la théorie des cordes peut être formulée seulement dans dix dimensions d'espace-temps, mais il semble qu'il y a beaucoup de façons à compactifier six parmi eux et ainsi rester avec quatre dimensions du monde réel.

En dehors de ce problème d'absence de la "théorie de tout" il y a beaucoup de questions ouvertes à l'intérieur du Modèle Standard. En particulier, le Modèle Standard décrit l'interaction forte, qui est en effet la plus forte interaction de la nature. Il est responsable de la majeure partie de la masse des baryons. L'interaction forte lie les nucléons dans les noyaux. La partie du Modèle Standard, décrivant l'interaction forte, la Chro-

modinamique Quantique (QCD), a les quarks et les gluons comme les degrés de liberté fondamentales. Toutefois, la compréhension du monde physique implique aussi la compréhension du fait comment ces constituants fondamentaux interagissent et produisent la diversité des objets physiques qui composent l'Univers. Une des propriétés importantes de l'interaction forte, le confinement des quarks, est toujours une énigme pour les théoriciens.

Si on connaissait la théorie duale à QCD, dans laquelle la théorie des perturbations donne le développement en puissances inverses de la constante de couplage g , on pourrait résoudre ces problèmes. Malheureusement on n'a pas encore trouvé une telle théorie. Mais cependant il y a quelques indications que cette théorie sera de type de la théorie des cordes.

L'origine de la théorie des cordes est étroitement liée à la théorie de l'interaction forte. D'abord, elle a été formulée comme une théorie des hadrons. Or, après l'apparition de QCD, la plupart de la recherche dans la théorie des cordes a été transférée à l'échelle de Planck. La théorie des cordes, dans la théorie de l'interaction forte, est devenue un outil phénoménologique. Néanmoins, l'espoir, que les théories de jauge avec le groupe de jauge $SU(N)$, peuvent être décrites par les cordes, provient de la limite de grand N de 't Hooft. À cette limite, les graphes de Feynman avec les topologies non-planaires sont supprimés par les puissances de $1/N$. Chaque graphe comporte un facteur topologique N^χ , où χ est la caractéristique d'Euler de la graphe. Cela rappelle fortement la théorie des cordes avec une constante du couplage $1/N$. En s'appuyant sur cela, 't Hooft a proposé une conjecture, qu'à cette limite QCD est décrit par une théorie des cordes. Cette idée est également soutenue par le fait expérimental que les hadrons se situent approximativement sur des trajectoires linéaires de Regge.

En soit même, la dualité de théorie jauge/corde est un sujet vieux mais toujours actuel qui apparaît dans de nombreuses situations. Un exemple très connu de cette dualité est une description par le modèle des matrices de la gravité quantique à deux dimensions et la théorie des cordes noncritiques. D'autre part, il y a des exemples des théories, qu'on peut résoudre exactement à la limite des grandes N . Les modèles des matrices et QCD à deux dimensions sont les deux exemples dans lesquels la limite des grands N est intégrable.

La découverte récente d'intégrabilité de la théorie de Yang-Mills avec la supersymétrie $\mathcal{N} = 4$ (SYM) à trois premières boucles, ainsi que l'observation d'intégrabilité au niveau classique de son dual, la corde sur le fond $AdS_5 \times S^5$ a fait renaître les espoirs, que quelques théories de jauge à 4 dimensions pourraient être exactement résolubles. Pour SYM $\mathcal{N} = 4$, l'intégrabilité se manifeste comme une possibilité de calculer, en utilisant les techniques de l'ansatz de Bethe, les dimensions, comme fonctions de constante de cou-

plage $\lambda = Ng^2$, de tous les opérateurs locaux de la théorie. Pour l’instant, cette fonction a été calculée jusqu’à $\mathcal{O}(\lambda^4)$, et la corde $AdS_5 \times S^5$ donne l’asymptotique de cette fonction à $\lambda \rightarrow \infty$ pour les “longues” opérateurs, qui sont un produit de beaucoup de champs fondamentaux de SYM dans le même point d’espace.

La thèse est consacrée à l’étude de cette intégrabilité.

L’approche quasi-classique est un des moyens les plus importants en mécanique quantique. Dans cette thèse nous considérons une méthode applicable aux théories des champs intégrables qui est basée sur la structure classique intégrable de la courbe algébrique. Nous appliquons cette méthode à la supercorde de Green - Schwarz sur l’espace $AdS_5 \times S^5$. Nous montrons que la méthode proposée reproduit parfaitement les résultats obtenus précédemment par l’expansion d’action autour des certaines solutions simples classiques. La construction est explicitement covariante, s’est à dire elle et n’est pas basée sur une paramétrisation particuliers des champs.

D’autre part, les corrections de taille finie, dans une certaine limite importante, sont étudiées dans cette thèse pour un système d’équations de Bethe. Dans le cas simple de la chaîne $\mathfrak{sl}(2)$ des spins de Heisenberg intégrable, les corrections sous-dominantes sont calculées. Ce calcul exige une analyse attentive de la position des racines Bethe près de leurs bords de distribution. Cela rappelle la limite de “double scaling” dans les modèles des matrices.

Les corrections $1/L$ ont aussi été obtenu pour le supergroupe général $\mathfrak{su}(N|K)$. Nous trouvons une équation qui décrit ces corrections dans une forme fermée. Comme un sous-produit de ce calcul, nous avons trouvé un nouveau type de la dualité entre les systèmes des équations de Bethe, “dualité particule-trou”, qui peut simplifier une distribution complexe des racines de Bethe.

Comme une application de la méthode développée pour les chaînes de Heisenberg, nous avons examiné les équations conjoncturées par Beisert et Staudacher (BS) corrigé par le “drerssing factor” de Hernandez et Lopez, où les corrections de taille finie devraient reproduire les calculs quasiclassiques autour du mouvement classique de supercorde dans l’espace $AdS_5 \times S^5$. En effet, nous montrons que notre équation intégrale peut être interprété comme une somme sur toutes les fluctuations physiques et ainsi nous prouvons, que les equations de BS sont cohérentes avec la quantification quasiclassique. Autrement dire, nous démontrons que toutes les charges locales (y compris l’énergie AdS) calculées à partir des équations BS sont effectivement données à la première boucle par la somme des charges des fluctuations, avec la precision exponentielle par rapport a une grandeur d’une impulsion angulaire de la corde. Pour les corrections de taille finie, qui ont été limitées aux configurations simples, le traitement présenté ici est totalement général.

Un autre resultat présenté ici: nous obtenons les équations BS pour le sous-sector $\mathfrak{su}(2)$

à partir de la matrice S de Zamolodchikov et Zamolodchikov, qui a été proposé il y a déjà 30 ans.

NOTATIONS

\mathcal{Q}_r - local conserved charges

$\lambda = g_{YM}^2 N$ - 't Hooft coupling

$z = x + 1/x$

m - winding of the string in S^5 around its angular momentum direction

n - mode number

L - total spin chain length

K_a - number of the Bethe roots of the type a

$\mathcal{J} = L/\sqrt{\lambda}$

$\alpha(x) = \frac{4\pi}{\sqrt{\lambda}} \frac{x^2}{x^2-1}$

Indexes

i, j, k - to number sheets of the Riemann surface, take values $1, \dots, 8$ or $\hat{1}, \dots, \hat{4}, \tilde{1}, \dots, \tilde{4}$

a, b - type of the magnon, corresponds to the node in the Dynkin diagram

i, j - take values $1, \dots, K_a$

Contents

1. <i>Introduction</i>	12
1.1 Integrability	14
1.1.1 Integrability and algebraic curve	16
1.2 Bethe ansatz equation	20
1.2.1 Bethe ansatz in the AdS/CFT correspondence	22
1.2.2 Thermodynamical limit	25
1.3 Overview	28
2. <i>Finite size corrections in Heisenberg spin chain</i>	31
2.1 Finite size corrections in $\mathfrak{sl}(2)$ Heisenberg spin chain	31
2.1.1 Hamiltonian, Transfer-matrix and Higher Charges of $\mathfrak{sl}(2)$ chain	33
2.1.2 $1/L$ expansion of BAE	34
2.1.3 Large L limit and $1/L$ -corrections from Baxter equation	35
2.1.4 Double scaling solution near the branch point	38
2.1.5 General solution for p_2 and E_2	42
2.1.6 Energy	43
2.1.7 One cut case	44
2.1.8 Local charges	47
2.1.9 Summary	49
2.2 Finite size corrections in $\mathfrak{su}(1,2)$ Heisenberg spin chain	50
2.2.1 Finite size correction to Nested Bethe Ansatz equations	55
2.2.2 Derivation using the transfer matrices	56
2.2.3 Re-derivation using the bosonic duality in the scaling limit	59
2.2.4 More about bosonic duality	60
2.2.5 Examples of the dual configurations	63
Appendix A: Transfer matrix invariance and bosonic duality for $SU(K M)$ su- pergroups	68
3. <i>Quasi-classical quantization and fluctuations</i>	72
3.1 Preface	72

3.2	Circular string solutions	75
3.3	Frequencies from the algebraic curve	76
3.3.1	The BMN string	80
3.3.2	The circular string in S^3 , the 1 cut $\mathfrak{su}(2)$ solution	82
3.3.3	The circular string in AdS_3 , the 1 cut $\mathfrak{sl}(2)$ solution	85
3.4	Results, interpretation and 1-loop shift	85
3.4.1	Simple $\mathfrak{su}(2)$ circular string	86
3.4.2	General $\mathfrak{sl}(2)$ circular string	87
3.4.3	Explanation of shifts	87
3.4.4	1-loop shift and prescription for labeling fluctuation frequencies	89
3.4.5	General $\mathfrak{su}(2)$ results	90
3.5	Summary	91
	Appendix A: Quasi-momenta for a generic rigid circular string	92
	Appendix B: BMN string, details	94
	Appendix C: $\mathfrak{su}(2)$ circular string, details	95
	Appendix D: $\mathfrak{sl}(2)$ circular string	97
	Appendix E: Ambiguities due to shifts	103
4.	<i>Matching finite size corrections and fluctuations</i>	105
4.1	Heisenberg spin chain	105
4.1.1	1-loop shift and fluctuations	106
4.1.2	Generalization	109
4.2	Matching of finite size corrections and fluctuations in AdS/CFT	111
4.2.1	Middle node anomaly	111
4.2.2	Dualities in the string Bethe ansatz	112
4.2.3	Integral equation	116
4.2.4	Fluctuations	117
4.3	The unit circle and the Hernandez-Lopez phase	119
	Appendix A: Large N limit	121
5.	<i>Relativistic bootstrap approach in AdS/CFT</i>	123
5.1	Classical $SU(2)$ Principal Chiral Field	124
5.1.1	Classical Integrability and Finite Gap Solution	125
5.2	Quantum Bethe Ansatz and Classical Limit: $O(4)$ Sigma-Model	127
5.2.1	Bethe Equations for Particles on a Circle	128
5.3	Quasi-classical limit	129
5.3.1	Energy and momentum	132
5.4	Elimination of θ 's and AFS equations	134

5.4.1	Derivation of AFS formula	135
5.4.2	Classical limit and KMMZ algebraic curve	136
5.4.3	Geometric proof	137
5.5	Virasoro modes	139
Appendix A: Derivation of AFS formula for asymptotic string BAE's		140

1. INTRODUCTION

THE HISTORY OF THE QUANTUM MECHANICS starts from Louis de Broglie, who suggested that the free particles could be described in terms of waves, like photons. This suggestion was brilliantly confirmed by the observed interference effects in the scattering of electrons from crystals. The next step was to describe the particles in external potential. This problem was solved by Schrodinger, who discovered the non-relativistic wave equation. However, its relativistic generalization had a puzzling property of negative densities and the description of systems of interacting relativistic particles turned out to be inconsistent.

After discovering the field theory, lots of old problems were resolved or at least clarified but new difficulties of divergences in perturbative theory appeared. However, to describe all physical phenomena, which can be observed on Earth, these difficulties can be overcome. The complete description of the existing experimental data so far is given by the Standard Model. The only ingredient of the Standard Model, which still lacks experimental support, is the Higgs boson particle. One can, therefore, conclude that at this moment there is no direct experimental need to go beyond the Standard Model.

On the other hand there are lots of theoretical reasons to go beyond the Standard Model. The Standard Model is a relativistic quantum field theory, which describes three fundamental interactions existing in nature. The consistent quantum theory, which describes all the four known interactions at the same time, does not exist today. One of the main problems of today physics is the integration of quantum mechanics and general relativity which leads to unification the gravitational interaction with the others. Until now, the most reasonable and the only existing candidate has been string theory. In this theory, several problems of the quantum gravity seem to be resolved. In particular, the divergencies are regularized on the Planck scale in some natural way. Unfortunately, string theory can be formulated consistently only in ten dimensional space-time and it seems that there are too many ways to compactify it to the four dimensions of the real world.

Besides the problem of finding the “theory of everything”, there are many open questions inside the Standard Model. In particular, the Standard Model describes the strong interaction, which is indeed the strongest force of nature. It is responsible for the major part of baryon mass, and thus for major part of all masses on the Earth. Strong interactions

bind nucleons in nuclei which, being dressed with electrons and bound into molecules by the much weaker electro-magnetic force, give rise to the variety of the chemical properties. The part of the Standard Model, describing the strong interaction, Quantum Chromodynamics (QCD), has quarks and gluons as fundamental degrees of freedom. However, understanding the physical world implies also understanding how these fundamental constituents interact and bring into existence the entire variety of physical objects composing the universe. One of the most important features of the strong interactions – quark confinement is still a mystery for the theorists.

String theory from its very origin is closely related to the theory of the strong interactions. It was first formulated as a theory of hadrons. However, after invention of QCD, the string research was shifted to the Planck scale. String theory in the theory of the strong interactions converted into a phenomenological tool. Nevertheless, the hope that the gauge theories with $SU(N)$ gauge group can be described by strings was coming from the large N 't Hooft limit. In this limit the Feynman graph with non-planar topology are suppressed by the powers of N . Each graph carries a topological factor N^χ , where χ is the Euler characteristic of the graph. This strongly reminds some string theory with $1/N$ coupling. Basing on this it was conjectured that in this limit QCD is described by some string theory. This idea is also supported by the experimental fact that hadrons approximately lie on linear Regge trajectories.

Then it was understood that the string theory dual to a particular 4 dimensional gauge theory lives on a curved, higher dimensional manifold [1]. The formulation of this duality could be made precise in the case of $\mathcal{N} = 4$ Super Yang-Mills. Maldacena conjectured that it is dual to the type IIB string theory on $AdS_5 \times S^5$ [2, 3, 4]. A great technical advantage of the string side of duality is that string theory in the tree approximation is a two dimensional σ -model and the string interactions are not relevant in the planar 't Hooft limit. On the other hand, there are numerous examples of the exactly solvable two-dimensional σ -models possessing an integrability. This gives us some hope that $\mathcal{N} = 4$ super Yang-Mills theory is the first interacting four dimensional gauge theory which could be solved at least in the planar 't Hooft limit.

In support of this hope, the 1-loop integrability was discovered in $\mathcal{N} = 4$ SYM in [5] for the bosonic sector¹ where the dilatation operator was identified with the Hamiltonian of an integrable 1-dimensional spin chain. Soon after, the classical integrability of the full superstring σ -model on $AdS_5 \times S^5$ was demonstrated in [8]. We will focus on this construction of major importance in the next section.

¹ Integrable spin chains have been discovered in (non-supersymmetric) gauge theories earlier [6, 7].

1.1 Integrability

THE GREEN-SCHWARZ (GS) SUPERSTRING on $AdS_5 \times S^5$ can be represented as a coset model with the target super-space [9]

$$\frac{PSU(2,2|4)}{SP(2,2) \times SP(4)}$$

whose bosonic part is $\frac{SU(2,2)}{SP(2,2)} \times \frac{SU(4)}{SP(4)}$ which is precisely $AdS_5 \times S^5$.

The matrix superalgebra $\mathfrak{su}(2,2|4)$ is spanned by the 8×8 supertraceless supermatrices

$$M = \begin{pmatrix} A & B \\ C & D \end{pmatrix} \quad (1.1)$$

where A and D belong to $\mathfrak{u}(2,2)$ and $\mathfrak{u}(4)$ respectively while the fermionic components are related by

$$C = B^\dagger \begin{pmatrix} \mathbb{I}_{2 \times 2} & 0 \\ 0 & -\mathbb{I}_{2 \times 2} \end{pmatrix}.$$

The $\mathfrak{psu}(2,2|4)$ superalgebra is the quotient of this algebra by the matrices proportional to the identity. Then we note that the $\mathfrak{psu}(2,2|4)$ algebra enjoys the automorphism

$$\Omega \circ M = \begin{pmatrix} EA^TE & -EC^TE \\ EB^TE & ED^TE \end{pmatrix}, \quad E = \begin{pmatrix} 0 & -1 & 0 & 0 \\ 1 & 0 & 0 & 0 \\ 0 & 0 & 0 & -1 \\ 0 & 0 & 1 & 0 \end{pmatrix}, \quad (1.2)$$

such that $\Omega^4 = 1$. This automatically implies that the algebra is endowed with a \mathbb{Z}_4 grading. This means that any algebra element can be decomposed into $\sum_{i=0}^3 M^{(i)}$, where $\Omega \circ M^{(n)} = i^n M^{(n)}$. More explicitly

$$\begin{aligned} M^{(0,2)} &= \frac{1}{2} \begin{pmatrix} A \pm EA^TE & 0 \\ 0 & D \pm ED^TE \end{pmatrix} \\ M^{(1,3)} &= \frac{1}{2} \begin{pmatrix} 0 & B \pm iEC^TE \\ C \mp iEB^TE & 0 \end{pmatrix}. \end{aligned} \quad (1.3)$$

We see that the $M^{(0)}$ elements belong, by definition, to the denominator algebra $\mathfrak{sp}(2,2) \times \mathfrak{sp}(4)$ of the coset. Then, the remaining bosonic elements, $M^{(2)}$, orthogonal to the former, generate the (orthogonal) complement of $\mathfrak{sp}(2,2) \times \mathfrak{sp}(4)$ in $\mathfrak{su}(2,2) \times \mathfrak{su}(4)$.

The Metsaev-Tseytlin action for the GS superstring in $AdS_5 \times S^5$ is then given in terms of the algebra current

$$J = -g^{-1}dg, \quad (1.4)$$

where $g(\sigma, \tau)$ is a group element of $PSU(2, 2|4)$, by

$$S = \frac{\sqrt{\lambda}}{4\pi} \int \text{str} \left(J^{(2)} \wedge *J^{(2)} - J^{(1)} \wedge J^{(3)} \right), \quad (1.5)$$

Besides the obvious global $PSU(2, 2|4)$ left multiplication symmetry the action (1.5) possesses a local gauge symmetry, $g \rightarrow gH$ with $H \in SP(2, 2) \times SP(4)$, under which

$$J^{(i)} \rightarrow H^{-1} J^{(i)} H, \quad i = 1, 2, 3$$

while $J^{(0)}$ transforms as a connection. The equations of motion following from (1.5) are equivalent to the conservation of the Noether current associated with the global left multiplication symmetry

$$d * k = 0 \quad (1.6)$$

where $k = gKg^{-1}$ and $K = J^{(2)} + \frac{1}{2} * J^{(1)} - \frac{1}{2} * J^{(3)}$.

For a purely bosonic representative g we can write

$$g = \left(\begin{array}{c|c} \mathcal{Q} & 0 \\ \hline 0 & \mathcal{R} \end{array} \right).$$

where $\mathcal{R} \in SU(4)$ and $\mathcal{Q} \in SU(2, 2)$. Then we see that $U \equiv \mathcal{R}E\mathcal{R}^T$ is invariant under the gauge transformation $U \rightarrow \mathcal{R}HEH^T\mathcal{R}^T = U$ for $H \in SP(4)$ and thus is a good parametrization of

$$SU(4)/SP(4) \sim S^5.$$

In the same way $V \equiv \mathcal{Q}E\mathcal{Q}^T$ describes the AdS_5 space. It is instructive to define the embedding coordinates u and v by the simple relations

$$u^j \Sigma_j^S = U, \quad v^j \Sigma_j^A = V, \quad (1.7)$$

where Σ^S, Σ^A are the gamma matrices of $SO(6)$ and $SO(4, 2)$. By construction these coordinates will automatically satisfy

$$\begin{aligned} 1 &= u_6^2 + u_5^2 + u_4^2 + u_3^2 + u_2^2 + u_1^2, \\ 1 &= v_6^2 + v_5^2 - v_4^2 - v_3^2 - v_2^2 - v_1^2. \end{aligned} \quad (1.8)$$

Then the bosonic part of the action can be expressed in the usual non-linear σ model form

$$S_b = \frac{\sqrt{\lambda}}{4\pi} \int_0^{2\pi} d\sigma \int d\tau \sqrt{-h} h^{\mu\nu} (\partial_\mu u \cdot \partial_\nu u - \partial_\mu v \cdot \partial_\nu v).$$

One can also expand the action in powers of fermions. It is convenient to use the following parametrization of the $PSU(2,2|4)$ group element [10]

$$g = \exp \left(\begin{array}{c|c} 0 & \theta \\ \hline \bar{\theta} & 0 \end{array} \right) \times \left(\begin{array}{c|c} \mathcal{Q} & 0 \\ \hline 0 & \mathcal{R} \end{array} \right) \quad (1.9)$$

In this parametrization the fermionic part of the action reads

$$\begin{aligned} \mathcal{S}_f &= \frac{\sqrt{\lambda}}{8\pi} \int d^2\sigma \sqrt{-h} h^{\mu\nu} \text{tr}_4 [V \partial_\mu \bar{V} (\theta \partial_\nu \bar{\theta} - \partial_\nu \theta \bar{\theta}) + U \partial_\mu \bar{U} (\partial_\nu \bar{\theta} \theta - \bar{\theta} \partial_\nu \theta)] \\ &\pm i \frac{\sqrt{\lambda}}{8\pi} \int d^2\sigma \epsilon^{\mu\nu} \text{tr}_4 [V \partial_\mu \bar{\theta}^t \bar{U} \partial_\nu \bar{\theta} + \partial_\mu \theta U \partial_\nu \theta^t \bar{V}] + \mathcal{O}(\theta^4) \end{aligned} \quad (1.10)$$

1.1.1 Integrability and algebraic curve

As follows from the equations of motion and the flatness condition,

$$dJ - J \wedge J = 0, \quad (1.11)$$

the connection

$$A(x) = J^{(0)} + \frac{x^2 + 1}{x^2 - 1} J^{(2)} - \frac{2x}{x^2 - 1} (*J^{(2)} - \Lambda) + \sqrt{\frac{x+1}{x-1}} J^{(1)} + \sqrt{\frac{x-1}{x+1}} J^{(3)} \quad (1.12)$$

is flat for any complex number x [8]. This is the crucial observation which indicates the model to be (at least classically) integrable. Indeed, we can define the monodromy matrix

$$\Omega(x) = \text{Pexp} \oint_\gamma A(x) \quad (1.13)$$

where γ is any path starting and ending at some point (σ, τ) and wrapping the worldsheet cylinder once. Since the flatness of the connection ensures path independence we can choose γ to be the constant τ path. Moreover, placing this loop at some other value of τ just amounts to a similarity transformation of the monodromy matrix. Thus we conclude that the eigenvalues of $\Omega(x)$ are time independent. Since they depend on a generic complex number x , we have obtained in this way an infinite number of conserved charges thus assuring integrability.

Let us construct the algebraic curve of Beisert, Kazakov, Sakai and Zarembo [11] which gives the classification of the classical motions of the super string on $AdS_5 \times S^5$. We will argue below that the action variables are represented in a transparent way in terms of the algebraic curve and thus give a good starting point for the quasi-classical quantization of the superstring action.

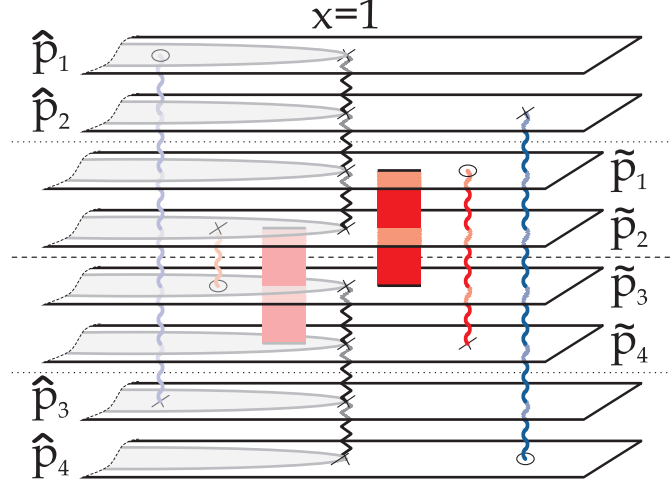


Fig. 1.1: The 8 sheets of the Riemann surface of the “Finite gap” method. The sheets could be connected by the cuts or have synchronized poles. The surface is also restricted by the $x \rightarrow 1/x$ symmetry. The singularities outside the unit circle are also reflected inside the unit circle.

To proceed, we notice that under periodic $SP(2,2) \times SP(4)$ gauge transformations the monodromy matrix transforms by a simple similarity transformation so that the eigenvalues are also gauge invariant. We denote them as follows

$$\{e^{i\hat{p}_1}, e^{i\hat{p}_2}, e^{i\hat{p}_3}, e^{i\hat{p}_4} | e^{i\tilde{p}_1}, e^{i\tilde{p}_2}, e^{i\tilde{p}_3}, e^{i\tilde{p}_4}\} . \quad (1.14)$$

In the rest of this section we shall review the results of [11] and analyze the analytical properties the quasi-momenta \hat{p} and \tilde{p} . The eigenvalues are the roots of the characteristic polynomial equation and thus they define an 8-sheet Riemann surface. These sheets are connected by several cuts – see fig.1.1 – whose branchpoints are the loci where the eigenvalues of the monodromy matrix become equal. The quasi-momenta can jump by a multiple of 2π at points connected by a cut². For example, for a cut going from the first to the second sheet, we will have

$$\hat{p}_1^+ - \hat{p}_2^- = 2\pi n, \quad x \in \mathcal{C}_n^{\hat{1}\hat{2}}, \quad (1.15)$$

where \tilde{p}^\pm stands for the value of the quasi-momenta immediately above/below the cut. This integer n , together with the filling fraction we shall introduce in next section, label each of the cuts. Generically, we can summarize all equations as

$$p_i^+ - p_j^- = 2\pi n_{ij}, \quad x \in \mathcal{C}_n^{ij}, \quad (1.16)$$

² Note that the derivative of the quasi-momenta is a single valued function on the Riemann surface while $p(x)$ is not.

where the indices i and j take values

$$i = \tilde{1}, \tilde{2}, \hat{1}, \hat{2}, \quad j = \tilde{3}, \tilde{4}, \hat{3}, \hat{4} \quad (1.17)$$

and we denote

$$p_{\tilde{1}, \tilde{2}, \tilde{3}, \tilde{4}} \equiv \tilde{p}_{1,2,3,4}, \quad p_{\hat{1}, \hat{2}, \hat{3}, \hat{4}} \equiv \hat{p}_{1,2,3,4}. \quad (1.18)$$

For each cut we also associate the filling fraction

$$S_{ij} = \pm \frac{\sqrt{\lambda}}{8\pi^2 i} \oint_{C_{ij}} \left(1 - \frac{1}{x^2}\right) p_i(x) dx. \quad (1.19)$$

obtained by integrating the quasi-momenta around the square root cut. As before, the indices run over (1.17) and we should chose the plus sign for $i = \hat{1}, \hat{2}$ and the minus sign for the remaining excitations with $i = \tilde{1}, \tilde{2}$. Let us explain why we chose to integrate the quasi-momenta $p(x)$ around the cut with the seemingly mysterious $1 - 1/x^2$ weight. It was pointed out in [12, 11] and shown in [13] that these filling fractions are the action variables of the theory. From the AdS/CFT correspondence these filling fractions are also expected to be integers since they correspond to an integer number of Bethe roots [14, 15]. Indeed, the likely existence of the Bethe ansatz description [16, 18] of the $AdS_5 \times S^5$ superstring also implies this pole structure of the exact quasi-momentum in a semi-classical limit. Moreover, in chapter 5 where the S^5 subsector is studied from the “Bootstrap” point of view we will clearly see that the quasi-momenta $p(z)$ coming from the quantum Bethe ansatz equations appears in the usual form $\oint p(z) dz$, for the Zhukovsky variable $z = x + 1/x$. Thus (1.19) is the good starting point for the string quasi-classical quantization.

From (1.3),(1.12) it follows that

$$C^{-1} \Omega(x) C = \Omega^{-ST}(1/x), \quad C = \left(\begin{array}{c|c} E & 0 \\ \hline 0 & -E \end{array} \right) \quad (1.20)$$

which translates into the inversion symmetry

$$\begin{aligned} \tilde{p}_{1,2}(x) &= -2\pi m - \tilde{p}_{2,1}(1/x) \\ \tilde{p}_{3,4}(x) &= +2\pi m - \tilde{p}_{4,3}(1/x) \\ \hat{p}_{1,2,3,4}(x) &= -\hat{p}_{2,1,4,3}(1/x) \end{aligned} \quad (1.21)$$

for the quasi-momenta³.

³ Note that for \hat{p} there is no $2\pi m$ imposed by requiring absence of time windings [19, 11].

The singularities of the connection at $x = \pm 1$ result in simple poles for the quasi-momenta. These singularities come from the current $J^{(2)}$ in (1.12). This current is super-traceless because it belongs to $\mathfrak{psu}(2,2|4)$ and so is its square due to the Virasoro constraints following from the variation of the action with respect to the worldsheet metric. Together with the inversion symmetry this forces the various residues to organize as follows

$$\{\hat{p}_1, \hat{p}_2, \hat{p}_3, \hat{p}_4 | \tilde{p}_1, \tilde{p}_2, \tilde{p}_3, \tilde{p}_4\} \simeq \frac{\{\alpha_{\pm}, \alpha_{\pm}, \beta_{\pm}, \beta_{\pm} | \alpha_{\pm}, \alpha_{\pm}, \beta_{\pm}, \beta_{\pm}\}}{x \pm 1}. \quad (1.22)$$

i.e. the residues at these points are synchronized and must be the same for the S^5 and the AdS_5 quasi-momenta \hat{p}_i and \tilde{p}_i . This is the crucial role of the Virasoro constraints which will be of utmost importance in the remaining of this chapter.

Finally, for large x , one has

$$A_{\sigma} \simeq -g^{-1} \left(\partial_{\sigma} + \frac{2}{x} k_{\tau} \right) g \quad (1.23)$$

where k , defined below (1.6), is the Noether current associated with the left global symmetry. Thus, from the behavior at infinity we can read the conserved global charges⁴[20]

$$\begin{pmatrix} \hat{p}_1 \\ \hat{p}_2 \\ \hat{p}_3 \\ \hat{p}_4 \\ \tilde{p}_1 \\ \tilde{p}_2 \\ \tilde{p}_3 \\ \tilde{p}_4 \end{pmatrix} \simeq \frac{2\pi}{x\sqrt{\lambda}} \begin{pmatrix} +E - S_1 + S_2 \\ +E + S_1 - S_2 \\ -E - S_1 - S_2 \\ -E + S_1 + S_2 \\ +J_1 + J_2 - J_3 \\ +J_1 - J_2 + J_3 \\ -J_1 + J_2 + J_3 \\ -J_1 - J_2 - J_3 \end{pmatrix}. \quad (1.24)$$

The finite gap method allow us to build, at least implicitly, classical solutions of the nonlinear equations of motion from the analytical properties of the quasi-momenta⁵.

As we shall see in chapter 3, the algebraic curve can also be turned into a powerful tool to study the quantum spectrum, i.e. the energy level spacing, for energies close to that of a given classical string solution.

⁴ These are the bosonic charges, the ones which are present for a classical solution. Latter we shall consider all kind of fluctuations, including the fermionic ones. Then we shall slightly generalize this expression to (3.19).

⁵ For the inverse problem of recovering the solutions from the algebraic curve see the monographs [21, 22] for the general formalism and [13] where this is carried over in the context of string theory for the classical bosonic string in $R \times S^3 \subset AdS_5 \times S^5$ described by the KMMZ algebraic curve [14].

Integrability from the string side appears in the classical theory and its essence is contained in the algebraical curve. From the gauge side of the duality, the integrability shows up in the study of the anomalous dimensions of the long operators, where the mixing matrix acts on the single trace operators as a spin chain Hamiltonian. An important tool in studying the integrable spin chains is Bethe ansatz reviewed in the next sections.

1.2 Bethe ansatz equation

IN 1931 HANS BETHE presented a method for obtaining the exact eigenvalues and eigenvectors of the one dimensional spin-1/2 Heisenberg model, a linear array of electrons with uniform interaction between nearest neighbors. Bethe's parametrization of the eigenvectors, the Bethe ansatz, has become influential to an extent not imagined at the time. Today, many other systems are known to be solvable by some variant of the Bethe ansatz, and the method has been generalized and expanded far beyond the calculational tool it was originally. In particular, it seems to be a key ingredient in the AdS/CFT duality [2, 3, 4] between $\mathcal{N} = 4$ SYM and type IIB superstring theory on $AdS_5 \times S^5$.

It is very instructive to follow the Bethe's original work to understand the physics beyond the algebraical constructions. The spin-1/2 Heisenberg spin chain is described in terms of the spin operators $\hat{\sigma}_n$ by the Hamiltonian

$$H = -2 \sum_{n=1}^L \left(\hat{\sigma}_n \cdot \hat{\sigma}_{n+1} - \frac{1}{4} \right) \quad (1.25)$$

with periodic boundary conditions $\hat{\sigma}_{L+1} = \hat{\sigma}_1$. H acts on a Hilbert space of dimension 2^L spanned by the orthogonal basis vectors $|\sigma_1 \dots \sigma_L\rangle$, where each σ_n is \uparrow or \downarrow .

The ferromagnetic state $|F\rangle = |\uparrow \dots \uparrow\rangle$ is obviously an eigenstate with zero energy. To diagonalize the sector with one spin flipped we can use the translational symmetry, which implies the plane wave form of the eigenstates

$$|p\rangle = \sum_{n=1}^L e^{ipn} |n\rangle \quad (1.26)$$

where $|n\rangle$ is the ferromagnetic state with the n^{th} spin flipped. We can also express it as $|n\rangle = \hat{\sigma}_n^- |F\rangle$. Since the states $|p\rangle$ with $Lp = 2\pi m$, $m = 0, \dots, L-1$ constitute the basis in the sector with one flipped spin they are automatically eigenstates of the Hamiltonian with eigenvalues

$$E = 2(1 - \cos p) \quad (1.27)$$

one can also use the parametrization $u = \frac{1}{2} \cot \frac{p}{2}$ of the momentum of the excitation. We will call this new quantity u - the Bethe root. In the new parametrization one has

$$E = \frac{1}{u^2 + 1/4} . \quad (1.28)$$

Let us consider two excitations (or magnons). When the two flipped spins are far from each other the Hamiltonian acts on them independently and so it is natural to assume the plane wave behavior of the wave-function

$$|\psi\rangle = \sum_{1 \leq n_1 < n_2 \leq L} e^{i(p_1 n_1 + p_2 n_2)} \hat{\sigma}_{n_1}^- \hat{\sigma}_{n_2}^- |F\rangle + A \sum_{1 \leq n_2 < n_1 \leq L} e^{i(p_1 n_1 + p_2 n_2)} \hat{\sigma}_{n_1}^- \hat{\sigma}_{n_2}^- |F\rangle \quad (1.29)$$

where the second term represent the result of the scattering of one excitation on another. Acting on this state by the Hamiltonian one finds

$$A = -\frac{e^{i(p_1+p_2)} + 1 - 2e^{ip_2}}{e^{i(p_1+p_2)} + 1 - 2e^{ip_1}} = \frac{u_1 - u_2 - i}{u_1 - u_2 + i} \quad (1.30)$$

we see that the scattering phase take a nice form in terms of u 's. The periodicity of the wave function implies

$$Ae^{ip_1 L} = 1 , \quad e^{ip_2 L} = A \quad (1.31)$$

or

$$\left(\frac{u + i/2}{u - i/2} \right)^L = 1 , \quad i = 1, \dots, K \quad (1.32)$$

$$e^{ipL} = 1 , \quad i = 1, \dots, K \quad (1.33)$$

$$\left(\frac{u_i + i/2}{u_i - i/2} \right)^L = \prod_{j \neq i}^K \frac{u_i - u_j + i}{u_i - u_j - i} , \quad i = 1, \dots, K \quad (1.34)$$

with $K = 2$. Increasing further the number of excitations will simply lead to the same equation with K equal to the number of the magnons. This set of the equations is called the Bethe ansatz equations. Energy of the state is given by

$$E = \sum_i \frac{1}{u_i^2 + 1/4} . \quad (1.35)$$

This seemingly surprising fact that the multi-magnon scattering is described by the product of the two magnon phases is due to the existence of the large number of the conserved charges. They are commuting with the hamiltonian and thus can be diagonalized in the same basis. Their eigenvalues are given by

$$\mathcal{Q}_r = \sum_{j=1}^K \frac{i}{r-1} \left(\frac{1}{(u_j + i/2)^{r-1}} - \frac{1}{(u_j - i/2)^{r-1}} \right) . \quad (1.36)$$

1.2.1 Bethe ansatz in the AdS/CFT correspondence

The $\mathcal{N} = 4$ SYM dilatation operator in the planar limit can be perturbatively computed in powers of the 't Hooft coupling λ . In the seminal work of Minahan and Zarembo [5] it was shown that the 1-loop dilatation operator acts on the six real scalars of the theory exactly like an integrable $SO(6)$ Heisenberg spin chain Hamiltonian. Restricting ourselves to two complex scalars we obtain the same Hamiltonian considered above. The full $\mathcal{N} = 4$ 1-loop dilatation operator [23] is also governed by an integrable Hamiltonian whose spectrum is given by a system of seven Bethe equations [24], corresponding to the seven nodes of the $\mathfrak{psu}(2,2|4)$ Dynkin diagram. In [25] the all loop generalization of the Bethe equation for the $SU(2)$ sector (1.34) was conjectured to be

$$\left(\frac{y_j^+}{y_j^-}\right)^L = \prod_{j \neq i}^K \frac{u_i - u_j + i}{u_i - u_j - i}, \quad (1.37)$$

where $y_j(u_j)$ and $y_j^\pm(u_j)$ are given by

$$y + \frac{1}{y} = \frac{4\pi}{\sqrt{\lambda}} u, \quad y^\pm + \frac{1}{y^\pm} = \frac{4\pi}{\sqrt{\lambda}} \left(u \pm \frac{i}{2}\right). \quad (1.38)$$

On the other hand, for the same sector but from the string side of the correspondence, a map between classical string solutions and Riemann surfaces was proposed [14] and then generalized to the full super string coset [11], as we review above.

The resemblance between the cuts connecting the different sheets of these Riemann surfaces and the distribution of roots of the Bethe equations in some limit seemed to indicate that the former could be the continuous limit of some quantum string Bethe ansatz. We will give more details about this so-called scaling limit in the next sections. In [16] these equations were proposed to be

$$\left(\frac{y_j^+}{y_j^-}\right)^L = \prod_{j \neq i}^K \frac{u_i - u_j + i}{u_i - u_j - i} \sigma_{\text{AFS}}^2(u_i, u_j), \quad (1.39)$$

where

$$\sigma_{\text{AFS}}(u_i, u_j) = \frac{1 - 1/(y_j^+ y_i^-)}{1 - 1/(y_j^- y_i^+)} \left(\frac{y_j^- y_i^- - 1}{y_j^- y_i^+ - 1} \frac{y_j^+ y_i^+ - 1}{y_j^+ y_i^- - 1} \right)^{i(u_j - u_i)}. \quad (1.40)$$

In Chapter 5 we will show how to derive (1.39) from the Bootstrap approach. The striking similarity between (1.37) and (1.39) naturally leads to the proposal that both sides of the correspondence would be described by the same equation with a scalar factor σ^2 interpolating from σ_{AFS}^2 for large 't Hooft coupling to 1 for small λ .

In [17, 18] Beisert and Staudacher (BS) conjectured the all-loop Bethe equations for the full $PSU(2, 2|4)$ group is

$$\begin{aligned}
e^{i\eta\phi_1 - i\eta\phi_2} &= \prod_{j=1}^{K_2} \frac{u_{1,k} - u_{2,j} + \frac{i}{2}}{u_{1,k} - u_{2,j} - \frac{i}{2}} \prod_{j=1}^{K_4} \frac{1 - 1/x_{1,k}x_{4,j}^+}{1 - 1/x_{1,k}x_{4,j}^-}, \\
e^{i\eta\phi_2 - i\eta\phi_3} &= \prod_{j \neq k}^{K_2} \frac{u_{2,k} - u_{2,j} - i}{u_{2,k} - u_{2,j} + i} \prod_{j=1}^{K_3} \frac{u_{2,k} - u_{3,j} + \frac{i}{2}}{u_{2,k} - u_{3,j} - \frac{i}{2}} \prod_{j=1}^{K_1} \frac{u_{2,k} - u_{1,j} + \frac{i}{2}}{u_{2,k} - u_{1,j} - \frac{i}{2}}, \\
e^{i\eta\phi_3 - i\eta\phi_4} &= \prod_{j=1}^{K_2} \frac{u_{3,k} - u_{2,j} + \frac{i}{2}}{u_{3,k} - u_{2,j} - \frac{i}{2}} \prod_{j=1}^{K_4} \frac{x_{3,k} - x_{4,j}^+}{x_{3,k} - x_{4,j}^-}, \\
e^{i\eta\phi_4 - i\eta\phi_5} &= \left(\frac{x_{4,k}^-}{x_{4,k}^+} \right)^{\eta L} \prod_{j \neq k}^{K_4} \frac{u_{4,k} - u_{4,j} + i}{u_{4,k} - u_{4,j} - i} \prod_j^{K_4} \left(\frac{1 - 1/x_{4,k}^+ x_{4,j}^-}{1 - 1/x_{4,k}^- x_{4,j}^+} \right)^{\eta - 1} \sigma_{\text{AFS}}^{2\eta}(x_{4,k}, x_{4,j}) e^{-i\eta \mathcal{V}(u_{4,k}, u_{4,j})} \\
&\quad \times \prod_{j=1}^{K_1} \frac{1 - 1/x_{4,k}^- x_{1,j}}{1 - 1/x_{4,k}^+ x_{1,j}} \prod_{j=1}^{K_3} \frac{x_{4,k}^- - x_{3,j}}{x_{4,k}^+ - x_{3,j}} \prod_{j=1}^{K_5} \frac{x_{4,k}^- - x_{5,j}}{x_{4,k}^+ - x_{5,j}} \prod_{j=1}^{K_7} \frac{1 - 1/x_{4,k}^- x_{7,j}}{1 - 1/x_{4,k}^+ x_{7,j}}, \quad (1.41) \\
e^{i\eta\phi_5 - i\eta\phi_6} &= \prod_{j=1}^{K_6} \frac{u_{5,k} - u_{6,j} + \frac{i}{2}}{u_{5,k} - u_{6,j} - \frac{i}{2}} \prod_{j=1}^{K_4} \frac{x_{5,k} - x_{4,j}^+}{x_{5,k} - x_{4,j}^-}, \\
e^{i\eta\phi_6 - i\eta\phi_7} &= \prod_{j \neq k}^{K_6} \frac{u_{6,k} - u_{6,j} - i}{u_{6,k} - u_{6,j} + i} \prod_{j=1}^{K_5} \frac{u_{6,k} - u_{5,j} + \frac{i}{2}}{u_{6,k} - u_{5,j} - \frac{i}{2}} \prod_{j=1}^{K_7} \frac{u_{6,k} - u_{7,j} + \frac{i}{2}}{u_{6,k} - u_{7,j} - \frac{i}{2}}, \\
e^{i\eta\phi_7 - i\eta\phi_8} &= \prod_{j=1}^{K_6} \frac{u_{7,k} - u_{6,j} + \frac{i}{2}}{u_{7,k} - u_{6,j} - \frac{i}{2}} \prod_{j=1}^{K_4} \frac{1 - 1/x_{7,k}x_{4,j}^+}{1 - 1/x_{7,k}x_{4,j}^-}.
\end{aligned}$$

Where $\eta = \pm 1$. Sets of equations with different η are related between each other by duality transformation, which we will discuss below. We inserted some additional parameters ϕ_i , called twists. Strictly speaking they all should be zero. However, as we will see the situation when all the twists are vanishing is a very degenerate one. We will also assume that the twists are restricted by

$$\phi_1 - \phi_2 - \phi_3 + \phi_4 = \phi_7 - \phi_8 - \phi_5 + \phi_6 = 2\pi m - \eta \sum_{j=1}^{K_4} \frac{1}{i} \log \frac{x_{4,j}^+}{x_{4,j}^-}. \quad (1.42)$$

The phase $\mathcal{V}(y_{4,j})$ should be responsible for the interpolation between the YM and the string equations for small and large t'Hooft coupling λ .

When some configuration of the Bethe roots $u_{a,j}$ is found the energy of the state (or anomalous dimension of the SYM operators) is given by

$$\Delta = \frac{\sqrt{\lambda}}{2\pi} \sum_{i=1}^{K_4} \left(\frac{i}{y_{4,j}^+} - \frac{i}{y_{4,j}^-} \right). \quad (1.43)$$

and the generalized expression for the local conserved changes is

$$\mathcal{Q}_r = \frac{1}{r-1} \sum_{j=1}^{K_4} \left(\frac{i}{(y_{4,j}^+)^{r-1}} - \frac{i}{(y_{4,j}^-)^{r-1}} \right). \quad (1.44)$$

In terms of them one can rewrite the AFS phase (1.40) as

$$\sigma_{\text{AFS}}^2(u_j, u_k) = \exp \left(2ig \sum_{r=2}^{\infty} (\mathcal{Q}_r(u_k) \mathcal{Q}_{r+1}(u_j) - \mathcal{Q}_{r+1}(u_k) \mathcal{Q}_r(u_j)) \right). \quad (1.45)$$

In [26], based on an hypothesis for a natural extension for the quantum symmetry of the theory, Beisert found (up to a scalar factor) an S-matrix from which the BS equations would be derived. The scalar factor \mathcal{V} was then conjectured in [27, 28] from the string side – using the Janik’s crossing relation [29] – and Beisert, Eden and Staudacher (BES) in [30, 31] from the gauge theory point of view – based on several heuristic considerations [32]. Similarly to (1.45) one can write

$$\mathcal{V}(u_k, u_j) = \sum_{r=2} \sum_{s=r+1} c_{r,s}(g) (\mathcal{Q}_r(u_k) \mathcal{Q}_s(u_j) - \mathcal{Q}_s(u_k) \mathcal{Q}_r(u_j)) \quad (1.46)$$

with

$$\begin{aligned} c_{r,s}(g) &= \sum_{n=1}^{\infty} g^{1-n} \frac{((-1)^{r+s} - 1) \zeta(n)}{(-2\pi)^n \Gamma(n-1)} (r-1)(s-1) \frac{\Gamma^{\frac{s+r+n-3}{2}} \Gamma^{\frac{s-r+n-1}{2}}}{\Gamma^{\frac{s+r-n+1}{2}} \Gamma^{\frac{s-r-n+3}{2}}} \\ &\simeq ((-1)^{r+s} - 1) \left(\frac{2(r-1)(s-1)}{\pi(r-s)(r+s-2)} + \frac{1}{12g} (r-1)(s-1) + \dots \right). \end{aligned} \quad (1.47)$$

The leading coefficient for $g \rightarrow \infty$ was first obtained by Hernandez and Lopez [89].

From the gauge theory side these equations were tested quite recently up to four loops [44, 34, 35]. From the string theory point of view the scalar factor recently passed several nontrivial checks [36, 37, 38, 39] where several loops were probed at strong coupling. Also at strong coupling, the full structure of the BS equations was derived up to two loops in [40, 41] in a particular limit [42] where the sigma model is drastically simplified.

Another efficient way of testing the predictions of the Bethe ansatz equations is via anomalous dimensions of the twist-two operators (i.e. local operators with two scalars and S derivatives, traceless and symmetric in Lorenz indexes). In the regime of large number of derivatives, their anomalous dimensions scale logarithmical $\Delta - S = f(g) \log S$. $f(g)$ is a universal scaling function, computed up to four loops in YM [43, 44, 45]. It is also can be computed up to 2-loops from the string side [46, 47, 48].

It is therefore fair to say that the advance in the last four years was spectacular. On the other hand it is also true that there is a great deal of conjectures involved one should both check and, hopefully, prove (or disprove).

In this work we will check that the BS equations reproduce the 1-loop shift around *any* classical string soliton solution with exponential precision in the large angular momentum of the string state $\mathcal{J} \equiv L/\sqrt{\lambda}$.

1.2.2 Thermodynamical limit

IN THIS SECTION we will review a special limit of the Bethe ansatz equations, following closely [14, 19]. It is so-called thermodynamical or scaling limit. It corresponds to the ferromagnetic regime of low energies $E \sim 1/L$.⁶ Consider for example an $\mathfrak{sl}(2)$ Heisenberg spin chain Bethe ansatz, which will be studied in details in the next chapter

$$-\left(\frac{u_j - i/2}{u_j + i/2}\right)^L = \prod_{k=1}^K \frac{u_j - u_k + i}{u_j - u_k - i}, \quad j = 1, \dots, K. \quad (1.48)$$

Note that under the formal replacement $L \rightarrow -L$ it becomes the described above $\mathfrak{su}(2)$ spin chain. An important property which simplifies the analysis is that the solutions of this set of the equations are always real, which is not the case for the $\mathfrak{su}(2)$ spin chain.

Taking log of both parts of (2.2) we have⁷

$$2\pi i n_j + L \log \frac{u_j - i/2}{u_j + i/2} = \sum_{k=1}^{K'} \log \frac{u_j - u_k + i}{u_j - u_k - i}. \quad (1.49)$$

As we shall see in a moment in the limit $L \rightarrow \infty, K \sim L$ and with $n_j \sim 1$ the Bethe roots scales like L . It means that the chain is very long and the spins are very smoothly changing along it. The typical length of spin-waves (magnons) is of the order of the length L . And it is instructive to introduce $x_j = u_j/L$. We can then write (1.49) in the form

$$2\pi n_j - \frac{1}{x_j} = \frac{2}{L} \sum_{k=1}^{K'} \frac{1}{x_j - x_k} \quad (1.50)$$

where we expanded (1.49) for large L . There is a potential danger arises from the right hand side, since $u_j - u_k$ could be of order of 1. As we will see in the chapter 2 this terms with $u_j - u_k \sim 1$ are responsible for the $1/L$ correction and are not important at the leading order.

Now let us consider the situation with a finite number of different mode numbers n_j , and assume that the number of Bethe roots with the same mode number is of order L .

⁶ It is different from a more traditional regime $E \sim L$ widely studied since many years, especially in the condensed matter literature.

⁷ Note that $\frac{i}{2} \log \frac{x+i}{x-i} = \arctan(x) - \frac{\pi}{2} \text{sign}(x)$ for standard definition of the log.

If we take the ratio K/L to be small we can neglect the right hand side of (1.50) to get $x_j = 1/(2\pi n_j)$. We see that the points x_j with the same mode number are very close to each other and separated from the others roots by ~ 1 . For $K/L \sim 1$ the picture is similar. The points x_j with the same mode number are constituting some continuous distributions. The supports of these distributions corresponding to the different mode numbers are separated by a finite distance ~ 1 . Hence, roots with the same mode number form a continuous cut in the complex plane x . One can characterize the distributions by the density

$$\rho(x) \equiv \frac{1}{L} \sum_j \delta(x - x_j) \quad (1.51)$$

or by resolvent

$$G(x) \equiv \frac{1}{L} \sum_{j=1}^K \frac{1}{x - x_j} \simeq \int_{\mathcal{C}} \frac{\rho(y) dy}{x - y}. \quad (1.52)$$

The density is non-zero on a set of cuts in the complex plane which in general consists of several non-overlapping cuts, $\mathcal{C} = \bigcup_i \mathcal{C}_i$, where the i^{th} cut \mathcal{C}_i represents roots with mode number n_i . In the considered case of the $\mathfrak{sl}(2)$ spin chain the roots are always real and the cuts belong to the real axe.

In the scaling limit of the Bethe equations can be rewritten as an integral equation for the density

$$2\mathcal{G} = 2 \oint_{\mathcal{C}} \frac{\rho(y) dy}{x - y} = 2\pi n_i - \frac{1}{x}, \quad x \in \mathcal{C}_i, \quad (1.53)$$

where $2\mathcal{G}(x) \equiv G(x + i0) + G(x - i0)$. One can solve this integral equation numerically and compare with the actual density of the Bethe roots, also found numerically. For the three cut configuration this comparison is given on the fig.1.2 revealing the perfect consistence of the above analysis.

Let us introduce

$$p(x) = \frac{1}{2x} + G(x) \quad (1.54)$$

which we shall call the quasi-momentum for reasons which will be clear soon. In terms of the analytic function $p(x)$ the above equation becomes

$$\not{p}(x) = \pi n_i, \quad x \in \mathcal{C}_i \quad (1.55)$$

by another words it implies that e^{ip} and e^{-ip} are two sheets of the same two sheet Riemann surface. This reminds the eigenvalues of the monodromy matrix in the classical finite gap analysis of 1.1.1. However we see that our $p(x)$ has a simple pole in the origin, whereas the quasimomenta of the $AdS_5 \times S^5$ string had two poles at ± 1 . But, the BS equations (1.41) are designed in such a way that the analogous quasimomenta arising in

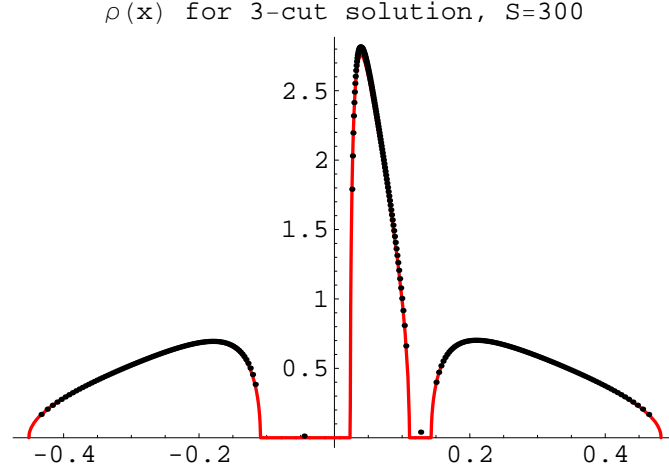


Fig. 1.2: Density of roots. The dots correspond to numerical 3-cut solution with total number of Bethe roots $K = 300$ and equal fractions $\alpha_i = 1/6$, and $n_i = \{-1, 3, 1\}$. They are fixed from the numerical values of the roots by the (2.13). Solid line is the density at $L = \infty$ computed analytically from the corresponding hyper-elliptic curve. x coordinates of the dots are $\frac{u_j + u_{j+1}}{2L}$ so that the solitary points in the middle of empty cuts are artifacts of this definition.

the thermodynamical limit have exactly the same analytical properties as the ones of the classical “finite-gap” analysis.

Indeed, for $\mathcal{J} = L/\sqrt{\lambda}$ fixed and $L \sim K_a \gg 1$ the BS equations can be summarized by $\not{p}_i - \not{p}_j = 2\pi n_{ij}$ for

$$\begin{aligned}
 p_1 &= + \frac{2\pi \mathcal{J} x - \delta_{\eta,+1} \mathcal{Q}_1 + \delta_{\eta,-1} \mathcal{Q}_2 x}{x^2 - 1} + \eta(-H_1 - \bar{H}_3 + \bar{H}_4) + \phi_1 \\
 p_2 &= + \frac{2\pi \mathcal{J} x - \delta_{\eta,-1} \mathcal{Q}_1 + \delta_{\eta,+1} \mathcal{Q}_2 x}{x^2 - 1} + \eta(-H_1 + H_2 + \bar{H}_2 - \bar{H}_3) + \phi_2 \\
 p_3 &= + \frac{2\pi \mathcal{J} x - \delta_{\eta,-1} \mathcal{Q}_1 + \delta_{\eta,+1} \mathcal{Q}_2 x}{x^2 - 1} + \eta(-H_2 + H_3 + \bar{H}_1 - \bar{H}_2) + \phi_3 \\
 p_4 &= + \frac{2\pi \mathcal{J} x - \delta_{\eta,+1} \mathcal{Q}_1 + \delta_{\eta,-1} \mathcal{Q}_2 x}{x^2 - 1} + \eta(+H_3 - H_4 + \bar{H}_1) + \phi_4 \\
 p_5 &= - \frac{2\pi \mathcal{J} x - \delta_{\eta,+1} \mathcal{Q}_1 + \delta_{\eta,-1} \mathcal{Q}_2 x}{x^2 - 1} + \eta(-H_5 + H_4 - \bar{H}_7) + \phi_5 \\
 p_6 &= - \frac{2\pi \mathcal{J} x - \delta_{\eta,-1} \mathcal{Q}_1 + \delta_{\eta,+1} \mathcal{Q}_2 x}{x^2 - 1} + \eta(-H_5 + H_6 + \bar{H}_6 - \bar{H}_7) + \phi_6 \\
 p_7 &= - \frac{2\pi \mathcal{J} x - \delta_{\eta,-1} \mathcal{Q}_1 + \delta_{\eta,+1} \mathcal{Q}_2 x}{x^2 - 1} + \eta(-H_6 + H_7 + \bar{H}_5 - \bar{H}_6) + \phi_7 \\
 p_8 &= - \frac{2\pi \mathcal{J} x - \delta_{\eta,+1} \mathcal{Q}_1 + \delta_{\eta,-1} \mathcal{Q}_2 x}{x^2 - 1} + \eta(+H_7 + \bar{H}_5 - \bar{H}_4) + \phi_8
 \end{aligned} \tag{1.56}$$

Where we introduced

$$G_a(x) = \sum_{j=1}^{K_a} \frac{\alpha(y_{a,j})}{x - y_{a,j}}, \quad H_a(x) = \sum_{j=1}^{K_a} \frac{\alpha(x)}{x - y_{a,j}}, \quad \alpha(x) = \frac{4\pi}{\sqrt{\lambda}} \frac{x^2}{x^2 - 1}.$$

For $\eta = 1$ we will also use the following notations

$$\begin{aligned} \tilde{p}_1 &= p_1, \quad \tilde{p}_2 = p_4, \quad \tilde{p}_3 = p_5, \quad \tilde{p}_4 = p_8, \\ \hat{p}_1 &= p_2, \quad \hat{p}_2 = p_3, \quad \hat{p}_3 = p_6, \quad \hat{p}_4 = p_7. \end{aligned} \quad (1.57)$$

The local conserved charges are encoded into the “middle node” resolvent $G_4(x) \equiv -\sum_{n=0}^{\infty} \mathcal{Q}_{n+1} x^n$. To leading order, these quasi-momenta define an eight-sheet Riemann surface with exactly the same properties as in the classical analysis of the first section.

1.3 Overview

IN THIS THESIS we will perform several nontrivial tests of the conjectures involved into the AdS/CFT correspondence.

- In chapter 2 we show how the finite size corrections to the scaling limit could be computed in a systematic way to arbitrary order in $1/L$. The procedure is similar to the standard WKB expansion. We find Airy type behavior of the Bethe roots close to the edge of the distribution. The Bethe roots are located at zeros of the function

$$f(v) = Ai \left[a^{1/3} \left(v - \frac{1}{4ax_*^2 L^{1/3}} + \frac{a^2 + 12b}{60aL^{2/3}} v^2 \right) \right], \quad (1.58)$$

where $v = (x - x_*)L^{2/3}$, x_* is a position of the branch point of the quasi-momenta, a and b are two paratemers, which could be fixed. Matching asymptotic expansion for large v 's with the expansion in powers of $1/L$ of quasi-momenta allows us to fix all ambiguities.

For a single cut solution for the $\mathfrak{sl}(2)$ subsector we explicitly computed the energy up to the $1/L^2$ order. The result is quite complicated and is given in (2.76).

Then we consider nested Bethe ansatz. As a technical tool we use a curious duality among the systems of the Bethe ansatz equations, which we call bosonic duality. In the scaling limit it allows one to interchange the sheets of the Riemann surface. We find some integral equation describing the leading finite size corrections in a closed form. For an $\mathfrak{su}(1|2)$ spin chain we have

$$\frac{1}{x} + 2 \oint_{c_{23}} \frac{\rho(y) dy}{x - y} + \int_{c_{13}} \frac{\rho(y) dy}{x - y} = 2\pi n_{23}^A + \phi_2 - \phi_3 - \frac{1}{L} \left[\cot_{23} - \int_{c_{13}} \frac{\Delta \cot_{12}}{x - y} \frac{dy}{2\pi i} \right]$$

where \cot_{ij} are some functions of the leading densities.

- In chapter 3 we propose a method of computation of the quasiclassical corrections to the classical spectrum of string theory in the $AdS_5 \times S^5$ background, based solely on the classical integrable structure of the theory. The idea of this method is inspired by the analytical structure of the quasi-momenta of the one-dimensional quantum mechanical systems. The quantum excitations are identified with the poles on the algebraic surface (see fig.1.1) with the residue fixed by the integer value of the classical action variables of the theory.

For a circular string solution we get the following spectrum of excitations

$$\begin{aligned}
\kappa \delta E = & \sum_n \left(N_n^{\hat{1}\hat{3}} + N_n^{\hat{2}\hat{4}} \right) \left(\omega_{n+m}^S - \mathcal{J} \right) + N_n^{\hat{2}\hat{3}} \omega_{n+2m}^{S_-} + N_n^{\hat{1}\hat{4}} \left(\omega_n^{S_+} - 2\mathcal{J} \right) \\
& + \sum_n \left(N_n^{\hat{1}\hat{4}} + N_n^{\hat{2}\hat{4}} + N_n^{\hat{3}\hat{1}} + N_n^{\hat{4}\hat{1}} \right) \left(\omega_n^F - \mathcal{J} + \frac{\kappa}{2} \right) \\
& + \sum_n \left(N_n^{\hat{1}\hat{3}} + N_n^{\hat{2}\hat{3}} + N_n^{\hat{3}\hat{2}} + N_n^{\hat{4}\hat{2}} \right) \left(\omega_{n+m}^F - \frac{\kappa}{2} \right) \\
& + \sum_n \left(N_n^{\hat{1}\hat{3}} + N_n^{\hat{1}\hat{4}} + N_n^{\hat{2}\hat{3}} + N_n^{\hat{2}\hat{4}} \right) \omega_n^A.
\end{aligned} \tag{1.59}$$

where

	eigenmodes	notation
S^5	$\sqrt{2\mathcal{J}^2 + n^2 \pm 2\sqrt{\mathcal{J}^4 + n^2\mathcal{J}^2 + m^2n^2}}$ $\sqrt{\mathcal{J}^2 + n^2 - m^2}$	$\omega_n^{S_{\pm}}$ ω_n^S
Fermions	$\sqrt{\mathcal{J}^2 + n^2}$	ω_n^F
AdS₅	$\sqrt{\mathcal{J}^2 + n^2 + m^2}$	ω_n^A

In this way we reproduced results of the previous direct calculations based on the string action. The developed method could be as well applied to the wide range of the integrable field theories for which the classical curve is known.

- In chapter 4 we show that the finite size corrections are related to the sea of the virtual quasi classical fluctuations and can be interpreted as zero point energy oscillations. The condition that the finite size corrections match the quasi classical excitations is a very nontrivial restriction of the underling system of the Bethe ansatz equation. We also note that to match BS equations in the infinite volume \mathcal{J} with exponential precision one have to introduce an extra potential into the BAE

$$\frac{1}{2} \left[\sum_{i \leq 4} \oint \alpha(x) \frac{(-1)^{F_{i5}}(p'_i - p'_5)}{x - y} \text{sign}(\text{Im } y) \frac{dy}{2\pi} + \dots \right] \tag{1.60}$$

$$= \oint \left[\frac{\alpha(x)}{x-y} - \frac{\alpha(1/x)}{1/x-y} \right] (p'_4 - p'_3 - p'_2 + p'_1) \operatorname{sign}(\operatorname{Im} y) \frac{dy}{2\pi} = -2\eta \mathcal{V}(x)$$

which one can rewrite as

$$\mathcal{V}(x) = \alpha(x) \sum_{\substack{r,s=2 \\ r+s \in \text{Odd}}}^{\infty} \frac{1}{\pi} \frac{(r-1)(s-1)}{(s-r)(r+s-2)} \left(\frac{\mathcal{Q}_r}{x^s} - \frac{\mathcal{Q}_s}{x^r} \right) \quad (1.61)$$

where we recognize precisely the Hernandez-Lopez coefficients (1.47).

- Finally in chapter 5 we show how the BS equations in $\mathfrak{su}(2)$ sector could be derived from the old bootstrap approach. We show that in the $\mathfrak{su}(2)$ sector the BS equations (which are AFS equations in this case) could be considered as effective equations coming from the simple nested equations with a clear physical meaning. Namely, by excluding rapidities θ_α of the relativistic particles from the set of the usual BAE equations

$$\begin{aligned} 2\pi m_\alpha &= \mu \sinh \pi \theta_\alpha - \sum_{\beta \neq \alpha}^L i \log S_0^2(\theta_\alpha - \theta_\beta) \\ &\quad - \sum_j^{J_u} i \log \frac{\theta_\alpha - u_j + i/2}{\theta_\alpha - u_j - i/2}, \end{aligned} \quad (1.62)$$

$$2\pi n_j^u = \sum_\beta^L i \log \frac{u_j - \theta_\beta - i/2}{u_j - \theta_\beta + i/2} + \sum_{i \neq j}^{J_u} i \log \frac{u_j - u_i + i}{u_j - u_i - i}, \quad (1.63)$$

we get precisely AFS equations with non-relativistic dispersion relation for the magnons! All the complicated structure of the AFS phase should thus be a manifestation of the existence of a hidden extra degree of freedom which was integrated out.

2. FINITE SIZE CORRECTIONS IN HEISENBERG SPIN CHAIN

THIS CHAPTER IS DEVOTED to the study of the $1/L$ finite size corrections in Bethe ansatz equations. Our main motivation to study the finite size corrections in Bethe ansatz comes from the AdS/CFT correspondence. From the string side of the duality the finite size corrections corresponds to the worldsheet loop expansion. Thus the careful analysis of the finite size corrections can bring a new insight and can serve as a very nontrivial test of the different conjectures involved into the AdS/CFT correspondence. The main result of this chapter will be the integral equation, describing in a closed form the finite size corrections to the classical limit in the BS equation.

The similarity, and even the coincidence in a certain regime of the finite size corrections from the Bethe ansatz side and 1-loop corrections to the classical limit from the string side was already observed earlier on particular string and chain solutions, having only one support for the Bethe roots distribution [49, 50, 51, 52, 53, 54, 55, 56]. $1/L$ corrections were first studied for BMN states in [5], where the integrable spin chain for $\mathcal{N} = 4$ SYM was first proposed, and then in [16]. The Airy edge behavior, we will find in this chapter, also seems to be an important feature, because it provides some information about the system at all orders in $1/L$.

2.1 *Finite size corrections in $\mathfrak{sl}(2)$ Heisenberg spin chain*

IN THIS SECTION WE STUDY the integrable periodic Heisenberg XXX_s chain of noncompact quantum spins transforming under the representation $s = -1/2$ of $\mathfrak{sl}(2)$, in the thermodynamical limit reviewed in the introduction. We will develop some general methods of the systematic $1/L$ expansion. In the next section we will generalize it to the so called nested Bethe ansatz, which arises for the spin chains with a higher rank symmetry group.

The $\mathfrak{sl}(2)$ spin chain is known to be solvable by the Bethe ansatz (see for example [57]) and the energy of a state of K magnons in dimensionless units is given by a simple formula

$$E = \sum_{k=1}^K \frac{1}{u_k^2 + 1/4} , \quad (2.1)$$

where the Bethe roots u_j , $j = 1, 2, \dots, K$, parameterizing the momenta of magnons, are solutions of a system of polynomial Bethe ansatz equations (BAE)

$$-\left(\frac{u_j - i/2}{u_j + i/2}\right)^L = \prod_{k=1}^K \frac{u_j - u_k + i}{u_j - u_k - i}, \quad j = 1, \dots, K. \quad (2.2)$$

It can be proven that for this model the roots are always real.

Our goal is to study the limiting $L \rightarrow \infty$ distributions of Bethe roots and the finite volume $1/L$ corrections to these distributions, to the energy and higher conserved charges. As we mentioned in the introduction in the main order this thermodynamical limit for the compact Heisenberg $XX_{1/2}$ chain of $\mathfrak{su}(2)$ spins was already considered in [58], and later in [59] in relation to the integrable dilatation hamiltonian in planar perturbative superconformal $\mathcal{N} = 4$ super-Yang-Mills (SYM) theory. Its description and the general solution in terms of algebraic curves was proposed in [14] for the $\mathfrak{su}(2)$ case¹ and in [61, 19] for the $\mathfrak{sl}(2)$ chain.

The study of $1/L$ corrections in these systems was started recently in the papers [49, 50] for the simplest single support, or one cut distribution, whereas a similar quantum \hbar correction to the classical KdV solitons was already found earlier in the general multi-cut case in [62].

This section we will get the following results:

1. The explicit formulas for the $1/L$ and $1/L^2$ corrections to the general multi-cut distribution of Bethe roots and to the corresponding energy of a Bethe state in terms of the underlying algebraic curve.
2. The universal description of the distribution of Bethe roots in the vicinity of an edge of a support in terms of zeroes of the Airy function, similar to the double scaling limit in the matrix models.
3. Asymptotics of conserved local charges $\mathcal{Q}_n(K, L)$ in the large n limit.

Unlike the papers [49, 50] using the method of singular integral equation corrected by so called anomaly term², we will use here the exact Baxter equation written directly for the analytical function - the resolvent of the root distribution (similar approach was used in [61]). This approach is more general and can be generalized to the higher orders in $1/L$. As an example we apply the method to the simplest 1-cut configuration.

In the next sections we will generalize the method developed here for the more general systems of the equations and finally apply it in chapter 4 to the conjectured string BS equations. Then in the next chapter we will show how the finite size corrections of BS

¹ Following a similar approach of [60] to a somewhat different limit of large spin

² This phenomenon of anomaly, or the contribution of close eigenvalues in the thermodynamical limit of BAE was first observed in [15]

equations match with the 1-loop corrections to the classical energy levels in the general classical background.

2.1.1 Hamiltonian, Transfer-matrix and Higher Charges of $\mathfrak{sl}(2)$ chain

The hamiltonian of interaction of the neighboring spins s_l, s_{l+1} can be written in an explicit way [63]

$$H_{-1/2} = \sum_{l=1}^L \hat{H}_{-1/2}^{l,l+1} \quad (2.3)$$

with the Hamiltonian density

$$\hat{H}_{-1/2}^{l,l+1} |k, m-k\rangle = \sum_{k'=0}^m \left(\delta_{k=k'} (h(k) + h(m-k)) - \frac{\delta_{k \neq k'}}{|k-k'|} \right) |k', m-k'\rangle, \quad (2.4)$$

where $|k_1, \dots, k_l, k_{l+1}, \dots, k_L\rangle$ is a state vector labeled by L integers k_j ($s = -1/2$ spin components) and $h(k) = \sum_{j=1}^k \frac{1}{j}$ are harmonic numbers.

The total momentum $P(u)$

$$e^{iP(u_j)} = \frac{u_j - i/2}{u_j + i/2} \quad (2.5)$$

satisfies the (quasi-)periodicity condition following directly from (2.2)

$$P_{tot} = \sum_{j=1}^K P(u_j) = 2\pi k/L, \quad k \in \mathbf{Z}. \quad (2.6)$$

In application to the anomalous dimensions of operators³ in $\mathcal{N} = 4$ SYM theory one selects only purely periodic Bethe states

$$P_{tot} = 2\pi m, \quad m \in \mathbf{Z}. \quad (2.7)$$

We can also study other physically interesting quantities of this model, such as the local conserved charges \hat{Q}_r . They are defined as follows

$$\hat{T}(v) = \exp \left(i \sum_{r=1}^{\infty} \hat{Q}_r v^{r-1} \right), \quad (2.8)$$

where the quantum transfer matrix $\hat{T}(v) \equiv \hat{T}(v; 0, 0, \dots, 0)$ is a particular case of the inhomogeneous transfer matrix

$$\hat{T}(v; v_1, \dots, v_L) = \text{Tr}_0 [\hat{R}_{0,1}(v - v_1) \cdots \hat{R}_{0,L}(v - v_L)] \quad (2.9)$$

³ The operators of the type $\text{Tr} (\nabla^{k_1} Z \cdots \nabla^{k_L} Z)$ in SYM, where $\nabla = \partial + A$ is a covariant derivative in a null direction and Z is a complex scalar, represent the state vectors $|k_1, \dots, k_l, k_{l+1}, \dots, k_L\rangle$ and the dilatation hamiltonian is given at one loop by the $\text{XXX}_{-1/2}$ hamiltonian.

and $\hat{R}_{0,j}$ is the universal $\mathfrak{sl}(2)$ R-matrix defined as [64]

$$\hat{R}_{0,1}(v) = \sum_{j=0}^{\infty} R_j(v) \mathcal{P}_{0,1}^{(j)}, \quad R_j(v) = \prod_{k=1}^j \frac{v - ik}{v + ik} \quad (2.10)$$

with $\mathcal{P}_{0,1}^{(j)}$ being the operator projecting the direct product of two neighboring spins $s_0 = s_1 = -1/2$ to the representation j . Recall that

$$[\hat{T}(v; v_1, \dots, v_L), \hat{T}(v'; v_1, \dots, v_L)] = 0 \quad (2.11)$$

for any pair v, v' , due to Yang-Baxter equations on the \hat{R} -matrix.

The direct calculation shows that $\hat{P}_{tot} = -\hat{Q}_1$ is the operator of the momentum and $\hat{H}_{-1/2} = \hat{Q}_2$ is the hamiltonian (2.3), etc. Those charges are local, in the sense that the charge density of \mathcal{Q}_k contains $\leq k$ consecutive spins.

Due to the integrability manifestly expressed by (2.11) all these charges commute and their eigenvalues on a Bethe state characterized by a set of Bethe roots satisfying (2.2) (enforcing the periodicity of the chain or the quasi-periodicity of the Bethe state) are given by [7]

$$\mathcal{Q}_r = \sum_{j=1}^K \frac{i}{r-1} \left(\frac{1}{(u_j + i/2)^{r-1}} - \frac{1}{(u_j - i/2)^{r-1}} \right). \quad (2.12)$$

We will later estimate the behavior of \mathcal{Q}_r at $r \rightarrow \infty$ and high orders of $1/L$ expansion.

2.1.2 $1/L$ expansion of BAE

Let us start from reviewing one of the method of solving (2.2) in the thermodynamical limit $L \rightarrow \infty$, $u_k \sim L \sim K$, before sticking with the most efficient one using the Baxter equation.

As we mentioned the (2.2) has only real solutions, i.e. all the roots lie on the real axis. We label the roots so that $u_{j+1} > u_j$. Suppose there exists a smooth function $X(x)$ parameterizing the Bethe roots

$$u_k = LX(k/L), \quad \varrho(X(x)) \equiv \frac{1}{X'(x)} \simeq \frac{1}{u_{k+1} - u_k}. \quad (2.13)$$

For large K the function $\varrho(x)$ has a meaning of density of Bethe roots. As follows from definition (2.13) its normalization is

$$\int dx \varrho(x) = \alpha \quad (2.14)$$

with $\alpha = K/L$. In the thermodynamical limit we can rewrite (1.49) assuming k to be far from the edges, as follows

$$\begin{aligned} \sum_j' i \log \left(\frac{u_j - u_k + i}{u_j - u_k - i} \right) &= -2 \sum_j' \frac{1}{u_j - u_k} + \frac{2}{3} \sum_j' \frac{1}{(u_j - u_k)^3} \\ &- \frac{2}{5} \sum_j' \frac{1}{(u_j - u_k)^5} + \frac{2}{7} \sum_j' \frac{1}{(u_j - u_k)^7} + \frac{\pi \varrho' [\coth(\pi \varrho)]_6}{L} \\ &- \frac{1}{12L^3} \left((\pi \varrho')^3 \left[\frac{\coth(\pi \varrho)}{\sinh^2(\pi \varrho)} \right]_2 - 2\pi^2 \varrho' \varrho'' \left[\frac{1}{\sinh(\pi \varrho)} \right]_3 + \pi \varrho^{(3)} [\coth(\pi \varrho)]_4 \right) + \mathcal{O} \left(\frac{1}{L^5} \right), \end{aligned} \quad (2.15)$$

where we introduce the notation defined by $[f(\varrho)]_n \equiv f(\varrho) - \sum_{i=0}^{n-1} f^{(i)}(0) \frac{\varrho^i}{i!}$ for the functions regular at zero. For singular functions the Taylor series should be substituted by the Laurent series so that $[f(\varrho)]_n$ is zero for $\varrho = 0$ and has first $n - 1$ zero derivatives at this point. The terms in the first line represent the naive expansion of the l.h.s. in $1/(u_j - u_k)$. It works well for the terms in the sum with $u_j \gg u_k$. The terms in the second line describe the anomalous contribution at $u_j \sim u_k$, for close roots with $i \sim j$. In this case we can expand

$$u_j - u_k = \frac{j - k}{\varrho(u_j/L)} + \mathcal{O}(1/L) \quad (2.16)$$

and calculate the corresponding converging sum giving the terms in the second line. This anomaly was noticed in the Bethe ansatz context in [15] although this phenomenon was known since long in the large N matrix integrals or similar character expansions [65, 66].

In our case when $L \rightarrow \infty$ it is obvious from (2.15, 1.49) that the anomaly does not contribute to the main order and the Bethe ansatz equation becomes a singular integral equation (see sec. 1.2.2)

$$2\pi n_k - \frac{1}{x} = 2 \int_{\mathcal{C}_{\text{tot}}} \frac{dy \varrho_0(y)}{x - y}, \quad x \in \mathcal{C}_k, \quad k = 1, \dots, K. \quad (2.17)$$

2.1.3 Large L limit and $1/L$ -corrections from Baxter equation

Eq. (2.2) can be also obtained as the condition that the transfer matrix eigenvalue $T(u)$ is a polynomial of degree L (see for example [67])

$$T(u) = W(u + i/2) \frac{Q(u + i)}{Q(u)} + W(u - i/2) \frac{Q(u - i)}{Q(u)}, \quad (2.18)$$

where $Q(u) = \prod_{k=1}^K (u - u_k)$, $W(u) = u^L$. That is clear from the very construction of a Bethe state in the algebraic Bethe ansatz approach [57]. The Bethe equations (2.2) is simply a condition that $T(u)$ has no poles.

Introducing notations: $x = u/L$, $\Phi(x) = \frac{1}{L} \sum_{k=1}^K \log(x - x_k)$, $V(x) = \log x$, $2t(x) = T(Lx)/(Lx)^L$ we rewrite (2.18) as

$$2t(x) = \exp L \left[\Phi \left(x + \frac{i}{L} \right) - \Phi(x) + V \left(x + \frac{i}{2L} \right) - V(x) \right] + \text{c.c.} \quad (2.19)$$

In this notations the quasi-momentum (1.54) takes the form (exactly in $1/L$)

$$p(x) \equiv \Phi' + V'/2 \quad (2.20)$$

and expanding the Baxter equation in $1/L$ we get

$$\begin{aligned} t(x) &= \cos p(x) \left[1 - \frac{1}{L} \left(\frac{p'(x)}{2} - \frac{V''(x)}{8} \right) + \frac{1}{2L^2} \left(\frac{p'(x)}{2} - \frac{V''(x)}{8} \right)^2 \right] \\ &+ \frac{1}{L^2} \sin p(x) \left(\frac{p''(x)}{6} - \frac{V^{(3)}(x)}{16} \right) + O\left(\frac{1}{L^3}\right). \end{aligned} \quad (2.21)$$

According to our definition $p(x)$ is a function of L . We will expand $p(x) = p_0(x) + \frac{1}{L}p_1(x) + \frac{1}{L^2}p_2(x) + \mathcal{O}(1/L^3)$, $t(x) = t_0(x) + \frac{1}{L}t_1(x) + \frac{1}{L^2}t_2(x) + \mathcal{O}(1/L^3)$ and plug it into the last equation. Since $t(x)$ has no singularities, except $x = 0$ it is natural to assume that the coefficients of expansion $t_0(x), t_1(x), t_2(x), \dots$ are the entire functions on the plane x with no cuts, having only a singularity at $x = 0$.

The quasi-periodicity property of the total momentum (2.6) reads up to 3 first orders as follows

$$P_{tot} = - \sum_j \frac{1}{u_j} + \sum_j \frac{1}{12u_j^3} + \mathcal{O}\left(\frac{1}{L^4}\right) = 2\pi k/L \quad (2.22)$$

and in the purely periodic case we select only the states with $k = mL$, with integer m .

Algebraical curve from Baxter equation

Let us restore from the Baxter equation the zero order result of the previous section. In the zero order approximation we get from (2.21)

$$\cos p_0(x) = t_0(x) \quad (2.23)$$

or

$$p'_0(x) = \frac{2t'_0(x)}{\sqrt{1 - t_0^2}}. \quad (2.24)$$

since $t_0(x)$ is an entire functions all the branch cuts of p_0 come from the square root in denominator, after the Bethe roots condense to a set $\mathcal{C}_1, \dots, \mathcal{C}_K$ of dense supports in the $L \rightarrow \infty$ limit. In this way we reproduced the thermodynamical limit.

1/L correction from Baxter equation

To find the $1/L$ correction to the leading approximation to the density of roots we deduce from (2.21)

$$p_1 = (-p'_0/2 + V''/8) \cot p_0 - \frac{t_1}{\sin p_0}, \quad (2.25)$$

From (2.24) and (1.55) we know about $p_0(x)$ that

$$p_0^+ = \pi n_j - \pi i \rho_0, \quad p_0^- = \pi n_j + \pi i \rho_0 \quad (2.26)$$

so that

$$\sin p_0^+ = -\sin p_0^- \quad (2.27)$$

and thus we have for the real and imaginary parts of $p_0(x)$ on the cuts

$$\pi i \rho_1 = \left(\frac{V''}{8} t_0 - t_1 \right) \frac{1}{\sin p_0^-}, \quad (2.28)$$

$$p_1 = -p'_0 \cot p_0/2. \quad (2.29)$$

We will solve these equations below and restore the explicit form p_1 .

Moreover we see from (2.22) that

$$p_1(0) = 0 \quad (2.30)$$

and $p_1(x)$ should decreases as $\mathcal{O}(1/x^2)$ for large x .

We can build a general solution of Riemann-Hilbert problem (2.29)

$$p_1(x) = \frac{x}{4\pi i f(x)} \oint_C \frac{f(y) p'_0(y) \cot p_0(y)}{y(y-x)} dy + \sum_{j=1}^{K-2} \frac{a_j x^j}{f(x)}, \quad (2.31)$$

where $f^2(x) = \prod_{j=1}^{2K} (x - x_j)$ and the contour encircles all cuts \mathcal{C}_k (but no other singularities). The first term in the r.h.s. represents the Cauchy integral restoring the function from its real part on the cuts and having a zero at the origin (the value of the quasi-momentum $p(x)$ at $x = 0, \infty$ was already fixed for p_0) whereas the second one is purely imaginary on the cuts, with the polynomial in the numerator chosen in such a way that it does not spoil the behavior of $p(x)$ at $x = 0, \infty$.⁴

Thus for $K < 3$ the solution is unique. In particular, for $K = 1$ we restore from here the 1-cut solution of [49]. For $K \geq 3$ we have to fix $K - 2$ parameters a_j . To do this we have to

⁴ We could also add terms $\frac{1}{f^3}, \frac{1}{f^5}, \dots$ but they are too singular at the branch points as we shell see in the next section.

use K additional conditions ensuring the right fractions α_j of the roots already chosen for p_0 :

$$\oint_{C_l} p_1(x) dx = 0, \quad l = 1, \dots, K, \quad (2.32)$$

in fact only $K - 2$ of them are linear independent (since we have already fixed the total filling fraction by the asymptotic properties of (2.31) at $x = \infty$: $p_1(x) = \mathcal{O}(1/x^2)$. Eq.(2.30) also restricts some linear combination of the conditions (2.32)). Hence we completely fixed all parameters of our K -cut solution for the $1/L$ correction p_1 knowing the zero order solution (algebraic curve) for p_0 .

$1/L^2$ corrections from Baxter relation

Expanding (2.21) up to $1/L^2$ we obtain

$$p_2 = -\frac{1}{2} \partial_x [\cot(p_0) I] - \frac{1}{8x^3} - \frac{\tilde{t}_2}{2 \sin(p_0)}, \quad (2.33)$$

where

$$I = -\frac{\tilde{t}_1}{\sin(p_0)} = p_1 + \frac{p'_0}{2} \cot p_0. \quad (2.34)$$

We introduced here the notations

$$\begin{aligned} \tilde{t}_1 &= t_1 + \frac{\cos p_0}{8x^2}, \\ \tilde{t}_2 &= t_2 - \frac{\cos p_0}{128x^4} + \frac{\tilde{t}_1}{8x^2} - \frac{\cos(2p_0) + 5}{24 \sin p_0} p''_0 + \frac{\cos p_0}{8 \sin^2 p_0} \left(3(p'_0)^2 + 4\tilde{t}_1^2 \right) \end{aligned} \quad (2.35)$$

so that \tilde{t}_1 and \tilde{t}_2 are single valued functions on the complex plane.

Note that above the cut $I^+ = \pi i \rho_1$. We will find the explicit solution of these equations later, but we will need for that some results of the next section where we study the behavior of $p(x)$ near the branch points.

2.1.4 Double scaling solution near the branch point

As we stated above the branch point singularities come only from the square roots of the denominator of (2.24). We define an exact branch point as a point x_* where $t(x_*) = \pm 1$. If we approach one of the branch points $x \rightarrow x_*$ we can expand

$$t(x) \simeq \pm [1 - a(x - x_*)/2 - b(x - x_*)^2/2]. \quad (2.36)$$

Note that x_*, a, b themselves depend on L . We assume that they have a regular expansion in $1/L$ and define $x_* = x_0 + x_1/L + \dots$. We call x_0 a classical branch point and x_1/L a branch point displacement.

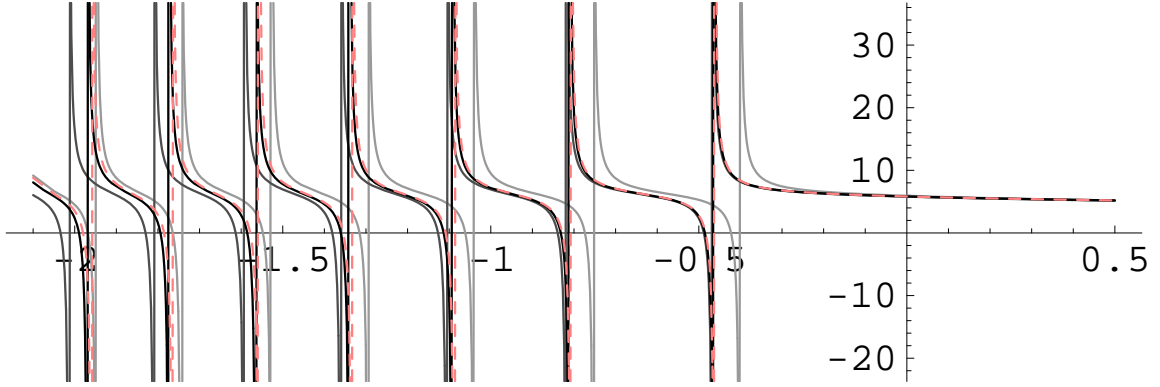


Fig. 2.1: Quasi-momentum near branch point as a function of the scaling variable v for $K = 200$. The poles corresponds to the positions of Bethe roots u_i . Red dashed line - "exact" numerical value, light grey - zero order approximation given by Airy function $\text{Ai}(a^{1/3}x)$, grey - first order and black - second order approximation.

Denoting $v = (x - x_*)L^{2/3}$ which will be our double scaling variable $v \sim 1$, we get from (2.18) up to $1/L^2$ terms

$$\pm 2 \left(1 - \frac{av}{2L^{2/3}} - \frac{bv^2}{2L^{4/3}} \right) Q(u) = Q(u+i) \frac{W(u+i/2)}{W(u)} + Q(u-i) \frac{W(u-i/2)}{W(u)}. \quad (2.37)$$

In terms of a new function

$$q(v) = e^{-n\pi v L^{1/3}} e^{\frac{v L^{1/3}}{2x_*}} Q(x_* L + v L^{1/3}), \quad (2.38)$$

where n is such that $t(x^*) = e^{i\pi n}$, and after expansion in $1/L$ the last eq. takes the form

$$q'' - avq = \frac{1}{L^{1/3}} \frac{4vq' + q}{4x_*^2} + \frac{1}{L^{2/3}} \left[\frac{1}{12} q^{(4)}(v) - \frac{v^2 q(v)}{4} \left(\frac{1}{x_*^4} - 4b \right) \right] + \mathcal{O}\left(\frac{1}{L}\right). \quad (2.39)$$

In fact, this equation can be easily solved in terms of q_0

$$q \propto \left[1 + \frac{v^2}{4x_*^2 L^{1/3}} + \frac{1}{L^{2/3}} \left(\frac{v^4}{32x_*^4} - \frac{3b - a^2}{15a} v \right) \right] q_0 \left(v - \frac{1}{4ax_*^2 L^{1/3}} + \frac{a^2 + 12b}{60a L^{2/3}} v^2 \right), \quad (2.40)$$

where $q_0(v) = \text{Ai}(a^{1/3}v)$ (the Airy function). The second solution of the (2.39), $\text{Bi}(a^{1/3}v)$ has a wrong asymptotic as we will see. The sign \propto means that the solution is defined up to a constant multiplier but this unknown multiplier doesn't affect the quasi-momentum. Now we can express the quasi-momentum only through our scaling function $q(v)$

$$p \left(x_* + \frac{v}{L^{2/3}} \right) = \frac{\partial_v q(v, L)}{q(v, L) L^{1/3}} + \pi n + \frac{1}{2x_*} \left(\frac{1}{1 + \frac{v}{x_* L^{2/3}}} - 1 \right). \quad (2.41)$$

The first two terms in the r.h.s., if we substitute $q(v) \rightarrow q_0(v)$, represent the principal contribution to the double scaling limit near the edge, valid up to the corrections of the

order $1/L^{2/3}$. We see from the definition (2.38) that the zeros of $q(v)$ are nothing but the positions u_i of Bethe roots. Thus we know these positions with a precision $1/L^{2/3}$ (see fig.3).

The large v asymptotic will be very helpful in fixing some unknown constant in the $1/L^2$ corrections given in the next section

$$p(x_* + vL^{-2/3}) = \pi n + \frac{1}{L^{1/3}} \left(\underbrace{-\sqrt{av}}_1 - \underbrace{\frac{1}{4v}}_{1/L} + \underbrace{\frac{5}{32v^2\sqrt{av}}}_{1/L^2} + \dots \right) \quad (2.42)$$

$$+ \frac{1}{L^{2/3}} \left(\underbrace{\frac{1}{8x_*^2\sqrt{av}}}_{1/L} - \underbrace{\frac{1}{16ax_*^2v^2}}_{1/L^2} + \dots \right) + \dots,$$

where the cut corresponds to negative v for $a > 0$. Introducing the notation $y = vL^{-2/3}$ and rearranging the terms by the powers $1/L$ we have

$$p(x_* + y) = \pi n + \left[-\sqrt{ay} - \frac{(a^2 + 12b)y^{3/2}}{24\sqrt{a}} + \dots \right]$$

$$+ \frac{1}{L} \left[-\frac{1}{4y} + \frac{1}{8x_*^2\sqrt{ay}} + \frac{a^2 - 4b}{16a} + \dots \right] \quad (2.43)$$

$$+ \frac{1}{L^2} \left[\frac{5}{32y^2\sqrt{ay}} - \frac{1}{16ay^2x_*^2} + \frac{6 - x_*^4(a^2 + 12b)}{768x_*^4(ay)^{3/2}} + \dots \right] + \dots$$

Doing this re-expansion we assume that $L^{-1} \ll y \ll 1$, trying to sew together the double scaling region with the $1/L$ corrections to the thermodynamical limit. This procedure is similar to the one used in higher orders of the WKB approximation in the usual one dimensional quantum mechanics (see for example [68]).

To compare with p_0 , p_1 and p_2 we have to re-expand around x_0

$$p(x_0 + y) = p(x_* + y) + \frac{x_1}{L} \frac{\sqrt{a}}{2\sqrt{y}} + \frac{1}{L^2} \left[-\frac{x_1}{4y^2} + \frac{x_1}{16x_0^2y\sqrt{ay}} + \frac{\sqrt{a}x_1^2}{8y\sqrt{y}} \right] \quad (2.44)$$

or, introducing notation

$$x_1 = \frac{2A}{\sqrt{a}} - \frac{1}{4x_0^2a} \quad (2.45)$$

we get

$$p(x_0 + y) = \pi n + \left[-\sqrt{ay} - \frac{(a^2 + 12b)y^2}{24\sqrt{ay}} + \dots \right] \quad (2.46)$$

$$\begin{aligned}
& + \frac{1}{L} \left[-\frac{1}{4y} + \frac{A}{\sqrt{y}} + \frac{a^2 - 4b}{16a} + \dots \right] \\
& + \frac{1}{L^2} \left[\frac{5}{32y^2\sqrt{ay}} - \frac{A}{2\sqrt{ay}^2} + \left(\frac{A^2}{2y\sqrt{ay}} - \frac{b}{64(ay)^{3/2}} - \frac{\sqrt{ay}}{768y^2} \right) + \dots \right] + \dots
\end{aligned}$$

Near the left branch point (i.e for $a < 0$ and $y < 0$) we have

$$\begin{aligned}
p(x_0 + y) &= \pi n + \left[\sqrt{ay} + \frac{(a^2 + 12b)y^2}{24\sqrt{ay}} + \dots \right] \\
& + \frac{1}{L} \left[-\frac{1}{4y} - \frac{A}{\sqrt{-y}} + \frac{a^2 - 4b}{16a} + \dots \right] \\
& + \frac{1}{L^2} \left[-\frac{5}{32y^2\sqrt{ay}} + \frac{A}{2\sqrt{-ay}^2} + \left(\frac{A^2}{2y\sqrt{ay}} + \frac{b}{64(ay)^{3/2}} + \frac{\sqrt{ay}}{768y^2} \right) + \dots \right] + \dots
\end{aligned} \tag{2.47}$$

Now we can compare it with our results of the previous sections and fix a, b and x_1 .

Let us note that similar Airy type oscillations were observed in the papers on random matrices where this behavior occurs near an endpoint of a distribution of eigenvalues [69].

Comparison with $1/L$ expansion

It is instructive to establish the relations between a, b, A and the parameters of the algebraic curve.

For that we use the expansion (2.36) defining a, b and find from (2.23) for $y > 0$

$$p_0(x_0 + y) = \pi n + \arccos t_0 \simeq \pi n - \sqrt{ay} - \frac{a^2 + 12b}{24\sqrt{a}} y^{3/2} + \mathcal{O}(y^{5/2}), \tag{2.48}$$

in agreement with (2.46, 2.47). We can fix a and b up to $\mathcal{O}(1/L)$ corrections from here through the parameters of the solution for p_0 .

To calculate a and b up to $\mathcal{O}(1/L)$ and to fix A , we use the expansion (2.36) with (2.25). Note that we have the minus sign in front of \sqrt{ay} which ensures the positivity of the density on the cut (i.e. for $y < 0$ and $a > 0$) $\rho(y) \simeq \sqrt{a(-y)}/\pi$. If we had Bi instead of Ai the sign would be plus and the density would be negative.

Now we compare this near-cut behavior to p_1 . Consider the regular part first

$$\not{p}_1 = -\frac{1}{2} p'_0 \cot p_0 \simeq -\frac{1}{4y} + \frac{a^2 - 4b}{16a} + \mathcal{O}(y), \tag{2.49}$$

which agrees with (2.43). From (2.31) we see that

$$p_1(x_0 + y) - \not{p}_1(x_0 + y) \simeq \frac{A}{\sqrt{y}} + \mathcal{O}\left(\frac{1}{y^{3/2}}\right), \tag{2.50}$$

where A can be written explicitly, again using p_0 .

For the example of one-cut solution see (2.73).

2.1.5 General solution for p_2 and E_2

Now we have enough of information to construct p_2 in the most general situation of an arbitrary number of cuts.

We start from a formula which immediately follows from (2.33)

$$p_2 = -\frac{1}{2}\partial_x \left[\cot(p_0) \left(p_1 + \frac{p'_0}{2} \cot p_0 \right) \right] - \frac{1}{8x^3}, \quad (2.51)$$

where p_1 is given by (2.31). The behaviors near zero and at infinity are the following. Since from (2.6) and (2.22) it follows that $G(0) - \frac{1}{24L^2}G''(0) = 2\pi k/L + \mathcal{O}(\frac{1}{L^4})$ we can conclude that

$$p_2(0) = \frac{1}{24}G''_0(0). \quad (2.52)$$

For large x we have again

$$p_2(x) = \mathcal{O}\left(1/x^2\right). \quad (2.53)$$

Repeating the arguments of the previous subsection we have

$$p_2(x) = \frac{x}{4\pi i f(x)} \oint_{\mathcal{C}} \frac{f(y)}{y(y-x)} \left(\frac{1}{4y^3} + \partial_y [\cot(p_0)p_1] \right) + \sum_{j=0}^{5K-1} \frac{c_j x^j}{f^5(x)}, \quad (2.54)$$

where the path \mathcal{C} is defined as in (2.31). Again the first term guarantees that p_2 satisfies (2.51). We drop out the $p'_0 \coth p_0$ for simplicity. We can do this since together with $f(y)$ it forms a single-valued function without cuts and the integral is given by the poles inside of the path of integration. In fact there are only poles at each branch point so that the result can be absorbed into the second term in (2.54).

So far the second term in (2.54) was restricted only by the conditions (2.52) and (2.53). Of course this does not explain why we should restrict ourselves by the fifth power of $f(x)$ in denominator. A natural explanation comes from the known behavior near the branch points (2.46, 2.47) from where we can see that

$$p_2(x_0^i + y) = \begin{cases} \frac{5}{32y^2\sqrt{a_i y}} - \frac{A_i}{2\sqrt{a_i y^2}} + \left(\frac{A_i^2}{2y\sqrt{a_i y}} - \frac{b_i}{64(a_i y)^{3/2}} - \frac{\sqrt{a_i y}}{768y^2} \right) + \mathcal{O}\left(\frac{1}{y}\right), & a_i, y > 0 \\ -\frac{5}{32y^2\sqrt{a_i y}} + \frac{A_i}{2\sqrt{-a_i y^2}} + \left(\frac{A_i^2}{2y\sqrt{a_i y}} + \frac{b_i}{64(a_i y)^{3/2}} + \frac{\sqrt{a_i y}}{768y^2} \right) + \mathcal{O}\left(\frac{1}{y}\right), & a_i, y < 0 \end{cases}, \quad (2.55)$$

where all $6K$ constants a_i, b, A_i for $i = 1, \dots, 2K$ are known since they can be determined from the near branch point behavior of p_0 and p_1 (2.46, 2.47). a_i and b_i follow from p_0

$$p_0(x_0^i + y) = \begin{cases} -\sqrt{a_i y} - \frac{(a_i^2 + 12b_i)y^2}{24\sqrt{a_i y}} + \mathcal{O}(y^{5/2}), & a_i > 0, y > 0 \\ \sqrt{a_i y} + \frac{(a_i^2 + 12b_i)y^2}{24\sqrt{a_i y}} + \mathcal{O}(y^{5/2}), & a_i < 0, y < 0 \end{cases} \quad (2.56)$$

and A_i comes from p_1

$$p_1(x_0^i + y) = \begin{cases} -\frac{1}{4y} + \frac{A_i}{\sqrt{y}} + \mathcal{O}(y^0), & a_i > 0, y > 0 \\ -\frac{1}{4y} - \frac{A_i}{\sqrt{-y}} + \mathcal{O}(y^0), & a_i < 0, y < 0 \end{cases}. \quad (2.57)$$

In fact (2.55) gives only two nontrivial conditions for each branch point which are the coefficient before the half-integer power of y so that we have $4K$ conditions. The extra K conditions come from zero A -period constraints signifying the absence of corrections to the filling fractions α_i .

$$\oint_{C_l} p_2(x) dx = 0, \quad l = 1, \dots, K. \quad (2.58)$$

To reduce the number of unknown constants consider a branch point x_0 . We can see that for small $y = x - x_0$ (we assume that the cut is on the left i.e. $a_i > 0$)

$$\begin{aligned} I_1 &\equiv \frac{x}{4\pi i f(x)} \oint_C \frac{f(z)}{z(z-x)} \left(\frac{1}{4z^3} + \partial_z(p_1 \cot p_0) \right) \\ &= \frac{3}{16y^2 \sqrt{ay}} - \frac{A}{2\sqrt{ay}^2} + \frac{1}{y^{3/2}} \left(\frac{b}{32a^{3/2}} - \frac{5\sqrt{a}}{128} \right) + \mathcal{O}\left(\frac{1}{y}\right). \end{aligned} \quad (2.59)$$

Introducing the following integral

$$\begin{aligned} I_2 &\equiv \frac{x}{4\pi i f(x)} \oint_C \frac{f(z)}{z(z-x)} \left((p_1 + p'_0 \cot p_0) p_1 \cot p_0 - \frac{p_0''}{12} \right) \\ &= -\frac{1}{32y^2 \sqrt{ay}} + \frac{1}{y^{3/2}} \left(\frac{A^2}{2\sqrt{a}} - \frac{3b}{64a^{3/2}} + \frac{29\sqrt{a}}{768} \right) + \mathcal{O}\left(\frac{1}{y}\right), \end{aligned} \quad (2.60)$$

we see that $I_1 + I_2$ reproduces the right series expansion near the branch points given by (2.43) and (2.43). Moreover, on the cuts $I_2(x + i0) + I_2(x - i0) = 0$ since the function under integral is single valued. We can simply take

$$p_2(x) = I_1(x) + I_2(x) + \sum_{j=0}^{K-1} \frac{\tilde{c}_j x^j}{f(x)}, \quad (2.61)$$

where the remaining K constants are fixed from (2.58). Using that $p_2(0) = G''(0)/24$ we can fix one constant $\tilde{c}_0 = \frac{G''(0)f(0)}{24}$ before imposing the condition (2.58).

This is our final result for the second quantum correction to the quasi-momentum. In the section 2.1.7 we will specify this result for the example of the one-cut solution where it can be made much more explicit.

2.1.6 Energy

To find $1/L$ corrections to the energy we represent the exact formula (2.1) as follows

$$E = -\frac{1}{L} G'(0) + \frac{1}{24L^3} G^{(3)}(0) + \mathcal{O}\left(\frac{1}{L^5}\right), \quad (2.62)$$

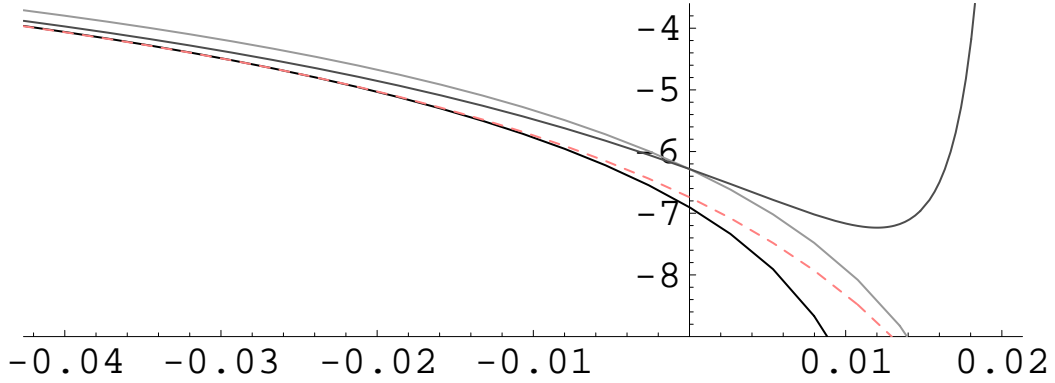


Fig. 2.2: Resolvent far from branch point as a function of x . Red dashed line - "exact" numerical value for one cut solution with $K = 10$, $n = 2$, $m = 1$, light grey - zero order approximation, grey - first order given by (2.31) and black - second order approximation given by (2.61). Note that near branch point ($x_0 = 0.02$) the approximation explodes and instead of it we should use the Airy function of (2.41), like in the usual WKB near a turning point.

We still have to expand $G(x) = -\frac{1}{2x} + p_0(x) + \frac{1}{L}p_1(x) + \frac{1}{L^2}p_2(x) + \mathcal{O}(1/L^3)$.

Finally, we obtain for the energy:

$$E = \frac{1}{L}E_0(x) + \frac{1}{L^2}E_1 + \frac{1}{L^3}E_2 + \mathcal{O}\left(\frac{1}{L^4}\right), \quad (2.63)$$

where

$$E_0 = -G'_0(0), \quad (2.64)$$

$$E_1 = -p'_1(0) = -\frac{Q'(0)}{4\pi i f(0)} \oint_C \frac{f(y)p'(y) \cot p(y)}{Q(y)y} dy, \quad (2.65)$$

and $Q(x) = \sum_{k=1}^{K-2} b_k x^k$ is related to the last term in (2.31). For E_2 we have from (2.61) the following representation

$$E_2 = \frac{G_0^{(3)}(0)}{24} - p'_2(0) = -\frac{c_1}{f(0)} + \frac{G_0''(0)f'(0)}{24f(0)} + \frac{G_0^{(3)}(0)}{24} - \frac{1}{4\pi i f(0)} \oint \frac{f(y)}{y^2} \left(\frac{1}{4z^3} + \partial_z(p_1 \cot p_0) - \frac{p_0''}{12} + (p_1 + p_0' \cot p_0)p_1 \cot p_0 \right). \quad (2.66)$$

Note that for 1-cut we should take $c_1 = 0$. We can compare our results with numerical calculations, as it is done for a few 1-cut solutions in the fig.2.3

2.1.7 One cut case

In this section we express corrections to the energy in terms of infinite sums for the simplest case of one-cut solution. For this solution the hyperelliptic curve is a sphere. It is

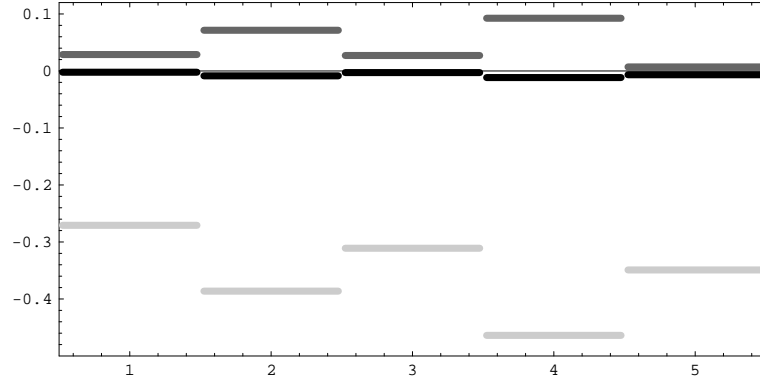


Fig. 2.3: Relative deviation $\delta E(K)/E(K)$ of analytical computations of the energy $E(K)$ from its "exact" value $E_{\text{exact}}(K)$ for the one cut distribution found numerically by Mathematica (solid line corresponds to $\delta E(K) = 0$), for a finite number of roots K and a finite length L for zero order (light gray), first order (gray) and second order (black) approximation. Details are summarized in the table

#	1	2	3	4	5
m, n	1, 2	2, 1	1, 3	2, 2	1, 5
E_0	$12\pi^2$	$24\pi^2$	$16\pi^2$	$32\pi^2$	$24\pi^2$
E_1	-558.4	-1563	-855.3	-2401	-1563
E_2	1160.	5464.	1592.	8982.	1504.
K	10	40	7	20	5
L	20	20	21	20	25
$E_{\text{numerical}}$	4.66004	8.54515	5.7359	10.7876	7.0232
$E_0 + \frac{E_1}{L} + \frac{E_2}{L^2}$	4.670	8.619	5.752	10.912	7.070

two complex planes connected by a single cut. The density of the Bethe roots is given by a simple formula [19]

$$\rho(x) = \frac{\sqrt{8\pi mx - (2\pi nx - 1)^2}}{2\pi x}. \quad (2.67)$$

We can easily find explicit expressions for a_i and b_i of (2.55). With the notation $M = \sqrt{m(m+n)}$ a_i and b_i become

$$a_1 = -\frac{8Mn^4\pi^3}{(\sqrt{4M^2 + n^2} - 2M)^2}, \quad (2.68)$$

$$b_1 = \frac{4\pi^4 n^6}{3(\sqrt{4M^2 + n^2} - 2M)^4} \left(12M\sqrt{4M^2 + n^2} + 3n^2 - 4n^2\pi^2 M^2 - 24M^2 \right)$$

and

$$a_2 = \frac{8Mn^4\pi^3}{(\sqrt{4M^2 + n^2} + 2M)^2}, \quad (2.69)$$

$$b_2 = -\frac{4\pi^4 n^6}{3(\sqrt{4M^2 + n^2} + 2M)^4} \left(12M\sqrt{4M^2 + n^2} - 3n^2 + 4n^2\pi^2 M^2 + 24M^2 \right).$$

It may be more convenient for comparison with string theory results [47] to express A defined by (2.46) as an infinite sum. We have to evaluate the integral in (2.31) and find A from the behavior near a branch point. We compute the integral by poles. To that end we use that the solutions to the equation $\sin(p_0(x_l^\pm)) = 0$ are

$$x_l^\pm = \frac{1}{2\pi} \frac{1}{\sqrt{4M^2 + n^2} \mp \sqrt{4M^2 + l^2}}, \quad l \geq 0. \quad (2.70)$$

The points $x_{l=0}^\pm$ are the branch points. They are inside the contour of integration and thus do not contribute.

Using that $f(x_l^\pm)/x_l^\pm = \pm \frac{l}{n}$ and

$$\begin{aligned} \frac{1}{x_l^+ - x_{0,1}} - \frac{1}{x_l^- - x_{0,1}} &= -\frac{\sqrt{l^2 + 4M^2}}{l^2} \frac{1}{\pi x_{0,1}^2} \\ \frac{1}{x_l^+ - x_{0,2}} - \frac{1}{x_l^- - x_{0,2}} &= -\frac{\sqrt{l^2 + 4M^2}}{l^2} \frac{1}{\pi x_{0,2}^2}. \end{aligned} \quad (2.71)$$

We can evaluate the integral (2.31) for $x \rightarrow x_0$ (we also take x inside the contour to drop irrelevant symmetric part of p_1)

$$\frac{1}{2\pi i} \oint_C \frac{f(y)p'(y) \cot p(y)}{y(y-x)} dy \rightarrow -\frac{1}{i\pi n x_0^2} \left[\sum_{l=1}^{\infty} \left(\frac{\sqrt{l^2 + 4M^2}}{l} - 1 \right) - \frac{1}{2} \right] \quad (2.72)$$

we can conclude that

$$\begin{aligned} A_2 &= -\frac{1}{2x_2^2 \sqrt{a_2}} \left[\sum_{l=1}^{\infty} \left(\frac{\sqrt{l^2 + 4M^2}}{l} - 1 \right) - \frac{1}{2} \right] \\ A_1 &= -\frac{1}{2x_1^2 \sqrt{-a_1}} \left[\sum_{l=1}^{\infty} \left(\frac{\sqrt{l^2 + 4M^2}}{l} - 1 \right) - \frac{1}{2} \right], \end{aligned} \quad (2.73)$$

We reproduce the result of [49] for E_1 in terms of a sum from (2.65)

$$E_1 = -p'_1(0) = 4\pi^2 \sum_{l=1}^{\infty} l \sqrt{l^2 + 4M^2} \quad (2.74)$$

with ζ -function regularization assumed.

We can also express our result for the next correction to the energy E_2 given by (2.66) as a double sum. We will need the following quantity

$$p_1(x_k^\pm) = \frac{\pm 1}{2\pi(x_k^\pm)^2 k} \left[\sum_{l=1}^{\infty} \left(\frac{l\sqrt{l^2 + 4M^2} - k\sqrt{k^2 + 4M^2}}{l^2 - k^2} - 1 \right) + \frac{\sqrt{k^2 + 4M^2}}{2k} - \frac{1}{2} \right]. \quad (2.75)$$

Evaluating the integrals in (2.66) we express E_2 as a double sum

$$E_2 = -(\mathcal{I}_1 + \mathcal{I}_2 + \mathcal{I}_3 + \mathcal{I}_4), \quad (2.76)$$

where

$$\begin{aligned} \mathcal{I}_1 &\equiv \frac{1}{4\pi i f(0)} \oint \frac{f(z)}{z^2} \partial_z (p_1 \cot p_0) = -2p'_1(0) \\ &\quad + \sum_{k=1}^{\infty} \left[2\pi \sum_{\pm} \left(\sqrt{4M^2 + n^2} \pm 2 \frac{k^2 + 2M^2}{\sqrt{k^2 + 4M^2}} \right) p_1(x_k^{\pm}) - 4p'_1(0) \right] \\ \mathcal{I}_2 &\equiv \frac{1}{4\pi i f(0)} \oint \frac{f(z)}{4z^5} = 4\pi^4 M^2 (n^2 + 5M^2) \\ \mathcal{I}_3 &\equiv I'_2(0) = \frac{1}{16} \left(\frac{1}{x_{0,1}^2} + \frac{1}{x_{0,2}^2} \right) + \frac{1}{x_{0,1}} \left(\frac{7a_1}{96} - \frac{b_1}{8a_1} - A_1^2 \right) + \frac{1}{x_{0,2}} \left(\frac{7a_2}{96} - \frac{b_2}{8a_2} + A_2^2 \right) \\ \mathcal{I}_4 &\equiv -\frac{G''_0(0)f'(0)}{24f(0)} - \frac{G_0^{(3)}(0)}{24} = \frac{4}{3} M^2 (2n^2 + 11M^2) \pi^4. \end{aligned} \quad (2.77)$$

Note that in our new notations $1/x_{0,i} = 4\pi M \pm 2\pi\sqrt{4M^2 + n^2}$. Expressions for a_i , b_i and A_i are given in (2.68, 2.69) and (2.73).

2.1.8 Local charges

In this we will calculate local charges Q_r in *all* powers of $1/L$ but for the *large* r from the behavior near the relevant branch point. The idea of this calculation is taken from the double scaling approach in matrix models. Namely, one can compare it to the calculation of the resolvent of eigenvalues in a gaussian unitary matrix ensemble

$$H_N(x) = \int \frac{d^{N^2} M}{(2\pi)^{N^2}} \exp \left(-\frac{N}{2} \text{Tr} M^2 \right) \text{Tr}(x - M)^{-1} = \sum_{g=1}^{\infty} N^{2-2g} \sum_{n=0}^{\infty} x^{-2n-1} H_{(g,n)} \quad (2.78)$$

where M is a hermitian matrix of large size N . The coefficients $H_{(g,n)}$ actually give the number of specific planar graphs: it is given by the number of surfaces of genus g which can be done from a polygon with $2n$ edges, by the pairwise gluing of these edges. To extract the large n asymptotics of $H_{(g,n)}$ for any g one can use that in the large N limit the density (which is the imaginary part of the resolvent on the support of eigenvalues) is given by the Wigner's semi-circle law, and the near-edge behavior is described by the Airy functional asymptotics [69, 70] showing the traces of individual eigenvalues in the continuous semi-circle distribution. We will try to extract the similar asymptotics for the distribution of Bethe roots. The role of $1/N$ expansion will be played by the $1/L$ expansion, whether as the order of the $1/x$ expansion in the matrix model will be now played by the label r of the charge.

We start from expanding (2.12)

$$\mathcal{Q}_r = \sum_{m=0}^{\infty} \frac{1}{L^{r+2m-1}} \frac{(-1)^{m+1} G^{(r+2m-1)}(0)}{(2m+1)!(r-1)!2^{2m}}. \quad (2.79)$$

As we shall see, for large r only the $m = 0$ term contributes. We express the derivative as a contour integral around cuts

$$G^{(n)}(0) = -\frac{n!}{2\pi i} \oint_{\mathcal{C}} \frac{G(x)}{x^{n+1}} dx. \quad (2.80)$$

For large n only a small neighborhood of the closest to zero branch point x_0 contributes due to the exponential suppression by the $1/x^{n+1}$ factor. Near the branch point x_0 we have from (2.46) (see also (2.47, 2.41))

$$G_k(x) = \delta_{k0} \left(\pi n_i - \frac{1}{2x_0} \right) + \begin{cases} c_k (x - x_0)^{\frac{1}{2} - \frac{3k}{2}} |a|^{\frac{1}{2} - \frac{k}{2}} + \mathcal{O} \left((x - x_0)^{1 - \frac{3k}{2}} \right), & a > 0, x_0 < 0 \\ (-1)^{k+1} c_k (x_0 - x)^{\frac{1}{2} - \frac{3k}{2}} |a|^{\frac{1}{2} - \frac{k}{2}} + \mathcal{O} \left((x_0 - x)^{1 - \frac{3k}{2}} \right), & a < 0, x_0 > 0 \end{cases} \quad (2.81)$$

where the universal constants c_k can be computed from the known asymptotic of Airy function

$$\text{Ai}(z) = \frac{e^{-\frac{2z^{3/2}}{3}}}{2\sqrt{\pi}z^{1/4}} \left[\sum_{k=0}^n \frac{\left(\frac{1}{6}\right)_k \left(\frac{5}{6}\right)_k}{k!} \left(-\frac{3}{4z^{3/2}}\right)^k + \mathcal{O} \left(\frac{1}{z^{3(n+1)/2}} \right) \right] \quad (2.82)$$

so that

$$c_k = \frac{\text{Ai}'(z)}{\text{Ai}(z)} \Big|_{z^{-\frac{3k-1}{2}}}, \quad (2.83)$$

in particular $c_0 = -1$, $c_1 = -\frac{1}{4}$, $c_2 = \frac{5}{32}$, $c_3 = -\frac{15}{64}$, $c_4 = \frac{1105}{2048}$, $c_5 = -\frac{1695}{1024}$, $c_6 = \frac{414125}{65536}$, $c_7 = -\frac{59025}{2048}$.

These coefficients behave asymptotically as $c_k \sim (-1)^k k!$ at $k \rightarrow \infty$.

We assume that $k \ll n, r$ and expand (for $x_0 < 0$)

$$\begin{aligned} \oint_{-y_0}^0 (y + x_0)^{-n} y^\beta dy &= |x_0|^{\beta+1-n} (-1)^n \oint_{-y_0}^0 y^\beta e^{-n \log(1-y)} dy \\ &\simeq |x_0|^{\beta+1-n} (-1)^n \oint_{-\infty}^0 y^\beta e^{ny} dy. \end{aligned} \quad (2.84)$$

For the last integral the path of integration starts at $-\infty - i0$, encircles the origin in the counterclockwise direction, and returns to the point $-\infty + i0$. For the first integral the path is finite: it starts at some point $-y_0 - i0$ where $0 < y_0 < |x_0|$ and ends at $-y_0 + i0$.

The dependence on the y_0 is exponentially suppressed. The last integral is nothing but the Hankel's contour integral

$$\oint_{-y_0}^0 (y + x_0)^{-n} y^\beta dy = (-1)^n |x_0|^{\beta+1-n} n^{-\beta-1} \frac{2\pi i}{\Gamma(-\beta)} \left(1 + \mathcal{O}\left(\frac{1}{n}\right)\right) \quad (2.85)$$

similarly

$$\oint_0^{y_0} (y + x_0)^{-n} (-y)^\beta dy = -|x_0|^{\beta+1-n} n^{-\beta-1} \frac{2\pi i}{\Gamma(-\beta)} \left(1 + \mathcal{O}\left(\frac{1}{n}\right)\right) \quad (2.86)$$

so that

$$\frac{G_k^{(n)}(0)}{n!} = \begin{cases} (-1)^n \frac{c_k |a|^{\frac{1}{2}-\frac{k}{2}} n^{\frac{3k}{2}-\frac{3}{2}} |x_0|^{\frac{1}{2}-\frac{3k}{2}-n}}{\Gamma(\frac{3k}{2}-\frac{1}{2})} \left(1 + \mathcal{O}\left(\frac{1}{n}\right)\right), & a > 0, x_0 < 0 \\ (-1)^{k+1} \frac{c_k |a|^{\frac{1}{2}-\frac{k}{2}} n^{\frac{3k}{2}-\frac{3}{2}} |x_0|^{\frac{1}{2}-\frac{3k}{2}-n}}{\Gamma(\frac{3k}{2}-\frac{1}{2})} \left(1 + \mathcal{O}\left(\frac{1}{n}\right)\right), & a < 0, x_0 > 0 \end{cases}. \quad (2.87)$$

As we can see from here, only the term with $m = 0$ in (2.79) contributes at large n . The others are suppressed as $1/n$ and the final result is

$$\mathcal{Q}_{k,r} = \begin{cases} (-1)^r \frac{c_k |a|^{\frac{1}{2}-\frac{k}{2}} r^{\frac{3k}{2}-\frac{3}{2}} |x_0|^{\frac{3}{2}-\frac{3k}{2}-r}}{\Gamma(\frac{3k}{2}-\frac{1}{2})} (1 + \mathcal{O}(r^{-1/2})), & a > 0, x_0 < 0 \\ (-1)^k \frac{c_k |a|^{\frac{1}{2}-\frac{k}{2}} r^{\frac{3k}{2}-\frac{3}{2}} |x_0|^{\frac{3}{2}-\frac{3k}{2}-r}}{\Gamma(\frac{3k}{2}-\frac{1}{2})} (1 + \mathcal{O}(r^{-1/2})), & a < 0, x_0 > 0 \end{cases}, \quad (2.88)$$

where we introduced the notation

$$\mathcal{Q}_r = \frac{1}{L^{r-1}} \sum_{k=0}^{\infty} \mathcal{Q}_{k,r} \frac{1}{L^k}. \quad (2.89)$$

Note that $\mathcal{Q}_{k,r}$ is similar to $H_{g,n}$ of the matrix model.

2.1.9 Summary

We showed in this section on the example of $\mathfrak{sl}(2)$ Heisenberg spin chain, how to find finite size corrections in the thermodynamical limit. We also propose a double scaling analysis of the near edge distribution of Bethe roots, which gives some interesting results for the asymptotics of high conserved charges for the finite size corrections of any order.

The methods presented here can be easily carried over to the $\mathfrak{su}(2)$ quantum chain as well, though some peculiarities of this model, like complex distributions of roots and the presence of "string" condensates with equally distributed roots [59], should be taken into account. Only slight modifications of our results will allow to find the $1/L$ corrections in the nonlocal integrable deformations of the $\mathfrak{su}(2)$ spin chain described in [71, 72]. As for more complicated models solved by nested Bethe ansatz, the $1/L$ will be discussed in the next section.

2.2 Finite size corrections in $\mathfrak{su}(1,2)$ Heisenberg spin chain

IN THIS SECTION we stick mainly to the simple example of $\mathfrak{su}(1,2)$ spin chain. This simple toy model has already contained all the nontrivial new features appearing due to the Nested nature of the Bethe ansatz. The generalization to other (super)groups is straightforward and in particular, we shall focus on the Bethe ansatz describing the superstring in $AdS_5 \times S^5$ in Chapter 4.

The scattering of excitations in this model is governed not by a simple phase factor as it was in $\mathfrak{su}(2)$ case considered in the introduction but rather by S -matrix. To derive the Bethe ansatz restricting the momenta of the excitations due to the periodical boundaries we have to solve a diagonalization problem

$$e^{-ip_k L} |\psi\rangle = \prod_{j \neq k}^K S(p_k, p_j) |\psi\rangle \quad (2.90)$$

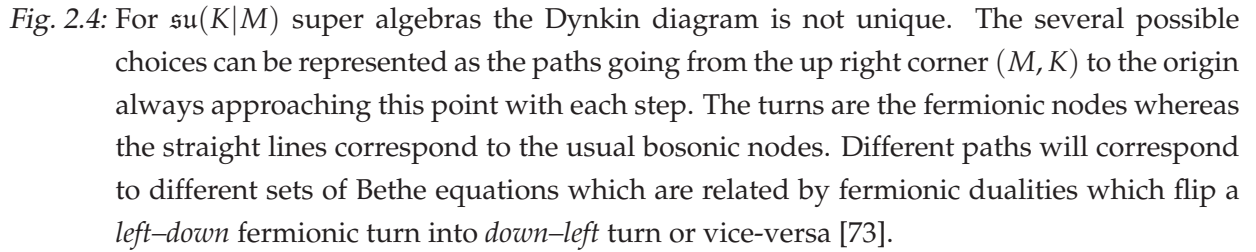
where $S(p_k, p_j)$ is a matrix and $|\psi\rangle$ is the multi-particle wave function. One can consider the matrix in the r.h.s. as a spin chain hamiltonian, depending on the momenta of the initial excitations p_i as on a parameters. One can show that this Hamiltonian is also integrable. The scattering of the excitations with some momenta \tilde{p}_i in this auxiliary spin chain is governed by a smaller size S -matrix. Continuing in this way we will get finally a scalar S -matrix for which (2.90) is trivial. Thus for integrable rank r spin chains each quantum state is parameterized by a set $\{u_{a,j}\}$ of Bethe roots where $a = 1, \dots, r$ and $j = 1, \dots, K_a$ where K_a is the excitation number of *magnons* of type a . The nested Bethe ansatz equations (NBA) from which we find these roots is given by

$$e^{i\tau_a} \left(\frac{u_{a,j} + \frac{i}{2}V_a}{u_{a,j} - \frac{i}{2}V_a} \right)^L = - \prod_{b=1}^r \frac{Q_b \left(u_{a,j} + \frac{i}{2}M_{ab} \right)}{Q_b \left(u_{a,j} - \frac{i}{2}M_{ab} \right)}, \quad (2.91)$$

where

$$Q_a(u) = \prod_{j=1}^{K_a} (u - u_{a,j})$$

are the Baxter polynomials, V_a are the Dynkin labels of the representation considered and M_{ab} the Cartan matrix. In fact, contrary to what happens for the usual Lie algebras, for super algebras the Dynkin diagram (and thus the Cartan matrix) is not unique. Take for example the $\mathfrak{su}(K|M)$ super algebra. The different possible Dynkin diagrams can be identified [73] as the different paths starting from (M, K) and finishing at $(0, 0)$ (always approaching this point with each step) in a rectangular lattice of size $M \times K$ as in figure 2.4. The turns in this path represent the fermionic nodes whereas the bosonic nodes are


$$M_{ab} = (p_a + p_{a+1}) \delta_{ab} - p_{a+1} \delta_{a+1,b} - p_a \delta_{a,b+1}$$

Here we are considering twisted (quasi-periodic) boundary conditions. I.e. we are restricting to the states which are periodical up to the multiplication by

$$g = \text{diag} \left(e^{i\phi_1}, \dots, e^{i\phi_K}, e^{i\varphi_1}, \dots, e^{i\varphi_M} \right) \in SU(K|M) \quad (2.92)$$

$$\begin{array}{ll} \tau_a = \phi_k - \phi_{k+1} & \text{for a bosonic along a vertical segment of the path} \\ \tau_a = \varphi_{m+1} - \varphi_m & \text{for a bosonic along a horizontal segment of the path} \\ \tau_a = \varphi_{m+1} - \phi_k + \pi & \text{for a fermionic node in a } \Gamma \text{ like turn that is with } p_{a-1} = -p_a = 1 \\ \tau_a = \phi_{k+1} - \varphi_m + \pi & \text{for a fermionic node with } p_{a-1} = -p_a = -1 \end{array}$$

Notice that since $g \in SU(K|M)$ we have $\sum_k \phi_k - \sum_m \varphi_m = 0 \bmod 2\pi$. We shall study these Bethe equations with generic twists and we will see that the usual case ($\tau_a = 0$) is in fact quite degenerate.

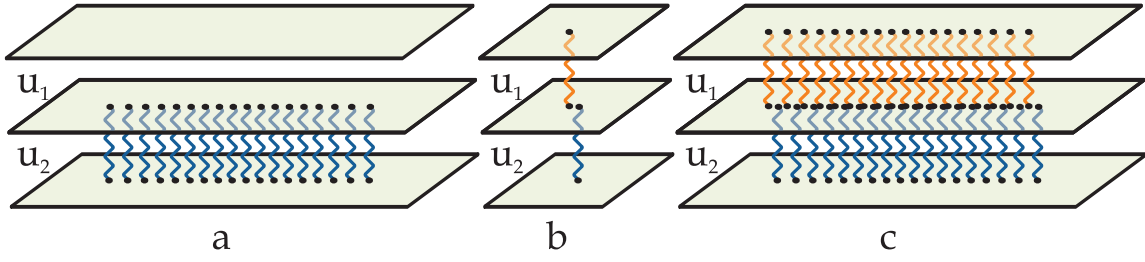


Fig. 2.5: The *middle node* Bethe roots u_2 can condense into a line as depicted in figure 2.5a (The spins in this spin chain transform in a non-compact representation and thus the cuts are typically real. For the $\mathfrak{su}(2)$ Heisenberg magnet the solutions are distributed in the complex plane as some *umbrella* shaped curves [59].). Roots of different types can form bound states, called *stacks* [15], as shown in figure 2.5b. The stacks behave as fundamental excitations and can also form cuts of stacks as represented in figure 2.5c.

As mentioned above, we find already all the ingredients we will need for the study of the BS equations in the simple example of a $\mathfrak{su}(1,2)$ spin chain in the fundamental representation described by the following system of NBA equations⁵

$$e^{i\phi_1 - i\phi_2} = -\frac{Q_1(u_{1,j} + i)}{Q_1(u_{1,j} - i)} \frac{Q_2(u_{1,j} - i/2)}{Q_2(u_{1,j} + i/2)}, \quad j = 1 \dots K_1 \quad (2.93)$$

$$e^{i\phi_2 - i\phi_3} \left(\frac{u_{2,j} - \frac{i}{2}}{u_{2,j} + \frac{i}{2}} \right)^L = -\frac{Q_2(u_{2,j} + i)}{Q_2(u_{2,j} - i)} \frac{Q_1(u_{2,j} - i/2)}{Q_1(u_{2,j} + i/2)}, \quad j = 1 \dots K_2. \quad (2.94)$$

The eigenvalues of the local conserved charges are functions of the roots $u_{2,j}$ only and are given by

$$Q_r = \sum_{j=1}^{K_2} \frac{i}{r-1} \left(\frac{1}{(u_{2,j} + i/2)^{r-1}} - \frac{1}{(u_{2,j} - i/2)^{r-1}} \right). \quad (2.95)$$

We will often call these momentum carrying roots carrying charges by *middle node* roots.⁶

First, consider only middle node excitations, $K_1 = 0 \neq K_2$ in the equations reduces to the $\mathfrak{sl}(2)$ case considered above

$$2\pi n^A + \phi_2 - \phi_3 = \frac{1}{x} + 2\mathcal{G}_2(x), \quad x \in \mathcal{C}^A \quad (2.96)$$

where we introduce the resolvents

$$G_a(x) = \int \frac{\rho_a(y)}{x-y}, \quad \rho_a(y) = \frac{1}{L} \sum_{j=1}^{K_a} \delta(x - x_{a,j}) \quad (2.97)$$

⁵ These equations are exactly the same as for the $\mathfrak{su}(3)$ spin chain except for the sign of the Dynkin labels which makes the system simpler because the Bethe roots are in general real.

⁶ This name is not very proper in this situation. For the BS equations the momentum carrying roots are indeed in the middle of the Dynkin diagram.

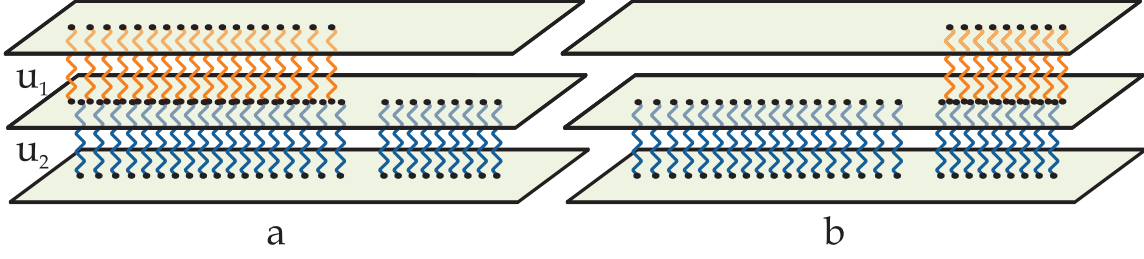


Fig. 2.6: In the scaling limit, to the leading order, the bosonic duality reads $Q_2 \simeq Q_1 \tilde{Q}_1$ with $Q_a = \prod_{k=1}^{K_a} (u - u_a)$. Thus, if we start with the configuration in figure 2.6a where the K_1 roots u_1 form a cut of stacks together with K_1 out of the K_2 middle node roots u_2 and apply the bosonic duality to this configuration, the $K_2 - K_1$ new roots \tilde{u}_1 must be close to the roots u_2 which were previously *single* while the cut of stacks in the left of figure 2.6a will become, after the duality, a cut of simple roots – see figure 2.6b.

Let us also introduce some notation useful for what will follow. Defining the quasi-momenta as

$$\begin{aligned} p_1 &= -\frac{1}{2x} + G_1 - \phi_1, \\ p_2 &= -\frac{1}{2x} - G_1 + G_2 - \phi_2, \\ p_3 &= -\frac{3}{2x} - G_2 - \phi_3, \end{aligned} \quad (2.98)$$

we can add the indices 23 to the mode number n^A and to the cut \mathcal{C}^A in (2.96) and recast this equation as

$$2\pi n_{23}^A = \not{p}_2 - \not{p}_3, \quad x \in \mathcal{C}_{23}^A. \quad (2.99)$$

Next let us consider a state with only two roots $u_{2,1} \equiv u$ and $u_{1,1} \equiv v$ with different flavors, that is $K_1 = K_2 = 1$. Bethe equations then yield

$$u = \frac{1}{2} \cot \frac{\phi_1 - \phi_3 + 2\pi n}{2L}, \quad v = u + \frac{1}{2} \cot \frac{\phi_1 - \phi_2}{2} \quad (2.100)$$

which tells us that if $n \sim 1$ we are in the scaling limit where $v \sim u \sim L$ and $v = u + \mathcal{O}(1)$ – the two Bethe roots form a bound state, called *stack* [15], and can be thought as a fundamental excitation – see figure 2.5b. On the other hand we notice that, strictly speaking, for the usual untwisted Bethe ansatz with $\phi_a = 0$ the stack no longer exists.

Since the stack in figure 2.5b seems to behave as a fundamental excitation one might wonder whether there exists a cut with $K_1 = K_2$ roots of type u_1 and u_2 , like in figure 2.5c, *dual* to the configuration plotted in figure 2.5a. To answer affirmatively to this question let us introduce a novel kind of duality in Bethe ansatz which we shall call *bosonic duality*.

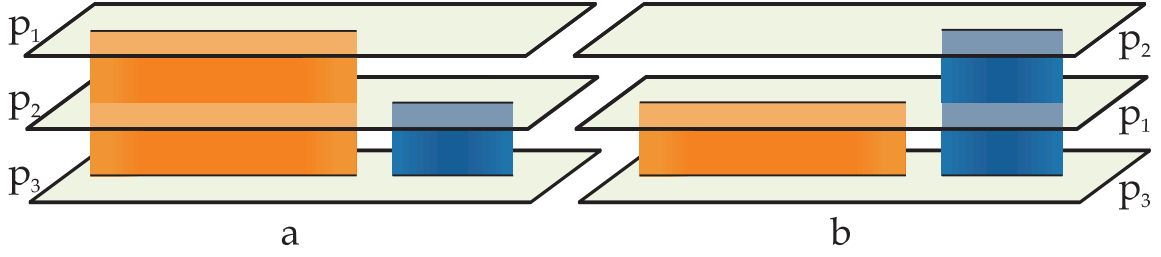


Fig. 2.7: In the scaling limit the configurations in figure 2.6 condense into some disjoint segments, cuts, and we obtain a Riemann surface whose sheets are the quasi-momenta. In this continuous limit the duality corresponds to the exchange of the Riemann sheets.

Indeed, as we explain in detail in section 2.2.4, given a configuration of K_1 roots of type u_1 and K_2 roots of type u_2 , we can write

$$2i \sin(\tau/2) Q_2(u) = e^{i\tau/2} Q_1(u - i/2) \tilde{Q}_1(u + i/2) - e^{-\tau/2} Q_1(u + i/2) \tilde{Q}_1(u - i/2), \quad (2.101)$$

where

$$\tilde{Q}_1(u) = \prod_{j=1}^{\tilde{K}_1} (u - \tilde{u}_{1,j}), \quad \tilde{K}_1 = K_2 - K_1,$$

and $\tau = \phi_1 - \phi_2$. Moreover this decomposition is unique and thus defines unambiguously the position of the new set of roots \tilde{u}_1 . Then, as we explain in section 2.2.4, the new set of roots $\{\tilde{u}_1, u_2\}$ is a solution of the same set of Bethe equations (2.91) with

$$\phi_1 \leftrightarrow \phi_2.$$

Let us then apply this duality to a configuration like the one in figure 2.5a where the roots $u_2 \sim L$ are in the scaling limit and where there are no roots of type u_1 , $K_1 = 0$. To the leading order, we see that the \tilde{u}_1 in (2.101) will scale like L so that the $\pm i/2$ inside the Baxter polynomials can be dropped and we find $Q_2 \simeq \tilde{Q}_1$, that is

$$\tilde{u}_{1,j} = u_{2,j} + \mathcal{O}(1)$$

and therefore we will indeed obtain a configuration like the one depicted in figure 2.5c. Moreover the local charges (2.95) of this dual cut are exactly the same as those of the original cut 2.5a since they are carried by the *middle node* roots u_2 which are untouched during the duality transformation.

Finally, if we apply the duality transformation to some configuration like that in figure 2.6a in the scaling limit we find, by the same reasons as above, that $Q_2(u) \simeq Q_1(u) \tilde{Q}_1(u)$. This means that the dual roots \tilde{u}_1 will be close to the roots u_2 which are not yet part of a stack – the ones making the cut in the right in figure 2.6a. Thus, after the duality, we will obtain a configuration like the one in figure 2.6b.

We conclude that, in the scaling limit with a large number of roots, the distributions of Bethe roots condense into cuts in such a way that the quasi-momenta p_i introduced above become the three sheets of a Riemann surface, see figure 2.7a, obeying

$$2\pi n_{ij}^A = \not{p}_i - \not{p}_j, \quad x \in \mathcal{C}_{ij}^A. \quad (2.102)$$

when x belongs to a cut joining sheets i and j with mode number n_{ij}^A . The duality transformation amounts to a reshuffling of sheets 1 and 2 of this Riemann surface⁷ so that a surface like the one plotted in figure 2.7a transforms into the one indicated in figure 2.7b.

2.2.1 Finite size correction to Nested Bethe Ansatz equations

In this section we will study the leading $1/L$ corrections to the scaling equations (2.102). Moreover since the charges of the solutions are expressed through *middle node roots* u_2 and since these roots are duality invariant it is useful to write the Bethe equations in terms of these roots only to have duality invariant equations. Let us then consider a given configuration of roots condensed into some simple cuts \mathcal{C}_{23} and some cuts of stacks \mathcal{C}_{13} . Then, to leading order, at cuts \mathcal{C}_{23} we have

$$\frac{1}{x} + 2 \oint_{\mathcal{C}_{23}} \frac{\rho_2(y)dy}{x-y} + \int_{\mathcal{C}_{13}} \frac{\rho_2(y)dy}{x-y} = 2\pi n_{23}^A + \phi_2 - \phi_3, \quad x \in \mathcal{C}_{23} \quad (2.103)$$

because in a cut \mathcal{C}_{13} we have $\rho_1 \simeq \rho_2 + \mathcal{O}(1/L)$. To study finite size corrections to this equation two contributions must be considered. On the one hand, as we saw in the previous section, when expanding the *self interaction* we get [53, 75, 49, 50, 52, 76]

$$\sum_{j \neq k} i \log \frac{u_{2,k} - u_{2,j} - i}{u_{2,k} - u_{2,j} + i} = 2 \oint_{\mathcal{C}_{23}} \frac{\rho_2(y)dy}{x-y} + 2 \int_{\mathcal{C}_{13}} \frac{\rho_2(y)dy}{x-y} + \frac{1}{L} \pi \rho'_2 \cot \pi \rho_2$$

where the $1/L$ correction comes from the contribution to the sum from the roots separated by $\mathcal{O}(1)$. On the other hand the auxiliary roots appear as⁸

$$\sum_j i \log \frac{u_{2,k} - u_{1,j} + i/2}{u_{2,k} - u_{1,j} - i/2} = - \int_{\mathcal{C}_{13}} \frac{\rho_1(y)dy}{x-y} = - \int_{\mathcal{C}_{13}} \frac{\rho_2(y)dy}{x-y} - \int_{\mathcal{C}_{13}} \frac{\rho_1(y) - \rho_2(y)}{x-y} dy$$

where the last term accounts for the mismatch in densities in cuts \mathcal{C}_{13} and is clearly also a $\mathcal{O}(1/L)$ effect. Below we will compute this mismatch and find

$$\rho_1(x) - \rho_2(x) = \frac{\Delta \cot_{12}}{2\pi i L} = \frac{\cot_{21}^+ - \cot_{23}^+}{2\pi i L}, \quad x \in \mathcal{C}_{13} \quad (2.104)$$

⁷ As we shall see in the next section this interpretation can be made exact, and not only valid in the scaling limit.

⁸ recall that the Bethe roots $u_{2,k}$ belongs to a \mathcal{C}_{23} cut and therefore is always well separated from $u_{1,j}$ roots which always belong to \mathcal{C}_{13} cuts.

where $\Delta f \equiv f(x + i0) - f(x - i0)$ and

$$\cot_{ij} \equiv \frac{p'_i - p'_j}{2} \cot \frac{p_i - p_j}{2}. \quad (2.105)$$

Thus we find, for $x \in \mathcal{C}_{23}$,

$$\frac{1}{x} + 2 \oint_{\mathcal{C}_{23}} \frac{\rho_2(y) dy}{x - y} + \int_{\mathcal{C}_{13}} \frac{\rho_2(y) dy}{x - y} = 2\pi n_{23}^A + \phi_2 - \phi_3 - \frac{1}{L} \left[\cot_{23} - \int_{\mathcal{C}_{13}} \frac{\Delta \cot_{12}}{x - y} \frac{dy}{2\pi i} \right] \quad (2.106)$$

As explained before, if we apply the duality transformation, cuts \mathcal{C}_{23} become cuts \mathcal{C}_{13} and vice-versa and, to leading order, $p_1 \leftrightarrow p_2$. Thus for cuts \mathcal{C}_{13} we find precisely the same equation (2.106) with $1 \leftrightarrow 2$, so that for $x \in \mathcal{C}_{13}$

$$\frac{1}{x} + 2 \oint_{\mathcal{C}_{13}} \frac{\rho_2(y) dy}{x - y} + \int_{\mathcal{C}_{23}} \frac{\rho_2(y) dy}{x - y} = 2\pi n_{13}^A + \phi_1 - \phi_3 - \frac{1}{L} \left[\cot_{13} - \int_{\mathcal{C}_{23}} \frac{\Delta \cot_{12}}{x - y} \frac{dy}{2\pi i} \right] \quad (2.107)$$

These two equations describing the finite size corrections for the two types of cuts of the $\mathfrak{su}(1,2)$ spin chain are the main results of this section.

In what follows we will derive this result from two different approaches. Namely, we will find this finite size corrections using a Baxter formalism, similar to the one considered in the previous section, based on transfer matrices for this spin chain in several representations and by exploiting the duality we mentioned in the previous section. It will become clear that the generalization to other NBA equations based on higher rank symmetry groups is straightforward.

2.2.2 Derivation using the transfer matrices

The central object in the study of integrable systems is the *transfer matrix* $\hat{T}(u)$. The algebraic Bethe ansatz formalism has the diagonalization of such objects as main goal and the Bethe equations appear in the process of diagonalization (see [57] and references therein for an introduction to the algebraic Bethe ansatz). As functions of a spectral parameter u and of the Bethe roots $u_{a,j}$ these transfer matrices seem to have some poles at the positions of the Bethe roots. On the other hand they are defined as a product of R operators which do not have these singularities. This means that the residues of these apparent poles must vanish. These analyticity conditions (on the Bethe roots) turn out to be precisely the Bethe equations, and thus, if we manage to obtain the eigenvalues of the transfer matrices, we can use this condition of pole cancelation to obtain the Bethe equations without going through the algebraic Bethe ansatz procedure, see for example [77, 78, 67, 73]. For the

$\mathfrak{su}(1,2)$ spin chain we have the following transfer matrices in the anti-symmetric representations:

$$\begin{aligned}
 T_{\square}(u) &= e^{-i\phi_2} \frac{Q_1(u - \frac{3i}{4})}{Q_1(u + \frac{i}{4})} \frac{Q_2(u + \frac{3i}{4})}{Q_2(u - \frac{i}{4})} \left(\frac{u - \frac{5i}{4}}{u - \frac{3i}{4}} \right)^L \\
 &+ e^{-i\phi_1} \frac{Q_1(u + \frac{5i}{4})}{Q_1(u + \frac{i}{4})} \left(\frac{u - \frac{5i}{4}}{u - \frac{3i}{4}} \right)^L + e^{-i\phi_3} \frac{Q_2(u - \frac{5i}{4})}{Q_2(u - \frac{i}{4})} \left(\frac{u - \frac{5i}{4}}{u + \frac{i}{4}} \right)^L, \\
 T_{\boxminus}(u) &= \bar{T}_{\square}(\bar{u}) \left(\frac{u - \frac{5i}{4}}{u + \frac{5i}{4}} \right)^L, \quad T_{\boxplus}(u) = \left(\frac{u - \frac{5i}{4}}{u + \frac{5i}{4}} \right)^L.
 \end{aligned} \tag{2.108}$$

One can easily see that the Bethe equations do follow from requiring analyticity of these transfer matrices.

In the previous section it was shown and emphasized that the TQ Baxter relations are the most powerful method to extract finite size corrections to the scaling limit of Bethe equations.

In this section we will use the transfer matrices presented above along with the fact that, due to the Bethe equations, they are good analytical functions of u to find what are the finite size corrections to this Nested Bethe ansatz. Since for generic (super) nested Bethe ansatz the transfer matrices in the several representations are known, this procedure can be easily generalized for other NBA's.

The key idea to find the finite size corrections to NBA is to use the transfer matrices in the various representations to define a new set of quasi-momenta q_i as the solutions of an algebraic equation whose coefficients are these transfer matrices. For example, to leading order,

$$\begin{aligned}
 T_{\square}(u) &\simeq e^{ip_1} + e^{ip_2} + e^{ip_3}, \\
 T_{\boxminus}(u) &\simeq e^{i(p_1+p_2)} + e^{i(p_2+p_3)} + e^{i(p_3+p_1)}, \\
 T_{\boxplus}(u) &\simeq e^{i(p_1+p_2+p_3)},
 \end{aligned}$$

so that if we define a set of *exact* quasimomenta q_i by

$$T_{\boxplus}(u) - e^{iq} T_{\boxminus}(u) \left(1 - \frac{L}{4u^2} \right) + e^{2iq} T_{\square}(u) \left(1 - \frac{L}{4u^2} \right) - e^{3iq} = 0, \tag{2.109}$$

then, to leading order, $q_i \simeq p_i$. Notice however that the coefficients in this equation have no singularities except some fixed poles close to $u = 0$. Thus, defined in this way, the quasi-momenta q_i constitute a 4 sheet algebraic surface (modulo 2π ambiguities) such that

$$q_i - q_j = 2\pi n_{ij}^A, \quad x \in \mathcal{C}_{ij}, \tag{2.110}$$

and, needless to say, this is an *exact* result in L , it is not a classical (scaling limit) leading result like (2.102). On the other hand, the expansion at large L of the above algebraic equation yields

$$\begin{aligned} q_1 &= p_1 + \frac{1}{2L} (+\cot_{12} + \cot_{13}) \\ q_2 &= p_2 + \frac{1}{2L} (-\cot_{21} + \cot_{23}) \\ q_3 &= p_3 + \frac{1}{2L} (-\cot_{31} - \cot_{32}) , \end{aligned}$$

which follows from the expansion

$$\begin{aligned} T_{\square}(u) \left(1 - \frac{L}{4u^2}\right) &= e^{ip_1} + e^{ip_2} + e^{ip_3} \\ &- \frac{1}{4L} \left[e^{ip_1}(2p'_1 - p'_2 - p'_3) + e^{ip_2}(p'_1 - p'_3) + e^{ip_3}(p'_1 + p'_2 - 2p'_3) \right] + \mathcal{O}\left(\frac{1}{L^2}\right) \\ T_{\boxplus}(u) \left(1 - \frac{L}{4u^2}\right) &= e^{i(p_1+p_2)} + e^{i(p_2+p_3)} + e^{i(p_3+p_1)} \\ &- \frac{1}{4L} \left[e^{i(p_1+p_2)}(p'_1 + p'_2 - 2p'_3) + e^{i(p_1+p_3)}(p'_1 - p'_3) + e^{i(p_2+p_3)}(2p'_1 - p'_2 - p'_3) \right] + \mathcal{O}\left(\frac{1}{L^2}\right) , \\ T_{\boxminus}(u) &= e^{i(p_1+p_2+p_3)} + \mathcal{O}\left(\frac{1}{L^2}\right) . \end{aligned}$$

of the several transfer matrices. Then, to the first order in $1/L$ the exact equation (2.110) gives, for the quasi-momenta p_i introduced in (5.15),

$$\not{p}_2 - \not{p}_3 = 2\pi n_{23}^A - \frac{1}{L} \cot_{23} , \quad x \in \mathcal{C}_{23} \quad (2.111)$$

$$\not{p}_1 - \not{p}_3 = 2\pi n_{13}^A - \frac{1}{2L} (\cot_{12} + 2\cot_{13} + \cot_{32}) , \quad x \in \mathcal{C}_{13} \quad (2.112)$$

where in (2.111) we use the fact that function $\cot_{31} - \cot_{21}$ vanishes under the slash on the cut \mathcal{C}_{23} since

$$\cot_{ij}^+ = \cot_{kj}^- , \quad x \in \mathcal{C}_{ik} . \quad (2.113)$$

Equations (2.111),(2.112) are the finite size corrections we aimed at.

Finally q_2 must have no discontinuity at a cut \mathcal{C}_{13} and therefore

$$\Delta p_2 = 2\pi i (\rho_1 - \rho_2) = \frac{1}{L} (\cot_{21}^+ - \cot_{23}^+) , \quad x \in \mathcal{C}_{13} . \quad (2.114)$$

Thus, replacing the quasi-momenta p_i by its expressions in terms of resolvents (5.15) and relating the density of *auxiliary roots* ρ_1 to that of the *middle node roots* ρ_2 through (2.114), we recover precisely (2.106) and (2.107) as announced.

We would like to stress the efficiency of the TQ relations. We were able to find the *usual* cot contributions (coming from the expansion of the log's of the Bethe equations when the Bethe roots are close to each other) plus the mismatch in densities of the different types of roots making the cuts of stacks using only the fact that due to Bethe equations the transfer matrices in several representations were analytical functions of u . The computation done in this way is by far more economical than a brute force expansion of the Bethe equations.

Finally let us make an important remark. To derive (2.107) from (2.112) one should use

$$\cot_{12} = -\frac{1}{2\pi i} \int_{\mathcal{C}_{13} \cup \mathcal{C}_{23}} \frac{\Delta \cot_{12}}{x-y} dy \quad (2.115)$$

which is clearly a valid relation if \cot_{12} has only branch cuts as singularities. For generic twists and for small enough cuts \mathcal{C}_{13} and \mathcal{C}_{23} this is the case. Indeed, in the absence of Bethe roots we have no cuts at all and thus $p_1 - p_2 = \phi_2 - \phi_1$. Suppose $\phi_2 - \phi_1 \neq 2\pi n$. Then, by continuity, when we slowly open some cuts \mathcal{C}_{23} and \mathcal{C}_{13} then $p_1 - p_2$ will start taking positive values around $\phi_2 - \phi_1$ without ever being zero. Thus, if the cuts are small enough we will never get poles in \cot_{12} . In the section 2.2.4 we will see that the stacks as described in [11] only exist when this assumption of absence of poles is right and are destroyed when $p_1 - p_2$ reaches $2\pi n$.

2.2.3 Re-derivation using the bosonic duality in the scaling limit

In this section let us re-derive the mismatch formula (2.104) using the bosonic duality (2.116). Besides the obvious advantage for what concerns our comprehension of having a second derivation there are systems for which the Bethe equations are known but the algebraic formalism behind these equations is still not well developed (this is the case for example for the *AdS/CFT* Bethe equations proposed by Beisert and Staudacher which we will study in chapter 4.2).

Denoting

$$u_{1,i} = u_{2,i} - \epsilon_i, \quad \tilde{u}_{1,i} = u_{2,i} - \tilde{\epsilon}_i, \quad \epsilon \sim 1$$

and expanding the bosonic duality (2.116) in the scaling limit ($L \rightarrow \infty$) we get

$$\sin(\tau/2) = \sin\left(\frac{1}{2}(\tilde{G}_1 - G_1 + \tau)\right) \exp\left(\sum_{i=1}^{K_1} \frac{\epsilon_i}{u - u_i^1} + \sum_{i=1}^{\tilde{K}_1} \frac{\tilde{\epsilon}_i}{u - u_i^1}\right),$$

where $\tau = \phi_1 - \phi_2$. Taking the logarithm of this equation and differentiating with respect to u we get

$$\sum \frac{\epsilon_i}{(u - u_i^1)^2} + \sum \frac{\tilde{\epsilon}_i}{(u - u_i^1)^2} = \frac{\tilde{G}'_1 - G'_1}{2L} \cot \frac{\tilde{G}_1 - G_1 + \tau}{2}$$

where we notice that the left hand side is precisely the difference of resolvents $G_2 - G_1 - \tilde{G}_1$. Thus we find

$$G_2 - G_1 - \tilde{G}_1 = \frac{\tilde{G}'_1 - G'_1}{2L} \cot \frac{\tilde{G}_1 - G_1 + \tau}{2} \simeq \frac{G'_2 - 2G'_1}{2L} \cot \frac{G_2 - 2G_1 + \tau}{2} = \frac{1}{L} \cot_{12}.$$

Finally, by computing the discontinuity of this expression at the cuts \mathcal{C}_{13} we will get the *mismatch* of the densities of the roots in a cut of stacks⁹

$$\rho_1 - \rho_2 = \frac{\Delta \cot_{12}}{2\pi i L} = \frac{\cot_{21}^+ - \cot_{23}^+}{2\pi i L},$$

which was the gap in the chain of arguments presented in the beginning of the section 2.2.1 and leading to (2.106).

Finally let us show that the bosonic duality amounts to a simple exchange of Riemann sheets in the scaling limit. Consider for example

$$\tilde{p}_1 = -\frac{1}{2x} + \tilde{G}_1 - \tilde{\phi}_1 = -\frac{1}{2x} + G_2 - G_1 - \tilde{\phi}_1 = p_2$$

since, as we will see more carefully in the next section, $\tilde{\phi}_{1,2} = \phi_{2,1}$.

2.2.4 More about bosonic duality

In this section we will explain some details behind the bosonic duality (2.101) mentioned in section 2.2. There are two main steps to be considered. On the one hand we have to prove that for a set of K_2 generic complex numbers u_2 and K_1 roots u_1 obeying the auxiliary Bethe equations (2.93) it is possible to write ($\tau = \phi_1 - \phi_2$)

$$2i \sin(\tau/2) Q_2(u) = e^{i\tau/2} Q_1(u - i/2) \tilde{Q}_1(u + i/2) - e^{-i\tau/2} Q_1(u + i/2) \tilde{Q}_1(u - i/2), \quad (2.116)$$

and that, in doing so, we define the position of a new set of numbers \tilde{u}_1 . A priori this is not at all a trivial statement because we have a polynomial of degree K_2 on the left whereas on the right hand side we have only $K_2 - K_1$ parameters to fix. However, as we will see, if K_1 equations (2.93) are satisfied it is possible to write $Q_2(u)$ in this form. This will be the subject of the section 2.2.4.

Assuming (2.116) to be proved we can use this relation to show that in the original Bethe equations we can replace the roots u_1 by the new roots \tilde{u}_1 with the simultaneous exchange $\phi_1 \leftrightarrow \phi_2$. Indeed if we evaluate the duality at $u = u_{2,j}$ we find

$$\frac{Q_1(u_{2,j} - i/2)}{Q_1(u_{2,j} + i/2)} = e^{i(\phi_2 - \phi_1)} \frac{\tilde{Q}_1(u_{2,j} - i/2)}{\tilde{Q}_1(u_{2,j} + i/2)},$$

⁹ $\Delta f = f^+ - f^-$, so that $\rho = -\frac{\Delta G}{2\pi i}$

meaning that in the equation (2.94) for the u_2 roots we can replace the roots u_1 by the dual roots \tilde{u}_1 provided we replace $\phi_1 \leftrightarrow \phi_2$. Moreover if we take $u = \tilde{u}_{1,j} \pm i/2$ we will get

$$e^{i\phi_2 - i\phi_1} = -\frac{\tilde{Q}_1(\tilde{u}_1 + i)}{\tilde{Q}_1(\tilde{u}_1 - i)} \frac{Q_2(\tilde{u}_1 - i/2)}{Q_2(\tilde{u}_1 + i/2)},$$

which we recognize as equation (2.93) with $K_2 - K_1$ roots \tilde{u}_1 in place of the K_1 original roots u_1 and with $\phi_1 \leftrightarrow \phi_2$. Finally evaluating (2.116) at $u = u_{1,j} \pm i/2$ we will get the original equation (2.93) so that we see that it must be satisfied in order to equation (2.116) to be valid.

In section 2.2.4 we will also see that the transfer matrices are invariant under the bosonic duality accompanied by an appropriate reshuffling of the phases ϕ_a . In section 2.2.5 some curious examples of dual states will be given.

Decomposition proof

In this section we shall prove that one can always decompose $Q_2(u)$ as in (2.116) and that this decomposition uniquely fixes the position of the new set of roots \tilde{u}_1 . In other words, let us show that we can set the polynomial

$$P(u) \equiv e^{+i\frac{\tau}{2}} Q_1(u - i/2) \tilde{Q}_1(u + i/2) - e^{-i\frac{\tau}{2}} Q_1(u + i/2) \tilde{Q}_1(u - i/2) - 2i \sin \frac{\tau}{2} Q_2(u)$$

to zero through a unique choice of the dual roots \tilde{u}_1 .

- Consider first the case $K_1 = 0$. Then it is trivial to see that we can always find unique polynomial $\tilde{Q}_1 = u^{K_2} + \sum_{n=1}^{K_2} a_n u^{n-1}$ such that

$$e^{+i\frac{\tau}{2}} \tilde{Q}_1(u + i/2) - e^{-i\frac{\tau}{2}} \tilde{Q}_1(u - i/2) = 2i \sin \frac{\tau}{2} Q_2(u).$$

because this amounts to solving K_2 linear equations for K_2 coefficients a_n with non-degenerate triangular matrix.

- Next let us consider $K_1 \leq K_2/2$. First we choose \tilde{Q}_1 to satisfy K_1 equations

$$\tilde{Q}_1(u_p^1) = 2ie^{-i\frac{\tau}{2}} \sin \frac{\tau}{2} \frac{Q_2(u_p^1 - i/2)}{Q_1(u_p^1 - i)} \equiv c_p, \quad p = 1, \dots, K_1$$

these conditions will define $\tilde{Q}_1(u)$ up to a homogeneous solution proportional to $Q_1(u)$,

$$\tilde{Q}_1(u) = Q_1(u) \tilde{q}_1(u) + \sum_{p=1}^{K_1} \frac{Q_1(u)}{Q_1'(u_p^1)(u - u_p^1)} c_p$$

where $\tilde{q}_1(u)$ is some polynomial of the degree $K_2 - 2K_1$. Now from (2.93) we notice that with this choice of \tilde{Q}_1 we have

$$\frac{P(u_p^1 + i/2)}{Q_2(u_p^1 + i/2)} = \frac{P(u_p^1 - i/2)}{Q_2(u_p^1 - i/2)} = 0, \quad p = 1, \dots, K_3$$

and thus

$$P(u) = Q_1(u + i/2)Q_1(u - i/2)p(u)$$

where

$$p(u) = e^{i\frac{\tau}{2}}\tilde{q}_1(u + i/2) - e^{-i\frac{\tau}{2}}\tilde{q}_1(u - i/2) - 2i \sin \frac{\tau}{2} q_2(u)$$

and q_2 is a polynomial. Thus we are left to the same problem as above where $K_1 = 0$. For completeness let us note that we can write $q_2(u)$ explicitly in terms of the original roots u_1 and u_2 ,

$$q_2(u) = \frac{Q_2(u)}{Q_1(u + i/2)Q_1(u - i/2)} - \text{poles}$$

where the last term is a simple collection of poles at $u = u_p^1 \pm i/2$ whose residues are such that $q_2(u)$ is indeed a polynomial.

- We can see that the number of the solutions of (2.93) with $K_1 = K$ and $K_1 = K_2 - K$ is the same (see [57] for examples of states counting). Thus for each solution with $K_1 \geq K_2/2$ we can always find one dual solution with $K_1 \leq K_2/2$ and in this way we prove our statement for $K_1 \geq K_2/2$
- Finally let us stress the uniqueness of the \tilde{Q}_1 . If $K_1 > \tilde{K}_1$ we have nothing to show since we saw explicitly above how the bosonic duality constrains uniquely the dual polynomial \tilde{Q}_1 . Let us then consider $K_1 < \tilde{K}_1$ and assume we have two different solutions \tilde{Q}_1^1 and \tilde{Q}_1^2 . Then from the duality relation (2.116) for either solution we find

$$\begin{aligned} e^{i\frac{\tau}{2}}Q_1(u - i/2) \left(\tilde{Q}_1^1(u + i/2) - \tilde{Q}_1^2(u + i/2) \right) = \\ e^{-i\frac{\tau}{2}}Q_1(u + i/2) \left(\tilde{Q}_1^1(u - i/2) - \tilde{Q}_1^2(u - i/2) \right). \end{aligned}$$

Evaluating this expression at $u = u_{1,j} + i/2$ we find that $\tilde{Q}_1^1(u_{1,j}) - \tilde{Q}_1^2(u_{1,j}) = 0$ so that $\tilde{Q}_1^1(u_1) - \tilde{Q}_1^2(u_1) = Q_1(u)h(u)$ and therefore

$$e^{i\frac{\tau}{2}}h(u + i/2) = e^{-i\frac{\tau}{2}}h(u - i/2)$$

which is clearly impossible for polynomial $h(u)$ – for large u we can neglect the $i/2$'s to obtain $e^{i\tau} = 1$ thus leading to a contradiction.

Transfer matrix invariance under the bosonic duality

In this section we will examine the transformation properties of the transfer matrices under the bosonic duality. In Appendix A we consider this problem for the general $\mathfrak{su}(N|M)$ group. For now let us just take T_{\square} for $\mathfrak{su}(1,2)$ from (2.108). Using (2.116) we can express ratios of Q_1 's through \tilde{Q}_1 and Q_2 so that

$$\begin{aligned} T_{\square}(u) = & e^{-i\phi_2} \left(+ \frac{2i \sin \frac{\tau}{2} e^{-i\frac{\tau}{2}} Q_2(u - \frac{i}{4})}{Q_1(u + \frac{i}{4}) \tilde{Q}_1(u + \frac{i}{4})} + e^{-i\tau} \frac{\tilde{Q}_1(u - \frac{3i}{4})}{\tilde{Q}_1(u + \frac{i}{4})} \right) \frac{Q_2(u + \frac{3i}{4})}{Q_2(u - \frac{i}{4})} \left(\frac{u - \frac{5i}{4}}{u - \frac{3i}{4}} \right)^L \\ & + e^{-i\phi_1} \left(- \frac{2i \sin \frac{\tau}{2} e^{+i\frac{\tau}{2}} Q_2(u + \frac{3i}{4})}{Q_1(u + \frac{i}{4}) \tilde{Q}_1(u + \frac{i}{4})} + e^{+i\tau} \frac{\tilde{Q}_1(u + \frac{5i}{4})}{\tilde{Q}_1(u + \frac{i}{4})} \right) \left(\frac{u - \frac{5i}{4}}{u - \frac{3i}{4}} \right)^L \\ & + e^{-i\phi_3} \frac{Q_2(u - \frac{5i}{4})}{Q_2(u - \frac{i}{4})} \left(\frac{u - \frac{5i}{4}}{u + \frac{i}{4}} \right)^L. \end{aligned}$$

We see that for $\tau = \phi_1 - \phi_2$ the terms with $\sin \frac{\tau}{2}$ cancel and we get the old expression for T_{\square} with u_1 replaced by \tilde{u}_1 and $\phi_1 \leftrightarrow \phi_2$.

This simple transformation property of the transfer matrices automatically implies that the Riemann surface defined by the algebraic equation (2.109) is untouched under the duality transformation (to all orders in L), so that the duality can cause at most some reshuffling of the sheets. However, as we will see in the next section, not necessarily the sheets as a whole are exchanged – this operation will be in general done in a piecewise manner.

2.2.5 Examples of the dual configurations

In this section we will study some curious Bethe roots distributions for the twisted $\mathfrak{su}(1,2)$ spin chain described by the nested Bethe equations (2.93) and (2.94) and for the usual $\mathfrak{su}(2)$ Heisenberg chain,

$$\left(\frac{u_{1,j} + \frac{i}{2}}{u_{1,j} - \frac{i}{2}} \right)^L = - \frac{Q_1(u_{1,j} + i)}{Q_1(u_{1,j} - i)}. \quad (2.117)$$

Using the first example we shall understand the importance of twists to stabilize big cuts of stacks like the ones depicted in figures 2.5a, 2.5b and explain how the stacks gets destroyed as we decrease the twists.

We can dualize $\mathfrak{su}(2)$ solutions of the twisted¹⁰ Heisenberg ring using the same duality (2.101) as before with $Q_2(u) \rightarrow u^L$. We will consider the dual solutions to the vacuum and to a 1-cut solution for the Heisenberg spin chain (2.117).

¹⁰ For zero twist the duality becomes degenerate and we will see below that it needs to be slightly modified.

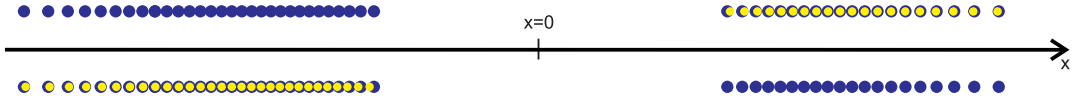


Fig. 2.8: The upper and the lower configuration of Bethe roots are dual to one another. Big blue dots are middle node roots u_2 , yellow dots are auxiliary roots u_1 . The formation of cuts of stacks is manifest for this situation where the twists are large (like $\pi/2$) and the filling fractions are small.

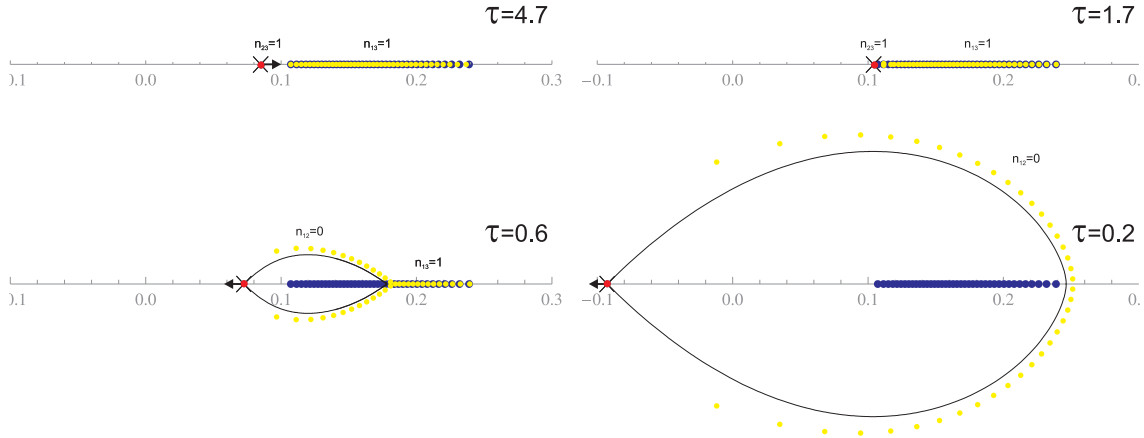


Fig. 2.9: Disintegration of the stack configuration. When the twist is large (the top left corner) the auxiliary roots form bound states together with the middle node ones and constitute a cut of stacks. As we decrease the twist fluctuation $n_{23} = 1$ (the red crossed dot) enters the cut of stacks (the top right corner) and subsequently partly *disintegrate* the cut of stacks forming some zipper like configuration (the bottom left corner). At some very small value of the twist the configuration of Bethe roots bears no resemblance with a cut of stacks.

Big enough twists, small enough fillings and zippers

In the previous sections we saw that the introduction of twists in the NBA equations are needed to have a configuration with auxiliary roots u_1 close to some momentum carrying roots u_2 . In figure 2.8 we have two numerical solutions of the Bethe equations which are related by the bosonic duality. In either of them we see a configuration of Bethe roots with a simple cut with middle roots only (in blue) and a cut of stacks (containing blue and yellow roots). In this situation it is clearly reasonable to think of stacks as bound states of different types of roots and we see that they indeed condense into *multicolor* cuts.

We will examine what happens when we decrease the twists (or increase filling fractions, which is the same qualitatively). For simplicity we consider the configuration, dual to the simple one cut solution ($K_2 = K$ and $K_1 = 0$) with no twist for the middle node roots, $\phi_2 - \phi_3 = 0$, and some generic twist $\phi_1 - \phi_2 = \tau$ for the auxiliary roots. Bosonic duality will leave untouched middle node roots u_2 and create K new axillary roots u_1 .

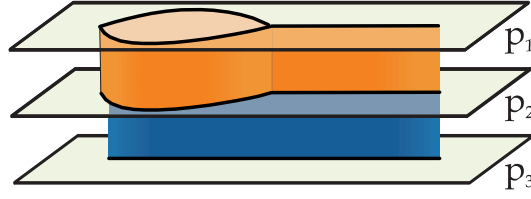


Fig. 2.10: In the scaling limit the algebraic curves for e^{ip_j} are the same before the duality (blue cut only) and after the duality (when the auxiliary roots are created). The duality causes interchange of the sheets outside the bubble, while keeping the order untouched inside. This follows from the need of a positive density for the “virtual” cut. In other words the duality is indeed only interchanging the sheets of the Riemann surface although it is interchanging them in a piecewise way.

In the upper left corner of figure 2.9 we applied the duality for some big twist $\tau = 4.6$ while in the bottom right corner of the same figure we have a configuration of Bethe roots with some small twist $\tau = 0.2$. In this latter case the auxiliary (yellow) roots clearly do *not* form stacks together with the middle node (blue) roots!, rather they form a bubble, containing the original cut of roots u_2 .

To understand what happens in the scaling limit consider the position of $n_{23} = 1$ fluctuation, given by (4.3), which would be a small infinitesimal cut between p_2 and p_3 . In figure 2.9 the position of this virtual fluctuation is marked by a red crossed dot. When the twist is big enough (and filling fraction is small enough) the fluctuation is to the left from the cut. When we start decreasing the twist the fluctuation approaches the cut (upper right picture on fig 2.9) and at this point we have at the same time

$$p_2(x_n) - p_3(x_n) = 2\pi$$

and

$$p_1(x_n) - p_3(x_n) = 2\pi ,$$

which implies $p_1 - p_2 = 0$ so that equation (2.115) becomes wrong at this point. When we continue decreasing the twist the fluctuation passes through the cut and becomes a $n_{12} = 0$ fluctuation. If we think of the fluctuation as being a small cut along the real axis we see that density becomes negative after crossing the cut:

$$0 < \rho_{23}^{fluc} = -\frac{\Delta(p_2 - p_3)}{4\pi i} = -\frac{\Delta(-p_1 - p_2)}{4\pi i} = -\rho_{12}^{fluc}$$

This means that two branch points of the infinitesimal cut should not be connected directly, but rather by some macroscopical curve with real positive density! This curves $z(t)$ can be calculated from the equation $\rho(z)dz \in \mathbb{R}^+$ or

$$\frac{p_1(z) - p_2(z)}{2\pi i} \partial_t z = \pm 1$$

and the resulting curve is plotted in black on the two bottom pictures on the figure 2.9. This is very similar to what happens when a fluctuation passes through the 1 cut $\mathfrak{su}(2)$ configuration [79]. In the scaling limit the black curve corresponds to the cut connecting p_1 and p_2 like on the figure 2.10.

At first sight these figures seem to be defying our previous results. Indeed we checked in the previous section that the transfer matrices themselves are invariant under the bosonic duality. Thus the algebraic curves obtained from (2.109) should be the same after and before duality and thus what one naturally expects is a simple interchange of Riemann sheets $p_1 \leftrightarrow p_2$ under the duality transformation. What really happens is a bit more tricky. The quasimomenta are indeed only exchanged but this exchange operation is done in a piecewise manner. That is, if we denote the new quasi-momenta by p_i^{new} and the old ones by p_i^{old} and if we denote the bubble in figure 2.10 by \mathcal{R} then we have

$$p_1^{new} = \begin{cases} p_2^{old} & , \text{ outside } \mathcal{R} \\ p_1^{old} & , \text{ inside } \mathcal{R} \end{cases} , \quad p_2^{new} = \begin{cases} p_1^{old} & , \text{ outside } \mathcal{R} \\ p_2^{old} & , \text{ inside } \mathcal{R} \end{cases} , \quad p_3^{new} = p_3^{old}$$

where the border of the region \mathcal{R} can be precisely determined in the scaling limit as explained above.

Dualizing momentum carrying roots

In this section we will consider an example of application of the bosonic duality to the Heisenberg magnet¹¹. The duality (2.101) can be applied to the roots u_1 obeying (2.117) provided we replace $Q_2(u) \rightarrow u^L$. In fact if we want to consider strictly zero twist we need a new duality because that one is clearly degenerate in this limiting case. The proper modified expression is in this case

$$i(\tilde{K}_1 - K_1)u^L = Q_1(u - i/2)\tilde{Q}_1(u + i/2) - Q_1(u + i/2)\tilde{Q}_1(u - i/2).$$

and the number of dual roots is now $L - K_1 + 1$. Contrary to what happened with non-zero twists, here, the dual solution is not unique. Indeed if $\tilde{K}_1 > K_1$ we can as well use

$$\tilde{Q}_1^\alpha \equiv \alpha Q_1 + \tilde{Q}_1. \quad (2.118)$$

All these solutions, parameterized by the constant α , have the same charges because the transfer matrix is invariant under this transformation – see Appendix A. Notice that if initially we have a physical state with $K_1 < L/2$ roots then all dual states (2.118) are unphysical with $\tilde{K}_1 > L/2$ violating the half-filling condition. Still, it is interesting, at the

¹¹ This section benefited a lot from the insightful discussions with T. Bargheer and N. Beisert whom we should thank.

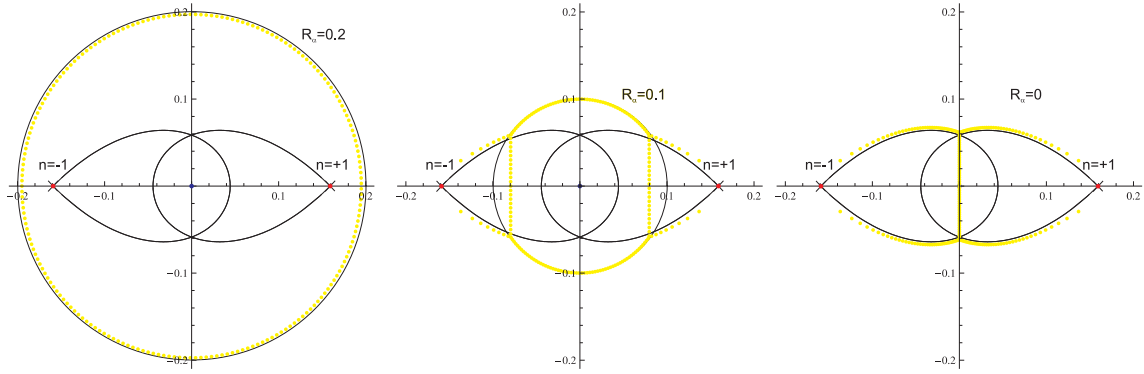


Fig. 2.11: Three configurations of Bethe roots dual to the ferromagnetic vacuum of the untwisted Heisenberg spin chain. For each physical solution (below half filling) of the Bethe equations there is a one parameter (α) family of dual unphysical solutions. To the left, α is large and the roots distribute themselves along a circle with radius R_α given by $(R_\alpha L)^L = \alpha$. Decreasing α the circle will touch the fluctuations $n = \pm 1$. Similarly to the previous section the virtual infinitesimal cuts become macroscopical bubble cuts with cusps at the position of the fluctuations. Intersection points of the new cuts with the circle are connected by condensates, which are logarithmic cuts on the algebraic curve [79].

level of Bethe equations, to understand how these solutions look like. First of all let us single out a particular \tilde{Q}_1 out of the various solutions to (2.118) so that

$$\tilde{Q}_1^\alpha = u^{\tilde{K}_1} + \sum_{l=0}^{\tilde{K}_1-1} c_l^\alpha u^l \quad (2.119)$$

becomes well defined through (2.118). We chose $\tilde{Q}_1 = \tilde{Q}_1^0$ to be the dual solution with $c_0^0 = 0$.

Consider for example the vacuum state for which $Q_1 = 1$. Let us first take α to be very large so that we can write

$$\alpha + \tilde{Q}_1^0 \simeq \alpha + (xL)^L. \quad (2.120)$$

We see for large α the dual roots will be on a circle of radius $\frac{|\alpha|^{1/L}}{L}$. The corresponding configuration is present on the first picture on the figure 2.11. In this figure we also plotted a circle with this radius and one can see that the Bethe roots belong perfectly to the circle.

Let us now understand this configuration from the algebraic curve point of view. The the quasi-momenta $p_1 = -p_2 \equiv p = \frac{1}{2x} - G$, in the absence of Bethe roots, are simply given by $p = \frac{1}{2x}$. Let us find the curves with positive densities and mode number $n = 0$. The density is given by $\rho(x) = \frac{1}{2\pi i} \frac{1}{x}$ and we have to find the curves where $\rho(x)dx$ is real. It is easy to see that the only possibility is the circle centered at the origin with an arbitrary radius. From the above arguments one can expect that for any α the roots will belong to

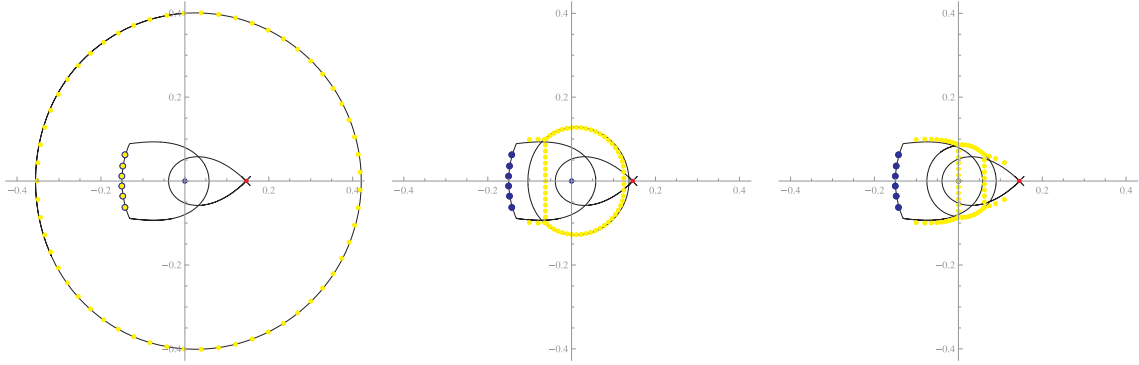


Fig. 2.12: Dual configuration to 1-cut solution. Similar to the previous example for the large α the dual roots are distributed along the big circle and cut (first picture). When the α decreases and the circle crosses the cut we have to choose another curve with the positive density (second and third pictures).

some circle. However, we analyzed only the curves with zero mode number and as we see on the figure 2.11 for smaller α 's the circle develops four tails and two vertical lines. Along these vertical lines the roots are separated by i (for $L \rightarrow \infty$) forming the so called *condensates* or *Bethe strings*. The tails meet at the points where the virtual fluctuation is and the corresponding curves are given by

$$\frac{p(z) \pm \pi}{\pi i} \partial_t z = \pm 1 \quad (2.121)$$

analogously to the previous section. In the last configuration on figure 2.11 the circle is completely absent. There are only two $n = \pm 1$ curves which, at the interceptions, become a 4π jump log condensate with the Bethe roots separated by $i/2$.

We also built the dual configurations to the 1-cut solution (see figure 2.12). The situation is similar to the vacuum, the only difference being that two tails (out of four) do not tend to touch each other, but rather end at the branch points of the initial cut.

Appendix A: Transfer matrix invariance and the bosonic duality for $SU(K|M)$ supergroups

In this section we review the formalism of [73] which allows one to derive the transfer matrices of usual (super) spin chains in any representation. We will use this general formalism to prove the invariance under the bosonic dualities of all possible transfer matrices one can build. The transfer matrices presented in section 2.108 can be obtained trivially using this formalism¹².

As mentioned in section 2.2, for the standard $SU(K|M)$ super spin chains (based on the standard R -matrix $R(u) = u + i\mathcal{P}$ with \mathcal{P} the super permutation) we can find the (twisted) transfer matrix eigenvalues for the single column young tableau with a boxes through the *non-commutative generating functions* [73, 74]

$$\sum_{a=0}^{\infty} (-1)^a e^{ia\partial_u} \frac{T_a(u)}{Q_{K,M}(u + (a - K + M + 1)i/2)} e^{ia\partial_u} = \prod_{(x,n) \in \gamma} \hat{V}_{x,n}^{-1}(u) \quad (2.122)$$

where γ is a path starting from (M, K) and finishing at $(0, 0)$ (always approaching this point with each step) in a rectangular lattice of size $M \times K$ as in figure 2.4¹³, $x = (m, k)$ is point in this path and $n = (0, -1)$ or $(-1, 0)$ is the unit vector looking along the next step of the path. Each path describes in this way a possible Dynkin diagram of the $SU(K|M)$ super group with corners denoting fermionic nodes and straight lines bosonic ones, see figure 2.4. Finally,

$$\begin{aligned} \hat{V}_{(m,k),(0,-1)}^{-1}(u) &= e^{i\phi_k} \frac{Q_{k,m}(u + i(m - k - 1)/2)}{Q_{k,m}(u + i(m - k + 1)/2)} \frac{Q_{k-1,m}(u + i(m - k + 2)/2)}{Q_{k-1,m}(u + i(m - k + 0)/2)} - e^{i\partial_u} \\ \hat{V}_{(m,k),(-1,0)}^{-1}(u) &= \left(e^{i\phi_m} \frac{Q_{k,m-1}(u + i(m - k - 2)/2)}{Q_{k,m-1}(u + i(m - k + 0)/2)} \frac{Q_{k,m}(u + i(m - k + 1)/2)}{Q_{k,m}(u + i(m - k - 1)/2)} - e^{i\partial_u} \right)^{-1} \end{aligned}$$

where $Q_{k,m}$ is the Baxter polynomial for the roots of the corresponding node¹⁴ and $\{\phi_k, \phi_m\}$ are twists introduced in the transfer matrix [74]. Let us then consider a bosonic node like the one in the middle of figure 2.4 (the *vertical* bosonic node is treated in the same fashion). If the position of this node on the $M \times K$ lattice is given by (m, k) then it is obvious that the only combination containing $Q_{m,k}$ in the right hand side of (2.122) comes from the product of $\hat{V}_{(m,k),(-1,0)}^{-1}(u) \hat{V}_{(m+1,k),(-1,0)}^{-1}(u)$ which reads

$$\begin{aligned} &\left[e^{i\phi_m + \phi_{m+1}} \frac{Q_{k,m+1}(u + i(m - k + 2)/2)}{Q_{k,m+1}(u + i(m - k + 0)/2)} \frac{Q_{k,m-1}(u + i(m - k - 2)/2)}{Q_{k,m-1}(u + i(m - k + 0)/2)} + e^{2i\partial_u} - \right. \\ &- \left(e^{i\phi_{m+1}} \frac{Q_{k,m}(u + i(m - k - 1)/2)}{Q_{k,m}(u + i(m - k + 1)/2)} \frac{Q_{k,m+1}(u + i(m - k + 2)/2)}{Q_{k,m+1}(u + i(m - k + 0)/2)} + \right. \\ &\left. + e^{i\phi_m} \frac{Q_{k,m-1}(u + i(m - k + 0)/2)}{Q_{k,m-1}(u + i(m - k + 2)/2)} \frac{Q_{k,m}(u + i(m - k + 3)/2)}{Q_{k,m}(u + i(m - k + 1)/2)} \right) e^{i\partial_u} \Big]^{-1} \quad (2.123) \end{aligned}$$

¹² We should mention that the transfer matrices in section 2.108 are not exactly the same we have in this Appendix but can be obtained from these via a trivial rescaling in u which obviously does not spoil the invariance of these objects.

¹³ Notice that the path goes in opposite direction compared to the labeling a of the Baxter polynomial Q_a used before. In the notation of this section $Q_{k,m}$ corresponds to the node is at position (m,k) in this lattice.

¹⁴ $\hat{Q}_{0,0}$ is normalized to 1. If we are considering a spin in the representation where the first Dynkin node has a nonzero Dynkin label then $Q_{M,K}$ will play the role of the potential term. In general the situation is more complicated, see [73]. In any case we are mainly interested in the dualization of roots which are not momentum carrying thus we need not care about such matters.

So, if we want to study the bosonic duality on the node (k, m) and its relation with the invariance of several transfer matrices we need to study the last two lines of this expression. For simplicity let us shift u , omit the subscript k in the Baxter polynomials $Q_{k,m-1}, Q_{k,m}, Q_{k,m+1}$ and define the reduced transfer matrix as

$$t(u, \varphi_m, \varphi_{m+1}) \equiv e^{i\varphi_{m+1}} \frac{Q_m(u-i)}{Q_m(u)} \frac{Q_{m+1}(u+i/2)}{Q_{m+1}(u-i/2)} + e^{i\varphi_m} \frac{Q_{m-1}(u-i/2)}{Q_{m-1}(u+i/2)} \frac{Q_m(u+i)}{Q_m(u)}. \quad (2.124)$$

Notice that the absence of poles at the zeros of Q_m yields precisely the Bethe equations for this auxiliary node.

Bosonic duality \Rightarrow Transfer matrices invariance

Thus, to check the invariance of the transfer matrices in all representations it suffices to verify that the reduced transfer matrix $t(u, \varphi_m, \varphi_{m+1})$ is invariant under $\varphi_m \leftrightarrow \varphi_{m+1}$ and $Q_m \rightarrow \tilde{Q}_m$ where

$$2i \sin\left(\frac{\varphi_{m+1} - \varphi_m}{2}\right) Q_{m-1}(u) Q_{m+1}(u) = \quad (2.125)$$

$$e^{i\frac{\varphi_{m+1}-\varphi_m}{2}} Q_m(u-i/2) \tilde{Q}_m(u+i/2) - e^{-i\frac{\varphi_{m+1}-\varphi_m}{2}} Q_m(u+i/2) \tilde{Q}_m(u-i/2).$$

which can be easily verified. It suffices to replace, in $t(u, \varphi_m, \varphi_{m+1})$ in (2.124),

$$\begin{aligned} \frac{Q_m(u-i)}{Q_m(u)} &\rightarrow e^{-i(\varphi_{m+1}-\varphi_m)} \frac{\tilde{Q}_m(u-i)}{\tilde{Q}_m(u)} \\ &\quad + 2ie^{-i\frac{\varphi_{m+1}-\varphi_m}{2}} \sin\left(\frac{\varphi_{m+1}-\varphi_m}{2}\right) \frac{Q_{m-1}(u+i/2) Q_{m+1}(u+i/2)}{Q_m(u) \tilde{Q}_m(u)}, \\ \frac{Q_m(u+i)}{Q_m(u)} &\rightarrow e^{+i(\varphi_{m+1}-\varphi_m)} \frac{\tilde{Q}_m(u+i)}{\tilde{Q}_m(u)} \\ &\quad - 2ie^{-i\frac{\varphi_{m+1}-\varphi_m}{2}} \sin\left(\frac{\varphi_{m+1}-\varphi_m}{2}\right) \frac{Q_{m-1}(u-i/2) Q_{m+1}(u-i/2)}{Q_m(u) \tilde{Q}_m(u)}, \end{aligned}$$

which are obvious consequences of the bosonic duality.

Transfer matrix invariance \Rightarrow Bosonic duality

On the other hand suppose we have two solutions of Bethe equations, one of them characterized by the Baxter polynomials $\{\dots, Q_{m-1}, Q_m, Q_{m+1}, \dots\}$ with twists $\{\dots, \varphi_m, \varphi_{m+1}, \dots\}$ and another with $\{\dots, Q_{m-1}, \tilde{Q}_m, Q_{m+1}, \dots\}$ with twists $\{\dots, \varphi_{m+1}, \varphi_m, \dots\}$ for which the transfer matrices are the same, that is

$$t(u, \varphi_m, \varphi_{m+1}) = \tilde{t}(u, \varphi_{m+1}, \varphi_m). \quad (2.126)$$

Then we can show that these two solutions are related by the bosonic duality (2.125). Indeed if we build the Wronskian¹⁵ like object

$$W(u) \equiv e^{i\frac{\varphi_{m+1}-\varphi_m}{2}} \frac{Q_m(u-i/2)\tilde{Q}_m(u+i/2)}{Q_{m-1}(u)Q_{m+1}(u)} - e^{-i\frac{\varphi_{m+1}-\varphi_m}{2}} \frac{Q_m(u+i/2)\tilde{Q}_m(u-i/2)}{Q_{m-1}(u)Q_{m+1}(u)}.$$

we can easily check that

$$W(u+i/2) - W(u-i/2) = -e^{-i\frac{\varphi_{m+1}+\varphi_m}{2}} \frac{Q_m(u)\tilde{Q}_m(u)}{Q_{m-1}(u-i/2)Q_{m+1}(u+i/2)} (t(u, \varphi_m, \varphi_{m+1}) - \tilde{t}(u, \varphi_{m+1}, \varphi_m)) = 0$$

Since by definition $W(u)$ is a rational function this means it must be a constant. Thus if $\varphi_m \neq \varphi_{m+1}$ we must have $K_m + \tilde{K}_m = K_m + K_{m+1}$ and the value of W can be read from the large u behavior. In this way we obtain precisely the bosonic duality (2.125). If $\varphi_m = \varphi_{m+1}$ then we see that $K_m + \tilde{K}_m = K_m + K_{m+1} + 1$ and we will obtain a different value for the constant W which will correspond to the untwisted bosonic duality described in section 2.2.5.

¹⁵ We would like to thank A.Zabrodin and V.Kazakov for suggesting this nice interpretation for the bosonic duality

3. QUASI-CLASSICAL QUANTIZATION AND FLUCTUATIONS

3.1 Preface

IN THIS CHAPTER we will study the semi-classical quantization of the $AdS_5 \times S^5$ Metsaev-Tseytlin superstring [9]. We will see that the semi-classical quantization of this very nontrivial field theory is not conceptually much difficult the one-dimensional non-relativistic particle in a smooth potential. Let us consider this very instructive example.

In terms of the quasi-momenta

$$p(x) \equiv \frac{\hbar \psi'(x)}{i \psi(x)}, \quad (3.1)$$

the Schrodinger equation for the wave function ψ takes the Riccati form

$$p^2 - i\hbar p' = 2m(E - V). \quad (3.2)$$

What do we know about $p(x)$? It is an analytical function which has, by definition (3.1), a pole with residue

$$\alpha = \frac{\hbar}{i} \quad (3.3)$$

at each of the zeros of the wave function. For the N -th excited state we will have N poles. On the other hand, for very excited states, the right hand side in (3.2) is much larger than \hbar and

$$p \simeq p_{\text{cl}} \equiv \sqrt{2m(E - V)} \quad (3.4)$$

describes now a two-sheet Riemann surface. What happened was that, as $N \rightarrow \infty$, the poles in $p(x)$ started to be denser and denser, condensing in a square root cut. Thus, in the semiclassical limit we retrieve the Bohr-Sommerfeld quantization

$$\frac{1}{2\pi\hbar} \oint_{\mathcal{C}} p_{\text{cl}}(z) dz \simeq \frac{1}{2\pi\hbar} \oint_{\mathcal{C}} p(z) dz = N, \quad (3.5)$$

where \mathcal{C} encircles the cut. The first integral is precisely the action variable of the classical motion.

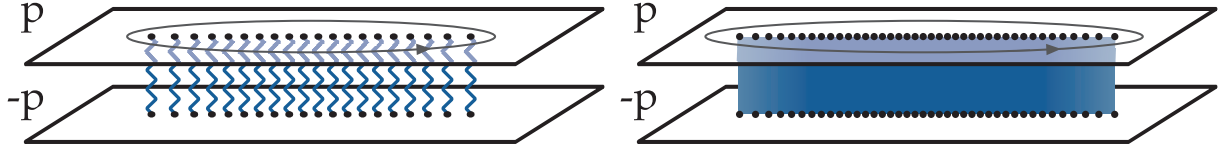


Fig. 3.1: Analytical structure of a quasi-momenta $p(x)$ of a one dimensional system. Left: for low lying states $p(x)$ is a collection of poles. Right: for high energy states the poles condense into a square root branch cut.

When we consider more degrees of freedom, in particular when we move to higher dimensions, let us say two, the situation is not just a little worse. Indeed, we have no proper *generic* recipe, except from lattice calculations, to extract the quantum spectrum, or a part of it, of an interacting quantum field theory. However, if we are lucky, it might happen that the theory is integrable. If it is the case, we can identify the action variables, apply the Bohr-Sommerfield condition and find the quasi-classical spectrum of the theory.

For a wide class of two dimensional sigma models this happens to be the case and the procedure is known explicitly. The central object is a collection of quasi-momenta, $p_i(x)$, whose derivative defines a many-sheet Riemann surface. These sheets can be connected by several cuts, to each of which we can associate a *filling fraction* by integrating the quasi-momenta around the cut as in (3.5). These are the action variables of the theory. Grosso modo, these filling fractions measure the size of the cut. Finally, when going through these cuts the quasi-momenta can jump by $2\pi n$ with n being an integer labeling the cut.

The superstring on $AdS_5 \times S^5$ background falls into this class of theories – the model is known to be classically integrable [80, 8], as we show in the introduction. The algebraic curve was built [11], and thus one can try to quasi-classically quantize the string. In the string language, when we choose which Riemann sheets we connect by a cut we are choosing which string polarization, i.e. which degree of freedom, to excite. The number n and the filling fraction associated to the cut are in strict analogy with the mode number and amplitude of a Fourier mode in a free theory such as the string in flat space [11].

Going back to our simple example, we can see that the existence of such discrete equations is indeed highly natural. For that purpose let us consider a simple harmonic oscillator, $V = \frac{m\omega^2 x^2}{2}$. From (3.2) it follows that $p(x) = im\omega x + \mathcal{O}(1/x)$. Since the quasi-momentum is a meromorphic function with N poles on the real axis, it must be given by

$$p(x) = im\omega x + \frac{\hbar}{i} \sum_{i=1}^N \frac{1}{x - x_i}. \quad (3.6)$$

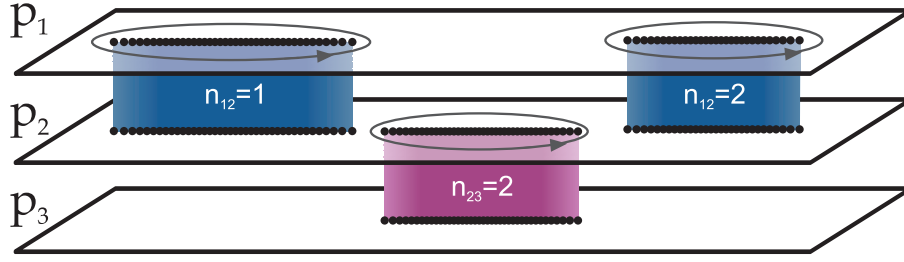


Fig. 3.2: A possible analytical structure of the quasi-momenta of an integrable sigma model. Many types of cuts are now possible. Cuts can join different sheets and each cut is marked by its “mode number” n_{ij} . In flat space limit they become numbers of Fourier modes. The number of microscopical poles constituting the given cut is called a “filling fraction” and can be calculated as a contour integral (3.5).

Then, from the large x behavior in (3.2) we read immediately

$$E = \hbar\omega \left(N + \frac{1}{2} \right) \quad (3.7)$$

while from the cancelation of each of the x_i poles in the same equation we get¹

$$x_i = \frac{\hbar}{2\omega m} \sum_{j \neq i}^N \frac{1}{x_i - x_j} \quad (3.8)$$

which strongly resembles the equations one finds in the Bethe ansatz context.

When we expand the superstring action around some classical solution, characterized by some conserved charges, we obtain, for the oscillations, a quadratic Lagrangian whose quantization yields, for the semiclassical spectrum,

$$E = E_{cl} + \sum_{A,n} N_{A,n} \mathcal{E}_{A,n}, \quad (3.9)$$

where we have dropped the zero energy excitation and denoted the number of quanta with energy $\mathcal{E}_{A,n}$ by $N_{A,n}$. The subscript A labels the several possible string polarizations we can excite while the mode number n is the Fourier mode of the quantum fluctuation. In this article we shall address the question of finding this quasi-classical spectrum for the $AdS_5 \times S^5$ superstring using the algebraic curve mentioned above.

Let us explain the idea behind the computation. There are basically two main steps involved. First we construct the curve associated with the classical solution around which we want to consider the quantum fluctuations following the procedure explained in the introduction. The second step consist of considering the small excitations around this

¹ Its solution is given by the zeros of the Hermite polynomials, $H_N \left(\sqrt{\frac{2m\omega}{\hbar}} x_i \right) = 0$.

classical solution in the spirit of [52]. In terms of the algebraic curve this means adding some microscopic cuts to this Riemann surface. By microscopic cuts we mean some finite number of poles, just like in the simple example (3.3). Then, by construction, the energy of the perturbed configuration is quantized as in (3.9).

As an application of this method we compute the fluctuation frequencies around the circular $\mathfrak{su}(2)$ and $\mathfrak{sl}(2)$ string. These solutions belong to a family of circular solutions whose quasi-momenta we computed explicitly in Appendix A. The frequencies we compute in this way were obtained in [81, 82] and [83, 84] by direct analysis of the expanded Lagrangian around these solutions in the Metsaev-Tseytlin GS superstring action.

3.2 Circular string solutions

IN THIS SECTION we will write down an important class of rigid circular strings studied in [83]. As we explain below they are particularly simple from the algebraic curve point of view and will therefore provide us an excellent playground to check our method for some simple choice of parameters. In terms of the AdS_5 and S^5 embedding coordinates, we can represent this general class of strings solutions with global charges $E = \sqrt{\lambda} \mathcal{E}$, $J_1 = \sqrt{\lambda} \mathcal{J}_1, \dots$, as [83]

$$\begin{aligned} u_2 + iu_1 &= \sqrt{\frac{\mathcal{J}_3}{w_3}} e^{i(w_3\tau + m_3\sigma)} , & v_2 + iv_1 &= \sqrt{\frac{\mathcal{S}_2}{w_2}} e^{i(w_2\tau + k_2\sigma)} , \\ u_4 + iu_3 &= \sqrt{\frac{\mathcal{J}_2}{w_2}} e^{i(w_2\tau + m_2\sigma)} , & v_4 + iv_3 &= \sqrt{\frac{\mathcal{S}_1}{w_1}} e^{i(w_1\tau + k_1\sigma)} , \\ u_6 + iu_5 &= \sqrt{\frac{\mathcal{J}_1}{w_1}} e^{i(w_1\tau + m_1\sigma)} , & v_6 + iv_5 &= \sqrt{\frac{\mathcal{E}}{\kappa}} e^{i\kappa\tau} , \end{aligned} \quad (3.10)$$

where the equations of motion and Virasoro constraints impose

$$\begin{aligned} 1 &= \sum_{i=1}^3 \frac{\mathcal{J}_i}{w_i} , \quad 1 = \frac{\mathcal{E}}{\kappa} - \sum_{j=1}^2 \frac{\mathcal{S}_j}{w_j} , \quad 0 = \sum_{j=1}^2 k_j \mathcal{S}_j + \sum_{i=1}^3 m_i \mathcal{J}_i , \\ w_j^2 &= \kappa^2 + k_j^2 , \quad \kappa^2 = \sum_{j=1}^2 \mathcal{S}_j \frac{2k_j^2}{w_j} + \sum_{i=1}^3 \mathcal{J}_i \frac{w_i^2 + m_i^2}{w_i} , \\ w_i^2 &= v^2 + m_i^2 , \quad v^2 \equiv \sum_{i=1}^3 \mathcal{J}_i \frac{w_i^2 - m_i^2}{w_i} . \end{aligned} \quad (3.11)$$

As explained in Appendix A, for this family of solutions the representative g can be written as

$$g = e^{\varphi_\sigma \sigma + \varphi_\tau \tau} \cdot g_0$$

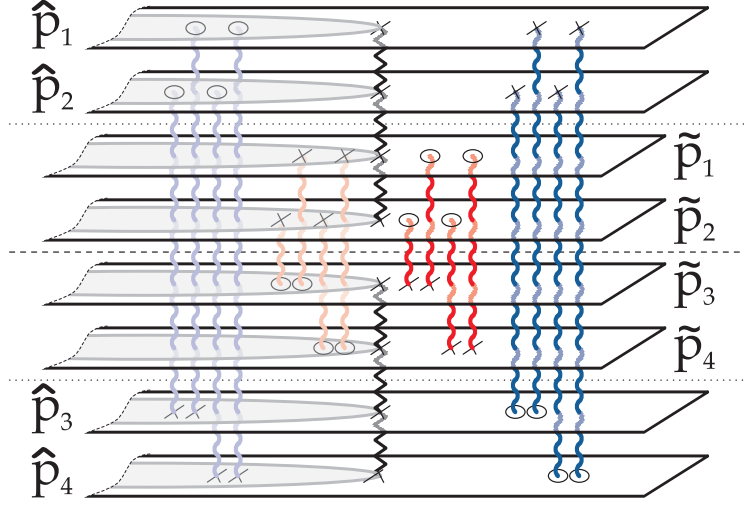


Fig. 3.3: Some configuration of poles on the algebraic curve corresponding to the S^5 excitations (red) and AdS_5 excitations (blue). Black line denotes poles at ± 1 , connecting 4 sheets with equal residues. The crosses correspond to the residue $+\alpha(x)$, while circles to residue $-\alpha(x)$. Physical domain of the surface lies outside the unit circle.

where $\varphi_{\sigma,\tau}$ are linear combinations of Cartan generators and g_0 is a constant matrix. Then we see that the current

$$J = -g^{-1}dg,$$

and therefore also the flat connection $A(x)$ in (1.12), are constant matrices! Then the computation of the path order exponential (1.13) is trivial and the quasi-momenta $p(x)$ are simply obtained from the eigenvalues of $\frac{2\pi}{i}A(x)$. For a detailed account see Appendix A.

3.3 Frequencies from the algebraic curve

IN THIS SECTION we will consider the quasi-classical quantization of the $AdS_5 \times S^5$ superstring in the language of the algebraic curve. As an example we will find the low lying energy spectrum for the excitations around some simple classical string solutions.

As we have already mentioned in the introduction and in section 1.1.1 the *exact* quasi-momenta is made out of a large collection of poles. From (1.19) we infer the residue of each pole,

$$p \simeq \sum_{a=k}^{S_n} \frac{\alpha(x_k)}{x - x_k} + \dots, \quad (3.12)$$

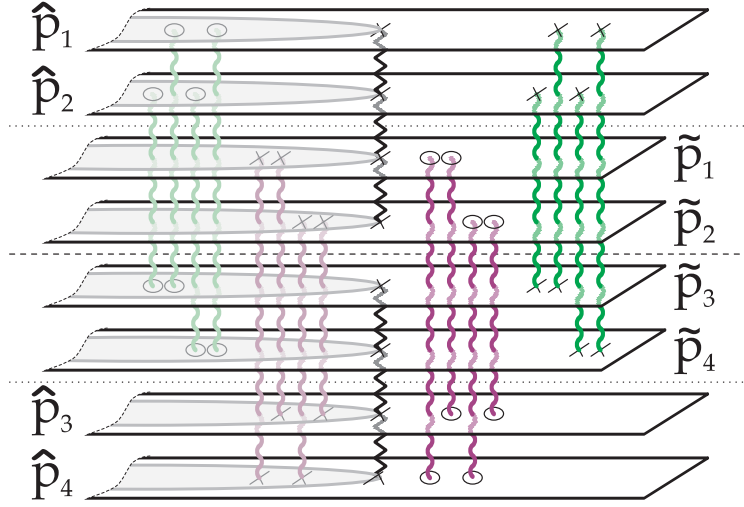


Fig. 3.4: Some configuration of poles on the algebraic curve corresponding to the 8 fermionic excitations. Black line denotes poles at ± 1 , connecting 4 sheets with equal residues. The crosses correspond to the residue $\alpha(x)$, while circles to residue $-\alpha(x)$. Physical domain of the surface lies outside the unit circle.

with

$$\alpha(x) = \frac{4\pi}{\sqrt{\lambda}} \frac{x^2}{x^2 - 1}. \quad (3.13)$$

These poles may then condense into square root cuts forming a classical Riemann surface like in fig. 3.1. The filling fraction and mode number of the cuts are in strict analogy with the amplitude and mode number of a fourier mode in the usual flat space string. Then, to consider the quantum fluctuations around this classical solution, amounts to adding small cuts, i.e. poles, to this curve. The key ingredient allowing us to do so is the knowledge of the residue (3.13) just like in the example (3.3) in the introduction. The several possible choices of sheets to be connected by these poles correspond to the several possible polarizations of the superstring, i.e. to the different quantum numbers. The 16 physical excitations are the $4 + 4$ modes in AdS_5 and S^5 (fig 3.3) plus the 8 fermionic fluctuations (fig 3.4).

Let us give a bit more of flavor to the discussion above. As we mentioned in the introduction, the equations describing the eight sheet quasi-momenta can be discretized [16] yielding a set of Bethe ansatz equations for the roots x_i making up the cuts. The resulting equations resemble (3.8) with an extra $2\pi n_i$ in the left hand side

$$\sum_{j \neq i} \frac{1}{x_i - x_j} = 2\pi n_i + V(x_i).$$

This means that we can think of x_i as being the position of a particle interacting with many other particles via a two-dimensional Coulomb interaction, placed in an external

potential² and feeling an external force $2\pi n_i$. What we are doing is, then, first considering a large number of particles which will condense in some disjoint supports, the cuts, with each cut being made out of particles with the same mode number n_i . Then we add an extra particle with some other mode number n . At the leading order, two things happen. The particle will seek its equilibrium point in this background and will backreact, shifting this background slightly by its presence [52]. The (AdS global time) energy E of the new configuration is then shifted. When adding N particles we get precisely the quantum steps in the spectrum, i.e. (3.9).

Technically the computations can be divided into two main steps. In what follows we will use the notation (1.18) intensively. We must solve (1.16) for all cuts of the Riemann surface where we now have $p(x) \rightarrow p(x) + \delta p(x)$ where $p(x)$ is the quasi-momenta associated with the classical solution.

- When applied to the microscopic cut, i.e. pole, equation (1.16) gives us, to leading order, the position x_n^{ij} of the pole,

$$p_i(x_n^{ij}) - p_j(x_n^{ij}) = 2\pi n, \quad |x_n^{ij}| > 1, \quad (3.14)$$

where $i < j$ are taking values $\hat{1}, \hat{2}, \hat{3}, \hat{4}, \tilde{1}, \tilde{2}, \tilde{3}, \tilde{4}$ and indicate which two sheets share the pole. We refer to domain $|x| > 1$ as *physical domain*. The interior of the unit circle is just the mirror image of the physical domain, as we saw in the previous section (1.21).

- Then, to find δp , and in particular the energy shift δE , we must solve the same equations but now in the macroscopic cuts

$$\delta p_i^+ - \delta p_j^- = 0, \quad x \in \mathcal{C}_n^{ij}. \quad (3.15)$$

This linear problem is to be supplemented with the known analytical properties of $\delta p(x)$ namely the asymptotic behavior presented below and the simple pole singularities with residues (3.13). In this way we are computing the backreaction described above.

Before proceeding it is useful to introduce some simple notation. We shall consider N_n^{ij} excitations with mode number n between sheet p_i and p_j such that

$$N_{ij} \equiv \sum_n N_n^{ij} \quad (3.16)$$

is the total number of poles connecting these two sheets. Moreover, each excitation has their own quantum numbers according to the global symmetry. The S^5 , AdS_5 and

² in (3.8) the potential is a quadratic one, for the actual Bethe equations it is something else

fermionic excitations can then be identified as the several possible choices of sheets to be connected, see figs 3.3 and 3.4,

$$\begin{aligned}
S^5 & , \quad (i,j) = (\tilde{1},\tilde{3}), (\tilde{1},\tilde{4}), (\tilde{2},\tilde{3}), (\tilde{2},\tilde{4}) \\
AdS_5 & , \quad (i,j) = (\hat{1},\hat{3}), (\hat{1},\hat{4}), (\hat{2},\hat{3}), (\hat{2},\hat{4}) \\
\text{Fermions} & , \quad (i,j) = (\tilde{1},\hat{3}), (\tilde{1},\hat{4}), (\tilde{2},\hat{3}), (\tilde{2},\hat{4}), \\
& \quad (\hat{1},\tilde{3}), (\hat{1},\tilde{4}), (\hat{2},\tilde{3}), (\hat{2},\tilde{4})
\end{aligned} \tag{3.17}$$

The 16 physical degrees of freedom of the superstring are precisely these 16 elementary excitations, also called *momentum carrying excitations* [11, 15].

When adding extra poles to the classical solutions its energy will be shifted by

$$\delta E = \delta \Delta + \sum_{AdS^5} N_{ij} + \frac{1}{2} \sum_{\text{Ferm}} N_{ij}, \tag{3.18}$$

where we isolated the anomalous part $\delta \Delta$ of the energy shift from the trivial bare part. Then, it is convenient to recast (1.24), for the excitations, as

$$\delta \begin{pmatrix} \hat{p}_1 \\ \hat{p}_2 \\ \hat{p}_3 \\ \hat{p}_4 \\ \tilde{p}_1 \\ \tilde{p}_2 \\ \tilde{p}_3 \\ \tilde{p}_4 \end{pmatrix} \simeq \frac{4\pi}{x\sqrt{\lambda}} \begin{pmatrix} +\delta\Delta/2 & +N_{\hat{1}\hat{4}} + N_{\hat{1}\tilde{3}} & +N_{\hat{1}\tilde{3}} + N_{\hat{1}\hat{4}} \\ +\delta\Delta/2 & +N_{\hat{2}\hat{3}} + N_{\hat{2}\hat{4}} & +N_{\hat{2}\hat{4}} + N_{\hat{2}\tilde{3}} \\ -\delta\Delta/2 & -N_{\hat{2}\hat{3}} - N_{\hat{1}\tilde{3}} & -N_{\hat{1}\tilde{3}} - N_{\hat{2}\hat{3}} \\ -\delta\Delta/2 & -N_{\hat{1}\hat{4}} - N_{\hat{2}\hat{4}} & -N_{\hat{2}\hat{4}} - N_{\hat{1}\hat{4}} \\ & -N_{\tilde{1}\hat{4}} - N_{\tilde{1}\tilde{3}} & -N_{\tilde{1}\tilde{3}} - N_{\tilde{1}\hat{4}} \\ & -N_{\tilde{2}\hat{3}} - N_{\tilde{2}\hat{4}} & -N_{\tilde{2}\hat{4}} - N_{\tilde{2}\hat{3}} \\ & +N_{\tilde{2}\hat{3}} + N_{\tilde{1}\tilde{3}} & +N_{\tilde{1}\tilde{3}} + N_{\tilde{2}\hat{3}} \\ & +N_{\tilde{1}\hat{4}} + N_{\tilde{2}\hat{4}} & +N_{\tilde{2}\hat{4}} + N_{\tilde{1}\hat{4}} \end{pmatrix} \tag{3.19}$$

These filling fractions N_{ij}^n are not independent. Any algebraic curve must obey the Riemann bilinear identity (see eqs. 3.38 and 3.44 in [11]). Since this was already the case for the classical solution around which we are expanding, the new filling fractions are constrained by

$$\sum_n n \sum_{\text{All } ij} N_n^{ij} = 0, \tag{3.20}$$

which is nothing but the string level matching condition in the algebraic curve language.

It is also important to note that sign of the residues can be summarized by the following formula

$$\text{res}_{x=x_n^{ij}} \hat{p}_k = \left(\delta_{i\hat{k}} - \delta_{j\hat{k}} \right) \alpha(x_n^{ij}) N_n^{ij}, \quad \text{res}_{x=x_n^{ij}} \tilde{p}_k = \left(\delta_{j\tilde{k}} - \delta_{i\tilde{k}} \right) \alpha(x_n^{ij}) N_n^{ij}, \tag{3.21}$$

with $k = 1, 2, 3, 4$ and $i < j$ taking values $\hat{1}, \hat{2}, \hat{3}, \hat{4}, \tilde{1}, \tilde{2}, \tilde{3}, \tilde{4}$, as summarized in figs.3.3 and 3.4.

In the following sections we shall analyze the quantum fluctuations around some simple classical solutions belonging to the family of rigid circular strings (3.10). We will do it in three main steps. First we compute the quasi-momenta³ associated to each classical solution as explained in section 3.2 and in greater detail in Appendix A. Then we shall consider the fluctuations around the classical solution which appear as new poles in the quasi-momenta. As explained above, we start by finding the position of these new roots using (3.14) and then we shall compute the perturbation δp of the quasi-momenta by using, again, the analytical properties described in section 1.1.1 plus the knowledge of the poles' positions found in the second step.

We can already notice that, using this procedure, one relies uniquely on considerations of analyticity and *needs not* introduce any particular parametrization of the group element $g(\sigma, \tau)$ for the fluctuations around the classical solution, contrary to what is usually done in this type of analysis [81, 82, 83, 84]. It is also nice to see that the fermionic and bosonic frequencies appear, in our approach, on a completely equal footing, both corresponding to simple poles which differ only by the sheets they unite - see figs.3.3 and 3.4. Finally, in principle, we can apply our method to any classical solution whereas the same generalization seems to be highly non-trivial to do directly in the action since we no longer have a simple field redefinition to make it time and space independent as was the case in [82, 84]. This method will allow us to prove some general statements about the quasi-classical spectrum and its relation to the finite-size corrections in the BS equations.

3.3.1 The BMN string

We shall consider the simplest possible solution amongst the family of circular strings presented in section 3.2, the rotating point like BMN string [85] moving around a big circle of S^5 . For this solution all spins except for

$$\mathcal{J}_1 = \mathcal{J}$$

are set to zero. Then we have $m_1 = 0$, $w_1 = \mathcal{J}$, $\mathcal{E} = \kappa = \mathcal{J}$. For this solution the connection $A(x)$ presented in Appendix A is not only constant but also diagonal so we immediately find

$$\tilde{p}_{1,2} = -\tilde{p}_{3,4} = \hat{p}_{1,2} = -\hat{p}_{3,4} = \frac{2\pi\mathcal{J}x}{x^2 - 1}. \quad (3.22)$$

³ Due to the simplicity of these solutions we could have computed the quasi-momenta by an alternative method, namely using just the analytical properties presented in section 1.1.1. This was done for the $\mathfrak{su}(2)$ and $\mathfrak{sl}(2)$ circular solutions in [14] and [19].

We see that this is indeed the simplest 8 sheet algebraic curve we could have built – it has neither poles nor cuts connecting its sheets other than the trivial ones at $x = \pm 1$ (1.22).

We shall now study the quantum fluctuations around this solution. For the sake of clarity we shall not write explicitly many of the quantities computed in the intermediate steps – they can be found in Appendix B.

To consider the 16 types of physical excitations we add all types of poles on the fig 3.3 and 3.4. From (3.14) we find that the poles in the physical domain with $|x| > 1$, for this simple case, are all located at the same position

$$x_n^{ij} = x_n = \frac{1}{n} \left(\mathcal{J} + \sqrt{\mathcal{J}^2 + n^2} \right). \quad (3.23)$$

Now we must find the quasi-momenta $p(x) + \delta p(x)$

- with poles located at (3.23) with residues (3.21) connecting the several sheets,
- obeying the $x \rightarrow 1/x$ symmetry property (1.21),
- with residues ± 1 grouped as in (1.22),
- with large x behavior given by (3.19).

From the requirements listed above one can easily write the expression for the quasi-momenta. For example

$$\delta \hat{p}_2 = \hat{a} + \frac{\delta \alpha_+}{x-1} + \frac{\delta \alpha_-}{x+1} + \sum_{i=3,4,\bar{3},\bar{4}} \sum_n \frac{\alpha(x_n^{2i}) N_n^{2i}}{x - x_n^{2i}} - \sum_{i=3,4,\bar{3},\bar{4}} \sum_n \frac{\alpha(x_n^{\hat{1}i}) N_n^{\hat{1}i}}{1/x - x_n^{\hat{1}i}} \quad (3.24)$$

$$\delta \hat{p}_3 = \hat{b} + \frac{\delta \beta_+}{x-1} + \frac{\delta \beta_-}{x+1} - \sum_{i=1,2,\bar{1},\bar{2}} \sum_n \frac{\alpha(x_n^{\hat{3}i}) N_n^{\hat{3}i}}{x - x_n^{\hat{3}i}} + \sum_{i=1,2,\bar{1},\bar{2}} \sum_n \frac{\alpha(x_n^{\hat{4}i}) N_n^{\hat{4}i}}{1/x - x_n^{\hat{4}i}} \quad (3.25)$$

where \hat{a}, \hat{b} and $\delta \alpha_{\pm}, \delta \beta_{\pm}$ are constants to be fixed and the last terms ensure the right poles in physical domain for $\delta \hat{p}_{1,4}(x) = -\delta \hat{p}_{2,3}(1/x)$. Similar expressions can be immediately written down for $\delta \hat{p}_{2,3}$ with the introduction of two new constants \tilde{a} and \tilde{b} .

At this point we are left with the problem of fixing the eight constants

$$\hat{a}, \hat{b}, \tilde{a}, \tilde{b}, \delta \alpha_+, \delta \alpha_-, \delta \beta_+, \delta \beta_-.$$

This is precisely the number of conditions one obtains by imposing the $1/x$ behavior at large x for the quasi-momenta (3.19). The asymptotic of $\hat{p}_2, \hat{p}_3, \tilde{p}_2, \tilde{p}_3$ fix the first four constants while the remaining four equations, solvable only if the level matching condition (3.20) is satisfied, fix the remaining coefficients and yield

$$\delta E = \sum_{\text{All}} \sum_n \frac{\sqrt{n^2 + \mathcal{J}^2} - \mathcal{J}}{\mathcal{J}} N_n^{ij} + \sum_{\text{AdS}^5} N^{ij} + \frac{1}{2} \sum_{\text{Ferm}} N^{ij} \quad (3.26)$$

where we indeed recognize the famous BMN frequencies [85] in the anomalous part of the energy shift.

3.3.2 The circular string in S^3 , the 1 cut $\mathfrak{su}(2)$ solution

The next less trivial example is the simple $\mathfrak{su}(2)$ rigid circular string [81]. Still it is simple enough so that all results are explicit. This solution is obtained from the family of circular strings in section 3.2 by setting

$$m_1 = -m_2 = m, \quad \mathcal{J}_1 = \mathcal{J}_2 = \mathcal{J} \quad (3.27)$$

with all other spins set to zero. For this solution

$$\mathcal{E} = \kappa = \sqrt{\mathcal{J}^2 + m^2}. \quad (3.28)$$

The quasi-momenta can be computed as explained in Appendix A. The AdS_5 quasi-momenta are obtained as for the BMN string

$$\hat{p}_{1,2} = -\hat{p}_{3,4} = \frac{2\pi\kappa x}{x^2 - 1} \quad (3.29)$$

while for the S^5 components \tilde{p}_i we find that this solution corresponds to 1 cut between \tilde{p}_2 and \tilde{p}_3 with mode number $k = -2m$, given by [14]

$$\begin{pmatrix} \tilde{p}_1 \\ \tilde{p}_2 \\ \tilde{p}_3 \\ \tilde{p}_4 \end{pmatrix} = 2\pi \begin{pmatrix} +\frac{x}{x^2-1}K(1/x) \\ +\frac{x}{x^2-1}K(x) - m \\ -\frac{x}{x^2-1}K(x) + m \\ -\frac{x}{x^2-1}K(1/x) \end{pmatrix}, \quad K(x) \equiv \sqrt{m^2x^2 + \mathcal{J}^2}. \quad (3.30)$$

where we assume that $m > 0$ and branch cut goes to the left of $x = -1$ so that

$$\begin{aligned} K(x) &= mx + \mathcal{O}(1/x), \quad K(x) = \mathcal{J} + \mathcal{O}(x) \\ K(1) &= K(-1) = \kappa > 0 \end{aligned}$$

In the rest of this section we will compute the quantum spectrum of the low lying excitations around this solution. For simplicity we will consider the AdS_5 , S^5 and fermionic fluctuations independently assuming the level matching condition (3.20) to be satisfied *for each of the sectors separately*. The result we give, however, is valid under the softer constraint (3.20) for all sectors, as one can easily check.

Method of computation

Suppose we want to compute the variation of the quasi-momenta $\delta p(x)$ when a small pole is added to some general finite gap solution with some square root cuts. Since the branch points will be slightly displaced we conclude that $\delta p(x)$ behaves like $\partial_{x_0} \sqrt{x - x_0} \sim 1/\sqrt{x - x_0}$ near each such point.

We are dealing with a 1-cut finite gap solution. Then, for $\delta \tilde{p}_2$, we can assume the most general analytical function with one branch cut, namely $f(x) + g(x)/K(x)$ where f and g are some rational functions and $K(x)$ was defined in (3.30). To obtain $\delta \tilde{p}_3$ it suffices to notice that (3.15) is simply telling us that $\delta \tilde{p}_3$ is the analytical continuation of $\delta \tilde{p}_2$ through the cut. The remaining quasi-momentum $\delta \tilde{p}_{1,4}$ can then be obtained from this ones by the inversion symmetry (1.21). We conclude that

$$\begin{pmatrix} \delta \tilde{p}_1 \\ \delta \tilde{p}_2 \\ \delta \tilde{p}_3 \\ \delta \tilde{p}_4 \end{pmatrix} = \begin{pmatrix} -f(1/x) - \frac{g(1/x)}{K(1/x)} \\ f(x) + \frac{g(x)}{K(x)} \\ f(x) - \frac{g(x)}{K(x)} \\ -f(1/x) + \frac{g(1/x)}{K(1/x)} \end{pmatrix}. \quad (3.31)$$

The only singularity of $\delta \tilde{p}_2$ apart from the branch cut are eventual simple poles at ± 1 and x_n and so the same must be true for $f(x)$ and $g(x)$. Then, just like in the previous example, these functions are uniquely fixed by the large x asymptotics (3.19) and by the residues at x_n (3.21) of the quasi-momenta.

Finally, since the AdS_5 part of the quasi-momenta of the non-perturbed finite gap solution has no branch cuts their variations $\delta \hat{p}_i$ have the same form (3.24),(3.25) as for simplest BMN string.

The AdS_5 excitations

This part is the simplest. The excitations live in the empty AdS_5 sheets where the only impact of the S^5 classical solution comes through the Virasoro constraints, by the residues at ± 1 (1.22). Thus the \tilde{p} are nonperturbed and $\delta \hat{p}_i$ are the same as in BMN case (3.24,3.25) with only AdS_5 filling fractions N 's being nonzero. Indeed, comparing (3.22) and (3.29) we see that we can completely recycle the previous computation provided we replace \mathcal{J} by κ in the expression (3.23) for the pole's position. This leads immediately to

$$\delta E = \sum_{AdS^5} \sum_n \frac{\sqrt{\mathcal{J}^2 + m^2 + n^2}}{\sqrt{\mathcal{J}^2 + m^2}} N_n^{ij} \quad (3.32)$$

The S^5 excitations

We must now analyze the shift in quasi-momenta due to the excitation of the algebraic curve by the four type of poles $(\tilde{1}\tilde{3}, \tilde{2}\tilde{4}, \tilde{2}\tilde{3}, \tilde{1}\tilde{4})$. Since the AdS quasi-momenta are trivial, with no cuts, we obtain for $\delta\hat{p}$ the same kind of expression we had for the BMN string (3.22), that is

$$\delta\hat{p}_{1,2} = -\delta\hat{p}_{3,4} = \frac{2\pi\delta E}{\sqrt{\lambda}} \frac{x}{x^2 - 1}, \quad (3.33)$$

where the constant factor was fixed by the asymptotics (3.19)

$$\delta\hat{p}_{1,2} \simeq -\delta\hat{p}_{3,4} \simeq \frac{2\pi\delta E}{\sqrt{\lambda}} \frac{1}{x}. \quad (3.34)$$

Due to the Virasoro constraints the poles at ± 1 in the AdS_5 and S^5 sectors are synchronized (1.22) so that we merely need to compute $f(x)$ and $g(x)$ from the large x asymptotics (3.19) and the residue condition (3.21) and extract, from these two functions, the residues at ± 1 . This is done in Appendix C.1. Let us just provide a glimpse of reasoning involved. Since the difference

$$\delta\tilde{p}_3 = f(x) - g(x)/K(x)$$

must have a single pole at $x_n^{\tilde{1}\tilde{3}}$ with residue $\alpha(x_n^{\tilde{1}\tilde{3}})$ whereas the sum

$$\delta\tilde{p}_2 = f(x) + g(x)/K(x)$$

must be analytical, we can, in this way, read the residues of both f and g at this point. This kind reasoning should be carried over for all the other excitations and for the points $x = \pm 1$ and leads to the ansatz (3.58,3.61) where the only 3 constants left to be found can be fixed by the large x asymptotics of the quasi-momenta.

One can then read of the energy shift from the large x asymptotics of the quasi-momenta

$$\delta E = \sum_n (N_n^{\tilde{1}\tilde{3}} + N_n^{\tilde{2}\tilde{4}}) \frac{x_n^{\tilde{1}\tilde{3}}(m+n) - \mathcal{J} - K(x_n^{\tilde{1}\tilde{3}})}{\kappa} + N_n^{\tilde{1}\tilde{4}} \frac{n x_n^{\tilde{1}\tilde{4}} - 2\mathcal{J}}{\kappa} + N_n^{\tilde{2}\tilde{3}} \frac{2m+n}{x_n^{\tilde{2}\tilde{3}}\kappa} \quad (3.35)$$

in terms of the positions of the roots obtained from the original algebraic curve through (3.14).

Fermionic excitations

We have 8 fermionic excitations but since $\hat{p}_1 = \hat{p}_2 = -\hat{p}_3 = -\hat{p}_4$ and $\tilde{p}_{1,2} = -\tilde{p}_{4,3}$ we will get the same result for the $(\hat{1}\hat{3}, \hat{2}\hat{3}, \hat{3}\hat{2}, \hat{4}\hat{2})$ poles and possibly another result for the $(\hat{1}\hat{4}, \hat{2}\hat{4}, \hat{3}\hat{1}, \hat{4}\hat{1})$ excitations. We can repeat the same kind of calculations we did for the

S^5 excitations to fix completely the quasi-momenta – see Appendix C.2. Then, from the asymptotics (3.19) we get

$$\delta\Delta = \sum_n \left(N_n^{\hat{1}\hat{3}} + N_n^{\hat{2}\hat{3}} + N_n^{\hat{3}\hat{2}} + N_n^{\hat{4}\hat{2}} \right) \frac{m+n}{x_n^{\hat{1}\hat{3}}\kappa} + \left(N_n^{\hat{1}\hat{4}} + N_n^{\hat{2}\hat{4}} + N_n^{\hat{3}\hat{1}} + N_n^{\hat{4}\hat{1}} \right) \frac{n x_n^{\hat{1}\hat{4}} - \mathcal{J} - \kappa}{\kappa} \quad (3.36)$$

3.3.3 The circular string in AdS_3 , the 1 cut $\mathfrak{sl}(2)$ solution

In section 3.3.2 we analyzed in detail a simple $\mathfrak{su}(2)$ solution with a particular mode number $k = -2m$. In Appendix D we repeat the analysis for the general $\mathfrak{sl}(2)$ circular string [83, 84] which also corresponds to a 1-cut algebraic curve but this time with an arbitrary mode number k for the cut [19]. This solution is again contained in the family of circular strings written in section 3.2. It corresponds to two non zero spins

$$S_1 = S, \quad \mathcal{J}_1 = \mathcal{J}$$

with mode numbers $m_1 = m, k_1 = k$ constrained by the level matching condition

$$Sk + \mathcal{J}m = 0$$

and frequencies $w_1 = \mathcal{J}$ and $w_1 = w$ fixed by

$$w^3 - (k^2 + m^2 + \mathcal{J}^2)w + 2km\mathcal{J} = 0. \quad (3.37)$$

For this solution $\kappa = \sqrt{w^2 - k^2}$ and the energy can be found from

$$\mathcal{E} = \kappa \left(1 + \frac{S}{w} \right) \quad (3.38)$$

In Appendix D we present the quasi-momenta associated to this classical solution and compute the fluctuation frequencies as we did for the $\mathfrak{su}(2)$ string. These results, together with the ones for the $\mathfrak{su}(2)$ circular string, are summarized and discussed in the following sections.

3.4 Results, interpretation and 1-loop shift

IN THIS SECTION we list all our results and introduce the notations usually used in the literature. In the next section we shall analyze them, compare them and draw some conclusions.

3.4.1 Simple $\mathfrak{su}(2)$ circular string

In section 3.3.2 we found the level spacings around the simple $\mathfrak{su}(2)$ circular solution, that is the fluctuation frequencies of the effective quadratic Lagrangian obtained by expanding the Metsaev-Tseytlin action (1.5) around this classical solution. In [82] this computation was performed having in mind the stability analysis and computation of the one loop shift. The various frequencies and corresponding degeneracies and origin can be summarized in table 3.1⁴. Using the notation introduced in this table we can replace the

Tab. 3.1: Simple $\mathfrak{su}(2)$ frequencies

	eigenmodes	notation
\mathbf{S}^5	$\sqrt{2\mathcal{J}^2 + n^2 \pm 2\sqrt{\mathcal{J}^4 + n^2\mathcal{J}^2 + m^2n^2}}$ $\sqrt{\mathcal{J}^2 + n^2 - m^2}$	$\omega_n^{S_{\pm}}$ ω_n^S
Fermions	$\sqrt{\mathcal{J}^2 + n^2}$	ω_n^F
AdS₅	$\sqrt{\mathcal{J}^2 + n^2 + m^2}$	ω_n^A

explicit expressions for the position of the roots found from (3.14) and recast our results (3.32,3.35,3.36) as

$$\begin{aligned}
\kappa \delta E &= \sum_n \left(N_n^{\hat{1}\hat{3}} + N_n^{\hat{2}\hat{4}} \right) \left(\omega_{n+m}^S - \mathcal{J} \right) + N_n^{\hat{2}\hat{3}} \omega_{n+2m}^{S_-} + N_n^{\hat{1}\hat{4}} \left(\omega_n^{S_+} - 2\mathcal{J} \right) \\
&+ \sum_n \left(N_n^{\hat{1}\hat{4}} + N_n^{\hat{2}\hat{4}} + N_n^{\hat{3}\hat{1}} + N_n^{\hat{4}\hat{1}} \right) \left(\omega_n^F - \mathcal{J} + \frac{\kappa}{2} \right) \\
&+ \sum_n \left(N_n^{\hat{1}\hat{3}} + N_n^{\hat{2}\hat{3}} + N_n^{\hat{3}\hat{2}} + N_n^{\hat{4}\hat{2}} \right) \left(\omega_{n+m}^F - \frac{\kappa}{2} \right) \\
&+ \sum_n \left(N_n^{\hat{1}\hat{3}} + N_n^{\hat{1}\hat{4}} + N_n^{\hat{2}\hat{3}} + N_n^{\hat{2}\hat{4}} \right) \omega_n^A.
\end{aligned} \tag{3.39}$$

We notice the appearance of constant shifts and relabeling of the frequencies when compared to those in table 3.1. We shall discuss this point below.

⁴ By expanding the GS action without imposing the Virasoro conditions from the beginning, one obtains, apart from the frequencies listed in the above table, some massless modes with $\omega = n$ [81]. In the chapter 5 we will see this Virasoro modes from the Bethe ansatz point of view if an extra level of particles with rapidities θ is introduced [86]

3.4.2 General $\mathfrak{sl}(2)$ circular string

The same analysis can be carried over for the $\mathfrak{sl}(2)$ circular string. In [83, 84] this frequencies were computed and the result can be summarized in table 3.2⁵.

Tab. 3.2: General $\mathfrak{sl}(2)$ frequencies

	eigenmodes	notation
AdS₅	$\frac{(\omega^2 - n^2)^2}{\sqrt{n^2 + \kappa^2}} + \frac{4\mathcal{S}}{w}\kappa^2\omega^2 - \frac{4\mathcal{E}}{\kappa}(\omega w - kn)^2 = 0$	$\omega_n^{A+} > \omega_n^{A-}$ ω_n^A
Fermions	$\sqrt{\left(n + \frac{\sqrt{w^2 - \mathcal{J}^2}}{2}\right)^2 + \frac{1}{2}(\kappa^2 + \mathcal{J}^2 - m^2)}$	ω_n^F
S⁵	$\sqrt{\mathcal{J}^2 + n^2 - m^2}$	ω_n^S

In the notation of the above table, the results (3.78),(3.73),(3.66)(3.65) derived in Appendix D can be put together as

$$\begin{aligned}
\kappa \delta E = & \sum_n \left(N_n^{\hat{1}\hat{3}} + N_n^{\hat{2}\hat{4}} \right) \omega_n^A + N_n^{\hat{2}\hat{3}} \left(\omega_{n-k}^{A-} + w \right) + N_n^{\hat{1}\hat{4}} \left(\omega_{n+k}^{A+} - w \right) \\
& + \sum_n \left(N_n^{\hat{2}\hat{3}} + N_n^{\hat{2}\hat{4}} + N_n^{\hat{3}\hat{1}} + N_n^{\hat{3}\hat{2}} \right) \left(\omega_{n+m/2-k/2}^F - \omega_{m/2-k/2}^F + \frac{1}{2}\kappa \right) \\
& + \sum_n \left(N_n^{\hat{1}\hat{3}} + N_n^{\hat{1}\hat{4}} + N_n^{\hat{4}\hat{1}} + N_n^{\hat{4}\hat{2}} \right) \left(\omega_{-n-m/2-k/2}^F - \omega_{-m/2-k/2}^F + \frac{1}{2}\kappa \right) \\
& + \sum_n \left(N_n^{\tilde{1}\tilde{3}} + N_n^{\tilde{1}\tilde{4}} + N_n^{\tilde{2}\tilde{3}} + N_n^{\tilde{2}\tilde{4}} \right) \left(\omega_{n+m}^S - \mathcal{J} \right). \tag{3.40}
\end{aligned}$$

3.4.3 Explanation of shifts

Let us first look at the $\mathfrak{su}(2)$ result (3.39) and pick one if the frequencies, say the first one

$$\omega_{n+m}^S - \mathcal{J}. \tag{3.41}$$

We find two kinds of shifts relatively to the frequencies listed in the table 1, namely the constant shift \mathcal{J} and the shift in the fourier mode $n \rightarrow n + m$. The same shifts we observe for the $\mathfrak{sl}(2)$ frequencies.

⁵ The results in this table are slightly simplified compared to those usually presented in the literature, especially the fermionic frequencies.

Let us understand the origin of this shifts. For that purpose consider a system of two harmonic oscillators,

$$L_x = \frac{\dot{x}_1^2 + \dot{x}_2^2}{2} - \frac{\omega^2}{2} (x_1^2 + x_2^2) ,$$

and suppose that, instead of quantizing this system, we chose to quantize the system obtained by rotating x_1, x_2 with angular velocity \mathcal{J} , i.e. we move to the y frame

$$x_1 + ix_2 = (y_1 + iy_2) e^{i\mathcal{J}t} . \quad (3.42)$$

Then, we obtain⁶

$$H_y = H_x + \mathcal{J}L_z ,$$

where L_z is the usual angular momentum, so that

$$E_{n_1, n_2}^y = \omega + (\omega - \mathcal{J}) n_1 + (\omega + \mathcal{J}) n_2 .$$

Thus for the radially symmetric wave function, for which $n_1 = n_2$ (and in particular for the ground state energy), the constant shifts cancel and we obtain the same energies as for the first system. That, in general, the two results are different is obvious since the energy depends on the observer.

The constant shifts mentioned above have exactly this origin. In fact, when expanding the Metsaev-Tseytlin string action around the classical $\mathfrak{su}(2)$ circular string one obtains an effective *time and space dependent* Lagrangian whose σ, τ dependence can be killed by a change of frame

$$\delta X = R(\sigma, \tau) \delta Y \quad (3.43)$$

where δX are the (bosonic) components of the fluctuations and R is a time and space dependent rotation matrix – see for instance expression (2.14) in [82]⁷. The same kind of field redefinitions are also present for the fermion fields. The time dependence of the rotation matrix gives the constant shifts as in the simple example we just considered while the space dependence in this change of frame is responsible for the relabeling of the mode numbers.

To make contact with the algebraic curve let us return to the frequency (3.41) we picked as illustration. It corresponds to a pole from sheet \tilde{p}_1 to \tilde{p}_3 (or from \tilde{p}_2 to \tilde{p}_4)

⁶ In the y frame the Lagrangian takes the form $2L_y = \dot{y}_1^2 + \dot{y}_2^2 - (\omega^2 - \mathcal{J}^2) (x_1^2 + x_2^2) + 2\mathcal{J}y_1\dot{y}_2 - 2\mathcal{J}\dot{y}_1y_2$.

⁷ The same is true for the $\mathfrak{sl}(2)$ circular string. The authors have moved to a different frame through a time and space dependent rotation – see for instance equation 4.11 in [84] – and should, therefore, measure shifted energies.

whose position is fixed by (3.14). The result in the rotated frame, ω_n^S , would correspond to a pole with mode number $n + m$ whose position is given by

$$\tilde{p}_1(x_n^{\tilde{1}\tilde{3}}) - \tilde{p}_3(x_n^{\tilde{1}\tilde{3}}) = 2\pi n + 2\pi m. \quad (3.44)$$

When plugging the actual expressions (3.30) for \tilde{p}_1 and \tilde{p}_3 in this equation we see that the $2\pi m$ disappears and the equation looks simpler than (3.14). However, for several cut solutions there is no such obvious choice of mode numbers (or field redefinition which kills the time dependence in the Lagrangian).

3.4.4 1-loop shift and prescription for labeling fluctuation frequencies

To compute the 1-loop shift to the classical energy of a given solution, according to [47], one has to sum over all energies of the modes in the expansion around the classical configuration

$$\delta E_{1\text{-loop}} = \frac{1}{2\kappa} \lim_{N \rightarrow \infty} \sum_{n=-N}^N \left(\sum_{i=1}^8 \Omega_{i,n}^B - \sum_{i=1}^8 \Omega_{i,n}^F \right). \quad (3.45)$$

However, the right hand side is hard to define rigorously. For $n \rightarrow \pm\infty$ each frequency behaves like

$$\Omega_{i,n}^B \simeq |n| \pm c_i^B + d_i^B, \quad \Omega_{i,n}^F \simeq |n| \pm c_i^F + d_i^F, \quad (3.46)$$

and thus the sum is sensible to the labeling of the frequencies. The seemingly innocent redefinition

$$\Omega_{i,n}^B \rightarrow \Omega_{i,n+k_i}^B, \quad \Omega_{i,n}^F \rightarrow \Omega_{i,n+l_i}^F, \quad (3.47)$$

with integer shifts constrained by $\sum_i k_i - l_i = 0$ to ensure the convergence of the sum, *does* change the result

$$\delta E_{1\text{-loop}} \rightarrow \delta E_{1\text{-loop}} + \sum (k_i^2 - l_i^2 + 2c_i^B k_i - 2c_i^F l_i). \quad (3.48)$$

In appendix E we discuss in greater detail the effect of these shifts.

One way to compute the frequencies is to expand the Metsaev-Tseytlin action around some classical solution. Generically, the resulting quadratic Lagrangian is time and space dependent. To eliminate this dependence, when possible, a field redefinition is performed. However, there are several ways to do the field redefinition to get a time and space independent action. Different choices will give different sets of frequencies related by transformations like (3.47) and will therefore lead to different results. In appendix E we analyze this kind of dangers by focusing on two explicit examples. Thus we need a solid prescription for the labeling of the frequencies.

Suppose we were semi-classically quantizing around some classical string solution in flat space. Then we would expect to find some fluctuation frequencies, the zero modes,

corresponding to an overall translation of the string solution and which should, therefore, carry no energy at all. Then the usual prescription is to take $\Omega_{i,0} = 0$.

The zero modes should also exist for a string in the $AdS_5 \times S^5$ space with a large amount of isometries. Indeed, let us take our results and denote the contribution at $n = 0$ in (3.39) and (3.40) by $\delta E_0^{\mathfrak{su}(2)}$ and $\delta E_0^{\mathfrak{sl}(2)}$. Then we find that they are equal and given by

$$\delta E_0 = \sum_{AdS^5} N_{ij} + \frac{1}{2} \sum_{Ferm} N_{ij}. \quad (3.49)$$

In other words, the contribution to the anomalous part $\delta\Delta$ of zero modes for our labeling is zero! Thus the prescription we used seems to be the precise analogue of the flat space fourier modes prescription.

Moreover, by construction, we have a good BMN limit. That is, when in the limit of very small cuts with $m \rightarrow 0$ we recover the result (3.26) without any unusual shifts⁸.

Then, from (3.39) and (3.40), we can write the 1-loop shifts for the 1-cut circular solutions⁹

$$E_{1-loop}^{\mathfrak{su}(2)} = \frac{1}{2\kappa} \lim_{N \rightarrow \infty} \sum_{n=-N}^N 4\omega_n^A + \omega_{n+m}^S + \omega_{n+2m}^{S_-} + \omega_n^{S_+} - 4\omega_n^F - 4\omega_{n+m}^F,$$

$$E_{1-loop}^{\mathfrak{sl}(2)} = \frac{1}{2\kappa} \lim_{N \rightarrow \infty} \sum_{n=-N}^N 2\omega_n^A + \omega_{n+k}^{A_+} + \omega_{n-k}^{A_-} + 4\omega_{n+m}^S - 4\omega_{n+\frac{m-k}{2}}^F - 4\omega_{-n-\frac{m+k}{2}}^F.$$

3.4.5 General $\mathfrak{su}(2)$ results

Another interesting solution contained in the family of circular solutions described in section 3.2 is the generalization of the simple $\mathfrak{su}(2)$ solution to the case of two non-equal spins $\mathcal{J}_{1,2}$ with two different mode numbers $m_{1,2}$. The fluctuation frequencies associated with this solution can be listed in table 3.3 [83]¹⁰

Now, armed with our prescription, we can write the one loop shift unambiguously. Imposing

⁸ This is not the case for the frequencies listed in table 2 for instance. For example, from this expression, we find, for the fermionic frequencies, $\omega_n^F \simeq \sqrt{(n+k/2)^2 + \mathcal{J}^2}$. See also discussion in Appendix E.

⁹ As for the simple example of the harmonic oscillators in the previous section, the sum of all constant shifts appearing in (3.39) and (3.40) cancel so that only the shifts in mode number lead to a change of the final result. The difference with respect to the sum with no shifts can be obtained from (3.48) and is equal to m^2/κ in both cases.

¹⁰ The fermionic frequencies for the general circular string of section 3.2 can be computed (we shall publish our findings elsewhere). In particular, for the $\mathfrak{su}(2)$ general circular string we find the results listed in table 3.3.

Tab. 3.3: General $\mathfrak{su}(2)$ frequencies

	eigenmodes	notation
S^5	$(\omega^2 - n^2)^2 - \frac{4\mathcal{J}_2}{w_2} (\omega w_1 - m_1 n)^2 - \frac{4\mathcal{J}_1}{w_1} (\omega w_2 - m_2 n)^2 = 0$ $\sqrt{n^2 + v^2}$	$\omega_n^{S+} > \omega_n^{S-}$ ω_n^S
Fermions	$\sqrt{\left(n - \frac{\sqrt{w_1^2 + m_2^2 - \kappa^2}}{2}\right)^2 + \mathcal{J}_1 w_1 + \mathcal{J}_2 w_2}$	ω_n^F
AdS_5	$\sqrt{n^2 + \kappa^2}$	ω_n^A

- Good BMN limit (3.26) for vanishing filling fractions,
- Proper zero mode behavior with $n = 0$ frequencies having trivial anomalous, part (3.49).
- For $m_1 = -m_2 = m$ we should retrieve the simple $\mathfrak{su}(2)$ result (3.39),

we get (for $m_1 + m_2 \leq 0$)

$$\begin{aligned}
\kappa \delta E &= \sum_n \left(N_n^{\hat{1}\hat{3}} + N_n^{\hat{2}\hat{4}} \right) \left(\omega_{n+m_1}^S - w_1 \right) + N_n^{\hat{2}\hat{3}} \left(\omega_{n+m_1-m_2}^{S-} + w_2 - w_1 \right) \\
&+ \sum_n N_n^{\hat{1}\hat{4}} \left(\omega_{n+m_1+m_2}^{S+} - w_2 - w_1 \right) + \sum_n \left(N_n^{\hat{1}\hat{3}} + N_n^{\hat{1}\hat{4}} + N_n^{\hat{2}\hat{3}} + N_n^{\hat{2}\hat{4}} \right) \omega_n^A \\
&+ \sum_n \left(N_n^{\hat{1}\hat{4}} + N_n^{\hat{2}\hat{4}} + N_n^{\hat{3}\hat{1}} + N_n^{\hat{4}\hat{1}} \right) \left(\omega_{n+\frac{m_1+m_2}{2}}^F - \omega_{\frac{m_1+m_2}{2}}^F + \frac{\kappa}{2} \right) \\
&+ \sum_n \left(N_n^{\hat{1}\hat{3}} + N_n^{\hat{2}\hat{3}} + N_n^{\hat{3}\hat{2}} + N_n^{\hat{4}\hat{2}} \right) \left(\omega_{-n-\frac{m_1-m_2}{2}}^F - \omega_{-\frac{m_1-m_2}{2}}^F + \frac{\kappa}{2} \right).
\end{aligned}$$

3.5 Summary

IN THIS CHAPTER we explain how to compute the quantum fluctuations around *any* classical superstring motion in $AdS_5 \times S^5$. These excitations include the fermionic, AdS_5 and S^5 modes. We showed that each mode correspond to adding a pole to a specific pair of sheets i, j of the algebraic curve. The position of the pole is determined from the equation

$$p_i(x_n^{ij}) - p_j(x_n^{ij}) = 2\pi n, \quad (3.50)$$

and thus provides one with an *unambiguous* labeling for the frequencies. In particular we observe the nice feature that for $n = 0$ this equation prescribes the pole at infinity,

that is we find the expected zero modes associated with global transformations under the isometries of the target superspace.

Technically we computed the change in quasi-momenta due to the addition of these new poles and read, from the large x asymptotics, the global charge corresponding to the AdS Energy, that is the frequencies. However, since we computed explicitly the perturbed quasi-momenta we have obtained not only the energy shift but actually all conserved charges!

In the next chapters we will use this method to prove some general statements about the quasi-classical spectrum around *any* classical string solution.

Appendix A: Quasi-momenta for a generic rigid circular string

To establish the link between the embedding coordinates solution (3.10) with the coset's notations we introduce the matrices

$$\mathcal{R} = \prod_{i=1}^3 e^{\frac{i}{2}(w_i\tau + m_i\sigma)\Phi_i} \cdot \mathcal{R}_0 \in SU(4)$$

and

$$\mathcal{Q} = e^{\frac{i}{2}\kappa\tau\Phi_1} \cdot \prod_{i=1}^2 e^{-\frac{i}{2}(w_i\tau + k_i\sigma)\Phi_{i+1}} \cdot \mathcal{Q}_0 \in SU(2,2).$$

where Φ_i are the Cartan generators,

$$\Phi_1 = \text{diag}(+, +, -, -), \quad \Phi_2 = \text{diag}(+, -, +, -), \quad \Phi_3 = \text{diag}(-, +, +, -),$$

and $\mathcal{R}_0 = e^{\Phi_{42}\theta} e^{\Phi_{64}\gamma}$ and $\mathcal{Q}_0 = e^{\Phi'_{42}\psi} e^{\Phi'_{64}\rho}$ are constant matrices with

$$\begin{aligned} (\cos \gamma, \sin \gamma \cos \theta, \sin \gamma \sin \theta) &= \left(\sqrt{\frac{\mathcal{J}_1}{w_1}}, \sqrt{\frac{\mathcal{J}_2}{w_2}}, \sqrt{\frac{\mathcal{J}_3}{w_3}} \right), \\ (\cosh \rho, \sinh \rho \cos \psi, \sinh \rho \sin \psi) &= \left(\sqrt{\frac{\mathcal{E}}{\kappa}}, \sqrt{\frac{\mathcal{S}_1}{w_1}}, \sqrt{\frac{\mathcal{S}_2}{w_2}} \right) \end{aligned}$$

and $\Phi_{42}, \Phi_{64}, \Phi'_{42}, \Phi'_{64}$ given respectively by

$$\frac{1}{2} \begin{pmatrix} 0 & -1 & 0 & 0 \\ 1 & 0 & 0 & 0 \\ 0 & 0 & 0 & -1 \\ 0 & 0 & 1 & 0 \end{pmatrix}, \begin{pmatrix} 0 & 0 & 0 & 0 \\ 0 & 0 & -1 & 0 \\ 0 & 1 & 0 & 0 \\ 0 & 0 & 0 & 0 \end{pmatrix}, \frac{1}{2} \begin{pmatrix} 0 & -1 & 0 & 0 \\ 1 & 0 & 0 & 0 \\ 0 & 0 & 0 & 1 \\ 0 & 0 & -1 & 0 \end{pmatrix}, \frac{1}{2} \begin{pmatrix} 0 & 0 & 0 & 1 \\ 0 & 0 & -1 & 0 \\ 0 & -1 & 0 & 0 \\ 1 & 0 & 0 & 0 \end{pmatrix}.$$

Let us ignore for a moment the fact that, for a generic choice of mode numbers m_i, k_j , these matrices are not always periodic. Then, to describe the circular solutions we can use, as representative $g \in PSU(2, 2|4)$, the block diagonal matrix

$$g = \left(\begin{array}{c|c} \mathcal{Q} & 0 \\ \hline 0 & \mathcal{R} \end{array} \right), \quad (3.51)$$

which indeed leads to (3.10) under the map (1.7).

What is particular about this solution is that, as follows trivially from the form of the matrices \mathcal{R} and \mathcal{Q} , the current

$$J = -g^{-1}dg,$$

and therefore also the flat connection $A(x)$ in (1.12), are constant matrices! Then the computation of (1.13) is trivial and the quasi-momenta $p(x)$ are simply obtained from the eigenvalues of $\frac{2\pi}{i}A(x)$.

Before going on let us comment on the subtle point ignored above – the periodicity of the rotation matrices \mathcal{R} (and \mathcal{Q}). For some integers m_i we see that this matrix could become anti-periodic. This means that in principle we should use another representative, $\mathcal{R}^{periodic}$, for which we should still have (1.7) but which should be periodic. However, if both \mathcal{R} and $\mathcal{R}^{periodic}$ obey these equations this means that they are related by an anti-periodic $SP(4)$ gauge transformation. This means that for the purpose of computing the quasi-momenta $p(x)$ we can indeed always use the element (3.51) provided we keep in mind that if \mathcal{R} is antiperiodic we can recover the real quasi-momenta through

$$\begin{aligned} & \{e^{i\hat{p}_1}, e^{i\hat{p}_2}, e^{i\hat{p}_3}, e^{i\hat{p}_4} | e^{i\tilde{p}_1}, e^{i\tilde{p}_2}, e^{i\tilde{p}_3}, e^{i\tilde{p}_4}\} \quad \text{For the true} \\ & \hspace{15em} \text{representative } \mathcal{R}^{periodic} \\ & = \{e^{i\hat{p}_1}, e^{i\hat{p}_2}, e^{i\hat{p}_3}, e^{i\hat{p}_4} | -e^{i\tilde{p}_1}, -e^{i\tilde{p}_2}, -e^{i\tilde{p}_3}, -e^{i\tilde{p}_4}\} \quad \text{Using the anti - periodic} \\ & \hspace{15em} \mathcal{R}^{instead} \end{aligned}$$

The same kind of statement hold for the AdS element \mathcal{Q} .

The computation of the quasi-momenta is then straightforward. The S^5 components

\tilde{p}_i are given in terms of the eigenvalues¹¹ of the symmetric matrix

$$\tilde{A}(x) = \pi \begin{pmatrix} -\tilde{a}_+(1/x) & \tilde{b}_+ & -\tilde{c}(1/x) & \tilde{d}(x) \\ \tilde{b}_+ & \tilde{a}_+(x) & \tilde{d}(1/x) & \tilde{c}(x) \\ -\tilde{c}(1/x) & \tilde{d}(1/x) & \tilde{a}_-(x) & \tilde{b}_- \\ \tilde{d}(x) & \tilde{c}(x) & \tilde{b}_- & -\tilde{a}_-(1/x) \end{pmatrix} \quad (3.52)$$

with

$$\begin{aligned} \tilde{a}_\pm(x) &= \pm \tilde{a}(x) - m_3 \cos \theta \\ \tilde{a}(x) &= -\frac{m_1 - w_1 x + (m_2 - w_2 x) \cos \theta + x \cos 2\gamma (-w_1 + m_1 x + (w_2 - m_2 x) \cos \theta)}{x^2 - 1} \\ \tilde{b}_\pm &= (m_2 \mp m_3) \cos \gamma \sin \theta \\ \tilde{c}(x) &= \frac{(m_2 + m_3)x^2 - (m_2 - m_3) - 2w_3 x}{x^2 - 1} \sin \gamma \sin \theta \\ \tilde{d}(x) &= \frac{-m_1 + w_1 x + (m_2 - w_2 x) \cos \theta}{x^2 - 1} \sin 2\gamma \end{aligned}$$

while the AdS quasi-momenta \hat{p}_i are the eigenvalues of

$$\hat{A}(x) = \pi \begin{pmatrix} -\hat{a}_+(1/x) & \hat{b}_+ & -\hat{c}(x) & \hat{d}(x) \\ \hat{b}_+ & \hat{a}_+(x) & \hat{d}(x) & \hat{c}(x) \\ \hat{c}(x) & -\hat{d}(x) & \hat{a}_-(x) & \hat{b}_- \\ -\hat{d}(x) & -\hat{c}(x) & \hat{b}_- & -\hat{a}_-(1/x) \end{pmatrix} \quad (3.53)$$

with

$$\begin{aligned} \hat{a}_\pm(x) &= \pm \frac{2\pi\kappa - k_1 (x^2 - 1) \cos \theta}{x^2 - 1} \cosh \rho + k_2 \cos \psi \\ \hat{b}_\pm &= (k_2 \cosh \rho \mp k_1) \sin \psi \\ \hat{c}(x) &= \frac{k_2 (x^2 + 1) - 2w_2 x}{x^2 - 1} \sin \psi \sinh \rho \\ \hat{d}(x) &= \frac{k_1 (x^2 + 1) - 2w_1 x}{x^2 - 1} \cos \psi \sinh \rho \end{aligned}$$

For the simple $\mathfrak{su}(2)$ or $\mathfrak{sl}(2)$ solutions we have, amongst other conditions, $\theta = \psi = 0$ which simplifies the computation drastically.

¹¹ To each eigenvalues we might need to add a multiple of π in such a way that its asymptotics become those prescribed in section 1.1.1. If \mathcal{R} is periodic this multiple should contain an even number of π 's whereas if it is anti-periodic, we should add πn with n odd to each quasi-momenta – see discussion in the text.

Appendix B: BMN string, details

This appendix serves as a complement to section 3.3.1. The quasi-momenta with the correct poles located at (3.23) and residues given by (3.21) is given by

$$\begin{aligned}\delta\hat{p}_2 &= \hat{a} + \frac{\delta\alpha_+}{x-1} + \frac{\delta\alpha_-}{x+1} + \sum_{i=\hat{3},\hat{4},\tilde{3},\tilde{4}} \sum_n \frac{\alpha(x_n^{\hat{2}i})N_n^{\hat{2}i}}{x-x_n^{\hat{2}i}} - \sum_{i=\hat{3},\hat{4},\tilde{3},\tilde{4}} \sum_n \frac{\alpha(x_n^{\hat{1}i})N_n^{\hat{1}i}}{1/x-x_n^{\hat{1}i}} \\ \delta\hat{p}_3 &= \hat{b} + \frac{\delta\beta_+}{x-1} + \frac{\delta\beta_-}{x+1} - \sum_{i=\hat{1},\hat{2},\tilde{1},\tilde{2}} \sum_n \frac{\alpha(x_n^{\hat{3}i})N_n^{\hat{3}i}}{x-x_n^{\hat{3}i}} + \sum_{i=\hat{1},\hat{2},\tilde{1},\tilde{2}} \sum_n \frac{\alpha(x_n^{\hat{4}i})N_n^{\hat{4}i}}{1/x-x_n^{\hat{4}i}}\end{aligned}$$

where the last term guaranties that $\delta\hat{p}_{1,4}(x) = -\delta\hat{p}_{2,3}(1/x)$ have the right poles with the appropriate residues in the physical domain. Analogously

$$\delta\tilde{p}_2 = \tilde{a} + \frac{\delta\alpha_+}{x-1} + \frac{\delta\alpha_-}{x+1} - \sum_{i=\hat{3},\hat{4},\tilde{3},\tilde{4}} \sum_n \frac{\alpha(x_n^{\tilde{2}i})N_n^{\tilde{2}i}}{x-x_n^{\tilde{2}i}} + \sum_{i=\hat{3},\hat{4},\tilde{3},\tilde{4}} \sum_n \frac{\alpha(x_n^{\tilde{1}i})N_n^{\tilde{1}i}}{1/x-x_n^{\tilde{1}i}} \quad (3.54)$$

$$\delta\tilde{p}_3 = \tilde{b} + \frac{\delta\beta_+}{x-1} + \frac{\delta\beta_-}{x+1} + \sum_{i=\hat{1},\hat{2},\tilde{1},\tilde{2}} \sum_n \frac{\alpha(x_n^{\tilde{3}i})N_n^{\tilde{3}i}}{x-x_n^{\tilde{3}i}} - \sum_{i=\hat{1},\hat{2},\tilde{1},\tilde{2}} \sum_n \frac{\alpha(x_n^{\tilde{4}i})N_n^{\tilde{4}i}}{1/x-x_n^{\tilde{4}i}} \quad (3.55)$$

and $\delta\tilde{p}_{1,4}(x) = -\delta\tilde{p}_{2,3}(1/x)$. From the large x behavior of these quasi-momenta one obtains

$$\begin{aligned}\hat{a} &= -\sum_n \frac{2\pi n}{\sqrt{\lambda}\mathcal{J}} \sum_{i=\hat{3},\hat{4},\tilde{3},\tilde{4}} N_n^{\hat{1}i}, & \hat{b} &= +\sum_n \frac{2\pi n}{\sqrt{\lambda}\mathcal{J}} \sum_{i=\hat{1},\hat{2},\tilde{1},\tilde{2}} N_n^{\hat{4}i}, \\ \tilde{a} &= +\sum_n \frac{2\pi n}{\sqrt{\lambda}\mathcal{J}} \sum_{i=\hat{3},\hat{4},\tilde{3},\tilde{4}} N_n^{\tilde{1}i}, & \tilde{b} &= -\sum_n \frac{2\pi n}{\sqrt{\lambda}\mathcal{J}} \sum_{i=\hat{1},\hat{2},\tilde{1},\tilde{2}} N_n^{\tilde{4}i},\end{aligned}$$

the level matching condition (3.20) and

$$\begin{aligned}\delta\alpha^+ - \delta\alpha^- &= -\sum_n \frac{2\pi n}{\sqrt{\lambda}\mathcal{J}} \sum_{i=\hat{3},\hat{4},\tilde{3},\tilde{4}} \sum_{j=\hat{1},\hat{2}} N_n^{ij}, \\ \delta\beta^+ - \delta\beta^- &= -\sum_n \frac{2\pi n}{\sqrt{\lambda}\mathcal{J}} \sum_{i=\hat{3},\hat{4},\tilde{3},\tilde{4}} \sum_{j=\tilde{3},\tilde{4}} N_n^{ij}.\end{aligned}$$

Appendix C: $\mathfrak{su}(2)$ circular string, details

In this appendix we present the details of the calculations from section 3.3.2 of the fluctuation frequencies around the 1-cut $\mathfrak{su}(2)$ solution.

C.1 S^5 modes

We start from the ansatz (3.31). We have four types of poles ($\tilde{1}\tilde{3}, \tilde{2}\tilde{4}, \tilde{2}\tilde{3}, \tilde{1}\tilde{4}$). Thus

$$f(x) = \frac{1}{2} (\delta\tilde{p}_2(x) + \delta\tilde{p}_3(x)) \quad (3.56)$$

must have simple poles at $x_n^{\tilde{2}\tilde{4}}, x_n^{\tilde{1}\tilde{3}}$ with residues $\frac{1}{2}\alpha(x_n^{\tilde{1}\tilde{3}})$ and $-\frac{1}{2}\alpha(x_n^{\tilde{2}\tilde{4}})$ respectively (see fig.3.3 or (3.21)). The same holds for

$$f(1/x) = -\frac{1}{2} (\delta\tilde{p}_4(x) + \delta\tilde{p}_1(x)) . \quad (3.57)$$

Moreover, since the residues of $\delta\tilde{p}_i$ are connected to the AdS quasi-momenta (1.22) and these are given by (3.33) we conclude that $f(x)$ should be regular at $x = \pm 1$. Thus we obtain

$$f(x) = -\sum_n \left(\frac{N_n^{\tilde{2}\tilde{4}}}{2} \left[\frac{\alpha(x_n^{\tilde{2}\tilde{4}})}{x - x_n^{\tilde{2}\tilde{4}}} + \frac{\alpha(x_n^{\tilde{2}\tilde{4}})}{x_n^{\tilde{2}\tilde{4}}(1 - xx_n^{\tilde{2}\tilde{4}})} \right] - (\tilde{2}\tilde{4} \rightarrow \tilde{1}\tilde{3}) \right) \quad (3.58)$$

Then

$$g(x) = \frac{K(x)}{2} (\delta\tilde{p}_2(x) - \delta\tilde{p}_3(x)) \quad (3.59)$$

must have simple poles at $x_n^{\tilde{2}\tilde{4}}, x_n^{\tilde{1}\tilde{3}}$ and $x_n^{\tilde{2}\tilde{3}}$ with residues $-\frac{1}{2}\alpha(x_n^{\tilde{1}\tilde{3}})$, $-\frac{1}{2}\alpha(x_n^{\tilde{2}\tilde{4}})$ and $-\alpha(x_n^{\tilde{2}\tilde{3}})$ respectively while

$$g(1/x) = \frac{K(x)}{2} (\delta\tilde{p}_4(x) - \delta\tilde{p}_1(x)) \quad (3.60)$$

must have simple poles at $x_n^{\tilde{2}\tilde{4}}, x_n^{\tilde{1}\tilde{3}}$ and $x_n^{\tilde{1}\tilde{4}}$ with residues $\frac{1}{2}\alpha(x_n^{\tilde{1}\tilde{3}})$, $\frac{1}{2}\alpha(x_n^{\tilde{2}\tilde{4}})$ and $\alpha(x_n^{\tilde{1}\tilde{4}})$ respectively. Contrary to $f(x)$, this function may have poles at ± 1 so we arrive at

$$\begin{aligned} g(x) = & a + \frac{\alpha_-}{x^2 - 1} + \frac{x\alpha_+}{x^2 - 1} + \sum_n \left(N_n^{\tilde{1}\tilde{4}} \frac{\alpha(x_n^{\tilde{1}\tilde{4}})K(1/x_n^{\tilde{1}\tilde{4}})}{x_n^{\tilde{1}\tilde{4}}(1 - xx_n^{\tilde{1}\tilde{4}})} - N_n^{\tilde{2}\tilde{3}} \frac{\alpha(x_n^{\tilde{2}\tilde{3}})K(x_n^{\tilde{2}\tilde{3}})}{x - x_n^{\tilde{2}\tilde{3}}} \right) \\ & + \sum_n \left(\frac{N_n^{\tilde{2}\tilde{4}}}{2} \left[\frac{\alpha(x_n^{\tilde{2}\tilde{4}})K(1/x_n^{\tilde{2}\tilde{4}})}{x_n^{\tilde{2}\tilde{4}}(1 - xx_n^{\tilde{2}\tilde{4}})} - \frac{\alpha(x_n^{\tilde{2}\tilde{4}})K(x_n^{\tilde{2}\tilde{4}})}{x - x_n^{\tilde{2}\tilde{4}}} \right] + (\tilde{2}\tilde{4} \rightarrow \tilde{1}\tilde{3}) \right) . \end{aligned} \quad (3.61)$$

Finally the remaining constants are fixed by the large x asymptotic (3.19) to be

$$\begin{aligned} a &= -\frac{2\pi}{\sqrt{\lambda}} \sum_n \left[m(N_n^{\tilde{1}\tilde{3}} + N_n^{\tilde{2}\tilde{4}}) + 2mN_n^{\tilde{2}\tilde{3}} \right] \\ \alpha_+ &= \frac{2\pi}{\sqrt{\lambda}} \sum_n \left[(N_n^{\tilde{1}\tilde{3}} + N_n^{\tilde{2}\tilde{4}}) \left(x_n^{\tilde{1}\tilde{3}}(m+n) - \mathcal{J} - K(x_n^{\tilde{1}\tilde{3}}) \right) + N_n^{\tilde{1}\tilde{4}}(x_n^{\tilde{1}\tilde{4}}n - 2\mathcal{J}) + N_n^{\tilde{2}\tilde{3}} \frac{2m+n}{x_n^{\tilde{2}\tilde{3}}} \right] \\ \alpha_- &= \frac{2\pi}{\sqrt{\lambda}} \sum_n \left[N_n^{\tilde{1}\tilde{3}} + N_n^{\tilde{1}\tilde{4}} + N_n^{\tilde{2}\tilde{3}} + N_n^{\tilde{2}\tilde{4}} \right] n . \end{aligned}$$

Then, from the residue at $x = 1$ we read $\delta E = \frac{\alpha_+}{\sqrt{m^2 + \mathcal{J}^2}}$.

C.2 Fermionic modes

Arguments similar to the ones in the previous section lead to

$$f(x) = \frac{2\pi}{\sqrt{\lambda}} \frac{x}{x^2 - 1} \sum_n \left[\frac{N_n^{\hat{1}\hat{4}} + N_n^{\hat{2}\hat{4}} - N_n^{\hat{3}\hat{1}} - N_n^{\hat{4}\hat{1}}}{xx_n^{\hat{1}\hat{4}} - 1} + x \frac{N_n^{\hat{3}\hat{2}} + N_n^{\hat{4}\hat{2}} - N_n^{\hat{1}\hat{3}} - N_n^{\hat{2}\hat{3}}}{x - x_n^{\hat{3}\hat{2}}} \right]$$

and

$$\begin{aligned} g(x) = & b + \frac{\beta_-}{x^2 - 1} + \frac{x\beta_+}{x^2 - 1} \\ & + \frac{2\pi}{\sqrt{\lambda}} \sum_n \left[\frac{\left(\sqrt{m^2 + \mathcal{J}^2} x_n + n(1 - x_n^2) \right) (N_n^{\hat{1}\hat{4}} + N_n^{\hat{2}\hat{4}} + N_n^{\hat{3}\hat{1}} + N_n^{\hat{4}\hat{1}})}{(1 - xx_n)(x_n^2 - 1)} \right. \\ & \left. - x_n \frac{\left(\sqrt{m^2 + \mathcal{J}^2} x_n + (n + m)(1 - x_n^2) \right) (N_n^{\hat{3}\hat{2}} + N_n^{\hat{4}\hat{2}} + N_n^{\hat{1}\hat{3}} + N_n^{\hat{2}\hat{3}})}{(x - x_n)(x_n^2 - 1)} \right] \end{aligned}$$

where

$$\begin{aligned} b &= \frac{2\pi m}{\sqrt{\lambda}} \sum_n (N_n^{\hat{1}\hat{3}} + N_n^{\hat{2}\hat{3}} + N_n^{\hat{1}\hat{3}} + N_n^{\hat{1}\hat{3}}) \\ \beta_- &= \frac{2\pi}{\sqrt{\lambda}} \sum_n \left(\frac{x_n \sqrt{m^2 + \mathcal{J}^2}}{x_n^2 - 1} - n \right) (N_n^{\hat{1}\hat{3}} + N_n^{\hat{1}\hat{4}} + N_n^{\hat{2}\hat{3}} + N_n^{\hat{2}\hat{4}} + N_n^{\hat{3}\hat{1}} + N_n^{\hat{3}\hat{2}} + N_n^{\hat{4}\hat{1}} + N_n^{\hat{4}\hat{2}}) \\ \beta_+ &= \frac{2\pi}{\sqrt{\lambda}} \sum_n \left[\left(\mathcal{J} - nx_n + \frac{x_n^2 \sqrt{m^2 + \mathcal{J}^2}}{x_n^2 - 1} \right) (N_n^{\hat{1}\hat{4}} + N_n^{\hat{2}\hat{4}} + N_n^{\hat{3}\hat{1}} + N_n^{\hat{4}\hat{1}}) \right. \\ & \quad \left. + \left(\frac{\sqrt{m^2 + \mathcal{J}^2}}{x_n^2 - 1} - \frac{m + n}{x_n} \right) (N_n^{\hat{1}\hat{3}} + N_n^{\hat{2}\hat{3}} + N_n^{\hat{3}\hat{2}} + N_n^{\hat{4}\hat{2}}) \right]. \end{aligned}$$

The AdS_5 part of the quasi-momenta is given by

$$\begin{aligned} \delta \hat{p}_2(x) &= \frac{2\pi}{\sqrt{\lambda}} \frac{x}{x^2 - 1} \left(+\delta\Delta - 2 \frac{N_n^{\hat{1}\hat{3}} + N_n^{\hat{1}\hat{4}}}{xx_n - 1} - 2x \frac{N_n^{\hat{2}\hat{3}} + N_n^{\hat{2}\hat{4}}}{x_n - x} \right) \\ \delta \hat{p}_3(x) &= \frac{2\pi}{\sqrt{\lambda}} \frac{x}{x^2 - 1} \left(-\delta\Delta + 2 \frac{N_n^{\hat{4}\hat{1}} + N_n^{\hat{4}\hat{2}}}{xx_n - 1} + 2x \frac{N_n^{\hat{3}\hat{1}} + N_n^{\hat{3}\hat{2}}}{x_n - x} \right) \end{aligned}$$

and $\delta \hat{p}_{1,4}(x) = -\delta \hat{p}_{2,3}(1/x)$. The constant Δ can be found from fixing the residues at ± 1 for $\delta \hat{p}_i$ and $\delta \tilde{p}_i$ to be equal (1.22) and is given in the main text (3.36).

Appendix D: $\mathfrak{sl}(2)$ circular string

The eigenvalues of (3.52) and (3.53) for the $\mathfrak{sl}(2)$ circular string described in the beginning of section 3.3.3 yield the most general 1-cut quasi-momentum connecting \hat{p}_2 and \hat{p}_3 (Due

to the $x \rightarrow 1/x$ symmetry, \hat{p}_1 and \hat{p}_4 will be also connected by a cut, but this will be in unphysical domain, that is inside the unit circle). Explicitly, we find

$$\tilde{p}_{1,2} = -\tilde{p}_{3,4} = 2\pi \frac{\mathcal{J}x + m}{x^2 - 1}. \quad (3.62)$$

and

$$\begin{pmatrix} \hat{p}_1 \\ \hat{p}_2 \\ \hat{p}_3 \\ \hat{p}_4 \end{pmatrix} = \begin{pmatrix} -\hat{p}_2(1/x) \\ +\hat{p}_2(x) \\ -\hat{p}_2(x) \\ +\hat{p}_2(1/x) \end{pmatrix}.$$

where [19]

$$\hat{p}_2 = k\pi \left(1 - \frac{(Cx + 1)\sqrt{x^2 - 2BCx + C^2}}{C(x^2 - 1)} \right). \quad (3.63)$$

and

$$w \equiv \frac{k}{2} \left(C + \frac{1}{C} \right), \quad B = 1 + \frac{2\mathcal{S}}{w}. \quad (3.64)$$

From all solutions of (3.37,3.64) for solutions for C and B we should pick the one for which we have a real cut outside the unit circle.

In the rest of this appendix we will excite this solution by adding poles to quasi-momenta as we did for the $\mathfrak{su}(2)$ solution. In this way we shall find the energy shifts around this classical solution. Moreover, as for the $\mathfrak{su}(2)$ string, we shall consider the AdS_5, S^5 and fermions separately, assuming for simplicity the Riemann identity (3.20) to be satisfied *for each of the sectors separately* – the result, as before, holds if we relax this stronger assumption.

D.1 The AdS_5 excitations

For these excitations the S^5 quasi-momenta remains untouched because its asymptotics do not change and it is still only allowed to have simple poles at ± 1 . Due to the Virasoro coupling of these quasi-momenta to the AdS_5 ones through the poles at ± 1 (1.22), we see that $\delta\hat{p}_i$ must have no poles at these points. The only poles of these quasi-momenta should be located at $x_n^{\hat{i}\hat{j}}$ with residues given by (3.21) – see fig.3.3. Finally, as explained in section 3.3.2, the perturbed quasi-momenta should have inverse square behavior close to the branch points of the classical solution.

Thus, from the same kind of reasoning we saw in the previous section for the $\mathfrak{su}(2)$ circular string, we find (3.67) for the AdS_3 excitations connecting sheets (\hat{p}_2, \hat{p}_3) and (\hat{p}_1, \hat{p}_4)

and (3.70) for the remaining AdS_5 excitations uniting (\hat{p}_1, \hat{p}_3) and (\hat{p}_2, \hat{p}_4) . From the large x behavior (3.19) of these quasi-momenta we read the energy shifts¹²

$$\delta E = \sum_n \left(N_n^{\hat{2}\hat{3}} \left[\frac{k - n}{k} \frac{x_n^{\hat{2}\hat{3}} - C^{-1}}{x_n^{\hat{2}\hat{3}} + C^{-1}} + \frac{nw}{k\kappa} \right] + N_n^{\hat{1}\hat{4}} \left[\frac{k + n}{k} \frac{x_n^{\hat{1}\hat{4}} - C}{x_n^{\hat{1}\hat{4}} + C} + \frac{nw}{k\kappa} \right] \right) \quad (3.65)$$

and

$$\delta E = \sum_n N_n^{\hat{1}\hat{3}} \left[\frac{K(x_n^{\hat{1}\hat{3}})k + n(x_n^{\hat{1}\hat{3}} - C)}{k(x_n^{\hat{1}\hat{3}} + C)} + \frac{nw}{k\kappa} \right] + N_n^{\hat{2}\hat{4}} \left[\frac{K(x_n^{\hat{2}\hat{4}})k + n(x_n^{\hat{2}\hat{4}} - C)}{k(x_n^{\hat{2}\hat{4}} + C)} + \frac{nw}{k\kappa} \right] \quad (3.66)$$

where, as for the $\mathfrak{su}(2)$ string, we denote the square root in the classical solution (3.63) by $K(x)$.

D.1.1 AdS_3 excitations – details

In strict analogy to what we have already seen in for $\mathfrak{su}(2)$ solution, the two (left and right) physical excitations inside the $\mathfrak{sl}(2)$ sector described by the AdS_3 σ -model, are given by the poles, connecting the pairs of sheets (\hat{p}_2, \hat{p}_3) and (\hat{p}_1, \hat{p}_4) . The number of such poles we denote $N_{\hat{2}\hat{3}}$ and $N_{\hat{1}\hat{4}}$ respectively.

As explained above, the AdS_5 excitations shifts of \hat{p} 's have no poles at ± 1 and must present an inverse square root behavior close to the branch points of the classical solution. Thus we can write

$$\delta \hat{p}_2(x) = \frac{2\pi}{\sqrt{\lambda}K(x)} \sum_n \left(N_n^{\hat{2}\hat{3}} \frac{x a_n}{x - x_n^{\hat{2}\hat{3}}} + N_n^{\hat{1}\hat{4}} \frac{x \bar{a}_n}{x - 1/x_n^{\hat{1}\hat{4}}} \right) \quad (3.67)$$

where

$$K(x) \equiv \sqrt{x^2 - 2BCx + C^2}$$

and the position of the roots is given by (3.14). Fixing the residues at $x_n^{\hat{2}\hat{3}}$ and $x_n^{\hat{1}\hat{4}}$ according to (3.21) we have

$$a_n = \frac{2Cx_n^{\hat{2}\hat{3}}(k - n)}{k(Cx_n^{\hat{2}\hat{3}} + 1)}, \quad \bar{a}_n = -\frac{2C(k + n)}{k(C + x_n^{\hat{1}\hat{4}})} \quad (3.68)$$

The large x asymptotic (3.19) is consistent if Riemann bilinear identity (3.20) is satisfied

$$\sum_n \left(N_n^{\hat{2}\hat{3}} + N_n^{\hat{1}\hat{4}} \right) n = 0 \quad (3.69)$$

and then the energy shift is given by (3.65).

¹² these AdS_3 excitations were also found in a similar way by K.Zarembo in relation with the finite size corrections computation [51] (according to the private communication).

D.1.2 The remaining AdS_5 excitations – details

These correspond to simple poles connecting (\hat{p}_1, \hat{p}_3) and (\hat{p}_2, \hat{p}_4) for which

$$\delta \hat{p}_2(x) = \frac{2\pi}{\sqrt{\lambda}} \sum_n \left[\frac{N_n^{\hat{1}\hat{3}} x \left(a_n + \frac{b_n + c_n x}{K(x)} \right)}{(x - x_n^{\hat{1}\hat{3}})(x - 1/x_n^{\hat{1}\hat{3}})} + \frac{N_n^{\hat{2}\hat{4}} x \left(\bar{a}_n + \frac{\bar{b}_n + \bar{c}_n x}{K(x)} \right)}{(x - x_n^{\hat{2}\hat{4}})(x - 1/x_n^{\hat{2}\hat{4}})} \right]. \quad (3.70)$$

Then $\delta \hat{p}_3$, just as we saw for the $\mathfrak{su}(2)$ solution, is the analytical continuation of $\delta \hat{p}_2$ through the cut. In simpler terms, it corresponds to a simple change of sign of $K(x)$ in the above expression. Finally $\delta \hat{p}_{1,4}(x) = -\delta \hat{p}_{2,3}(1/x)$.

The undetermined coefficients are fixed by the residues

$$\begin{aligned} \text{res}_{x=x_n^{\hat{1}\hat{3}}} \hat{p}_{1,3} &= \pm \alpha \left(x_n^{\hat{1}\hat{3}} \right) N_n^{\hat{1}\hat{3}}, & \text{res}_{x=x_n^{\hat{1}\hat{3}}} \hat{p}_{2,4} &= 0 \\ \text{res}_{x=x_n^{\hat{2}\hat{4}}} \hat{p}_{2,4} &= \pm \alpha \left(x_n^{\hat{2}\hat{4}} \right) N_n^{\hat{2}\hat{4}}, & \text{res}_{x=x_n^{\hat{2}\hat{4}}} \hat{p}_{1,3} &= 0 \end{aligned}$$

to be

$$\begin{aligned} a_n &= -1, & b_n &= C \frac{2n x_n^{\hat{1}\hat{3}} + kK(x_n^{\hat{1}\hat{3}})}{k(x_n^{\hat{1}\hat{3}} + C)}, & c_n &= \frac{kK(x_n^{\hat{1}\hat{3}}) - 2Cn}{k(C + x_n^{\hat{1}\hat{3}})} \\ \bar{a}_n &= 1, & \bar{b}_n &= C \frac{2n x_n^{\hat{2}\hat{4}} + kK(x_n^{\hat{2}\hat{4}})}{k(x_n^{\hat{2}\hat{4}} + C)}, & \bar{c}_n &= \frac{kK(x_n^{\hat{2}\hat{4}}) - 2Cn}{k(C + x_n^{\hat{2}\hat{4}})} \end{aligned}$$

Hence, with the level matching condition

$$\sum_n \left(N_n^{\hat{1}\hat{3}} + N_n^{\hat{2}\hat{4}} \right) n = 0, \quad (3.71)$$

we find, from the large x behavior, the energy shift (3.66).

D.2 The S^5 excitations

The S^5 quasi-momentum (3.62) has no branch cuts and thus $\delta \tilde{p}_i$ will be of the same form as we found for the BMN string except that the position of the roots, found from (3.14) is now given by

$$\tilde{x}_n \equiv x_n^{\hat{1}\hat{3}} = x_n^{\hat{1}\hat{4}} = x_n^{\hat{2}\hat{3}} = x_n^{\hat{1}\hat{4}} = \frac{\mathcal{J} + \sqrt{\mathcal{J}^2 + (n+m)^2 - m^2}}{n} \quad (3.72)$$

instead of (3.23). The explicit expressions for $\delta \tilde{p}_i$ are given in (3.74). This perturbation shifts the residues at ± 1 from

$$\pi(\mathcal{J} \mp m)$$

to some other values which we parameterize by

$$\pi \left(\mathcal{J} + \delta \mathcal{J}^{eff} \mp (m + \delta m^{eff}) \right).$$

The precise expressions for these shifts can be found in (3.74,3.75). But then, since the AdS_5 quasi-momenta only knows about the S^5 sector though the residues at these points, the perturbed quasi-momenta $\hat{p}_i + \delta \hat{p}_i$ will be given by the same expression (3.63) with the trivial replacement

$$\mathcal{J}, m \rightarrow \mathcal{J} + \delta \mathcal{J}^{eff}, m + \delta m^{eff}.$$

The same is true for the energy, given in (3.64) so that – see Appendix D.2 for details – we can immediately find

$$\delta E = \frac{1}{\kappa} \sum_n \left(N_n^{\tilde{1}\tilde{3}} + N_n^{\tilde{1}\tilde{4}} + N_n^{\tilde{2}\tilde{3}} + N_n^{\tilde{2}\tilde{4}} \right) \left(\sqrt{(n+m)^2 - m^2 + \mathcal{J}^2} - \mathcal{J} \right). \quad (3.73)$$

D.2.1 The S^5 excitations – details

As explained above the perturbed S^5 quasi-momenta are of the BMN form (3.54,3.55)

$$\begin{aligned} \delta \tilde{p}_2(x) &= + \frac{4\pi}{\sqrt{\lambda}} \frac{x^2}{x^2 - 1} \sum_n \left(\frac{N_n^{\tilde{2}\tilde{3}} + N_n^{\tilde{2}\tilde{4}}}{\tilde{x}_n - x} + \frac{N_n^{\tilde{1}\tilde{3}} + N_n^{\tilde{1}\tilde{4}}}{x^2 \tilde{x}_n - x} \right) \\ \delta \tilde{p}_3(x) &= - \frac{4\pi}{\sqrt{\lambda}} \frac{x^2}{x^2 - 1} \sum_n \left(\frac{N_n^{\tilde{1}\tilde{3}} + N_n^{\tilde{2}\tilde{3}}}{\tilde{x}_n - x} + \frac{N_n^{\tilde{2}\tilde{4}} + N_n^{\tilde{1}\tilde{4}}}{x^2 \tilde{x}_n - x} \right) \end{aligned}$$

where \tilde{x}_n is given by (3.72). Then, in the notation introduced above, the shift in the $x = \pm 1$ residues is given by

$$\delta \mathcal{J}^{eff} = \frac{\sum_n \left(N_n^{\tilde{1}\tilde{3}} + N_n^{\tilde{1}\tilde{4}} + N_n^{\tilde{2}\tilde{3}} + N_n^{\tilde{2}\tilde{4}} \right) \left(mn + \mathcal{J}^2 - \mathcal{J} \sqrt{\mathcal{J}^2 + n^2 + 2mn} \right)}{\sqrt{\lambda}(m^2 - \mathcal{J}^2)} \quad (3.74)$$

while δm^{eff} is given by

$$\mathcal{J} \delta m^{eff} + \delta \mathcal{J}^{eff} m = \frac{1}{\sqrt{\lambda}} \sum_n \left(N_n^{\tilde{1}\tilde{3}} + N_n^{\tilde{1}\tilde{4}} + N_n^{\tilde{2}\tilde{3}} + N_n^{\tilde{2}\tilde{4}} \right) n = 0 \quad (3.75)$$

due to the Riemann condition. Then, from (3.64,3.37), we have

$$\delta \mathcal{E} = \frac{w^3 - km\mathcal{J}}{w^2\kappa} \delta w = \frac{w(k^2 + m^2 + \mathcal{J}^2) - 3km\mathcal{J}}{w^2\kappa} \delta w \quad (3.76)$$

where, using (3.37,3.75), we have

$$\delta w = - \frac{\delta \mathcal{J}^{eff}}{\mathcal{J}} \frac{w^2(m^2 - \mathcal{J}^2)}{w(k^2 + m^2 + \mathcal{J}^2) - 3km\mathcal{J}} \quad (3.77)$$

so that δE will be given by (3.73)

D.3 Fermionic excitations

The fermionic excitations can be treated as for the $\mathfrak{su}(2)$ string. As before we expect at most two different answers for the energy shifts – one coming from the poles uniting the $(\hat{1}\tilde{3}, \hat{1}\tilde{4}, \hat{4}\tilde{1}, \hat{4}\tilde{2})$ sheets another result for the $(\hat{2}\tilde{3}, \hat{2}\tilde{4}, \hat{3}\tilde{1}, \hat{3}\tilde{2})$. From the expressions in Appendix C.3 we find

$$\delta\Delta = \sum_n \left(N_n^{\hat{1}\tilde{3}} + N_n^{\hat{1}\tilde{4}} + N_n^{\hat{4}\tilde{1}} + N_n^{\hat{4}\tilde{2}} \right) \delta\Delta_n^{(1)} + \sum_n \left(N_n^{\hat{2}\tilde{3}} + N_n^{\hat{2}\tilde{4}} + N_n^{\hat{3}\tilde{1}} + N_n^{\hat{3}\tilde{2}} \right) \delta\Delta_n^{(2)}, \quad (3.78)$$

where

$$\begin{aligned} \delta\Delta_n^{(1)} &= \frac{(2m+k) - 2\mathcal{J}C - kC^2}{k(C^2-1)(C^{-1}x_n^{\hat{1}\tilde{3}}+1)} + \frac{n(C^{-1}x_n^{\hat{1}\tilde{3}}-1)}{k(C^{-1}x_n^{\hat{1}\tilde{3}}+1)} + \frac{n\omega}{k\kappa} \\ \delta\Delta_n^{(2)} &= \frac{(2m-k)C^2 - 2\mathcal{J}C + k}{k(C^2-1)(Cx_n^{\hat{2}\tilde{3}}+1)} - \frac{n(Cx_n^{\hat{2}\tilde{3}}-1)}{k(Cx_n^{\hat{2}\tilde{3}}+1)} + \frac{n\omega}{k\kappa} \end{aligned}$$

with the position of the fermionic poles being given by (3.14), in terms of the algebraic curve for the classical solution.

D.3.1 Fermionic excitations – details

The S^5 part of the quasi-momenta is given by

$$\begin{aligned} \tilde{p}_2(x) &= + \frac{4\pi x}{\sqrt{\lambda}(x^2-1)} \sum_n \left(\frac{N_n^{\hat{3}\tilde{1}} + N_n^{\hat{4}\tilde{1}}}{xx_n^{\hat{3}\tilde{1}}-1} - x \frac{N_n^{\hat{3}\tilde{2}} + N_n^{\hat{4}\tilde{2}}}{x-x_n^{\hat{3}\tilde{1}}} \right) \\ \tilde{p}_3(x) &= - \frac{4\pi x}{\sqrt{\lambda}(x^2-1)} \sum_n \left(\frac{N_n^{\hat{1}\tilde{4}} + N_n^{\hat{2}\tilde{4}}}{xx_n^{\hat{3}\tilde{1}}-1} - x \frac{N_n^{\hat{1}\tilde{3}} + N_n^{\hat{2}\tilde{3}}}{x-x_n^{\hat{3}\tilde{1}}} \right) \end{aligned}$$

whereas the AdS_5 part is more complicated. Parameterizing $\delta\hat{p}$ as we did for the $\mathfrak{su}(2)$ string in (3.31), we have

$$\begin{aligned} f(x) &= \frac{x}{x^2-1} \sum_n \left(x \frac{N_n^{\hat{2}\tilde{3}} + N_n^{\hat{2}\tilde{4}} - N_n^{\hat{3}\tilde{1}} - N_n^{\hat{3}\tilde{2}}}{x-x_n^{\hat{2}\tilde{3}}} + \frac{N_n^{\hat{2}\tilde{3}} + N_n^{\hat{2}\tilde{4}} - N_n^{\hat{3}\tilde{1}} - N_n^{\hat{3}\tilde{2}}}{xx_n^{\hat{2}\tilde{3}}-1} \right) \\ g(x) &= \frac{x}{x^2-1} \sum_n \left(\left[\frac{xK(x_n^{\hat{2}\tilde{3}})}{x-x_n^{\hat{2}\tilde{3}}} + a_n x + b_n \right] (N_n^{\hat{2}\tilde{3}} + N_n^{\hat{2}\tilde{4}} + N_n^{\hat{3}\tilde{1}} + N_n^{\hat{3}\tilde{2}}) \right. \\ &\quad \left. - \left[\frac{xx_n^{\hat{1}\tilde{3}}K(1/x_n^{\hat{1}\tilde{3}})}{xx_n^{\hat{1}\tilde{3}}-1} + \bar{a}_n x + \bar{b}_n \right] (N_n^{\hat{1}\tilde{3}} + N_n^{\hat{1}\tilde{4}} + N_n^{\hat{4}\tilde{1}} + N_n^{\hat{4}\tilde{2}}) \right) \end{aligned}$$

where the remain constants are given by

$$a_n = C \frac{(C^2-1)(k-2n)x_n^{\hat{2}\tilde{3}} + 2Cm - 2\mathcal{J}}{(C^2-1)(Cx_n^{\hat{2}\tilde{3}}+1)k}$$

$$\begin{aligned}
\bar{a}_n &= C \frac{(C^2 - 1)k - 2(m + n) + 2C(Cn + \mathcal{J})}{(C^2 - 1)(C + x_n^{\hat{1}\hat{3}})k} \\
b_n &= C \frac{(C^2 - 1)k - 2C^2(m + n) + 2(n + C\mathcal{J})}{(C^2 - 1)(C + x_n^{\hat{2}\hat{3}})k} \\
\bar{b}_n &= -C \frac{(C^2 - 1)(k + 2n)x_n^{\hat{1}\hat{3}} + 2Cm - 2C^2\mathcal{J}}{(C^2 - 1)(C + x_n^{\hat{1}\hat{3}})k}
\end{aligned}$$

Then the energy shifts can be read from the large x asymptotics and are given in (3.78).

Appendix E: Ambiguities due to shifts

To compute the 1-loop shift one must sum all frequencies. This sum, however, is sensitive to the way the frequencies are labeled. Let us demonstrate this on a simple example. Consider the sum

$$\frac{1}{2} \sum_{n=-\infty}^{\infty} (2\omega_n - \omega_{n+m} - \omega_{n-m}) \quad (3.79)$$

with $\omega_n = \omega_{-n}$ and assume that for large mode number, $\omega_n \simeq |n| + \dots$. Naively this sum is zero if m is integer, since all terms cancel among each other if we allow renumbering of the terms. However a more careful analysis shows that this is not the case

$$\frac{1}{2} \sum_{n=-N}^N (2\omega_n - \omega_{n+m} - \omega_{n-m}) = \sum_{n=N-m+1}^N (\omega_n - \omega_{n-m}) = m^2 + \mathcal{O}(1/N). \quad (3.80)$$

Thus one should be very careful calculating 1-loop shift having a frequencies at hand because ambiguities can easily arise. Consider, for example, the equation for the bosonic frequencies for the general $3\mathcal{J}$ solution [83]

$$\begin{aligned}
P_8^{J_1 J_2 J_3}(\omega) &= (\omega^2 - n^2)^4 - 4(\omega^2 - n^2)^2 \sum_{i \neq j}^3 \frac{\mathcal{J}_i}{w_i} (w_j \omega - m_j n)^2 \\
&\quad + 8 \sum_{i \neq j \neq k \neq i}^3 \frac{\mathcal{J}_i}{w_i} (w_j \omega - m_j n)^2 (w_k \omega - m_k n)^2 = 0.
\end{aligned}$$

This solution can be smoothly deformed to general $\mathfrak{su}(2)$ solution for which $J_3 \rightarrow 0$ while preserving all constraints (1.8). In this limit we find

$$P_8^{J_1 J_2 0}(\omega) = P_4^{\mathfrak{su}(2)}(\omega) \left((\omega^2 - n^2)^2 - 4 \left(m_3 n - \omega \sqrt{m_3^2 + v^2} \right)^2 \right) \quad (3.81)$$

where the quartic polynomial $P_4^{\mathfrak{su}(2)}(\omega)$ is the one appearing in table 3 and gives us the usual $\mathfrak{su}(2)$ modes whereas the remaining equations yields the frequencies

$$\sqrt{(n + m_3)^2 + v^2} + w_3, \quad \sqrt{(n - m_3)^2 + v^2} - w_3 \quad (3.82)$$

instead of the two $\sqrt{n^2 + v^2}$ we read from table 3. From the above explanation this ambiguity converts into an extra contribution of m_3^2/κ to the 1-loop shift.

Moreover, we also found contradictory results in the literature. For the simple $\mathfrak{su}(2)$ solution, in [82, 87, 88] the sum over fermionic frequencies ω_n^F is taken over the integers for even m and over $\mathbb{Z} + 1/2$ for odd m while in [49, 89] the sum always goes over the integers. We found that the fermions will indeed be summed over integer n 's. The same kind of mismatch appears for the $\mathfrak{sl}(2)$ circular string. For example, in [51, 53, 89, 84] the fermionic frequencies ω_n^F are summed with n integer whereas we found $\omega_{n+m/2-k/2}^F$ and $\omega_{-n-m/2-k/2}^F$ that is, the frequencies have half-integer arguments if $m+k$ is odd – see (3.40). In view of this discrepancies we also repeated the calculation for the frequencies directly from the expansion of the string action using a coset representative parameterized as in [10]. We also found the same kind of field redefinitions which are trivially related to the \mathcal{R} and \mathcal{Q} matrices written in section 3.2. For the simple $\mathfrak{su}(2)$ solution the field redefinitions always leave the fermions periodic whereas for the $\mathfrak{sl}(2)$ string they are periodic (anti-periodic) for $m+k$ even (odd) in agreement with the calculation presented in this paper. Shifts changing integers into half-integers are no longer related by the simple expressions of the form m^2/κ like in the previous example. However, the sum over fermions can be replaced by integral with exponential precision and therefore this shifts may end up being not so harmful.

4. MATCHING FINITE SIZE CORRECTIONS AND FLUCTUATIONS

IN THE CHAPTER 2 we developed a method to compute the finite size corrections in the thermodynamical limit. The conjectured BS equations depend on the 't Hooft coupling λ and should describe the spectrum of the AdS/CFT system (in the planar limit) for the asymptotical states, i.e. for large angular momentum of the string $\mathcal{J} = L/\sqrt{\lambda} \gg 1$. The analog of the thermodynamical limit for the BS equations is $K_a \sim L \sim \sqrt{\lambda} \rightarrow \infty$ as we already mentioned in the introduction. The BS equations are constructed to reproduce the classical algebraical curve of the “finite-gap” method in the leading thermodynamical limit. The finite size $1/L$ corrections are also $1/\sqrt{\lambda}$ corrections to the classical spectrum and thus should be related to the quasi-classical quantization considered in chapter 3.

In this section we will apply the method developed in the chapter 2 to the BS equations to extract their finite size corrections. Then, we will show that they are, in fact, related to the fluctuations, considered in the previous chapter, in such a way, that the 1-loop $1/\sqrt{\lambda}$ correction to the classical energy of a state is given by a sum of zero point oscillations. This proves the complete 1-loop consistency of the BS equations.

4.1 Heisenberg spin chain

IN THIS SECTION we will demonstrate the interplay between fluctuations and finite size corrections in NBA's in the scaling limit. For simplicity we first consider the $\mathfrak{su}(1,2)$ spin chain and then generalize to the general $\mathfrak{su}(N)$ case.

In the chapter 2 we explained how to obtain the spectrum of the fluctuation energies around any classical string solution using the algebraic curve by adding a pole to this curve. In particular, we reproduced in this way some previous results [81, 82, 83, 84] where the semi-classical quantization around some simple circular string motions were computed by directly expanding the Metsaev-Tseytlin action [9] around some classical solutions and quantizing the resulting quadratic action. Using the fact that one extra pole in the algebraic curve means one quantum fluctuation, we can compute the leading quantum corrections to the classical energy of a state from the field theory considerations using the algebraic curve alone, as we mentioned in the introduction. This implies a nontrivial relation between fluctuations on algebraic curve and finite size corrections in

Bethe ansatz.

- Suppose we compute the energy shift $\delta\mathcal{E}_n^{ij}$ due to the addition of a stack with mode number n uniting sheets p_i and p_j to a given configuration with some finite cuts \mathcal{C} .
- Suppose on the other hand that we compute $1/L$ energy expansion $\mathcal{E} = \mathcal{E}^{(0)} + \frac{1}{L}\mathcal{E}^{(1)} + \dots$ of the configuration with the finite cuts \mathcal{C} .

From the field theory point of view the first quantity corresponds to *one of the fluctuation energies* around a classical solution parameterized by the configuration with the cuts \mathcal{C} whereas the second quantity, $\mathcal{E}^{(1)}$, is the *1-loop shift* [47] around this classical solution with energy $\mathcal{E}^{(0)}$. This 1-loop shift, or ground state energy, is given by the sum of halves of the fluctuation energies [47]

$$\mathcal{E}^{(1)} = \frac{1}{2} \sum_{n=-N}^N \sum_{ij} \delta\mathcal{E}_n^{ij} \quad (4.1)$$

In fact for usual (non super-symmetric) field theories this sum is divergent and needs to be regularized. We will see that (4.1) can be generalized and holds for arbitrary local charges

$$\mathcal{Q}_r^{(1)} = \frac{1}{2} \sum_{n=-N}^N \sum_{ij} \delta\mathcal{Q}_{r,n}^{ij}. \quad (4.2)$$

where N is some large cut-off.

Let us stress once more that from the Bethe ansatz point of view these quantities are computed independently and there is a priori no obvious reason why such relation between fluctuations and finite size corrections should hold. In this section we will show that Nested Bethe Ansatz's describing (super) spin chains with arbitrary rank do indeed obey such property with some particular regularization procedure (for the Heisenberg $su(2)$ spin chain a similar treatment was carried in [52]). Moreover we will see that the regularization mentioned above also appears naturally from the Bethe ansatz point of view as some integrals around the origin.

4.1.1 1-loop shift and fluctuations

We will follow the logic of the previous chapter to compute the charges of the fluctuations, around a given configuration of the roots. Let us pick the leading order integral equation for the densities of the Bethe roots in the scaling limit (2.103) and perturb it by a single stack, connecting p^i with p^j . According to (2.97) this simply implies $\rho_2 \rightarrow \rho_2 + \frac{1}{L}\delta(x - x^{ij})$, where x^{ij} is position of the new stack. Finally, the positions where one can put an extra

stack, as it follows from the BAE (2.93,2.94), can be parameterized by one integer mod number n

$$p_i(x_n^{ij}) - p_j(x_n^{ij}) = 2\pi n. \quad (4.3)$$

Therefore, for $i = 2, j = 3$ the perturbed equation (2.103) reads

$$\frac{1}{x} + 2 \oint_{\mathcal{C}_{23}} \frac{\rho(y)}{x-y} + \int_{\mathcal{C}_{13}} \frac{\rho(y)}{x-y} + \frac{1}{L} \frac{2}{x-x_n^{23}} = 2\pi k_{23} + \phi_2 - \phi_3, \quad x \in \mathcal{C}_{23}. \quad (4.4)$$

and this perturbation will lead to some perturbation of the density $\delta\rho(y)$, which will lead to the perturbation in the local charges (2.95) as

$$\delta Q_{r,n}^{23} = \int \frac{\delta\rho(y)}{y^r} dy + \frac{1}{L(x_n^{23})^r}, \quad (4.5)$$

the local charges of the fluctuation with polarization 23 and mode number n .

Thus, by linearity, if we want to obtain the 1-loop shift (4.2) (or rather a large N regularized version of this quantity where the sum over n goes from $-N$ to N) we have to solve the following integral equation for densities

$$\frac{1}{x} + 2 \oint_{\mathcal{C}_{23}} \frac{\rho(y)}{x-y} + \int_{\mathcal{C}_{13}} \frac{\rho(y)}{x-y} + \sum_{n=-N}^N \frac{1}{2L} \left[\frac{2}{x-x_n^{23}} + \frac{1}{x-x_n^{13}} \right] = 2\pi k_{23}, \quad x \in \mathcal{C}_{23}. \quad (4.6)$$

and then the 1-loop shifted charges are given

$$Q_r = \int_{\mathcal{C}_{13} \cup \mathcal{C}_{23}} \frac{\rho(y)}{y^r} dy + \sum_{n=-N}^N \frac{1}{2L} \left[\frac{1}{(x_n^{23})^r} + \frac{1}{(x_n^{13})^r} \right] \quad (4.7)$$

$$= \int_{\mathcal{C}_{13} \cup \mathcal{C}_{23}} \frac{\rho(y)}{y^r} dy + \sum_{n=-N}^N \frac{1}{2L} \left[\oint_{\mathcal{C}_{x_n^{23}}} \frac{\cot_{23}}{y^r} \frac{dy}{2\pi i} + \oint_{\mathcal{C}_{x_n^{13}}} \frac{\cot_{13}}{y^r} \frac{dy}{2\pi i} \right]. \quad (4.8)$$

To pass from the first line to the second in the above expression we use that \cot_{ij} has poles at x_n^{ij} with unit residue. We will now understand how to redefine the density in such a way that the second term is absorbed into the first one. We start by opening the contours in (4.8) around the excitation points x_n^{ij} . These contours will then end up around the cuts \mathcal{C}_{kl} of the classical solution and around the origin. We will not consider the contour around $x = 0$ – this contribution would lead to a regularization of the divergent sum in r.h.s. of (4.2). We will analyze it carefully in the super-string case, where it leads to the Hernandez-Lopez phase factor. Then we get

$$Q_r = \int_{\mathcal{C}_{13} \cup \mathcal{C}_{23}} \frac{\rho(y)}{y^r} dy + \frac{1}{2L} \left[\oint_{\mathcal{C}_{13}} \frac{\cot_{23}}{y^r} \frac{dy}{2\pi i} + \oint_{\mathcal{C}_{23}} \frac{\cot_{13}}{y^r} \frac{dy}{2\pi i} \right] \quad (4.9)$$

Fig. 4.1: Illustration of an identity used in the main text.

Noting that

$$\cot_{ij}^+ = \cot_{kj}^-, \quad x \in \mathcal{C}_{ik}, \quad (4.10)$$

where the superscript $+$ ($-$) indicates that x is slightly above (below) the cut, we can write

$$\mathcal{Q}_r = \int_{\mathcal{C}_{13} \cup \mathcal{C}_{23}} \frac{\rho(y)}{y^r} dy - \frac{1}{2L} \int_{\mathcal{C}_{13} \cup \mathcal{C}_{23}} \frac{\Delta \cot_{12}}{y^r} \frac{dy}{2\pi i} \quad (4.11)$$

so that we see that it is natural to introduce a new density, “dressed” by the virtual particles,

$$\varrho = \rho - \frac{1}{2L} \frac{\Delta \cot_{12}}{2\pi i} \quad (4.12)$$

so that the expression for the local charges takes the standard form

$$\mathcal{Q}_r = \int_{\mathcal{C}_{13} \cup \mathcal{C}_{23}} \frac{\varrho(y)}{y^r} dy.$$

Let us now rewrite our original integral equation (4.6) in terms of this dressed density. We will see that the integral equation we are constructing for this density by requiring a proper semi-classical quantization will be precisely the equation (2.106) (up to some contribution coming from the region around the $x = 0$. Subtraction of this contribution could be considered as a regularization of the divergent sum (4.2)) which is the finite size corrected integral equation arising from the NBA for the spin chain! This will thus prove the announced property relating finite size corrections and 1-loop shift.

Consider for example the first summand in (4.6) (recall that $x \in \mathcal{C}_{23}$),

$$\sum_n \frac{1}{x - x_n^{23}} = \sum_n \oint_{\mathcal{C}_{23}} \frac{\cot_{23}}{x - y} \frac{dy}{2\pi i} = \cot_{23} + \oint_{\mathcal{C}_{13}} \frac{\cot_{23}}{x - y} \frac{dy}{2\pi i} = \cot_{23} - \int_{\mathcal{C}_{13}} \frac{\Delta \cot_{12}}{x - y} \frac{dy}{2\pi i}, \quad (4.13)$$

Note that \cot_{23} has branch cut singularities at \mathcal{C}_{13} which we have to encircle when we blow up the contour, which leads to the second term. The first term comes from the pole at $x = y$. Finally, to write the second term as it is we used (4.10). Analogously (see figure 4.1 for a pictorial explanation of the second equality)

$$\sum_n \frac{1}{x - x_n^{13}} = \oint_{\mathcal{C}_{23}} \frac{\cot_{13}}{x - y} \frac{dy}{2\pi i} = \cot_{13} + \int_{\mathcal{C}_{23}} \frac{\Delta \cot_{13}}{x - y} \frac{dy}{2\pi i} = \cot_{13} - \int_{\mathcal{C}_{23}} \frac{\Delta \cot_{12}}{x - y} \frac{dy}{2\pi i}. \quad (4.14)$$

Then we note that (see (2.115))

$$\text{cot}_{13} = \text{cot}_{12} = - \oint_{\mathcal{C}_{13} \cup \mathcal{C}_{23}} \frac{\Delta \text{cot}_{12}}{x-y} \frac{dy}{2\pi i}$$

so that (4.6) reads

$$\frac{1}{x} + 2 \oint_{\mathcal{C}_{23}} \frac{\rho(y)}{x-y} + \int_{\mathcal{C}_{13}} \frac{\rho(y)}{x-y} + \frac{1}{2L} \left[2 \text{cot}_{23} - 2 \oint_{\mathcal{C}_{23}} \frac{\Delta \text{cot}_{12}}{x-y} \frac{dy}{2\pi i} - 3 \int_{\mathcal{C}_{13}} \frac{\Delta \text{cot}_{12}}{x-y} \frac{dy}{2\pi i} \right] = 2\pi k_{23} + \phi_2 - \phi_3$$

which in terms of the redefined density ϱ becomes

$$\frac{1}{x} + 2 \oint_{\mathcal{C}_{23}} \frac{\varrho(y)}{x-y} + \int_{\mathcal{C}_{13}} \frac{\varrho(y)}{x-y} + \frac{1}{L} \left[\text{cot}_{23} - \int_{\mathcal{C}_{13}} \frac{\Delta \text{cot}_{12}}{x-y} \frac{dy}{2\pi i} \right] = 2\pi k_{23} + \phi_2 - \phi_3$$

which coincides precisely with (2.106) as announced above! Thus the finite size corrections to the charge of any given configuration will indeed be equal to the field theoretical prediction, that is to the 1-loop shift around the classical solution.

4.1.2 Generalization

Here we consider a $\mathfrak{su}(n)$ NBA with the Dynkin labels V_a being $+1$ for a particular a only. In this section we generalize the results from the section 4.1.1. For the spin chain $\mathfrak{su}(n)$ NBA, in the classical limit, we will have n quasi-momenta each one above or below each of the $n-1$ Dynkin nodes¹. We label these quasi-momenta by p_i (p_j) with i, i' (j, j') taking positive (negative) values for quasi-momenta above (below) the node for which $V_a \neq 0$. Then let us mention how the equations in the previous section are generalized. We consider a *middle node* cut $\mathcal{C}_{1,-1}$. The analogue of equation (4.6) is now

$$-\frac{1}{x} + \sum_j \int_{\mathcal{C}_{1,j}} \frac{\delta\rho(y)}{x-y} + \sum_i \int_{\mathcal{C}_{i,-1}} \frac{\delta\rho(y)}{x-y} + \sum_{n=-N}^N \frac{1}{2L} \left[\sum_i \frac{1}{x-x_n^{i,-1}} + \sum_j \frac{1}{x-x_n^{1,j}} \right] = 0 \quad (4.15)$$

and the charges (4.7), (4.8), (4.9) and (4.11) become²

$$\mathcal{Q}_r - \int \frac{\rho(y)}{y^r} dy = + \sum_n \sum_{ij} \frac{1}{2L} \frac{1}{(x_n^{ij})^r} = + \frac{1}{2L} \sum_{ij} \frac{1}{2J} \oint_{\mathcal{C}_{ij}} \frac{\text{cot}_{ij}}{y^r} \frac{dy}{2\pi i} \quad (4.16)$$

¹ See figure 4.2 for an example of such pattern for a super group which clearly resembles $\mathfrak{su}(8)$.

² as in the previous section, we are ignoring the regularization of the charges coming from the contribution of the contour around the origin which would appear in the second line from opening the contours around the excitation points x_n^{ij} .

$$= +\frac{1}{2L} \sum_{ii'j} \oint_{\mathcal{C}_{i'j}} \frac{\cot_{ij}}{y^r} \frac{dy}{2\pi i} + \frac{1}{2L} \sum_{ijj'} \oint_{\mathcal{C}_{ij'}} \frac{\cot_{ij}}{y^r} \frac{dy}{2\pi i} \quad (4.17)$$

$$= -\frac{1}{2L} \sum_{ii'j} \oint_{\mathcal{C}_{i'j}} \frac{\cot_{ii'}}{y^r} \frac{dy}{2\pi i} - \frac{1}{2L} \sum_{ijj'} \oint_{\mathcal{C}_{ij'}} \frac{\cot_{jj'}}{y^r} \frac{dy}{2\pi i} \quad (4.18)$$

$$= -\frac{1}{2L} \int_{\mathcal{C}} \frac{\sum_{i<i'} \Delta \cot_{ii'} + \sum_{j<j'} \Delta \cot_{jj'}}{y^r} \frac{dy}{2\pi i}, \quad (4.19)$$

so that the natural definition of the dressed density becomes now

$$\varrho = \rho + \frac{1}{4L\pi i} \Delta \left(\sum_{i<i'} \cot_{ii'} + \sum_{j<j'} \cot_{jj'} \right). \quad (4.20)$$

Next step is to rewrite the integral equation (4.15) in terms of this new density. We proceed exactly as in (4.13), (4.14) using now

$$\cot_{1,i} = - \sum_j \left(\mathcal{I}_{1,j}^{1i} + \mathcal{I}_{i,j}^{1i} \right), \quad \mathcal{I}_{ij}^{kl} \equiv \int_{\mathcal{C}_{ij}} \frac{\cot_{kl}(y)}{x-y} \frac{dy}{2\pi i},$$

which is the analog of (2.115) for this $\mathfrak{su}(n)$ setup, so that at the end we obtain the following equation

$$\sum_j \int_{\mathcal{C}_{1,j}} \frac{\delta \varrho(y)}{x-y} + \sum_i \int_{\mathcal{C}_{i,-1}} \frac{\delta \varrho(y)}{x-y} + \frac{1}{L} \left(\cot_{1,-1} - \sum_{ij} \int_{\mathcal{C}_{ij}} \frac{\Delta \cot_{1,i} + \Delta \cot_{j,-1}}{x-y} \frac{dy}{2\pi i} \right) = 0 \quad (4.21)$$

for $\delta \varrho = \varrho - \varrho_0$ where ϱ_0 obeys the leading order equation

$$-\frac{1}{x} + \sum_j \int_{\mathcal{C}_{1,j}} \frac{\varrho_0(y)}{x-y} + \sum_i \int_{\mathcal{C}_{i,-1}} \frac{\varrho_0(y)}{x-y} = 2\pi k_{1,-1}. \quad (4.22)$$

This corrected equation is precisely the one we would obtain from finite size corrections to the $\mathfrak{su}(n)$ NBA equations. To find this equation from the Bethe ansatz point of view one can simply repeat either of the derivations in section 2.2.1, that is the known transfer matrices in various representations or the bosonic duality described in the previous sections. In section 4.2 we consider the AdS/CFT Bethe ansatz equations which are based on a large rank symmetry group, namely $PSU(2,2|4)$. There one can see an example of how this could be done explicitly.

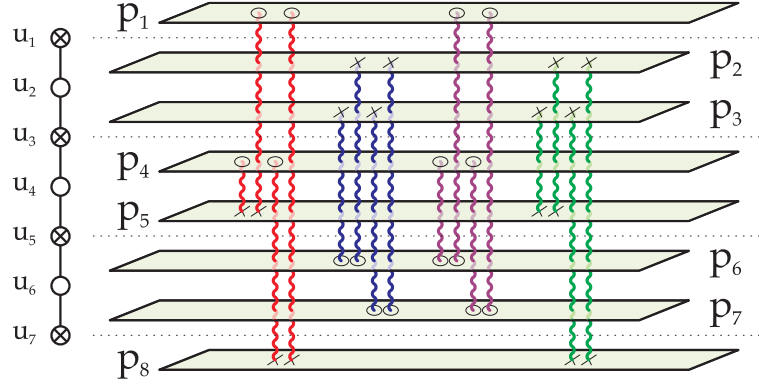


Fig. 4.2: The several physical fluctuations in the string Bethe ansatz. The 16 elementary physical excitations are the stacks (bound states) containing the middle node root. From the left to the right we have four S^5 fluctuations, four AdS_5 modes and eight fermionic excitations. The bosonic (fermionic) stacks contain an even (odd) number of fermionic roots represented by a cross in the $psu(2,2|4)$ Dynkin diagram in the left.

4.2 Matching of finite size corrections and fluctuations in AdS/CFT

4.2.1 Middle node anomaly

In this section we will expand BS equations in the scaling limit for the roots belonging to a cut containing middle node roots x_4 only. We do not assume that all the others cuts are of the same type, rather they can be cuts of stacks of several sizes. In the section 2.2.5 we will generalize the results obtained in this section to an arbitrary cut, assuming, as in the previous section, that the cuts are small enough and twists are not zero so that stacks are stable. We will discuss in section 4.3 what happens when one takes all twists to zero.

To leading order, the middle node equation (1.41) can be simply written as $\not{p}_4 - \not{p}_5 = 2\pi n$ while at 1-loop the first product in the r.h.s. of (1.41) corrects this equation due to (2.15)

$$\frac{1}{i} \log \prod_{j \neq k}^{K_4} \left(\frac{u_{4,k} - u_{4,j} + i}{u_{4,k} - u_{4,j} - i} \right) \simeq 2 F_4(x) + \alpha(x) \pi \rho'(x) \cot(\pi \rho(x)) \quad (4.23)$$

where $F_4(x) = \sum_j^{K_4} \frac{1}{u(x) - u_{4,j}}$, $\rho(x) = \frac{dk}{du_k}$. Expansion of the remaining terms in (1.41) will not lead to the appearance of such *anomaly* like terms since the roots of another types are separated by ~ 1 from $x_{4,k}$. Thus we have simply

$$2\pi n = \not{p}_4 - \not{p}_5 - \eta \alpha(x) \pi \rho'(x) \cot(\pi \rho(x)) , \quad x \in \mathcal{C}_{45} \quad (4.24)$$

In the next sections we will use dualities of the BS equations to get some extra information about cuts of stacks and generalize the above equation to any possible type of cut. To

achieve this we shall recast this equation in terms of the middle node roots x_4 only. Finally, in this section we will use

$$\cot_{ij} \equiv \alpha(x) \frac{p'_i - p'_j}{2} \cot \frac{p_i - p_j}{2}$$

which is similar (but should not be confused) with (2.105).

4.2.2 Dualities in the string Bethe ansatz

Obviously, the behavior of the Bethe roots will be as described in section 2.2 for a simpler example of a $\mathfrak{su}(1,2)$ spin chain, that is, we will have simple cuts made out of x_4 roots only and also cuts of stacks with x_2, x_3 and x_4 roots for example. Consider such cut of stacks. Clearly, to be able to write the middle node equation (1.41) or (4.24) we need to compute the density mismatches $\rho_2 - \rho_3$ and $\rho_3 - \rho_4$ which are 1-loop contributions we must take into account if we want to write an integral equation for the middle node equation in terms of the density ρ_4 of momentum carrying roots only. In this section we shall analyze the dualities present in the BS Bethe equations. By analyzing them in the scaling limit we will then be able to derive the desired density mismatches.

Fermionic duality in scaling limit

In [18] it was shown that the BS equations obey a very important fermionic duality. Since we chose to work with a subset of the possible Bethe equations, that is the ones with $\eta_1 = \eta_2 = \eta$ present in [18], we should apply the duality present below not only to the fermionic roots x_1 and x_3 (as described below) but also to the Bethe roots x_5 and x_7 . Obviously the duality for x_5 and x_7 is exactly the same as for x_1 and x_3 and so we will focus simply on the latter while keeping implicit that we always dualize all the fermionic roots at the same time.

We construct the polynomial ($\tau = \eta (\phi_4 - \phi_3)$)

$$\begin{aligned} P(x) &= e^{+i\frac{\tau}{2}} \prod_{j=1}^{K_4} (x - x_{4,j}^+) \prod_{j=1}^{K_2} (x - x_{2,j}^-) (x - 1/x_{2,j}^-) \\ &- e^{-i\frac{\tau}{2}} \prod_{j=1}^{K_4} (x - x_{4,j}^-) \prod_{j=1}^{K_2} (x - x_{2,j}^+) (x - 1/x_{2,j}^+) \end{aligned} \quad (4.25)$$

of degree $K_4 + 2K_2$ which clearly admits $x = x_{3,j}$ and $x = 1/x_{1,j}$ as $K_3 + K_1$ zeros³. The remaining $K_4 + 2K_2 - K_3 - K_1$ roots are denoted by $\tilde{x}_{3,j}$ or $1/\tilde{x}_{1,j}$ depending on whether

³ we also have $1/x_1$ has zeros because, due to (1.42), the equation for $x_{1,j}$ is the same as the equation for $x_{3,j}$ if we replace $x_{3,j}$ by $1/x_{1,j}$. This is why the restriction (1.42) of the twists is so important.

they are outside or inside the unit circle respectively,

$$P(x) = 2i \sin(\tau/2) \prod_{j=1}^{K_1} (x - 1/x_{1,j}) \prod_{j=1}^{\tilde{K}_1} (x - 1/\tilde{x}_{1,j}) \prod_{j=1}^{K_3} (x - x_{3,j}) \prod_{j=1}^{\tilde{K}_3} (x - \tilde{x}_{3,j}) \quad (4.26)$$

Then we can replace the roots $x_{1,j}, x_{3,j}$ by the roots $\tilde{x}_{1,j}, \tilde{x}_{3,j}$ in the BS equations provided we change the grading $\eta \rightarrow -\eta$ and interchange the twists $\phi_1 \leftrightarrow \phi_2$ and $\phi_3 \leftrightarrow \phi_4$. In fact, since we should also dualize the remaining fermionic roots, we should also change $\phi_5 \leftrightarrow \phi_6$ and $\phi_7 \leftrightarrow \phi_8$ and replace the remaining fermionic roots x_5 and x_7 .

Since to the leading order $x^\pm \simeq x$ each root will belong to a stack which must always contain a momentum carrying root x_4 . We have therefore $\tilde{K}_1 = K_2 - K_1$ and $\tilde{K}_3 = K_2 + K_4 - K_3$. Thus we label the Bethe roots as

$$\begin{aligned} x_{1,j} &= x_{4,j} - \epsilon_{1,j} \ , \quad j = 1, \dots, K_1 \\ \tilde{x}_{1,j} &= x_{4,j+K_1} - \tilde{\epsilon}_{1,j} \ , \quad j = 1, \dots, \tilde{K}_1 \\ x_{2,j} &= x_{4,j} - \epsilon_{2,j} \ , \quad j = 1, \dots, K_2 \\ x_{3,j} &= x_{4,j} - \epsilon_{3,j} \ , \quad j = 1, \dots, K_3 \\ \tilde{x}_{3,j} &= x_{4,j+K_3} - \tilde{\epsilon}_{3,j} \ , \quad j = 1, \dots, \tilde{K}_3 \end{aligned}$$

with $\epsilon \sim 1/\sqrt{\lambda}$. Dividing (4.25) and (4.26) by $\prod_{j=1}^{K_4} (x - x_{4,j}) \prod_{j=1}^{K_2} (x - x_{4,j})(x - 1/x_{4,j})$ we have

$$\begin{aligned} & e^{+i\frac{\tau}{2}} \prod_{j=1}^{K_4} \frac{x - x_{4,j}^+}{x - x_{4,j}} \prod_{j=1}^{K_2} \frac{x - x_{2,j}^-}{x - x_{4,j}} \frac{x - 1/x_{2,j}^-}{x - 1/x_{4,j}} - e^{-i\frac{\tau}{2}} \prod_{j=1}^{K_4} \frac{x - x_{4,j}^+}{x - x_{4,j}} \prod_{j=1}^{K_2} \frac{x - x_{2,j}^+}{x - x_{4,j}} \frac{x - 1/x_{2,j}^+}{x - 1/x_{4,j}} \\ &= 2i \sin(\tau/2) \prod_{j=1}^{K_1} \frac{x - 1/x_{1,j}}{x - 1/x_{4,j}} \prod_{j=1}^{\tilde{K}_1} \frac{x - 1/\tilde{x}_{1,j}}{x - 1/x_{4,K_1+j}} \prod_{j=1}^{K_3} \frac{x - x_{3,j}}{x - x_{4,j}} \prod_{j=1}^{\tilde{K}_3} \frac{x - \tilde{x}_{3,j}}{x - x_{4,K_3+j}} \quad (4.27) \end{aligned}$$

In this form it is easy to expand the duality relation in powers of $1/\sqrt{\lambda}$. By expanding all factors in (4.27) such as

$$\prod_{j=1}^{K_2} \frac{x - x_{2,j}^\pm}{x - x_{4,j}} = \exp \left(\sum_{j=1}^{K_2} \log \frac{x - x_{2,j}^\pm}{x - x_{4,j}} \right) \simeq \exp \left(\mp \frac{i}{2} G_2(x) + \sum_j \frac{\epsilon_{2,j}}{x - x_{2,j}} \right) \ ,$$

we find

$$\begin{aligned} \sin \left(\frac{\eta(p_4 - p_3)}{2} \right) &= \sin \left(\frac{\tau}{2} \right) \exp \left(+ \sum \frac{\epsilon_3}{x - x_3} + \sum \frac{\tilde{\epsilon}_3}{x - x_3} - \sum \frac{\epsilon_2}{x - x_2} \right) \\ &\times \exp \left(- \sum \frac{\epsilon_1/x_1^2}{x - 1/x_1} - \sum \frac{\tilde{\epsilon}_1/\tilde{x}_1^2}{x - 1/\tilde{x}_1} + \sum \frac{\epsilon_2/x_2^2}{x - 1/x_2} \right) . \end{aligned}$$

Then, similarly to what we had in section 2.2.3 for the bosonic duality, we notice that

$$\alpha(x)\partial_x \left(\sum \frac{\epsilon_3}{x-x_3} + \sum \frac{\tilde{\epsilon}_3}{x-\tilde{x}_3} - \sum \frac{\epsilon_2}{x-\tilde{x}_2} \right) = H_3 + H_{\tilde{3}} - H_4 - H_2 ,$$

with a similar expression for the argument of the second exponential. Thus finally we get

$$(H_4 + H_2 - H_3 - H_{\tilde{3}}) + (\bar{H}_2 - \bar{H}_1 - \bar{H}_{\tilde{1}}) = -\cot_{34} ,$$

or alternatively, using the $x \rightarrow 1/x$ symmetry transformation properties of the quasi-momenta,

$$(\bar{H}_4 + \bar{H}_2 - \bar{H}_3 - \bar{H}_{\tilde{3}}) + (H_2 - H_1 - H_{\tilde{1}}) = -\cot_{12} .$$

From this expressions we can deduce several properties of the density mismatches we wanted to obtain. For example, if we compute the discontinuity of (4.2.2) at a cut containing roots x_1 , that is in a large cut of stacks $\mathcal{C}_{1,i>4}$, we immediately get

$$\rho_1 - \rho_2 = -\frac{\Delta \cot_{12}}{2\pi i} , \quad x \in \mathcal{C}_{1,i>4} . \quad (4.28)$$

Proceeding in a similar way we find

$$\rho_3 - \rho_4 = -\frac{\Delta \cot_{34}}{2\pi i} , \quad x \in \mathcal{C}_{3,i>4} , \quad (4.29)$$

$$\rho_3 - \rho_4 = \rho_2 - \rho_{\tilde{3}} , \quad x \in \mathcal{C}_{1,i>4} \cup \mathcal{C}_{2,i>4} . \quad (4.30)$$

Let us now show that in the scaling limit the fermionic duality corresponds just to the exchange of the sheets $\{p_i\}$ of the Riemann surface. For illustration let us pick p_1 and see how it transforms under the duality. By definition the fermionic duality corresponds to the replacement $\eta \rightarrow -\eta, H_1 \rightarrow H_{\tilde{1}}, H_3 \rightarrow H_{\tilde{3}}$ and $\phi_1 \leftrightarrow \phi_2, \phi_3 \leftrightarrow \phi_4$, so that

$$p_1 \rightarrow \frac{2\pi \mathcal{I}x - \delta_{\eta,-1}Q_1 + \delta_{\eta,+1}Q_2x}{x^2 - 1} - \eta(-H_{\tilde{1}} - \bar{H}_{\tilde{3}} + \bar{H}_4) + \phi_2 = p_2 + \eta \cot_{12}$$

In the same way we get

$$p_2 \rightarrow p_1 + \eta \cot_{12} , \quad p_3 \rightarrow p_4 - \eta \cot_{34} , \quad p_4 \rightarrow p_3 - \eta \cot_{34} ,$$

and since $\cot_{ij} \sim 1/\sqrt{\lambda}$ we see that to the leading order the duality indeed just exchanges the sheets.

Bosonic duality in scaling limit

The bosonic nodes of the BS equations are precisely as in the usual Bethe ansatz discussed in the first sections so that we can just briefly mention the results. The duality ($\tau = \eta(\phi_2 - \phi_3)$)

$$e^{+i\frac{\tau}{2}} \tilde{Q}_2(u - i/2) Q_2(u + i/2) - e^{-i\frac{\tau}{2}} \tilde{Q}_2(u + i/2) Q_2(u - i/2) = 2i \sin \frac{\tau}{2} Q_1(u) Q_3(u)$$

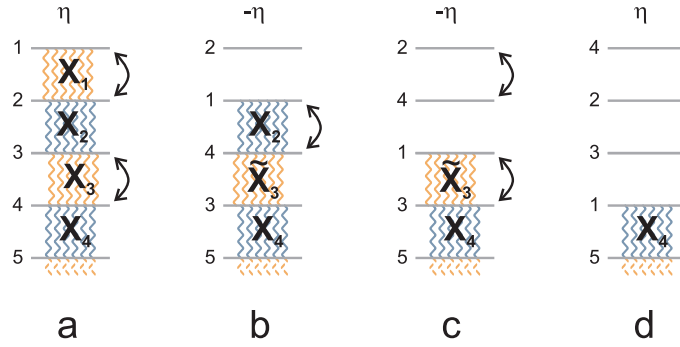


Fig. 4.3: Action of the duality on a long stack. By successively applying the fermionic and the bosonic dualities we can reduce the size of any large cut. One should not forget to change the sign of the grading η after applying the fermionic duality.

leads to

$$(H_1 + H_3 - H_2 - H_{\bar{2}}) + (\bar{H}_1 + \bar{H}_3 - \bar{H}_2 - \bar{H}_{\bar{2}}) = \cot_{23} \quad (4.31)$$

which implies

$$\rho_2 - \rho_3 = +\frac{\Delta \cot_{23}}{2\pi i}, \quad x \in \mathcal{C}_{2,i>4}.$$

As we already discussed in section 2.2 the bosonic duality also amounts to an exchange of Riemann sheets. Indeed, under the replacement $H_2 \rightarrow H_{\bar{2}}$ and $\phi_2 \leftrightarrow \phi_3$, we find

$$p_2 \rightarrow p_3 - \eta \cot_{23}, \quad p_3 \rightarrow p_2 + \eta \cot_{23}$$

which again, to the leading order in $\sqrt{\lambda}$, is just the exchange of the sheets of the curve.

Dualities and the missing mismatches

Using bosonic and fermionic dualities separately we already got some information about the several possible mismatches of the densities inside the stack. To compute the missing mismatches we have to use both dualities together. For example suppose we want to compute $\rho_3 - \rho_4$ in a cut $\mathcal{C}_{1,i>4}$. We start by one such large cut of stacks (see figure 4.3a) and we apply the fermionic duality to this configuration so that we obtain a smaller cut as depicted in figure 4.3b. For this configuration we can use (4.2.2) to get

$$\rho_2 - \rho_{\bar{3}} = +\frac{\Delta \cot_{14}}{2\pi i}.$$

However, from (4.30), this is also equal to the mismatch we wanted to compute, that is

$$\rho_3 - \rho_4 = +\frac{\Delta \cot_{14}}{2\pi i}, \quad x \in \mathcal{C}_{1,i>4}.$$

Tab. 4.1: Densities mismatches

	$\mathcal{C}_{1,i}$	$\mathcal{C}_{2,i}$	$\mathcal{C}_{3,i}$
$2\pi i(\rho_1 - \rho_2)$	$-\Delta \cot_{12}$		
$2\pi i(\rho_2 - \rho_3)$	$-\Delta \cot_{13}$	$+\Delta \cot_{23}$	
$2\pi i(\rho_3 - \rho_4)$	$+\Delta \cot_{14}$	$-\Delta \cot_{24}$	$-\Delta \cot_{34}$

To compute the last mismatch we apply the bosonic duality to get a yet smaller cut as in figure 4.3c for which we use (4.29) to get

$$\rho_3 - \rho_4 = -\frac{\Delta \cot_{13}}{2\pi i}.$$

Again, from (4.30), we can revert this result into a mismatch for the configuration before duality, that is

$$\rho_2 - \rho_3 = -\frac{\Delta \cot_{13}}{2\pi i}, \quad x \in \mathcal{C}_{1,i>4}.$$

Let us then summarize all densities mismatches in table 4.1.

4.2.3 Integral equation

In this section we shall recast equation (4.24) or

$$\eta \frac{4\pi \mathcal{J}x - 2\delta_{\eta,+1} \mathcal{Q}_1 - 2\delta_{\eta,-1} \mathcal{Q}_2 x}{x^2 - 1} + 2\mathcal{H}_4 - H_3 - H_5 - \bar{H}_1 - \bar{H}_7 = 2\pi n + \eta\phi_4 - \eta\phi_5 - \cot_{45} \quad (4.32)$$

in terms of the density $\rho_4(x)$ of the middle roots x_4 . To do so we only need to replace the several densities by the middle node density $\rho_4(x)$ using the several density mismatches presented in table 4.1. Defining

$$H_{ij}(x) \equiv \int_{\mathcal{C}_{ij}} \frac{\alpha(x)}{\alpha(y)} \frac{\rho_4(y)}{x - y} dy$$

we can then rewrite equation (4.32) in terms of the middle node roots only,

$$\begin{aligned} & \eta \frac{4\pi \mathcal{J}x - 2\delta_{\eta,+1} \mathcal{Q}_1 - 2\delta_{\eta,-1} \mathcal{Q}_2 x}{x^2 - 1} + 2\mathcal{H}_{45} + H_{15} + H_{48} - 2\bar{H}_{18} - \bar{H}_{15} - \bar{H}_{48} \\ & = 2\pi n + \eta\phi_4 - \eta\phi_5 - \cot_{45} + \sum_{\substack{1 \leq i \leq 4 \\ 5 \leq j \leq 8}} (\mathcal{I}_{ij}^{i4} + \mathcal{I}_{ij}^{5j}) + \sum_{\substack{1 \leq i \leq 4 \\ 5 \leq j \leq 8}} (\bar{\mathcal{I}}_{1j}^{i1} + \bar{\mathcal{I}}_{i8}^{8j}) \end{aligned} \quad (4.33)$$

where $x \in \mathcal{C}_{45}$ and

$$\mathcal{I}_{ij}^{kl}(x) = (-1)^{F_{kl}} \int_{\mathcal{C}_{ij}} \frac{\alpha(x)}{\alpha(y)} \frac{\Delta \cot_{kl}}{x - y} \frac{dy}{2\pi i}, \quad \mathcal{I}_{ij}^{kk}(x) \equiv 0, \quad \bar{\mathcal{I}}_{ij}^{kl}(x) = \mathcal{I}_{ij}^{kl}(1/x).$$

The several dualities amount to an exchange of Riemann sheets so that the cuts $\mathcal{C}_{ij} \rightarrow \mathcal{C}_{i'j'}$ with the subscripts in H_{ij} changing accordingly. The middle roots x_4 are never touched in the process. Moreover to leading order $p_i \leftrightarrow p_{i'}$ and thus the r.h.s. of (4.33) is also trivially changed under the dualities. Therefore, as in section 2.2.1 (see (2.106) and (2.107)), we can now trivially write the corrected equation when x belongs to any possible type of cut of stacks by applying the several dualities to equation (4.33).

4.2.4 Fluctuations

In this section we shall find the integral equation (4.33) from the field theoretical point of view like we did in section 4.1. That is, we will find what the corrections to the classical (leading order) equations [11]

$$\eta \frac{4\pi \mathcal{J}x - 2\delta_{\eta,+1}\mathcal{Q}_1 - 2\delta_{\eta,-1}\mathcal{Q}_2x}{x^2 - 1} + 2\mathcal{H}_4 - H_3 - H_5 - \bar{H}_1 - \bar{H}_7 = 2\pi n + \eta\phi_4 - \eta\phi_5, \quad (4.34)$$

should be in order to describe properly the semi-classical quantization of the string (and not only the classical limit). We will find that this construction leads precisely to the integral equation (4.33) thus showing that the BS nested Bethe ansatz equations do reproduce the 1-loop shift around any (stable) classical solution with exponential precision (in some large charge of the classical solution). This section is very similar to section 4.1 and thus we will often omit lengthy but straightforward intermediate steps. We assume $i = 1, \dots, 4$ and $j = 5, \dots, 8$ in all sums.

As in (4.6) and (4.15), we add $\frac{1}{2}(-1)^F$ of a virtual excitation for each possible mode number n and polarization ij to each quasi-momenta. Notice that for this super-symmetric model the fluctuations can also be fermionic and indeed the grading $(-1)^F$ equals $+1$ (-1) for bosonic (fermionic) fluctuations, see figure 4.2, as usual for bosonic (fermi-onic) harmonic oscillators.

We denote $\rho = \rho_0 + \delta\rho$ where ρ_0 is the leading density, solution of the leading (classical) equation (4.34), while ρ obeys the corrected (semi-classical) equation. For example, if we consider $x \in \mathcal{C}_{4,5}$, the starting point should be (see [90] for a similar analysis)

$$\begin{aligned} 0 = & \frac{-2x\delta_{\eta,-1}\delta\mathcal{Q}_1}{x^2 - 1} + 2 \int_{\mathcal{C}_{45}} \frac{\alpha(x)}{\alpha(y)} \frac{\delta\rho(y)}{x - y} + \int_{\mathcal{C}_{15}} \frac{\alpha(x)}{\alpha(y)} \frac{\delta\rho(y)}{x - y} + \int_{\mathcal{C}_{48}} \frac{\alpha(x)}{\alpha(y)} \frac{\delta\rho(y)}{x - y} \\ & - 2 \int_{\mathcal{C}_{18}} \frac{\alpha(1/x)}{\alpha(y)} \frac{\delta\rho(y)}{1/x - y} - \int_{\mathcal{C}_{15}} \frac{\alpha(1/x)}{\alpha(y)} \frac{\delta\rho(y)}{1/x - y} - \int_{\mathcal{C}_{48}} \frac{\alpha(1/x)}{\alpha(y)} \frac{\delta\rho(y)}{1/x - y} \\ & + \sum_{n=-N}^N \frac{1}{2} \left[\sum_{i \leq 4} \frac{(-1)^{F_{i5}} \alpha(x)}{x - x_n^{i5}} + \sum_{j \geq 5} \frac{(-1)^{F_{4j}} \alpha(x)}{x - x_n^{4j}} - \sum_{i \leq 4} \frac{(-1)^{F_{i8}} \alpha(1/x)}{1/x - x_n^{i8}} - \sum_{j \geq 5} \frac{(-1)^{F_{1j}} \alpha(1/x)}{1/x - x_n^{1j}} \right] \end{aligned} \quad (4.35)$$

Then, by construction, the charges

$$\mathcal{Q}_r = \int_{\mathcal{C}} \frac{\rho(y)}{y^r} dy + \sum_n \sum_{ij} (-1)^{F_{ij}} \frac{\alpha(x_n^{ij})}{2(x_n^{ij})^r} = \int_{\mathcal{C}} \frac{\rho(y)}{y^r} dy + \sum_{ij} \frac{(-1)^{F_{ij}}}{2} \oint_{x_n^{ij}} \frac{\cot_{ij}}{y^r} \frac{dy}{2\pi i} \quad (4.36)$$

will take the $1/\sqrt{\lambda}$ corrected values. It is clear that, as before, we do not include the new *virtual* excitations in the density $\rho(x)$. Similarly to (4.12) and (4.20), if we want the charges to have the standard form

$$\mathcal{Q}_r = \int \frac{\varrho(y)}{y^r} dy$$

we must redefine the density as

$$\varrho = \rho + \frac{1}{4\pi i} \left(\sum_{i < i' \leq 4} (-1)^{F_{i' i}} \Delta \cot_{i' i} + \sum_{j > j' \geq 5} (-1)^{F_{j' j}} \Delta \cot_{j' j} \right).$$

Now we want to go back to the integral equation (4.35) and rewrite it using the density $\delta\varrho = \varrho - \rho_0$. For example, for $x \in \mathcal{C}_{45}$,

$$\begin{aligned} & 2 \int_{\mathcal{C}_{45}} \frac{\alpha(x)}{\alpha(y)} \frac{\delta\rho(y)}{x-y} + \int_{\mathcal{C}_{15}} \frac{\alpha(x)}{\alpha(y)} \frac{\delta\rho(y)}{x-y} + \int_{\mathcal{C}_{48}} \frac{\alpha(x)}{\alpha(y)} \frac{\delta\rho(y)}{x-y} \\ & + \sum_{n=-N}^N \frac{1}{2} \left[\sum_i \frac{(-1)^{F_{i5}} \alpha(x)}{x - x_n^{i5}} + \sum_j \frac{(-1)^{F_{4j}} \alpha(x)}{x - x_n^{4j}} \right] = \\ & 2 \int_{\mathcal{C}_{45}} \frac{\alpha(x)}{\alpha(y)} \frac{\delta\varrho(y)}{x-y} + \int_{\mathcal{C}_{15}} \frac{\alpha(x)}{\alpha(y)} \frac{\delta\varrho(y)}{x-y} + \int_{\mathcal{C}_{48}} \frac{\alpha(x)}{\alpha(y)} \frac{\delta\varrho(y)}{x-y} \\ & + \cot_{45} - \sum_{ij} \left(\mathcal{I}_{ij}^{4i} + \mathcal{I}_{ij}^{j5} \right) - \frac{1}{2} \sum_{ij} \left(\bar{\mathcal{I}}_{8j}^{8i} + \bar{\mathcal{I}}_{1i}^{1j} + \bar{\mathcal{I}}_{ij}^{8i} + \bar{\mathcal{I}}_{ij}^{1j} \right) \end{aligned}$$

where the identity

$$(-1)^{F_{4i}} \cot_{4,i} = - \sum_j \left(\mathcal{I}_{4j}^{4i} + \mathcal{I}_{ij}^{4i} \right) - \sum_j \left(\bar{\mathcal{I}}_{1j}^{1i} + \bar{\mathcal{I}}_{ij}^{1i} \right),$$

where $\bar{1} = i$, $\bar{1} = 4$, $\bar{2} = 3$, is being used. Now, when $x \in \mathcal{C}_{18}$, we will get

$$\begin{aligned} & 2 \int_{\mathcal{C}_{18}} \frac{\alpha(x)}{\alpha(y)} \frac{\delta\rho(y)}{x-y} + \int_{\mathcal{C}_{15}} \frac{\alpha(x)}{\alpha(y)} \frac{\delta\rho(y)}{x-y} + \int_{\mathcal{C}_{48}} \frac{\alpha(x)}{\alpha(y)} \frac{\delta\rho(y)}{x-y} \\ & + \sum_{n=-N}^N \frac{1}{2} \left[\sum_i \frac{(-1)^{F_{i8}} \alpha(x)}{x - x_n^{i8}} + \sum_j \frac{(-1)^{F_{1j}} \alpha(x)}{x - x_n^{1j}} \right] = \\ & 2 \int_{\mathcal{C}_{18}} \frac{\alpha(x)}{\alpha(y)} \frac{\delta\varrho(y)}{x-y} + \int_{\mathcal{C}_{15}} \frac{\alpha(x)}{\alpha(y)} \frac{\delta\varrho(y)}{x-y} + \int_{\mathcal{C}_{48}} \frac{\alpha(x)}{\alpha(y)} \frac{\delta\varrho(y)}{x-y} \\ & - \frac{1}{2} \sum_{ij} \left(\mathcal{I}_{ij}^{1i} + \mathcal{I}_{ij}^{j8} - \mathcal{I}_{8j}^{8i} - \mathcal{I}_{1i}^{1j} \right) \end{aligned}$$

Finally we can use the x to $1/x$ symmetry to translate last equality into one for $x \in \mathcal{C}_{45}$. Subtracting it from the previous equation we see that the $1/\sqrt{\lambda}$ corrected equation will correspond to adding

$$-\cot_{45} + \sum_{ij} \left(\mathcal{I}_{ij}^{4i} + \mathcal{I}_{ij}^{5i} + \bar{\mathcal{I}}_{1j}^{1i} + \bar{\mathcal{I}}_{8i}^{8j} \right)$$

to the r.h.s. of (4.34) thus obtaining, after the identification $\varrho = \rho_4$, precisely the finite size corrected equation (4.33) obtained from the NBA point of view!

In this section we showed that the one loop shift as a sum of all fluctuation energies (or others local charges) perfectly matches the finite size corrections in the NBA equations. However we systematically dropped the contours around the unit circle. In the next section we will accurately take it into account.

4.3 The unit circle and the Hernandez-Lopez phase

CONSIDER again the sum in the equation (4.35). We can rewrite it as an integral around each x_n^{ij} and then blow the contour to encircle all the singularities of \cot_{ij} and the circle going through the points x_N^{ij} and x_{-N}^{ij} , which are close to 1 and -1 correspondingly. The contributions coming from the contours encircling the cuts of \cot_{ij} we have already considered in the previous section and show that they reproduce the finite size corrections in the BS equations. Let us show that the unit circle contributions accounts for the HL phase factor. We will drop systematically the contributions considered in the previous section.

$$\begin{aligned} & \sum_{n=-N}^N \frac{1}{2} \left[\sum_{i \leq 4} \frac{(-1)^{F_{i5}} \alpha(x)}{x - x_n^{i5}} + \sum_{j \geq 5} \frac{(-1)^{F_{4j}} \alpha(x)}{x - x_n^{4j}} - \sum_{i \leq 4} \frac{(-1)^{F_{i8}} \alpha(1/x)}{1/x - x_n^{i8}} - \sum_{j \geq 5} \frac{(-1)^{F_{1j}} \alpha(1/x)}{1/x - x_n^{1j}} \right] \\ &= \frac{1}{2} \left[\sum_{i \leq 4} \oint \frac{\alpha(x)}{\alpha(y)} \frac{(-1)^{F_{i5}} \cot_{i5}}{x - y} \frac{dy}{2\pi i} + \dots \right] \end{aligned} \quad (4.37)$$

Now let us assume that everywhere we can replace $\cot \left(\frac{p_i(x) - p_j(x)}{2} \right)$ by $i \operatorname{sign}(\operatorname{Im} x)$ with exponential precision in $\frac{L}{\sqrt{\lambda}} \gg 1$. This is reasonable for generic points in the unit circle, where the imaginary part of $p_i(x) - p_j(x)$ is large, but one has to carefully analyze the neighborhood of the real axis, where this imaginary part vanishes. We will analyze this step carefully in the next section. Assuming this could be done we will get

$$\begin{aligned} & \frac{1}{2} \left[\sum_{i \leq 4} \oint \alpha(x) \frac{(-1)^{F_{i5}} (p'_i - p'_5)}{x - y} \operatorname{sign}(\operatorname{Im} y) \frac{dy}{2\pi} + \dots \right] \\ &= \oint \left[\frac{\alpha(x)}{x - y} - \frac{\alpha(1/x)}{1/x - y} \right] (p'_4 - p'_3 - p'_2 + p'_1) \operatorname{sign}(\operatorname{Im} y) \frac{dy}{2\pi} = -2\eta \mathcal{V}(x) \end{aligned} \quad (4.38)$$

Finally, as we can see from (1.56), the combination of quasi-momenta appearing in (4.38) is precisely the one from which one reads the local charges Q_n ,

$$p'_4 - p'_3 - p'_2 + p'_1 = -\eta \partial_y [G_4(y) - G_4(1/y)] . \quad (4.39)$$

where

$$G_4(y) = - \sum_{n=0}^{\infty} Q_{n+1} y^n , \quad (4.40)$$

so that we can expand the denominators in (4.38) for large x and obtain

$$\mathcal{V}(x) = \alpha(x) \sum_{\substack{r,s=2 \\ r+s \in \text{Odd}}}^{\infty} \frac{1}{\pi} \frac{(r-1)(s-1)}{(s-r)(r+s-2)} \left(\frac{Q_r}{x^s} - \frac{Q_s}{x^r} \right) \quad (4.41)$$

where we recognize precisely the Hernandez-Lopez coefficients! To obtain the values of the potential for $|x| < 1$ we can simply use the exact symmetry $\mathcal{V}(x) = -\mathcal{V}(1/x)$ which is not manifest in the form (4.41).

Unit circle contribution

In this section we show that for the “unit circle” contribution we can replace \cot_{ij} by $i \operatorname{sign} \operatorname{Im}(x)$ if the ration $L/\sqrt{\lambda}$ is large.

Let us focus on the vicinity of $x = 1$ where we have the following expansion of the quasi-momenta

$$\frac{p_i(x) - p_j(x)}{2} = \frac{\beta_{ij}}{x-1} + \dots$$

where β_{ij} is usually of order $L/\sqrt{\lambda}$. We will consider the circle with radius $x_{N+1/2}^{ij} \simeq 1 + \frac{1}{\pi N \beta_{ij}}$, where N is some large cutoff in the sum of fluctuations (4.35). We want to estimate

$$\int \alpha(x) f(x) \left[\cot \left(\frac{p_i - p_j}{2} \right) + i \operatorname{sign}(\operatorname{Im} x) \right] (p'_i - p'_j) dx .$$

This integral is dominated for $x \simeq \pm 1$ and can be performed by saddle point. The contribution for $x \simeq 1$ is

$$\int \alpha(x) f(x) \left[\cot \left(\frac{p_i - p_j}{2} \right) + i \operatorname{sign}(\operatorname{Im} x) \right] (p'_i - p'_j) dx = \frac{i\pi^3 f(1)}{6\beta_{ij}\sqrt{\lambda}} + \mathcal{O} \left(\frac{1}{N} \right)$$

which is zero under the sum over all polarizations. For example

$$\frac{(-1)^{F_{45}}}{\beta_{45}} = - \frac{(-1)^{F_{35}}}{\beta_{35}} .$$

Thus we can indeed can replace \cot 's when integrating over the unit circle by a simple sign function. In the Appendix A we will carefully analyze the $N \rightarrow \infty$ limit and the numbering of the frequencies problem.

Summary

Although we always assumed the twists to be sufficiently large and the fillings to be sufficiently small we can always analytically continue the results towards zero twists or large filling fractions. Let us briefly explain why. In the scaling limit, for large twists, the bosonic duality we introduced amounts to a simple exchange of sheets in some Riemann surface, $p_a(x) \leftrightarrow p_b(x)$. As we saw in section 2.2.5 what happens when the twists start to become very small is that the quasi-momenta are still simply exchanged but in a piecewise manner, that is, we can always split the complex planes in some finite number of regions where the bosonic duality simply means $p_a(x) \leftrightarrow p_b(x)$. Thus, from the e^{ip} algebraic curve point of view nothing special occurs for what analyticity is concerned and therefore we can safely analytically continue our findings to any value of the twists. Exactly the same analysis holds for the filling fractions. Moreover, for the usual Bethe system, we defined a set of quasi-momenta, which constitute an algebraic curve to any order in $1/L$, and therefore we don't expect analyticity to break down at any order in $1/L$.

We also performed a high precision numerical check concluding that there is no singularity when the configuration of the Bethe roots is affected by this partial reshuffling of the sheets and that finite size corrections are still related to the same sum of fluctuations, which are analytical functions w.r.t. the twists.

Appendix A: Large N limit

In the x plane the contour in figure 4a is mapped to that in figure 4b. For large N the contour starts at $-1 - \epsilon_-^{ij}(N)$ and ends at $+1 + \epsilon_+^{ij}(N)$. In this appendix we perform a careful analysis of the large N limit.

A.1 Asymptotics of quasimomenta and expansion of x_n

Let us take $\eta = 1$ and use notations (1.57). Large n 's are mapped to the vicinity of ± 1 where

$$\begin{aligned}\hat{p}_2 &\simeq +\frac{\alpha_{\pm}}{x \mp 1} + \sum_{n=0} \hat{a}_n^{\pm} (x \mp 1)^n, & \tilde{p}_2 &\simeq +\frac{\alpha_{\pm}}{x \mp 1} + \sum_{n=0} \tilde{a}_n^{\pm} (x \mp 1)^n, \\ \hat{p}_3 &\simeq -\frac{\alpha_{\pm}}{x \mp 1} + \sum_{n=0} \hat{b}_n^{\pm} (x \mp 1)^n, & \tilde{p}_3 &\simeq -\frac{\alpha_{\pm}}{x \mp 1} + \sum_{n=0} \tilde{b}_n^{\pm} (x \mp 1)^n.\end{aligned}$$

The remaining quasimomenta are fixed by the $x \rightarrow 1/x$ symmetry

$$\begin{aligned}\tilde{p}_{1,2}(x) &= -2\pi m - \tilde{p}_{2,1}(1/x) \\ \tilde{p}_{3,4}(x) &= +2\pi m - \tilde{p}_{4,3}(1/x) \\ \hat{p}_{1,2,3,4}(x) &= -\hat{p}_{2,1,4,3}(1/x).\end{aligned}\tag{4.42}$$

From this expansion we can read the large n behavior of x_n^{ij} defined by (1.7). Let us, however, use a more general definition

$$p_i(x_n^{ij}) - p_j(x_n^{ij}) = 2\pi(n - m_i + m_j). \quad (4.43)$$

For $n \rightarrow \pm\infty$ all x_n^{ij} are close to ± 1 and we find

$$x_n^{ij} = \pm 1 + \frac{\alpha^\pm}{\pi n} + \mathcal{O}(1/n^2) \quad (4.44)$$

where we notice that the first $1/n$ coefficient is universal and fixed uniquely by the residues of the quasi-momenta.

A.2 Large N versus ϵ regularization

The main goal of this appendix is to justify the integration path used in the main text where for all ij the integral in the x plane starts from $-1 - \epsilon$ and ends at $1 + \epsilon$ as depicted on the figure 4.2b. However by definition (4.2) we have to start from the large N regularization. These two regularization in principal are not equivalent, since x_N^{ij} 's are not exactly equal for all ij and thus we should calculate the difference between both regularizations. In particular in (4.37) we will have slightly different contours of integrations after replacement of the cot's by sign. One would like to make all the contours to be the circle of the radius $1 + \epsilon$. However, while changing the contours of integration one will get some unwelcome contribution proportional to

$$\left(\frac{1}{\alpha_+} - \frac{1}{\alpha_-} \right) (m + m_{\bar{1}} + m_{\bar{2}} - m_{\bar{1}} - m_{\bar{2}}) (m + m_{\bar{3}} + m_{\bar{4}} - m_{\bar{3}} - m_{\bar{4}}) .$$

Fortunately it is possible to choose m_i in such a way that it is always zero, and this transformation is possible. For example

$$m_{\bar{1}} = m, \quad m_{\bar{4}} = -m \quad (4.45)$$

and all the others m_i are zero. This amounts to some prescription for the mode numbers. For obvious reasons let us denote it by Bethe ansatz friendly prescription. Contrary to what we had in the chapter 3 we have no obvious argument in favor of this new prescription. For the $sl(2)$ and $su(2)$ one cut solutions this prescription gives the same result (with exponential precision in large \mathcal{J}) as in [81, 82, 83, 84, 53, 51].

5. RELATIVISTIC BOOTSTRAP APPROACH IN ADS/CFT

THE CLASSICAL INTEGRABLE TWO-DIMENSIONAL NON-LINEAR SIGMA MODELS are relatively easy to solve. At least, when the corresponding Lax pair is known, one can construct a large class of the so called classical finite gap solutions [92]. These solutions are known to constitute a dense (in the sense of parameters of initial conditions) subset in the space of solutions of the model.

However, the quantization of such classically integrable sigma-models usually creates substantial problems and is known to be virtually impossible to do in the direct way, in terms of the original degrees of freedom of the classical action. The existing quantum solutions are usually based on plausible assumptions which are difficult to prove in a systematic way.

There were a few successful, though not completely justified, attempts to find the quantum solutions of $SU(N)$ principal chiral field model (PCF), starting from the original action. A. Zamolodchikov and Al. Zamolodchikov [93] found the factorizable bootstrap S-matrices for the $O(N)$ sigma models, later generalized to many other sigma models. The $O(4)$ case which we are focused on in this chapter, is equivalent to the $SU(2)$ PCF. Polyakov and Wiegmann [94, 95] found the equivalent non-relativistic integrable Thirring model reducible in a special limit to the PCF. Faddeev and Reshetikhin [96] proposed the "equivalent" double spin chain for the $SU(2)$ PCF. In both cases, the equivalence is based on subtle assumptions, difficult to verify.

The verification of such solutions is usually based on the perturbation theory, large N limit or Monte-Carlo simulations [93, 97, 98, 99].

Here we address this question in a more systematic way. Namely, we will reproduce all classical finite gap solutions of a sigma model from the Bethe ansatz solution for a system of physical particles on the space circle, in a special large density and large energy limit. We shall call it the continuous limit though, as we show, it is the actual classical limit of the theory. We will see that in this limit the Bethe Ansatz equations (BAE) diagonalizing the periodicity condition, will be reduced to a Riemann-Hilbert problem. This chapter is inspired by [100] and contains many original results.

In [86] we also repeated this construction for the $O(6)$ sigma-model and explained how the generalization to the $O(2n)$ model can be done in a trivial way. In fact, as it

will be clear below, the method seems to be general enough to work for all sigma-models described by a factorizable bootstrap S-matrix. Hence it gives a new way to relate, in a general and systematic way, the classical and quantum integrability.

The classical action of the $SU(2)$ PCF is

$$S = \frac{\sqrt{\lambda}}{8\pi} \int d\sigma d\tau \operatorname{tr} \partial_a g^\dagger \partial_a g, \quad g \in SU(2). \quad (5.1)$$

it is equivalent to the $O(4)$ sigma model where the fundamental field is the four dimensional unit vector $\vec{X}(\sigma, \tau)$. Therefore, at least classically, it can be used to study a string on the $S^3 \times R_1$ background. Indeed, our main motivation for this study was the search for new approaches in the quantization of the Green–Schwartz–Metsaev–Tseytlin superstring on the $AdS_5 \times S^5$ which is classically (and most-likely quantum-mechanically as well) an integrable field theory as we discuss in the introduction. The simplest nontrivial subsector of it is described by the sigma model on the subspace $S^3 \times R_t$, where R_t is the coordinate corresponding to the AdS time. The time direction will be almost completely decoupled from the dynamics of the rest of the string coordinates, appearing only through the Virasoro conditions. These conditions are a selection rule for the states of the theory or, better to say, for the classical solutions appearing when we pick the classical limit in Bethe equations. The degrees of freedom eliminated in this way are the longitudinal modes associated with the reparametrization invariance of the string.

Of course, in the absence of the fermions and of the AdS part of the full 10d superstring theory, this model will be asymptotically free and will not be suitable as a viable to describe the quantum string theory. Nevertheless, in the classical limit we shall encounter the full finite gap solution of the string in the $SO(4)$ sector found in [14]. The method can be generalized to the $SO(6)$ sector in [12] and hopefully to the full Green–Schwartz–Metsaev–Tseytlin superstring on the $AdS_5 \times S^5$ space, including fermions, where the finite gap solution was constructed in [12] (although it appears to be more difficult for the last, and the most interesting, system).

At the end of the paper we go slightly further and derive from these BAE the conjectured asymptotic string Bethe ansatz (the so called AFS-equation [16]) with its nontrivial dressing factor to the leading order in large λ . According to the quasi-classical analysis in the previous chapters it captures the information about the quantum spectrum up to the $1/\sqrt{\lambda}$ order for large $L/\sqrt{\lambda}$.

5.1 Classical $SU(2)$ Principal Chiral Field

In this section we will review the classical finite gap solution of the $SU(2)$ principal chiral field. This construction can be obtained by the reduction of the full $PSU(2,2|4)$ algebraic

curve constructed in the introduction to the $SU(2)$ subsector. This can be achieved by dropping all quasi-momenta except \tilde{p}_2 and \tilde{p}_3 . But for self consistency of this chapter and to fix some notations we will go through the construction of [14]¹ for the easy comparison with the quantum Bethe ansatz solution of the model.

Classically this model can be used to describe the string on $S^3 \times R_t \subset AdS_5 \times S^5$. At the quantum level, even dropping all the rest of the degrees of freedom, one might still expect to capture some features of the full superstring theory. As we will see in the latter sections, this is indeed the case.

The action (5.1) possesses the obvious global symmetry under the right and left multiplication by $SU(2)$ group element. The currents associated with this symmetry are, respectively,

$$j^R \equiv j = g^{-1}dg, \quad j^L = dg g^{-1}, \quad (5.2)$$

and the corresponding Noether charges read

$$Q_R = \frac{i\sqrt{\lambda}}{4\pi} \int_0^{2\pi} d\sigma \operatorname{tr} (j_\tau^R \tau^3), \quad Q_L = \frac{i\sqrt{\lambda}}{4\pi} \int_0^{2\pi} d\sigma \operatorname{tr} (j_\tau^L \tau^3). \quad (5.3)$$

In the quantum theory these charges are positive integers².

Virasoro conditions read $\operatorname{tr} (j_\tau \pm j_\sigma)^2 = -2\kappa_\pm^2$, where we used the residual reparametrization symmetry to fix the AdS global time Y to

$$Y = \frac{\kappa_+}{2}(\tau + \sigma) + \frac{\kappa_-}{2}(\tau - \sigma). \quad (5.4)$$

Finally, from the action, we read off the energy and momentum as

$$E^{\text{cl}} \pm P^{\text{cl}} = -\frac{\sqrt{\lambda}}{8\pi} \int_0^{2\pi} \operatorname{tr} (j_\tau \pm j_\sigma)^2 d\sigma = \frac{\sqrt{\lambda}}{2} \kappa_\pm^2. \quad (5.5)$$

5.1.1 Classical Integrability and Finite Gap Solution

The equations of motion can be encoded into a single flatness condition for a Lax connection over the world-sheet [92],

$$\left[\partial_\sigma - \frac{x j_\tau + j_\sigma}{x^2 - 1}, \partial_\tau - \frac{x j_\sigma + j_\tau}{x^2 - 1} \right] = 0. \quad (5.6)$$

In particular, we can then use this flat connection to define the monodromy matrix

$$\Omega(x) = \overleftarrow{P} \exp \int_0^{2\pi} d\sigma \frac{x j_\tau + j_\sigma}{x^2 - 1}. \quad (5.7)$$

¹ with a little generalization to the excitations of both left and right sectors

² It will be important for future comparisons to notice that the normalization of the generators is such that the smallest possible charge is 1 as follows from the Poisson brackets for the current.

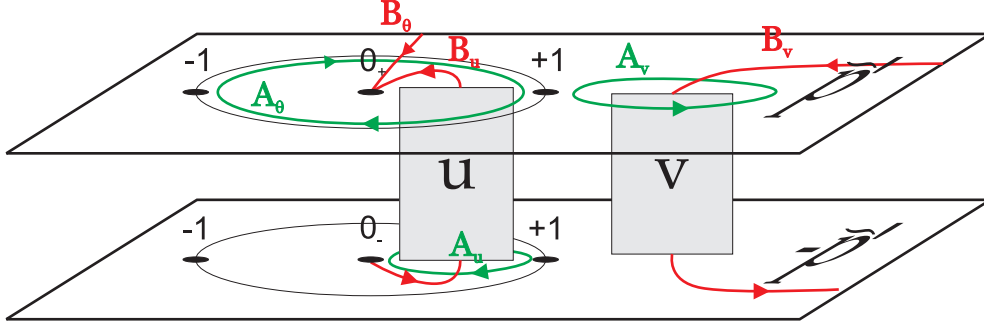


Fig. 5.1: Algebraic curve from the finite gap method. u and v cuts correspond to cuts inside and outside the unit circle respectively.

By construction $\Omega(x)$ is a unimodular matrix (and also unitary for real x) whose eigenvalues can therefore be written as

$$\left(e^{i\tilde{p}(x)}, e^{-i\tilde{p}(x)} \right) \quad (5.8)$$

where $\tilde{p}(x)$ is called the quasi-momentum. These *functions of x* do not depend on time τ due to (5.6) and provide therefore an infinite set of classical integrals of motion of the model.

From the explicit expression (5.7) we can determine the behavior of the quasi-momentum close to $x = \pm 1, 0, \infty$. Using (5.5) and (5.3), we obtain

$$\tilde{p}(x) \simeq -\frac{\pi\kappa_{\pm}}{x \mp 1}, \quad (5.9)$$

$$\tilde{p}(x) \simeq 2\pi m + \frac{2\pi Q_L}{\sqrt{\lambda}} x, \quad (5.10)$$

$$\tilde{p}(x) \simeq -\frac{2\pi Q_R}{\sqrt{\lambda}} \frac{1}{x}. \quad (5.11)$$

Since, by construction, $\Omega(x)$ is analytical in the whole plane except at $x = \pm 1$ where it develops essential singularities, it follows from (5.12) that for $x \neq \pm 1$ the only singularities of

$$\tilde{p}'(x) = -\frac{1}{\sqrt{4 - (\text{tr } \Omega(x))^2}} \frac{d}{dx} \text{tr } \Omega(x). \quad (5.12)$$

are of the form

$$\tilde{p}'(x \rightarrow x_k) \simeq \frac{1}{\sqrt{x - x_k}}. \quad (5.13)$$

If we are looking for a finite gap solution the number K of these cuts is finite and we conclude that $\tilde{p}'(x), -\tilde{p}'(x)$ are two branches of an analytical function defined by a

hyperelliptic curve (see fig.1),

$$(p')^2 = \frac{P^2(x)}{Q(x)}, \quad (5.14)$$

where $Q(x)$ has $2K$ zeros and the order of $P(x)$ is fixed by the large x asymptotics (5.11). We denote the branch cuts of $p'(x)$ by u (v) cuts if they are inside (outside) the unit circle. These cuts are the loci where the eigenvalues of the monodromy matrix become degenerate. Thus, when crossing such cut the quasi-momentum may at most jump by a multiple of 2π which characterizes each cut,

$$\tilde{p}'(x) = \pi n_k, \quad x \in \mathcal{C}_k \quad (5.15)$$

where $\tilde{p}'(x)$ is the average of the quasi-momentum above and below the cut,

$$\tilde{p}'(x) \equiv \frac{1}{2} (\tilde{p}(x + i0) + \tilde{p}(x - i0)). \quad (5.16)$$

Each cut is also parameterized by the filling fraction numbers which we define as integrals along A -cycles of the curve (see fig.1) ³

$$S_i^v = -\frac{\sqrt{\lambda}}{8\pi^2 i} \oint_{A_i^v} \tilde{p}(x) \left(1 - \frac{1}{x^2}\right) dx, \quad S_i^u = \frac{\sqrt{\lambda}}{8\pi^2 i} \oint_{A_i^u} \tilde{p}(x) \left(1 - \frac{1}{x^2}\right) dx. \quad (5.17)$$

Finally, imposing (5.15,5.17,5.9,5.10,5.11) one fixes completely the undetermined constants in (5.14).

5.2 Quantum Bethe Ansatz and Classical Limit: $O(4)$ Sigma-Model

WE WILL DESCRIBE a quantum state of the $O(4)$ sigma model by a system of L relativistic particles of mass $\mu/2\pi$ put on a circle of the length 2π . The momentum and the energy of each particle can be suitably parameterized by its rapidity as $p = \frac{\mu}{2\pi} \sinh \theta$ and $e = \frac{\mu}{2\pi} \cosh \theta$ so that the total energy and momentum will be given by

$$P = \frac{\mu}{2\pi} \sum_{\alpha=1}^L \sinh(\pi\theta_\alpha), \quad (5.18)$$

$$E = \frac{\mu}{2\pi} \sum_{\alpha=1}^L \cosh(\pi\theta_\alpha). \quad (5.19)$$

³ It was pointed out in [12, 15] and shown in [13] that $S_i^{u,v}$ are the action variables so that quasi-classically they indeed become integers. We will also find a striking evidence for this quantization on the string side when finding the classics from the quantum Bethe ansatz where these quantities are naturally quantized. Indeed, from the AdS/CFT correspondence these filling fractions are expected to be integers since this is obvious on the SYM side [14, 15]. We used their integrability to quasi-classically quantize the AdS/CFT string in chapter 3.

These particles transform in the vector representation under $O(4)$ symmetry group or in the bi-fundamental representations of $SU(2)_R \times SU(2)_L$. The scattering of the particles in this theory is known to be elastic and factorizable: the relativistic S-matrix $\hat{S}(\theta_1 - \theta_2)$ depends only on the difference of rapidities of scattering particles θ_1 and θ_2 and obeys the Yang–Baxter equations. As was shown in [93] (and in [95, 97, 101, 102] for the general principle chiral field) these properties, together with the unitarity and crossing-invariance, define essentially unambiguously the S-matrix \hat{S} . Let us recall briefly how the bootstrap program goes. From the symmetry of the problem we know that

$$\hat{S} = \hat{S}_L \times \hat{S}_R \quad (5.20)$$

where $S_{L,R}$ are built by use of the two $SU(2)$ invariant tensors and can therefore be written as

$$\hat{S}_{R,L}(\theta)_{ab}^{a'b'} = \frac{S_0(\theta)}{\theta - i} \left(\theta \delta_a^{a'} \delta_b^{b'} - i f(\theta) \delta_a^{b'} \delta_b^{a'} \right).$$

Imposing the Yang-Baxter equation on \hat{S} yields $f(\theta) = 1$, while the unitarity constrains the remaining unknown function to obey

$$S_0(\theta)S_0(-\theta) = 1 \quad (5.21)$$

and crossing symmetry requires

$$S_0(\theta) = \left(1 - \frac{i}{\theta}\right) S_0(i - \theta). \quad (5.22)$$

From (5.21), (5.22) and the absence of poles on the physical strip $0 < \theta < 2$ one can compute the scalar factor: $S_0(\theta) = \frac{\Gamma(-\frac{\theta}{2i})\Gamma(\frac{1}{2} + \frac{\theta}{2i})}{\Gamma(\frac{\theta}{2i})\Gamma(\frac{1}{2} - \frac{\theta}{2i})}$. For our purpose we just need the much easier to extract large θ asymptotics. From (5.22) and (5.21) it follows immediately that

$$i \log S_0^2(\theta) = 1/\theta + O(1/\theta^3). \quad (5.23)$$

5.2.1 Bethe Equations for Particles on a Circle

When this system of particles is put into a finite 1-dimensional periodic box of the length \mathcal{L} the set of rapidities of the particles $\{\theta_\alpha\}$ is constrained by the condition of periodicity of the wave function $|\psi\rangle$ of the system,

$$|\psi\rangle = e^{i\mu \sinh \pi \theta_\alpha} \prod_1^{\overleftarrow{\alpha-1}} \hat{S}(\theta_\alpha - \theta_\beta) \prod_N^{\overrightarrow{\alpha+1}} \hat{S}(\theta_\alpha - \theta_\beta) |\psi\rangle, \quad (5.24)$$

where the first term is due to the free phase of the particle and the second is the product of the scattering phases with the other particles. The arrows stand for ordering of the

terms in the product and $\mu = m_0 \mathcal{L}$ is a dimensionless parameter. Diagonalization of both the L and R factors in the process of fixing the periodicity (5.24) leads to the following set of Bethe equations [103] which may be found from (5.24) by the algebraic Bethe ansatz method [104, 64]. We took the logarithms of the Bethe ansatz equations in their standard, product form. This leads to the integers m_α, n_j^u, n_j^v defining the choice of the branch of logarithms

$$2\pi m_\alpha = \mu \sinh \pi \theta_\alpha - \sum_{\beta \neq \alpha}^L i \log S_0^2(\theta_\alpha - \theta_\beta) - \sum_j^{J_u} i \log \frac{\theta_\alpha - u_j + i/2}{\theta_\alpha - u_j - i/2} - \sum_k^{J_v} i \log \frac{\theta_\alpha - v_k + i/2}{\theta_\alpha - v_k - i/2}, \quad (5.25)$$

$$2\pi n_j^u = \sum_\beta^L i \log \frac{u_j - \theta_\beta - i/2}{u_j - \theta_\beta + i/2} + \sum_{i \neq j}^{J_u} i \log \frac{u_j - u_i + i}{u_j - u_i - i}, \quad (5.26)$$

$$2\pi n_j^v = \sum_\beta^L i \log \frac{v_k - \theta_\beta - i/2}{v_k - \theta_\beta + i/2} + \sum_{l \neq k}^{J_v} i \log \frac{v_k - v_l + i}{v_k - v_l - i}, \quad (5.27)$$

where u 's and v 's are the Bethe roots appearing from the diagonalization of (5.24) and characterizing each quantum state. A quantum state with no such roots corresponds to the highest weight ferromagnetic state where all spins of both kinds are up. Adding a u (v) roots corresponds to flipping one of the right (left) $SU(2)$ spins, thus creating a magnon. The left and right charges of the wave function, associated with the two $SU(2)$ spins are given by

$$Q_L = L - 2J_u, \quad Q_R = L - 2J_v. \quad (5.28)$$

This model with massive relativistic particles and the asymptotically free UV behavior cannot look like a consistent quantum string theory. Only in the classical limit we can view it as a string toy model obeying the classical conformal symmetry. In the classical case it is also easy to impose the Virasoro conditions. In the quasi-classical limit, we still can try to impose the Virasoro conditions as some natural constraints on the quantum states. We will discuss this point later.

5.3 Quasi-classical limit

IN THE CLASSICAL LIMIT the physical mass of the particle ⁴

⁴ For the $O(N)$ sigma model the beta function for the coupling is given by $\beta \equiv \frac{\partial}{\partial \log \Lambda} \sqrt{\lambda(\Lambda)} = N - 2$ where Λ is the cutoff of the theory. The dynamically generated mass must be of the form $\mu = \Lambda f(\sqrt{\lambda})$. The

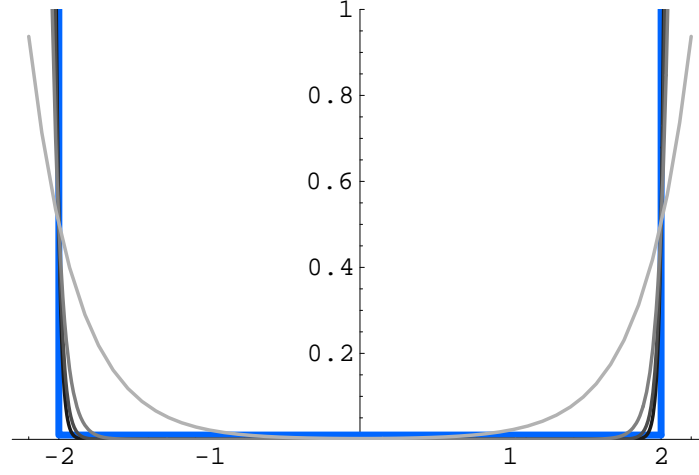


Fig. 5.2: We plot $V(z)$ for $M = 1, 5, 9, 13$ (lighter to darker gray). It is clear that the potential approaches the blue box potential as $M \rightarrow \infty$.

$$\frac{\mu}{2\pi} \sim e^{-\sqrt{\lambda}/2}, \quad (5.29)$$

where λ is the physical coupling at the scale of the size of the box 2π , vanishes since $\lambda \rightarrow \infty$. Moreover we should focus on quantum states with large quantum numbers, i.e. we shall consider a large number $L \rightarrow \infty$ of particles on the ring.

Let us now think of (5.25-5.27) as of the equations for the equilibrium condition for a system of three kinds of particles: $(\theta_\alpha, u_j$ and $v_k)$, interacting between themselves and experiencing the external constant forces $(2\pi m_\alpha, 2\pi n_j^u$ and $2\pi n_k^v)$. The particles of the θ kind are also placed into the external confining potential

$$V(z) = \mu \cosh(\pi M z), \quad z = \theta / M \quad (5.30)$$

where

$$M \equiv -\frac{\log \mu}{2\pi} \simeq \frac{\sqrt{\lambda}}{4\pi}. \quad (5.31)$$

In the classical limit the potential becomes a square box potential with the infinite walls at $z = \pm 2$ (see fig.5.2). Moreover, since this is a large box for the original variables we can use the asymptotics (5.23) for the force between particles of the θ (or z) type. The box potential provides the appropriate boundary conditions for the density of particles interacting by the Coulomb force. Since they repel each other the density should be peaked around $z = \pm 2$. To find the correct asymptotics close to these two points, we can consider (5.25) as the equilibrium condition for the gas of Coulomb particles in the box.

functional form of f is fixed by the β function upon imposing independence on the cutoff of this physical quantity. Thus, for general N , $-\log \mu = \frac{\sqrt{\lambda}}{N-2} + \mathcal{O}(1)$.

If the right and left modes (magnons) are not excited we have only the states with $U(1)$ modes. In the classical limit, using the Coulomb approximation (5.23), we have for this sector the following Bethe equation

$$\mu \sinh \pi M z_\alpha - 2\pi m = -\frac{1}{M} \sum_{\beta \neq \alpha}^L \frac{1}{z_\alpha - z_\beta}.$$

In the continuous limit, the equation for the asymptotic density, $L \sim M \rightarrow \infty$, is given, through the resolvent $G_\theta(z) = \frac{1}{M} \sum_{\beta=1}^L \frac{1}{z-z_\beta}$ by

$$\mathcal{Q}_\theta(z) = -2\pi m, \quad z \in \mathcal{C}_\theta, \quad (5.32)$$

with inverse square root boundary conditions near ± 2 . The analytical function $G_\theta(x)$ having a real part on the cut defined by (5.32), with support $[-2, 2]$, with inverse square root boundary conditions (the only compatible with the asymptotics at $z \rightarrow \infty$: $G_\theta(z) \rightarrow \frac{L}{M} \frac{1}{z}$, is completely fixed:

$$G_\theta(z) = \left(\frac{2\pi m z + \frac{L}{M}}{\sqrt{z^2 - 4}} - 2\pi m \right), \quad L > 4\pi|m|M \quad (5.33)$$

which gives for the density

$$\rho_\theta(z) = \frac{1}{\pi} \left(\frac{2\pi m z + \frac{L}{M}}{\sqrt{4 - z^2}} \right). \quad (5.34)$$

For a general solution with u and v magnons we will also find the same asymptotics

$$\rho(z) \equiv \frac{1}{M} \sum_{\alpha=1}^L \delta(z - z_\alpha) \simeq \frac{2\kappa_\pm}{\sqrt{2 \mp z}}, \quad z \rightarrow \pm 2. \quad (5.35)$$

with κ_\pm yet to be determined through the energy and momentum of the solution, as we shall explain in the next section.

We will be considering the scenario where we have the same mode number $m_\alpha = m$ for all z particles. As proposed in [86, 100] this is the adequate set of states which will obey the Virasoro constraints in the classical limit.

First, we will relate the z behavior close to the walls, characterized by the constants κ_\pm with the energy and momentum E, P of the quantum state, as given by (5.36, 5.19). Then we shall eliminate the θ 's from the system of Bethe equations by explicitly solving the first one in the considered limit. Finally, we will justify why we take the same mode number m for all θ 's by identifying the longitudinal modes to the excited mode numbers m_i in the Bethe ansatz setup. This constraint on the states will correspond to the Virasoro conditions, at least in the classical limit.

5.3.1 Energy and momentum

The total momentum can be calculated exactly, before any classical limit⁵

$$P = \frac{\mu}{2\pi} \sum_{\alpha} \sinh(\pi\theta_{\alpha}) = m_p L_p - \sum_p n_p S_p^u - \sum_p n_p S_p^v \quad (5.36)$$

where L_p, S_p^u, S_p^v are the numbers of Bethe roots with a given mode numbers $m_p, n_{u,p}, n_{v,p}$. To prove this, it suffices to sum the (5.25) for all roots θ_{α} . The contribution of $S_0(\theta)$ terms cancels due to antisymmetry while the second and third sums in the r.h.s. of (5.25) are replaced using (5.26) and (5.27), respectively.

Let us show how to calculate the energy (5.19) which is a far less trivial task [86]. As a byproduct we will also reproduce the total momentum from the behavior at the singularities at $z = \pm 2$ described by the residues κ_{\pm} . We want to compute the sum

$$E \equiv \frac{\mu}{2\pi} \sum_{\alpha} \cosh(\pi\theta_{\alpha}), \quad (5.37)$$

but we *cannot* simply replace this sum by an integral and use the asymptotic density $\rho_{\theta}(z)$ to compute the energy. That is because the main contribution to the energy comes from large θ 's, near the walls, where the expression for the asymptotic density is no longer accurate. It is natural for the classical limit since the particles become effectively massless and the contributions of right and left modes are clearly distinguishable and located far from $\theta = 0$. We notice that the energy is dominated by large θ 's where, with exponential precision, we can replace $\cosh \pi\theta_{\alpha}$ by $\pm \sinh \pi\theta_{\alpha}$ for positive (negative) θ_{α} . Furthermore, the contribution from the θ 's in the middle of the box is also exponentially suppressed since μ is very small. Thus we can pick a point a somewhere in the box not too close to the walls. One can think of a as being somewhere in the middle. Then,

$$E = \sum_{z_{\alpha} > a} \frac{\mu}{2\pi} \sinh(\pi z_{\alpha} M) - \sum_{z_{\alpha} < a} \frac{\mu}{2\pi} \sinh(\pi z_{\alpha} M), \quad (5.38)$$

where, let us stress, the result is *correct independently of the point a within the interval $-2 < a < 2$ with the exponential precision*. Each sum of $\sinh \pi\theta_{\alpha}$ can be substituted by the corresponding r.h.s. of the Bethe equation (5.25), thus giving

$$\begin{aligned} E &\simeq \frac{i}{\pi} \sum_{z_{\beta} < a < z_{\alpha}} \log S_0^2(M[z_{\alpha} - z_{\beta}]) + \sum_{\alpha} m \operatorname{sign}(z_{\alpha} - a) \\ &- \frac{1}{2\pi} \sum_{j,\alpha} \operatorname{sign}(z_{\alpha} - a) i \log \frac{Mz_{\alpha} - u_j + i/2}{Mz_{\alpha} - u_j - i/2} - \frac{1}{2\pi} \sum_{k,\alpha} \operatorname{sign}(z_{\alpha} - a) i \log \frac{Mz_{\alpha} - v_k + i/2}{Mz_{\alpha} - v_k - i/2} \end{aligned} \quad (5.39)$$

⁵ For the closed string theory we should take $P = 0$ which gives the level matching condition. Moreover, as we shall explain latter, we should also pick the same mode number for all particles, $m_{\alpha} = m$.

As mentioned above we assume all m_α to be the same ⁶. Now we can safely go to the continuous limit since in the first term the distances between z 's are now mostly of the order 1⁷. This allows to rewrite the energy, with $1/M$ precision, as follows

$$E \simeq -\frac{M}{\pi} \int_{-2}^a dz \int_a^2 dw \frac{\rho_\theta(z)\rho_\theta(w)}{z-w} - \frac{M}{2\pi} \int \frac{\rho_\theta(z)\rho_u(w)}{z-w} \text{sign}(z-a) dz dw \\ - \frac{M}{2\pi} \int \frac{\rho_\theta(z)\rho_v(w)}{z-w} \text{sign}(z-a) dz dw + m M \int \rho_\theta(z) \text{sign}(z-a) dz \quad (5.40)$$

where we are now free to use the asymptotic density $\rho_\theta(z)$. By the use of Bethe equations, we managed to transform the original sum over cosh's, highly peaked at the walls, into a much smoother sum where the main contribution is now softly distributed along the bulk and where the continuous limit does not look suspicious. From the previous discussion we know that this expression does not depend on a provided a is not too close to the walls. In fact, we can easily see that it does not depend on a *at all* after taking the continuous limit leading to the perfect box-like potential. To prove it one notices that due to Bethe equations (5.25) the a -derivative of (5.40) is zero for all $a \in]-2, 2[$. Hence we can even send a close to a wall: $a = -2 + \epsilon$, where ϵ is very small. But then the last three terms in (5.40) are precisely the momentum (5.36), as explained in the beginning of this section. To compute the first term we can now use the asymptotics (5.23,5.35). The contribution of this term is then given by

$$-\frac{M}{\pi} \int_{-2}^{-2+\epsilon} dz \int_{-2+\epsilon}^2 dw \frac{\rho_\theta(z)\rho_\theta(w)}{z-w} \\ \simeq - \int_{-2}^{-2+\epsilon} dz \int_{-2+\epsilon}^2 dw \frac{4M\kappa_-^2}{\pi(z-w)\sqrt{2+z}\sqrt{2+w}} \simeq 2\pi M\kappa_-^2 \quad (5.41)$$

so that

$$E \simeq 2M\kappa_-^2 \pi + P. \quad (5.42)$$

If we compute the a -independent integral (5.40) near the other wall, i.e. for $a = 2 - \epsilon$, we find

$$E \simeq 2M\kappa_+^2 \pi - P.$$

⁶ as we will show it is this choice of states which reproduces the finite gap solution of [14] we mentioned in the first section. We will come back to this point at a latter stage

⁷ Moreover, it is very important that the contribution from z 's near the walls ± 2 is now suppressed since (5.23)

$$|\log S_0^2(M(2-z_\beta))| > |\log S_0^2(M(2-a))| \sim 1/M.$$

Therefore, equating the results one obtains the desired expressions for the energy and momentum

$$E \pm P = 2\pi M \kappa_{\pm}^2 \quad (5.43)$$

through the singularities of the density of rapidities at $z = \pm 2$, described by κ_{\pm} . Together with (5.31) this is precisely the classical formula (5.5)!

5.4 Elimination of θ 's and AFS equations

IN THIS SECTION we will show how the AFS equations (1.39), which are restriction of the BS equations on the $\mathfrak{su}(2)$ subsector, can be derived from the bootstrap approach. It is useful for what follows, to introduce some new notations. Using the Zhukovsky map

$$z = x(z) + \frac{1}{x(z)}, \quad |x(z)| > 1 \quad (5.44)$$

we define

$$y_j^{\pm} \equiv x\left(\frac{u_j \pm i/2}{M}\right), \quad y_j \equiv x\left(\frac{u_j}{M}\right) \quad (5.45)$$

with the similar expressions for v_l given by \tilde{y}_l^{\pm} and \tilde{y}_l .

In this section, for the purposes of comparison with the asymptotic AFS Bethe ansatz for the N=4 SYM theory, let drop the v magnons, $J_v = 0$. Their contributions will be easily restored later. As explained at the beginning of this section we can write the first Bethe equation, (5.25) as

$$\mathcal{G}_{\theta}(z) + 2\pi m = \sum_{j=1}^K i \log \frac{Mz - u_j - i/2}{Mz - u_j + i/2}, \quad (5.46)$$

Where

$$G_{\theta}(z) = \frac{1}{M} \sum_{\alpha} \frac{1}{z - \theta_{\alpha}/M} = \int_{-2}^2 \frac{dz' \rho_{\theta}(z')}{z - z'} \quad (5.47)$$

and $\mathcal{G}_{\theta}(z)$ is a real part of $G_{\theta}(z)$. We can find $G_{\theta}(z)$ as a function of u_j .

Performing the inverse Zhukovsky map (5.44,5.45) we obtain the equation

$$\mathcal{G}_{\theta}(z) + 2\pi m = i \sum_{j=1}^K \left(\log \frac{x - y_j^+}{x - y_j^-} + \log \frac{x - 1/y_j^+}{x - 1/y_j^-} \right) \quad (5.48)$$

Introducing

$$H(x) = G_{\theta}(z(x)) \quad (5.49)$$

we obtain from (5.48)

$$\frac{1}{2} [H(x) + H(1/x)] = -2\pi m + i \sum_{j=1}^K \left(\log \frac{x - y_j^+}{x - y_j^-} + \log \frac{x - 1/y_j^+}{x - 1/y_j^-} \right). \quad (5.50)$$

The solution of this equation, with the right asymptotics at infinity $H(1/\epsilon) = G_\theta(1/\epsilon) \simeq L/M\epsilon$, is as follows

$$\begin{aligned} H(x) = & i \sum_{j=1}^K \left[\frac{2x}{x^2 - 1} \left(\frac{1}{y_j^+} - \frac{1}{y_j^-} \right) - \frac{2x^2 \log \frac{y_j^+}{y_j^-}}{x^2 - 1} + 2 \log \frac{y_j^+ x - 1}{y_j^- x - 1} \right] \\ & + \frac{\frac{L}{2M} + 2\pi m}{x - 1} + \frac{\frac{L}{2M} - 2\pi m}{x + 1}. \end{aligned} \quad (5.51)$$

We can also compute the density of θ 's as the imaginary part of the resolvent $G_\theta(z)$

$$\rho_\theta(Z(x)) = \frac{\text{Im} G_\theta(Z(x))}{\pi} = \frac{i}{2\pi} [H(x) - H(1/x)] \quad (5.52)$$

Then from (5.43,5.35) we see that in classical limit (5.36,5.19) can be expressed through poles of $H(x)$ in $x = \pm 1$. Extracting the residues of $H(x)$ at the poles $x = \pm 1$ we can see that

$$\Delta = L + 2iM \sum_{j=1}^K \left(\frac{1}{y_j^+} - \frac{1}{y_j^-} \right) \quad (5.53)$$

$$P = \left(m - \frac{i}{2\pi} \sum_{j=1}^K \log \frac{y_j^+}{y_j^-} \right) \Delta = 0 \quad (5.54)$$

(5.53) is precisely the expression for the anomalous dimension (1.43) and (5.54) gives precisely the zero momentum condition for the AFS equation (1.42) (for zero twists)!

5.4.1 Derivation of AFS formula

In this section we will exclude θ variables from (5.26,5.27) using the θ -density calculated above, and obtain the AFS equation (1.39). We are trying here to go the same way as the authors of [105], where the similar variables were excluded in favor of the magnon variables in Lieb-Wu equations for the Hubbard model.

Let us now exclude θ 's from (5.26), using the result (5.51). Taking the log of (5.26) we obtain

$$\sum_{j \neq k} \log \frac{u_k - u_j + i}{u_k - u_j - i} + 2\pi i n_k = \sum_{\beta} \log \frac{u_k - \theta_{\beta} + i/2}{u_k - \theta_{\beta} - i/2} \equiv i p_k \quad (5.55)$$

rewriting p_k through density we have

$$ip_k = M \int_{-2}^2 \log \frac{z - w_k^+}{z - w_k^-} \rho_\theta(z) dz \quad (5.56)$$

where $w_k^\pm = \frac{u_k \pm i/2}{M}$. The function $\rho_\theta(z)$ is given by (5.52,5.51). In Appendix A we perform the integration and obtain the following result

$$\begin{aligned} ip_k = & \sum_j \left[2 \log \frac{y_k^- y_j^+ (y_j^- y_k^+ - 1)}{y_k^+ y_j^- (y_j^+ y_k^- - 1)} - 2i(u_j - u_k) \log \frac{(y_j^- y_k^- - 1)(y_j^+ y_k^+ - 1)}{(y_j^- y_k^+ - 1)(y_j^+ y_k^- - 1)} \right] \\ & - 2M \left(\frac{1}{y_k^+} - \frac{1}{y_k^-} \right) \left[2\pi m - i \sum_j \log \frac{y_j^+}{y_j^-} \right] + L \log \frac{y_k^+}{y_k^-} \end{aligned} \quad (5.57)$$

It leads to the following equations

$$\left(\frac{y_k^+}{y_k^-} \right)^L = \prod_{j \neq k}^K \frac{y_k^+ - y_j^-}{y_k^- - y_j^+} \left(\frac{1 - 1/(y_j^- y_k^+)}{1 - 1/(y_j^+ y_k^-)} \right)^{-1} \left(\frac{(y_j^- y_k^- - 1)(y_j^+ y_k^+ - 1)}{(y_j^- y_k^+ - 1)(y_j^+ y_k^- - 1)} \right)^{2i(u_j - u_k)} \quad (5.58)$$

which precisely coincide with the AFS [16] (1.39), including the expressions for energy and momentum (5.53,5.54).

5.4.2 Classical limit and KMMZ algebraic curve

To consider the classical limit we trivially restore the v roots from the previous calculation, to find

$$\left(\frac{y_k^+}{y_k^-} \right)^L = \prod_{j \neq k}^{J_u} \frac{u_k - u_j + i}{u_k - u_j - i} \sigma^2(u_j, u_k) \prod_{l=1}^{J_v} \sigma^2(v_l, u_k), \quad (5.59)$$

and similarly for \tilde{y}_k , and consider the limit where $J_u, J_v, L \sim M$, so that the u and v roots also scale as M . Then the expansion of this equation, after taking the \log 's, gives to the leading order in $1/M$

$$\pi n_k = \frac{\frac{L}{2M} y_k + 2\pi m}{1 - y_k^2} + \frac{1}{y_k^2 - 1} \frac{1}{M} \sum_{l=1}^{J_v} \frac{1}{1/y_k - \tilde{y}_l} + \frac{y_k^2}{y_k^2 - 1} \frac{1}{M} \sum_{j \neq k}^{J_u} \frac{1}{y_k - y_j}. \quad (5.60)$$

Finally we can define the quasimomentum [106]

$$p(x) = \frac{\frac{L}{2M} x + 2\pi m}{1 - x^2} + \frac{1}{x^2 - 1} \frac{1}{M} \sum_{j=1}^{J_v} \frac{1}{1/x - \tilde{y}_j} + \frac{x^2}{x^2 - 1} \frac{1}{M} \sum_{j=1}^{J_u} \frac{1}{x - y_j}. \quad (5.61)$$

Let us explain how it becomes precisely the quasimomentum we had in the context of the algebraic curve in section 5.1.1 in the classical theory. It is clear that we indeed have the

asymptotics (5.10,5.11) close to $x = 0, \infty$. Then, to relate the residues of (5.61) to the ones found from the algebraic curve in (5.9), we expand (5.53) in our limit as follows:

$$\Delta = L + \sum_j \frac{2}{y_j^2 - 1} + \sum_l \frac{2}{\tilde{y}_l^2 - 1} \quad (5.62)$$

and check that this is indeed what one finds from the quasimomenta we just defined. Finally, when we consider a large number of magnons J_u, J_v the roots in (5.61) condense into a number of one dimensional supports, the sums becoming the integrals along these lines giving the same square root cuts as we had in the finite gap construction.

5.4.3 Geometric proof

The roots solving (5.25,5.26,5.27) with the same mode number will condense into a single square root cut. When we consider more than one type of mode numbers we see that the particles condense into a few distinct supports, one for each distinct mode number

$$\mathcal{C} = \mathcal{C}_1 \cup \dots \cup \mathcal{C}_K.$$

We can now rescale the Bethe roots

$$(u, v, \theta) = M(x, y, z) \quad (5.63)$$

and define

$$\begin{aligned} p_1 = -p_2 &= \frac{1}{M} \sum_{i=1}^{J_u} \frac{1}{z - x_i} - \frac{1}{2M} \sum_{\beta=1}^L \frac{1}{z - z_\beta} \\ p_3 = -p_4 &= \frac{1}{M} \sum_{l=1}^{J_v} \frac{1}{z - y_l} - \frac{1}{2M} \sum_{\beta=1}^L \frac{1}{z - z_\beta}. \end{aligned} \quad (5.64)$$

Then we can recast the Bethe equations in this scaling limit as follows

$$\begin{aligned} x \in \mathcal{C}_u, & \quad p_1^+ - p_2^- = 2\pi n_u \\ x \in \mathcal{C}_\theta, & \quad p_2^+ - p_3^- = 2\pi m \\ x \in \mathcal{C}_v, & \quad p_3^+ - p_4^- = 2\pi n_v \\ x \in \mathcal{C}_\theta, & \quad p_4^+ - p_1^- = 2\pi m, \end{aligned} \quad (5.65)$$

where we

- considered, as in the preceding section, one single mode number m for all rapidities;
- dropped the momentum $\mu \sinh \theta$. As we explained in section 5.3 we can do this provided we replace it by the boundary conditions (5.35).

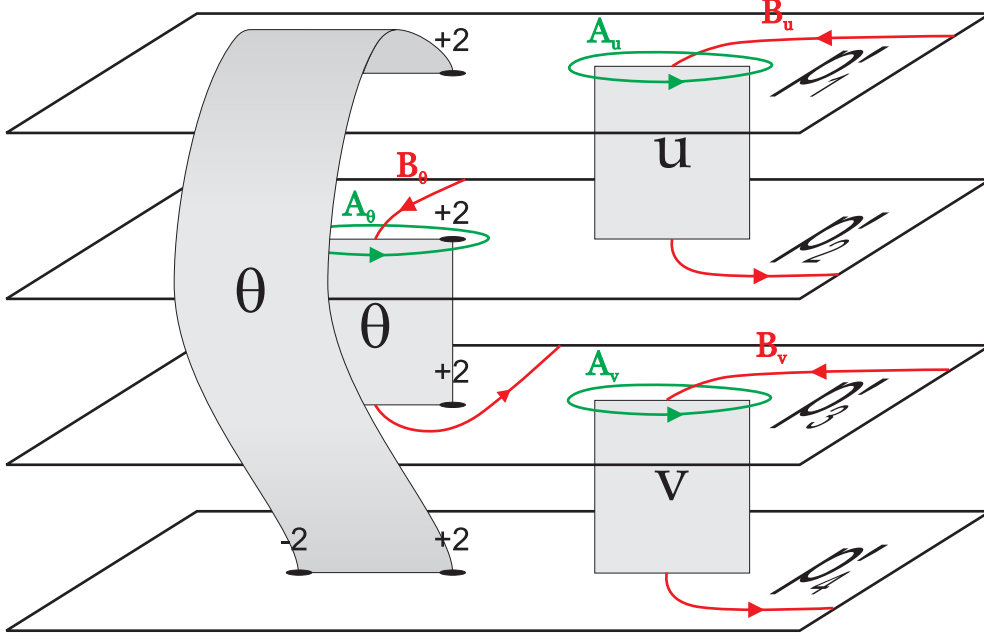


Fig. 5.3: Structure of the curve coming from the Bethe ansatz side. This figure is related with fig.1 by means of the Zhukovsky map.

These equations tell us that $p'_1(z), p'_2(z), p'_3(z), p'_4(z)$ form four sheets of the Riemann surface of an analytical function $p'(z)$ (see fig.5.3).

They can also be written as holomorphic integrals around the infinite B-cycles:

$$\begin{aligned}
 \oint_{B_j^u} dp &= 2\pi n_{u,j} & n_j &= 1, \dots, K_u \\
 \oint_{B_j^v} dp &= 2\pi n_{v,j} & n_j &= 1, \dots, K_v \\
 \oint_{B^\theta} dp &= 2\pi m
 \end{aligned} \tag{5.66}$$

where the first two conditions correspond to the equations in the first and third line of (5.65), respectively, while the last one corresponds to any of the equations of the second and fourth lines of (5.65). The B cycles are defined as in fig.5.3.

We found two Riemann surfaces which we plotted in figures 1 and 5.3. The equivalence between these two curves is achieved through the Zhukovsky map [86]

$$z = x + \frac{1}{x}$$

and amounts to the equivalence between the finite gap solutions for the classical theory and the Bethe ansatz solutions in the scaling limit.

5.5 Virasoro modes

WE ESTABLISHED THE EQUIVALENCE between

- all classical solutions following from the PCF action (5.1) and subject to the Virasoro conditions $\text{tr} (j_\tau \pm j_\sigma)^2 = -2\kappa_\pm^2$ as described by the construction of the algebraic curve of section 5.1.1.
- and the Bethe ansatz quantum solution (5.25-5.26) in the scaling limit (5.63) with all rapidities θ_α having the same mode number m .

In the context of string theory one is interested in quantizing the Polyakov string action

$$S = \frac{\sqrt{\lambda}}{8\pi} \int d\sigma d\tau \sqrt{h} h^{ab} \left(\text{tr} \partial_a g^\dagger \partial_b g - \partial_a Y \partial_b Y \right). \quad (5.67)$$

Due to its local reparametrization and Weyl symmetries one can then fix the target space time Y as in (5.4) and reduce the action to (5.1). However, due to the residual reparametrization symmetry

$$\tau \pm \sigma \rightarrow f_\pm(\tau \pm \sigma), \quad (5.68)$$

one must keep in mind that the original presence of the world-sheet metric field imposes that the stress energy tensor vanishes. This is precisely the Virasoro conditions.

On the other hand, from the field theory point of view the Bethe ansatz equations (5.25-5.27) should describe all possible states of the theory, not only those for which

$$\langle \psi | T^{ab} | \phi \rangle = 0. \quad (5.69)$$

Thus, in view of the equivalence we proved, we are lead to the conclusion that if we start with some classical solution with one θ cut and some u and v cuts, the excitation of additional microscopic θ cuts should correspond to the inclusion of the longitudinal modes which we drop in the context of string theory. Indeed, these massless (from the world-sheet point of view) excitations coming from our conformal gauge choice, appear if one expands the action around the classical solution without fixing the Virasoro conditions from the beginning (see for instance expression 2.7 and the discussion following it in [82]). In this section we verify this claim therefore justifying this single θ cut restriction, first proposed in [100] and given the interpretation as the Virasoro condition in [86].

In (5.39) we computed the energy of a quantum state where all mode numbers $m_\alpha = m$ were the same. If we change the mode numbers of a few θ 's we will have a macroscopic support with particles having the mode number m surrounded by some microscopic domains, linear supports, with mode numbers $m_\beta < m$ (to the left of it) and $m_\beta > m$ (to its right).

Let us assume that we excite them one at a time and focus on the first particle whose mode number we change. Before we do it, it is in equilibrium due to the exponential force exerted by the wall of the box (5.30) and by (an equal) force produced by all the other particles and by the constant force $2\pi m$ – see (5.25). When we change the particle mode number the constant force increases pushing the particle against the wall. However since the forces are exponential the shift will be very small, much smaller than $1/M$ – the characteristic distance between the neighboring rapidities. Then let us consider the particles in the middle of the box, the ones whose position is well described by the asymptotic density $\rho(z)$. They only feel the change in mode number through the new position of the corresponding θ particle. Since this shift is very small the asymptotic density, to the order we are interested, is not changed. Thus, in this procedure of changing a few mode numbers we conclude that, when going to the continuous limit in (5.39), only the second term will lead to a different result so that

$$\delta E = \sum_n |n| N_{m+n} \quad (5.70)$$

where N_n is the number of particles with mode number n . We found in this way the massless (world-sheet) modes associated with the local reparametrization symmetry of the world-sheet. These modes appear when considering the fluctuations around a classical solution [82] and are the only ones not taken into account by the finite gap algebraic curve (see chapter 3).

Appendix A: Derivation of AFS formula for asymptotic string BAE's

In this appendix we evaluate integral (5.56) and obtain AFS BAE.

We can simplify expression for $H(x)$ (5.51) assuming that in (5.54) $P = 0$

$$H(x) = -4\pi m + \frac{\Delta}{M} \frac{x}{x^2 - 1} + 2i \sum_j \log \frac{y_j^+ x - 1}{y_j^- x - 1} \quad (5.71)$$

we rewrite (5.56) in x variable

$$ip_k = -\frac{M}{2} \oint \frac{i}{2\pi} (H(x) - H(1/x)) \left(\log \frac{x - y_k^+}{x - y_k^-} + \log \frac{x - 1/y_k^+}{x - 1/y_k^-} \right) \left(1 - \frac{1}{x^2} \right) dx \quad (5.72)$$

where contour goes in counterclockwise direction around unit circle, $y_k^\pm = X(w_k^\pm)$. Note that terms with $H(1/x)$ are equal to that with $H(x)$ after change of the variable $x \rightarrow 1/x$. So that

$$ip_k = M \oint H(x) \left(\log \frac{x - y_k^+}{x - y_k^-} + \log \frac{x - 1/y_k^+}{x - 1/y_k^-} \right) \left(\frac{x^2 - 1}{x^2} \right) \frac{dx}{2\pi i} \quad (5.73)$$

Various terms are

$$I_1 \equiv \oint \left(-4\pi m + \frac{\Delta}{M} \frac{x}{x^2 - 1} \right) \log \frac{x - y_k^+}{x - y_k^-} \left(\frac{x^2 - 1}{x^2} \right) \frac{dx}{2\pi i} \quad (5.74)$$

$$I_2 \equiv \oint \left(-4\pi m + \frac{\Delta}{M} \frac{x}{x^2 - 1} \right) \log \frac{x - 1/y_k^+}{x - 1/y_k^-} \left(\frac{x^2 - 1}{x^2} \right) \frac{dx}{2\pi i} \quad (5.75)$$

$$I_3 \equiv 2i \oint \log \frac{y_j^+ x - 1}{y_j^- x - 1} \log \frac{x - y_k^+}{x - y_k^-} \left(\frac{x^2 - 1}{x^2} \right) \frac{dx}{2\pi i} \quad (5.76)$$

$$I_4 \equiv 2i \oint \log \frac{y_j^+ x - 1}{y_j^- x - 1} \log \frac{x - 1/y_k^+}{x - 1/y_k^-} \left(\frac{x^2 - 1}{x^2} \right) \frac{dx}{2\pi i} \quad (5.77)$$

Integral I_1 can be calculated by residue in $x = 0$, since $|y_k^\pm| > 1$.

$$I_1 = \frac{\Delta}{M} \log \frac{y_k^+}{y_k^-} - 4\pi m \left(\frac{1}{y_k^+} - \frac{1}{y_k^-} \right) \quad (5.78)$$

Similar I_2 and I_4 are given by residue at infinity.

$$I_2 = 4\pi m \left(\frac{1}{y_k^+} - \frac{1}{y_k^-} \right) \quad (5.79)$$

$$I_4 = -2i \left(\frac{1}{y_k^+} - \frac{1}{y_k^-} \right) \log \frac{y_j^+}{y_j^-} \quad (5.80)$$

Calculation of I_3 is slightly more difficult. One can differentiate it with respect to y_j^+ to kill one of the logarithms and then calculate it by poles at $x = 0$

$$\partial_{y_j^+} I_3 = 2i \log \frac{y_k^+}{y_k^-} + 2i \left(\frac{1}{y_j^{+2}} - 1 \right) \log \frac{y_k^+ y_j^+ - 1}{y_k^- y_j^+ - 1}, \quad I_3 = \int_{y_j^-}^{y_j^+} \partial_{y_j^+} I_3 dy_j^+ \quad (5.81)$$

thus

$$\begin{aligned} I_3 &= 2i \frac{u_j - u_k}{M} \log \frac{(y_j^+ y_k^- - 1)(y_j^- y_k^+ - 1)}{(y_j^+ y_k^+ - 1)(y_j^- y_k^- - 1)} + \frac{2}{M} \log \frac{y_j^- y_k^+ - 1}{y_j^+ y_k^- - 1} \\ &\quad + 2i \left((y_j^+ - y_j^-) \log \frac{y_k^+}{y_k^-} - (y_k^+ - y_k^-) \log \frac{y_j^+}{y_j^-} \right) \end{aligned} \quad (5.82)$$

Finally

$$\begin{aligned} ip_k &= M \sum_{a=1}^4 I_a = L \log \frac{y_k^+}{y_k^-} \\ &\quad + \sum_j \left(2 \log \frac{1 - 1/y_j^- y_k^+}{1 - 1/y_j^+ y_k^-} + 2i(u_j - u_k) \log \frac{(y_j^+ y_k^- - 1)(y_j^- y_k^+ - 1)}{(y_j^+ y_k^+ - 1)(y_j^- y_k^- - 1)} \right) \end{aligned} \quad (5.83)$$

thus we prove (5.57) assuming $P = 0$. This immediately leads to AFS BAE (5.58).

Bibliography

- [1] A. M. Polyakov, "String theory and quark confinement," Nucl. Phys. Proc. Suppl. **68** (1998) 1 [arXiv:hep-th/9711002].
- [2] J. M. Maldacena, "The large N limit of superconformal field theories and supergravity," Adv. Theor. Math. Phys. **2** (1998) 231 [Int. J. Theor. Phys. **38** (1999) 1113] [arXiv:hep-th/9711200].
- [3] S. S. Gubser, I. R. Klebanov and A. M. Polyakov, "Gauge theory correlators from non-critical string theory," Phys. Lett. B **428** (1998) 105 [arXiv:hep-th/9802109].
- [4] E. Witten, "Anti-de Sitter space and holography," Adv. Theor. Math. Phys. **2**, 253 (1998) [arXiv:hep-th/9802150].
- [5] J. A. Minahan and K. Zarembo, "The Bethe-ansatz for N = 4 super Yang-Mills," JHEP **0303** (2003) 013 [arXiv:hep-th/0212208].
- [6] L. N. Lipatov, JETP Lett. **59** (1994) 596 [Pisma Zh. Eksp. Teor. Fiz. **59** (1994) 571].
- [7] L. D. Faddeev and G. P. Korchemsky, "High-energy QCD as a completely integrable model," Phys. Lett. B **342**, 311 (1995) [arXiv:hep-th/9404173].
- [8] I. Bena, J. Polchinski and R. Roiban, "Hidden symmetries of the AdS(5) x S⁵ superstring," Phys. Rev. D **69** (2004) 046002 [hep-th/0305116].
- [9] R. R. Metsaev and A. A. Tseytlin, "Type IIB superstring action in AdS(5) x S(5) background," Nucl. Phys. B **533**, 109 (1998) [arXiv:hep-th/9805028].
- [10] L. F. Alday, G. Arutyunov and S. Frolov, JHEP **0601** (2006) 078 [arXiv:hep-th/0508140].
- [11] N. Beisert, V. A. Kazakov, K. Sakai and K. Zarembo, "The algebraic curve of classical superstrings on AdS(5) x S⁵," Commun. Math. Phys. **263** (2006) 659 [hep-th/0502226].
- [12] N. Beisert, V. A. Kazakov and K. Sakai, "Algebraic curve for the SO(6) sector of AdS/CFT," arXiv:hep-th/0410253.

-
- [13] N. Dorey and B. Vicedo, "On the dynamics of finite-gap solutions in classical string theory," JHEP **0607** (2006) 014 [arXiv:hep-th/0601194].
 - [14] V. A. Kazakov, A. Marshakov, J. A. Minahan and K. Zarembo, JHEP **0405** (2004) 024 [arXiv:hep-th/0402207].
 - [15] N. Beisert, V. A. Kazakov, K. Sakai and K. Zarembo, "Complete spectrum of long operators in $N = 4$ SYM at one loop," JHEP **0507** (2005) 030 [arXiv:hep-th/0503200].
 - [16] G. Arutyunov, S. Frolov and M. Staudacher, "Bethe ansatz for quantum strings," Phys. Rev. D **66** (2002) 010001 arXiv:hep-th/0406256.
 - [17] M. Staudacher, JHEP **0505** (2005) 054 [arXiv:hep-th/0412188].
 - [18] N. Beisert and M. Staudacher, "Long-range PSU(2,2;4) Bethe ansaetze for gauge theory and strings," Nucl. Phys. B **727** (2005) 1 [arXiv:hep-th/0504190].
 - [19] V. A. Kazakov and K. Zarembo, "Classical / quantum integrability in non-compact sector of AdS/CFT", JHEP **0410**, 060 (2004) [arXiv:hep-th/0410105].
 - [20] G. Arutyunov and S. Frolov, "Integrable Hamiltonian for classical strings on AdS(5) x S**5," JHEP **0502** (2005) 059 [arXiv:hep-th/0411089].
 - [21] O. Babelon, D. Bernard, M. Talon, "Introduction to Classical Integrable Systems", Cambridge University Press, June 2003.
 - [22] E. D. Belokolos, A. I. Bobenko, V. Z. Enolskii, A. R. Its, V. B. Matveev, "AlgebroGeometric Approach to Nonlinear Integrable Equations", Springer, Berlin, 1994
 - [23] N. Beisert, "The complete one-loop dilatation operator of $N = 4$ super Yang-Mills theory," Nucl. Phys. B **676**, 3 (2004) [arXiv:hep-th/0307015].
 - [24] N. Beisert and M. Staudacher, "The $N = 4$ SYM integrable super spin chain," Nucl. Phys. B **670** (2003) 439 [arXiv:hep-th/0307042].
 - [25] N. Beisert, V. Dippel and M. Staudacher, "A novel long range spin chain and planar $N = 4$ super Yang-Mills," JHEP **0407** (2004) 075 [arXiv:hep-th/0405001].
 - [26] N. Beisert, "The su(2—2) dynamic S-matrix," arXiv:hep-th/0511082.
 - [27] N. Beisert, R. Hernandez and E. Lopez, "A crossing-symmetric phase for AdS(5) x S**5 strings," JHEP **0611**, 070 (2006) [arXiv:hep-th/0609044].

-
- [28] N. Beisert, “On the scattering phase for $\text{AdS}(5) \times S^5$ strings,” *Mod. Phys. Lett. A* **22**, 415 (2007) [arXiv:hep-th/0606214].
- [29] R. A. Janik, “The $\text{AdS}(5) \times S^5$ superstring worldsheet S-matrix and crossing symmetry,” *Phys. Rev. D* **73**, 086006 (2006) [arXiv:hep-th/0603038].
- [30] N. Beisert, B. Eden and M. Staudacher, “Transcendentality and crossing,” *J. Stat. Mech.* **0701** (2007) P021 [arXiv:hep-th/0610251].
- [31] B. Eden and M. Staudacher, “Integrability and transcendentality,” *J. Stat. Mech.* **0611**, P014 (2006) [arXiv:hep-th/0603157].
- [32] A. V. Kotikov and L. N. Lipatov, “DGLAP and BFKL equations in the $N = 4$ supersymmetric gauge theory,” *Nucl. Phys. B* **661**, 19 (2003) [Erratum-ibid. *B* **685**, 405 (2004)] [arXiv:hep-ph/0208220].
- [33] Z. Bern, M. Czakon, L. J. Dixon, D. A. Kosower and V. A. Smirnov, “The Four-Loop Planar Amplitude and Cusp Anomalous Dimension in Maximally Supersymmetric Yang-Mills Theory,” *Phys. Rev. D* **75**, 085010 (2007) [arXiv:hep-th/0610248].
- [34] N. Beisert, T. McLoughlin and R. Roiban, “The Four-Loop Dressing Phase of $N=4$ SYM,” *Phys. Rev. D* **76** (2007) 046002 [arXiv:0705.0321 [hep-th]].
- [35] A. V. Kotikov, L. N. Lipatov, A. Rej, M. Staudacher and V. N. Velizhanin, “Dressing and Wrapping,” arXiv:0704.3586 [hep-th].
- [36] N. Dorey, D. M. Hofman and J. Maldacena, “On the singularities of the magnon S-matrix,” *Phys. Rev. D* **76** (2007) 025011 [arXiv:hep-th/0703104].
- [37] J. Ambjorn, R. A. Janik and C. Kristjansen, “Wrapping interactions and a new source of corrections to the spin-chain /string duality,” *Nucl. Phys. B* **736**, 288 (2006) [arXiv:hep-th/0510171].
- [38] M. Kruczenski, R. Roiban, A. Tirziu and A. A. Tseytlin, “Strong-coupling expansion of cusp anomaly and gluon amplitudes from quantum open strings in $\text{AdS}(5) \times S(5)$,” arXiv:0707.4254 [hep-th].
- [39] R. Roiban and A. A. Tseytlin, “Strong-coupling expansion of cusp anomaly from quantum superstring,” arXiv:0709.0681 [hep-th].
- [40] T. Klose and K. Zarembo, “Reduced sigma-model on $\text{AdS}(5) \times S(5)$: one-loop scattering amplitudes,” *JHEP* **0702**, 071 (2007) [arXiv:hep-th/0701240].

-
- [41] T. Klose, T. McLoughlin, J. A. Minahan and K. Zarembo, “World-sheet scattering in $AdS(5) \times S^5$ at two loops,” arXiv:0704.3891 [hep-th].
- [42] J. Maldacena and I. Swanson, “Connecting giant magnons to the pp-wave: An interpolating limit of $AdS_5 \times S^5$,” Phys. Rev. D **76**, 026002 (2007) [arXiv:hep-th/0612079].
- [43] Z. Bern, L. J. Dixon and V. A. Smirnov, Phys. Rev. D **72** (2005) 085001 [arXiv:hep-th/0505205].
- [44] Z. Bern, M. Czakon, L. J. Dixon, D. A. Kosower and V. A. Smirnov, Phys. Rev. D **75**, 085010 (2007) [arXiv:hep-th/0610248].
- [45] F. Cachazo, M. Spradlin and A. Volovich, Phys. Rev. D **75**, 105011 (2007) [arXiv:hep-th/0612309].
- [46] S. S. Gubser, I. R. Klebanov and A. M. Polyakov, Nucl. Phys. B **636**, 99 (2002) [arXiv:hep-th/0204051].
- [47] S. Frolov and A. A. Tseytlin, “Semiclassical quantization of rotating superstring in $AdS(5) \times S(5)$,” JHEP **0206** (2002) 007 [arXiv:hep-th/0204226].
- [48] R. Roiban, A. Tirziu and A. A. Tseytlin, JHEP **0707** (2007) 056 [arXiv:0704.3638 [hep-th]].
- [49] N. Beisert, A. A. Tseytlin and K. Zarembo, “Matching quantum strings to quantum spins: One-loop vs. finite-size corrections,” Nucl. Phys. B **715** (2005) 190 [arXiv:hep-th/0502173].
- [50] R. Hernandez, E. Lopez, A. Perianez and G. Sierra, “Finite size effects in ferromagnetic spin chains and quantum corrections to classical strings,” JHEP **0506**, 011 (2005) [arXiv:hep-th/0502188].
- [51] S. Schafer-Nameki, M. Zamaklar and K. Zarembo, “Quantum corrections to spinning strings in $AdS(5) \times S^5$ and Bethe ansatz: A comparative study,” JHEP **0509** (2005) 051 [arXiv:hep-th/0507189].
- [52] N. Beisert and L. Freyhult, “Fluctuations and energy shifts in the Bethe ansatz,” Phys. Lett. B **622**, 343 (2005) [arXiv:hep-th/0506243].
- [53] N. Beisert and A. A. Tseytlin, “On quantum corrections to spinning strings and Bethe equations,” Phys. Lett. B **629** (2005) 102 [arXiv:hep-th/0509084].
- [54] S. Schafer-Nameki and M. Zamaklar, “Stringy sums and corrections to the quantum string Bethe ansatz,” arXiv:hep-th/0509096.

-
- [55] J. A. Minahan, A. Tirziu and A. A. Tseytlin, “ $1/J$ corrections to semiclassical AdS/CFT states from quantum Landau-Lifshitz model,” arXiv:hep-th/0509071.
- [56] J. A. Minahan, A. Tirziu and A. A. Tseytlin, “ $1/J^2$ corrections to BMN energies from the quantum long range Landau-Lifshitz model,” arXiv:hep-th/0510080.
- [57] L. D. Faddeev, “How Algebraic Bethe Ansatz works for integrable model”, arXiv:hep-th/9605187.
- [58] B. Sutherland, “Low-Lying Eigenstates of the One-Dimensional Heisenberg Ferromagnet for any Magnetization and Momentum”, Phys. Rev. Lett. 74, 816 (1995).
- [59] N. Beisert, J. A. Minahan, M. Staudacher and K. Zarembo, “Stringing spins and spinning strings”, JHEP **0309**, 010 (2003) [arXiv:hep-th/0306139].
- [60] N. Reshetikhin and F. Smirnov “Quantum Floquet functions”, Zapiski nauchnikh seminarov LOMI (Notes of scientific seminars of Leningrad Branch of Steklov Institute) v.131 (1983) 128 (in russian).
- [61] G. P. Korchemsky, “WKB quantization of reggeon compound states in high-energy QCD,” arXiv:hep-ph/9801377.
- [62] F. A. Smirnov, “Quasi-classical study of form factors in finite volume”, Amer. Math. Soc. Transl. 201, 2000, 283 [arXiv:hep-th/9802132].
- [63] N. Beisert, “The dilatation operator of $N = 4$ super Yang-Mills theory and integrability”, Phys. Rept. **405**, 1 (2005) [arXiv:hep-th/0407277].
- [64] P. P. Kulish, N. Y. Reshetikhin and E. K. Sklyanin, “Yang-Baxter Equation And Representation Theory: I,” Lett. Math. Phys. **5**, 393 (1981).
- [65] A. Matytsin, “On the large N limit of the Itzykson-Zuber integral,” Nucl. Phys. B **411**, 805 (1994) [arXiv:hep-th/9306077].
- [66] J. M. Daul and V. A. Kazakov, “Wilson loop for large N Yang-Mills theory on a two-dimensional sphere,” Phys. Lett. B **335**, 371 (1994) [arXiv:hep-th/9310165].
- [67] I. Krichever, O. Lipan, P. Wiegmann and A. Zabrodin, “Quantum integrable models and discrete classical Hirota equations,” Commun. Math. Phys. **188**, 267 (1997) [arXiv:hep-th/9604080].
- [68] P. Bleher, “Quasi-classical expansions and the problem of quantum chaos”, in Lecture Notes in Mathematics, n.1469, “Geometrical Aspects of Functional Analysis”, Israel Seminar (GAFA) 1989-1990.

-
- [69] E. Brezin and V. A. Kazakov, “*Exactly Solvable Field Theories Of Closed Strings*”, Phys. Lett. B **236**, 144 (1990).
- [70] M. L. Mehta, Random Matrices, (Academic Press, New-York, 1967)
- [71] N. Beisert, C. Kristjansen and M. Staudacher, “*The dilatation operator of $N = 4$ super Yang-Mills theory*,” Nucl. Phys. B **664** (2003) 131 [arXiv:hep-th/0303060].
- [72] D. Serban and M. Staudacher, “*Planar $N = 4$ gauge theory and the Inozemtsev long range spin chain*,” JHEP **0406** (2004) 001 [arXiv:hep-th/0401057].
- [73] V. Kazakov, A. Sorin and A. Zabrodin, “*Supersymmetric Bethe ansatz and Baxter equations from discrete Hirota dynamics*,” arXiv:hep-th/0703147.
- [74] A. Zabrodin, “*Backlund transformations for difference Hirota equation and supersymmetric Bethe ansatz*,” arXiv:0705.4006 [hep-th].
- [75] S. Schafer-Nameki, M. Zamaklar and K. Zarembo, “*Quantum corrections to spinning strings in $AdS(5) \times S^5$ and Bethe ansatz: A comparative study*,” JHEP **0509**, 051 (2005) [arXiv:hep-th/0507189].
- [76] N. Gromov and V. Kazakov, “*Double scaling and finite size corrections in $sl(2)$ spin chain*,” Nucl. Phys. B **736** (2006) 199 [arXiv:hep-th/0510194].
- [77] N. y. Reshetikhin, “*A Method Of Functional Equations In The Theory Of Exactly Solvable Quantum Systems*,” Lett. Math. Phys. **7**, 205 (1983).
- [78] N. Y. Reshetikhin, “*INTEGRABLE MODELS OF QUANTUM ONE-DIMENSIONAL MAGNETS WITH $O(N)$ AND $SP(2K)$ SYMMETRY*,” Theor. Math. Phys. **63**, 555 (1985) [Teor. Mat. Fiz. **63**, 347 (1985)].
- [79] T.Bargheer, N.Beisert, N.Gromov, to appear
- [80] G. Mandal, N. V. Suryanarayana and S. R. Wadia, Phys. Lett. B **543** (2002) 81 [arXiv:hep-th/0206103].
- [81] S. Frolov and A. A. Tseytlin, “*Multi-spin string solutions in $AdS(5) \times S^5$* ,” Nucl. Phys. B **668**, 77 (2003) [arXiv:hep-th/0304255].
- [82] S. Frolov and A. A. Tseytlin, “*Quantizing three-spin string solution in $AdS(5) \times S^5$* ,” JHEP **0307**, 016 (2003) [arXiv:hep-th/0306130].
- [83] G. Arutyunov, J. Russo and A. A. Tseytlin, “*Spinning strings in $AdS(5) \times S^5$: New integrable system relations*,” Phys. Rev. D **69**, 086009 (2004) [arXiv:hep-th/0311004].

-
- [84] I. Y. Park, A. Tirziu and A. A. Tseytlin, "Spinning strings in $AdS(5) \times S^5$: One-loop correction to energy in $SL(2)$ sector," JHEP **0503**, 013 (2005) [arXiv:hep-th/0501203].
- [85] D. Berenstein, J. M. Maldacena and H. Nastase, "Strings in flat space and pp waves from $N=4$ Super Yang Mills," AIP Conf. Proc. **646**, 3 (2003).
- [86] N. Gromov, V. Kazakov, K. Sakai and P. Vieira, "Strings as multi-particle states of quantum sigma-models," Nucl. Phys. B **764** (2007) 15 [arXiv:hep-th/0603043].
- [87] S. A. Frolov, I. Y. Park and A. A. Tseytlin, "On one-loop correction to energy of spinning strings in $S(5)$," Phys. Rev. D **71**, 026006 (2005) [arXiv:hep-th/0408187].
- [88] S. Schafer-Nameki, Phys. Lett. B **639**, 571 (2006) [arXiv:hep-th/0602214].
- [89] R. Hernandez and E. Lopez, "Quantum corrections to the string Bethe ansatz," JHEP **0607** (2006) 004 [arXiv:hep-th/0603204].
- [90] N. Gromov and P. Vieira, "Constructing the AdS/CFT dressing factor," arXiv:hep-th/0703266.
- [91] N. Gromov and P. Vieira, "The $AdS(5) \times S^5$ superstring quantum spectrum from the algebraic curve," arXiv:hep-th/0703191.
- [92] S. Novikov, S. V. Manakov, L. P. Pitaevsky and V. E. Zakharov, "Theory Of Solitons. The Inverse Scattering Method,"
- [93] A. B. Zamolodchikov and A. B. Zamolodchikov, "Relativistic Factorized S Matrix In Two-Dimensions Having $O(N)$ Isotopic Symmetry," Nucl. Phys. B **133** (1978) 525 [JETP Lett. **26** (1977) 457].
- [94] A.M. Polyakov, P.B. Wiegmann, "Theory of Non-Abelian Goldstone Bosons", Phys.Lett.**131B** (1984) 121.
- [95] P. B. Wiegmann, "Exact Solution For The $SU(N)$ Main Chiral Field In Two-Dimensions," JETP Lett. **39** (1984) 214 [Pisma Zh. Eksp. Teor. Fiz. **39** (1984) 180].
- [96] L. D. Faddeev and N. Y. Reshetikhin, "Integrability Of The Principal Chiral Field Model In $(1+1)$ -Dimension," Annals Phys. **167** (1986) 227.
- [97] P. Wiegmann, "Exact Factorized S Matrix Of The Chiral Field In Two-Dimensions," Phys. Lett. B **142**, 173 (1984).
- [98] V.A. Fateev, V.A. Kazakov, P.B. Wiegmann, "Principal chiral field at large N ", Nucl. Phys. B424 [FS] (1994) 505-520, [arXiv:hep-th/9403099].

-
- [99] J. Balog, S. Naik, F. Niedermayer, P. Weisz, *Phys.Rev.Lett.* **46** (1992). 356.
- [100] N. Mann and J. Polchinski, "Bethe ansatz for a quantum supercoset sigma model," *Phys. Rev. D* **72** (2005) 086002 [arXiv:hep-th/0508232].
- [101] P. B. Wiegmann, "On The Theory Of Nonabelian Goldstone Bosons In Two-Dimensions: Exact Solution Of The $O(3)$ Nonlinear Sigma Model," *Phys. Lett. B* **141**, 217 (1984).
- [102] E. Ogievetsky, N. Reshetikhin and P. Wiegmann, "The Principal Chiral Field In Two-Dimension And Classical Lie Algebra," NORDITA-84/38
- [103] A. B. Zamolodchikov and A. B. Zamolodchikov, "Massless factorized scattering and sigma models with topological terms," *Nucl. Phys. B* **379** (1992) 602.
- [104] L. D. Faddeev, E. K. Sklyanin and L. A. Takhtajan, "The Quantum Inverse Problem Method. 1," *Theor. Math. Phys.* **40**, 688 (1980) [*Teor. Mat. Fiz.* **40**, 194 (1979)].
- [105] A. Rej, D. Serban and M. Staudacher, "Planar $N = 4$ gauge theory and the Hubbard model," *JHEP* **0603**, 018 (2006) [arXiv:hep-th/0512077].
- [106] N. Gromov and V. Kazakov, "Asymptotic Bethe ansatz from string sigma model on $S^3 \times \mathbb{R}$," arXiv:hep-th/0605026.